THE METABOLISM, DECOMPOSITION AND PHARMACOKINETICS OF ANTI-TUMOUR IMIDAZOTETRAZINONES.

by

Colin Goddard

A thesis submitted for the degree of

Doctor of Philosophy

in

Aston University, Birmingham

August 1985

The metabolism, decomposition and pharmacokinetics of anti-tumour imidazotetrazinones

by

Colin Goddard

A thesis submitted for the degree of Doctor of Philosophy, 1985 in Aston University.

Mitozolomide [8-carbamoyl-3-(2-chloroethyl)imidazo[5,1-3]-1,2,3,5-tetrazin-4(3H)-one], the lead compound in a series of imidazo[5,1-d]-1,2,3,5-tetrazin-4(3H)-ones, and CCRG 81045, its 3-methyl analogue, show promise as antitumour agents. Chemical, biochemical and experimental antitumour data revealed certain similarities with antitumour chloroethylnitrosoureas and triazenoimidazoles. Studies were undertaken using mitozolomide and CCRG 81045 in an attempt to establish the pharmacological basis to their therapeutic action and to identify potential areas of improvement over existing agents. Reversed-phase high performance liquid chromatographic methods were developed to facilitate these studies. The results of *in vitro* studies supported a decomposition mechanism *via* a monoalkyltriazene, the putative active intermediate, as the principal chemical fate of these compounds under physiological conditions. First-order kinetics, an exquisite pH dependence and a relative catalysis in plasma were features of this decomposition. The pharmacokinetics of mitozolomide and CCRG 81045 in mice and of mitozolomide in man were described using a simple one-compartment model supported by monophasic elimination and volumes of distribution approximating to total body water. Mitozolomide was administered clinically at doses up to 153 mg. m^{-2} where severe thrombocytopenia prevented further escalation. Mitozolomide pharmacokinetics were independent of dose and good oral bioavailability was demonstrated. Elimination half-lives for CCRG 81045 in mice and for mitozolomide in mice and man were in agreement with *in vitro* data implicating the importance of chemical degradation in the *in vivo* fate of these agents. Between 10 and 24% of administered mitozolomide was excreted unchanged in the urine of mice and there was some evidence of a metabolic contribution to elimination. The potential importance of local pH variations to the *in vivo* activity and in the interpretation of *in vitro* cytotoxicity data are discussed. The pharmacokinetics of these two imidazo[5,1-d]-1,2,3,5-tetrazin-4(3H)-ones suggest they may offer significant improvement on currently used drugs.

Key words: imidazo[5,1-d]-1,2,3,5-tetrazinones, mitozolomide, HPLC, pharmacokinetics, cancer

ACKNOWLEDGEMENTS

I would like to express my thanks to everyone within the Cancer Research Campaign Experimental Chemotherapy Group for their friendship, encouragement and advice during the course of this work and particularly to Dr J A Slack for his thorough and patient supervision throughout (thanks John!).

I would also like to thank W Isp for his invaluable technical assistance, the Science Research Council for financial support, Hazel Brown for her excellent typing and two very tolerant parents for their continued support over the last 8 years.

Dedicated to the memory of Barry Blenkinsop ..... one of the good guys.

CONTENTS

LIST OF FIGURES

LIST OF TABLES

ABBREVIATIONS

AIC	-	5-aminoimidazole-4-carboxamide
diazo-IC	-	5-diazoimidazole-4-carboxamide
MCTIC	-	5-[3-(2-chloroethyl)triazenyl]imidazole-4-carboxamide
DTIC	-	5-(3,3-dimethyl-1-triazenyl)imidazole-4-carboxamide
BCTIC	-	5-[3,3-bis(2-chloroethyl)-1-triazenyl]imidazole-4-carboxamide
MNNG	-	1-methyl-1-nitroso-guanidine
MNU	-	1-methyl-1-nitrosourea
BCNU	-	1,3-bis(2-chloroethyl)-1-nitrosourea
meCCNU	-	1-(2-chloroethyl)-3-(4-methylcyclohexyl)-1-nitrosourea
PCNU	-	1-(2-chloroethyl)-3-(2,6-dioxo-3-piperidyl)-1-nitrosourea
CCNU	-	1-(2-chloroethyl)-3-cyclohexyl-1-nitrosourea
MTIC	-	5-(3-methyl-1-triazenyl)imidazole-4-carboxamide
NADPH	-	nicotinamide adenine dinucleotide phosphate (reduced)
DNA	-	deoxyribose nucleic acid
GSH	-	glutathione (reduced)
GSSG	-	glutathione (oxidised)
DMSO	-	dimethylsulphoxide
TLC	-	thin layer chromatography
HPLC	-	high performance liquid chromatography
NCI	-	US National Cancer Institute
MTD	-	maximum tolerated dose
LD_{10}	-	lethal dose for 10% of test population
LD_{50}	-	lethal dose for 50% of test population
iv	-	intra venous
ip	-	intra-peritoneal
po	-	oral
ic	-	intra-cranium

λ max	-	wavelength of maximum UV absorbance
UV	-	ultraviolet
RT	-	retention time
Rf	-	relative index of movement from origin in TLC
k'	-	capacity factor
log P	-	relative index of lipophilicity
$t_{\frac{1}{2}}$	-	half-life
$t_{\frac{1}{2}\alpha}$	-	distribution phase half-life
$t_{\frac{1}{2}\beta}$	-	elimination phase half-life
Vd	-	volume of distribution
AUC	-	area under the curve
Cp.max.act.	-	measured maximum plasma concentration
Cp.max.ex.	-	calculated maximum plasma concentration
Cp.max	-	maximum plasma concentration
k_{el}	-	elimination rate constant
C_{WB}	-	concentration in whole blood
Cpt.	-	concentration at time 't'.

1. INTRODUCTION

1.1 General

Despite the investment of huge amounts of resource and time a cure for most forms of cancer remains elusive. The array of diseases described as cancer all appear to arise as the result of subtle failings in the normal development of cell populations. Whilst a tumour cell population is often diverse, large and invasive its constituent cells remain so similar to those found in normal tissues that specific, directed anti-tumour therapy currently remains beyond our capability.

Initial approaches to therapy centred on the surgical excision of the tumour and radiotherapy. Unfortunately at the time of presentation the primary tumour has often metastasized and the disease manifested itself into a systemic one. The development of the cytotoxic agent nitrogen mustard as an offshoot of research into nerve gases signalled the beginnings of attempts to treat cancer with systemically administered drugs.

The use of chemotherapy in the clinical management of cancer has achieved a high status over the last 25 years due largely to the success of a small number of agents and their combination in regimens that exploit differing toxicity profiles (towards normal cells) to obtain an improved therapeutic effect (1).

However the prognosis for many tumours (notably the solid, slow growing tumours such as lung, breast, and colon carcinomas) remains poor (2) and many of the drugs in use inflict deleterious side-effects upon patients. Because of this there is an urgent need to develop new agents which offer both an improved therapeutic benefit and decreased patient toxicity.

The imidazo[5,1-d]-1,2,3,5-tetrazin-4(3H)-ones are a novel class of compounds from which it is hoped suitable such agents may be found.

The parent ring system (see figure 1.1) contains a reactive NNN linkage fused via a fourth bridgehead nitrogen to an imidazole ring. The chemistry of this NNN linkage in both cyclic (triazine) and acyclic (triazene) systems has been studied in some depth (see references 3 and 4 for reviews) in an attempt to elucidate the potential of this reactive moiety in an anti-tumour setting. Ring opening of both 1,2,3-benzotriazin-4(3H)-ones and imidazo[5,1-c]-1,2,4-triazines have been shown to occur (3) and the potential ring cleavage of the imidazo[5,1-d]-1,2,3,5-tetrazin-4(3H)-one ring system in any one of the 4 positions (see figure 1.1) suggested clear possibilities with respect to the generation of reactive intermediates (5).

The current work focusses on two imidazo[5,1-d]-1,2,3,5-tetrazin-4(3H)-ones, mitozolomide, the lead compound in the series and its 3-methyl analogue CCRG 81045.

Figure 1.1 - The imidazo[5,1-d]-1,2,3,5-tetrazine heterocycle showing numbering system and potential sites of ring cleavage.

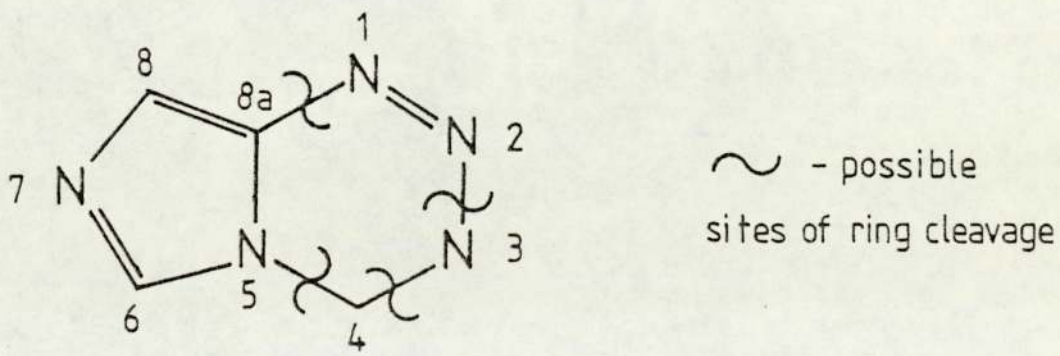

1.2 Synthesis and chemistry of mitozolomide

Mitozolomide, 8-carbamoyl-3-(2-chloroethyl)-imidazo[5,1-d]-1,2,3,5-tetrazin-4(3H)-one, was the first compound in the series to be prepared in a synthesis performed by Robert Stone in 1980 (6). Stone was working on cyclic and acyclic modifications of 5-aminoimidazole-4-carboxamide (AIC) an important salvage substrate via its ribonucleotide (AICAR) in purine biosynthesis (7). The starting material for much of the synthetic work was 5-diazoimidazole-4-carboxamide (diazo-IC) obtained from the diazotisation of AIC. Diazo-IC was known to be a reactive intermediate in the photolytic decomposition of DTIC[5-(3,3-dimethyl-1-triazenyl)-1H-imidazole-4-carboxamide] a clinically used anti-tumour agent (8) and one of many triazenoimidazoles extensively studied (see reference 9 for review).

Ege and Gilbert (10) had described a synthetic route to pyrazolo[5,1-d]-1,2,3,5-tetrazin-4(3H)-ones based on the reaction of diazoazoles and isocyanates (see figure 1.2). From this it was postulated that the analogous reaction using diazo-IC with aryl and alkyl isocyanates would generate a series of imidazo[5,1-d]-1,2,3,5-tetrazin-4(3H)-ones and that these novel heterocycles would have the potential to generate a range of reactive products upon their decomposition including diazo-IC and isocyanates.

Thus, diazo-IC and 2-chloroethylisocyanate were stirred in dichloromethane at 25°C, in the dark, for 20 days generating 8-carbamoyl-3-(2-chloroethyl)imidazo[5,1-d]-1,2,3,5-tetrazin-4(3H)-one in a 90% yield [(5); see figure 1.3]. The synthesis proved to be general with methyl, n-propyl and various aryl isocyanates reacting in either dichloromethane or ethyl acetate to generate 3-substituted imidazo[5,1-d]-1,2,3,5-tetrazin-4(3H)-ones in high yield.

Figure 1.2 - The synthesis of pyrazolo[5,1-d]-1,2,3,5-tetrazin-4(3H)-ones.

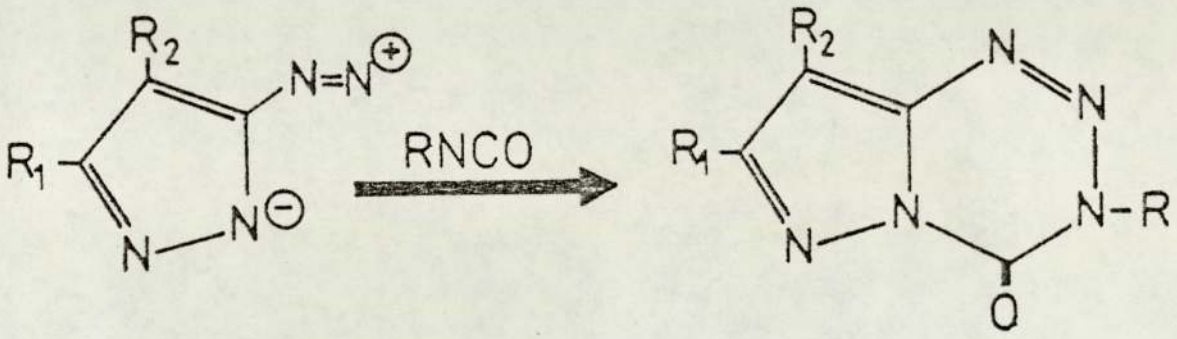

Figure 1.3 - The synthesis of mitozolomide, 8-carbamoyl-3-(2-chloroethyl)-imidazo[5,1-d]-1,2,3,5-tetrazin-4(3H)-one, from 2-chloroethylisocyanate and diazo-IC.

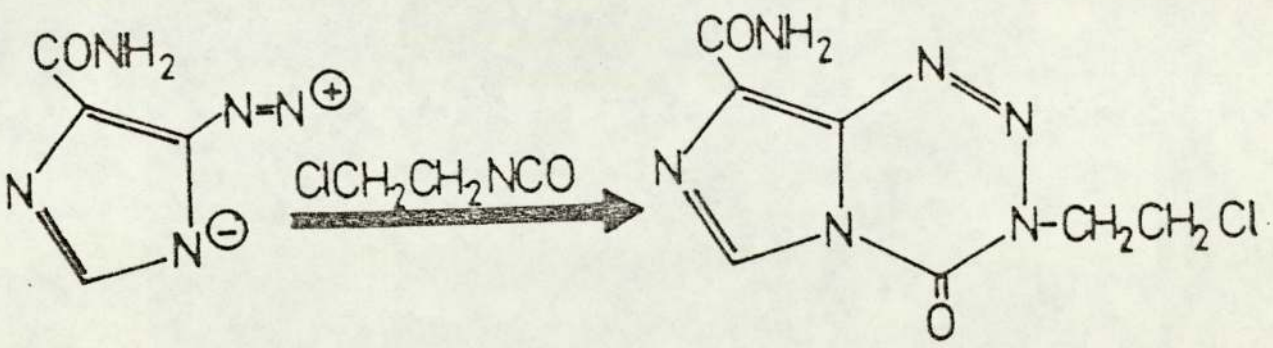

Figure 1.4 - Likely decomposition pathways for mitozolomide.

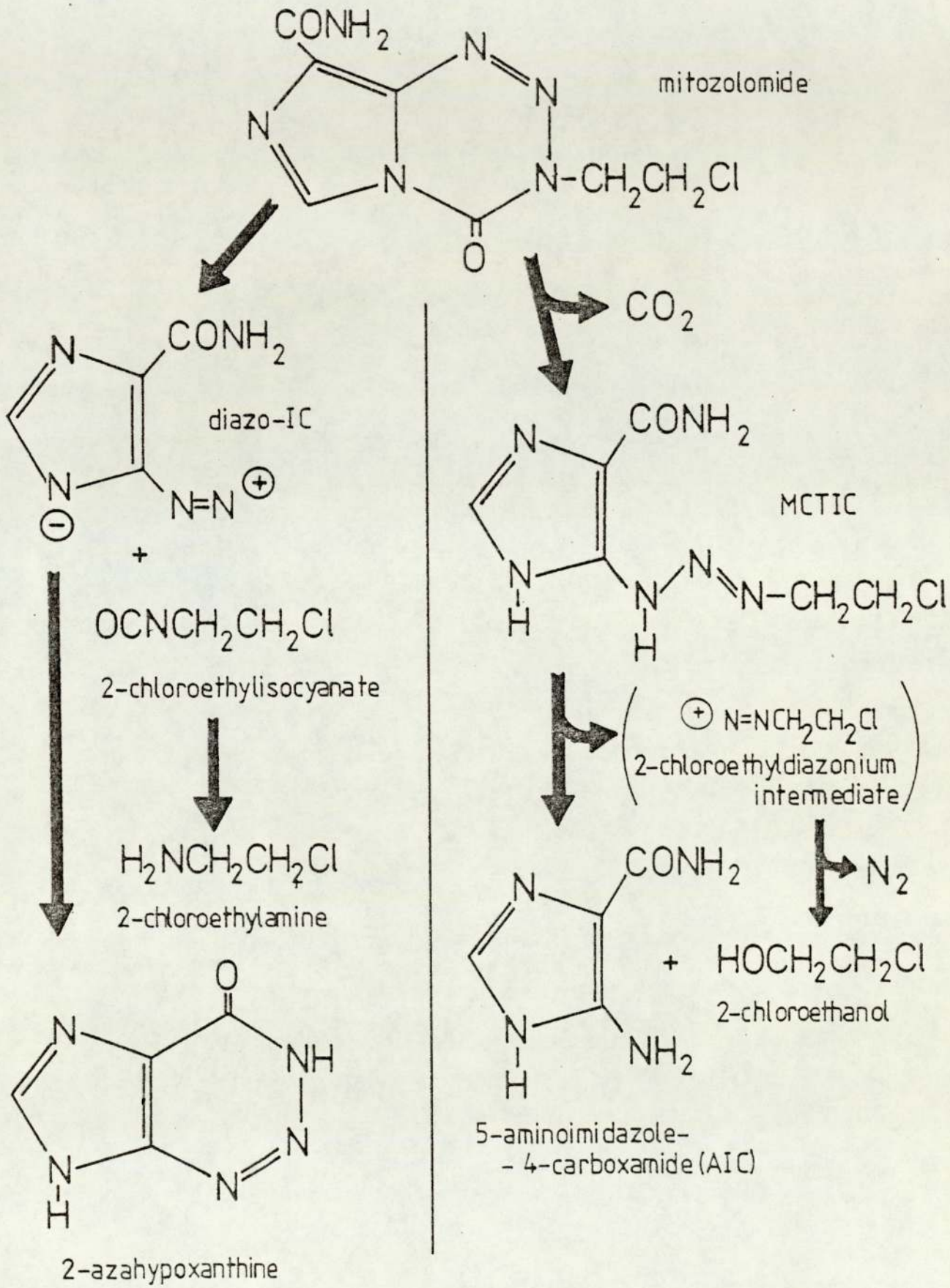

Both mitozolomide and CCRG 81045 were structurally confirmed by X-ray crystallography, characterized (5) and studies on the chemistry (principally of mitozolomide) conducted. Work on the 1,2,3-benzotriazin-4(3H)-ones (3) and the imidazo[5,1-c]-1,2,4-triazin-4(3H)-ones (11) suggested two likely decomposition routes, either via reversion to the diazoimidazole and chloroethylisocyanate or by nucleophilic attack at the C4 position with ring-opening and subsequent de-carboxylation to generate the triazene 5-[3-(2-chloroethyl)-triazenyl]imidazole-4-carboxamide, MCTIC (see figure 1.4). Early work indicated that the nature and kinetics of the decomposition were very dependent on reaction conditions.

Decomposition in alcohols (methanol and ethanol) was generally slow (complete in approximately 18 hours in boiling methanol). Product analysis by thin layer chromatography (TLC) and ^{1}H-nmr confirmed the presence of 2-azahypoxanthine and N-(2-chloroethyl)-carbamate, the expected end-products from the diazo-IC route of decomposition (5).

However, under aqueous conditions a pH dependence was evident. Mitozolomide appeared stable to even hot concentrated sulphuric acid whilst decomposition under basic conditions was rapid and in phosphate buffer at pH 7.4 a first order half-life of 98 minutes was seen at 28°C (6). A brief decomposition in 5% sodium bicarbonate enabled the characterization of an unstable solid as MCTIC. Prolonged treatment resulted in AIC and 2-chloroethanol together with various minor components (12).

Shealey had previously observed AIC and a similar range of minor components in the decomposition of MCTIC (13). Three of these by-products were subsequently identified as N-(2-chloroethyl)-AIC and the corresponding N-(2-hydroxyethyl)-and N-aziridino-derivatives [(12); see figure 1.5].

A consideration of these potential degradation pathways revealed many structural similarities to the triazenoimidazoles and the chloroethylnitrosoureas, important agents in cancer chemotherapy, which eventually led to the screening of mitozolomide as an anti-tumour agent.

Figure 1.5 - Minor products arising from the decomposition of MCTIC.

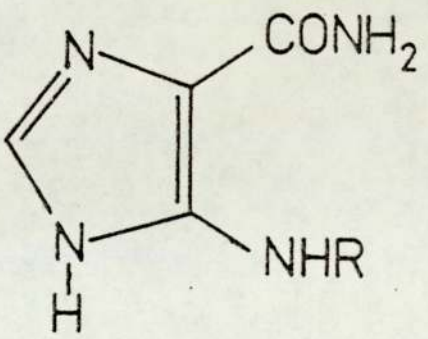

R_1= CH_2CH_2OH; N-(2-hydroxyethyl)-AIC

R_2= CH_2CH_2Cl; N-(2-chloroethyl)-AIC

R_3= HN CH_2 CH_2 ; N-aziridino-AIC

1.3 Historical perspective

1.3.1 The triazenoimidazoles

Interest in the triazene group and particularly its role in triazenoimidazoles has been extensive since the synthesis and screening of DTIC by Shealey et al in the early 1960's (14, 15). Of a series of triazenoimidazoles synthesized in this period the most active against the murine L1210 leukaemia was BCTIC, 5-[3,3-bis(2-chloroethyl)-1-triazenyl]-1H-imidazole-4-carboxamide; TIC-mustard, the bis(2-chloroethyl) analogue of DTIC (89). BCTIC elicited cures (taken as survival at the end of the study, 2-8 months) against this in vivo model (16, 17) and went on to be evaluated clinically (18-22). The drug was used in the

treatment of malignant melanoma (18), various childhood malignancies (19), glioma (20), and against cancers of the breast (21) and gastro-intestinal tract (22). Results showed extensive toxicity with nausea and haematopoetic depression being the most prevalent and despite some responses (18, 21) this toxicity coupled to the enormous problems in formulating and administering such an unstable agent (9, 17) prevented further clinical evaluation. BCTIC has a tendency, even in the solid state to convert to an inactive triazolinium salt [(17), see figure 1.6] and is also photosensitive. BCTIC was thought to exert its anti-tumour effect via decomposition to bis(2-chloroethyl)amine and diazo-IC (23) but in 1975 Shealey proposed a possible metabolic activation to MCTIC (see figure 1.6), in a manner analogous to the postulated activation of DTIC, and showed MCTIC to have excellent anti-tumour activity against a murine L1210 model (13). The putative role of MCTIC in the mode of action of BCTIC received further credence when Hill demonstrated the existence of a liver microsomal enzyme capable of N-dechlorethylating BCTIC at an appreciate rate (24). The instability of MCTIC precludes it from development as an agent in its own right but clearly this work hints at the possible value of a stable pro-drug form of this monoalkyltriazene.

Figure 1.6 - The fate of BCTIC, isomeric conversion to its inactive triazolinium salt or microsomally mediated activation to MCTIC.

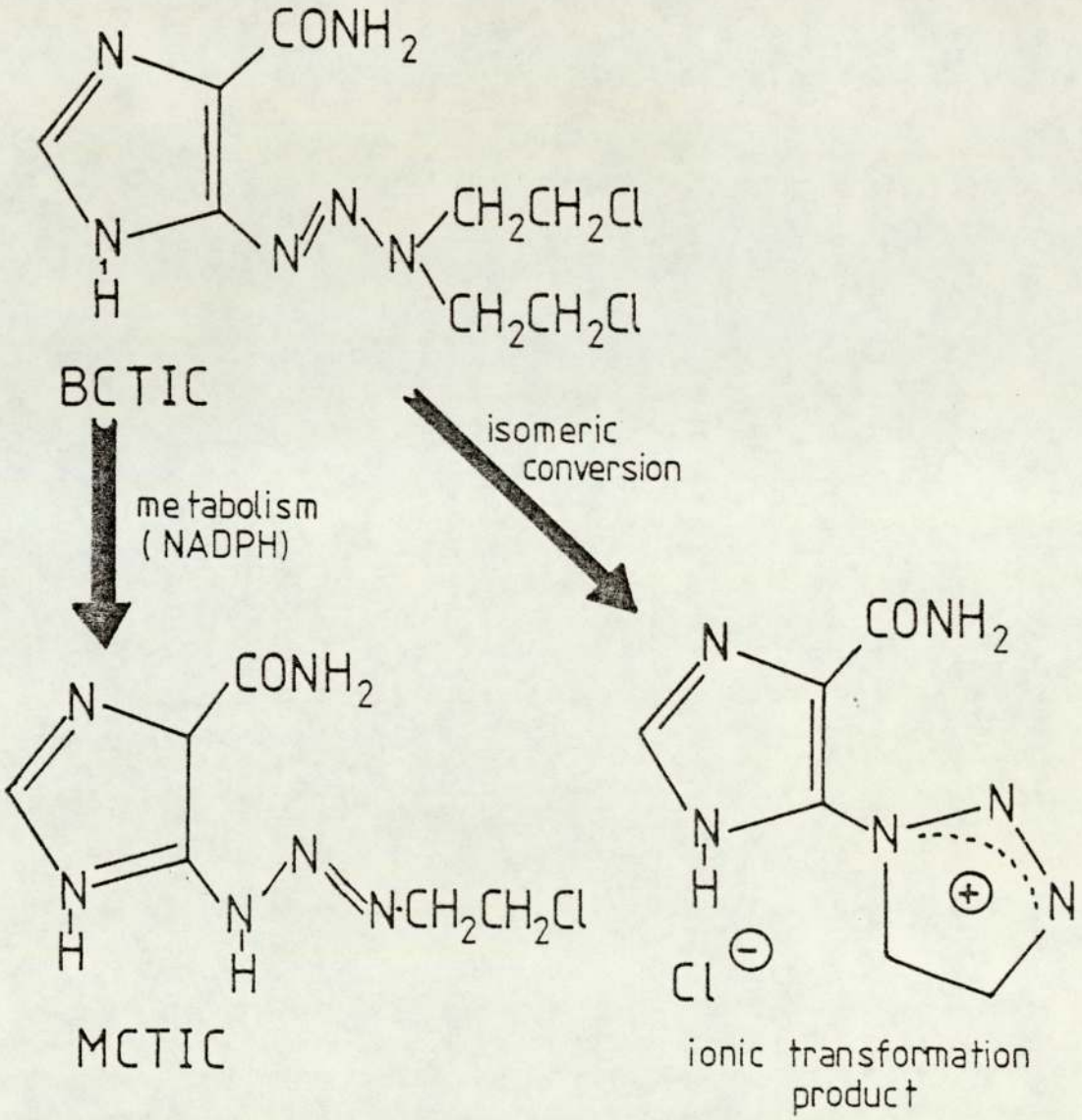

1.3.2 The chloroethylnitrosoureas

The correlation of the imidazo[5,1-d]-1,2,3,5-tetrazin-4(3H)-ones with the chloroethylnitrosoureas is a two-fold one. Early decomposition studies (6) indicated that mitozolomide may generate chloroethylisocyanate under certain conditions and a concurrent study by Hickman and Gibson at Aston was involved in assessing the importance of isocyanates in the toxicity and mode of action of the chloroethylnitrosoureas (25). However, decompositon via the triazene MCTIC could generate an intermediate chloroethyldiazonium species (5) which is also produced in the decomposition of the nitrosureas (26). Subsequent mode of action studies on mitozolomide have revealed many other close similarities with the nitrosoureas.

Interest in the nitroso group was first initiated in 1960 when Green and Greenberg demonstrated activity of nitrosoguanidines and particularly 1-methyl-1-nitroso-3-nitroso-guanidine(MNNG) against L1210 ascites in mice (27). Baker et al (28) proceeded to demonstrate the importance of the nitroso group to anti-leukaemic activity and showed that inclusion of a chloroethyl group in place of the terminal methyl group considerably enhanced this activity. This led to the synthesis of 1-(2-chloroethyl)-1-nitrosourea (CENU) which proved curative in tests against the L1210 leukaemia. Simultaneously Montgomery et al working on possible diazomethane releasers found that 1-methyl-1-nitrosourea (MNU) produced superior activity to MNNG against intraperitoneally (ip) implanted L1210 cells in mice and that, more importantly, unlike the drugs in use at the time, limited but reproducible activity was seen against intra-cranially (ic) implanted L1210 (29). This suggested a solution to the apparent problem of tumour cell sanctuaries and resulted in a large scale analogue synthesis programme based on MNU.

One of the first products of this programme was 1,3-bis(2-chloroethyl)-1-nitrosourea, BCNU, which proved curative against the L1210 leukaemia (30,31). Further research showed the more lipophilic 3-cyclohexyl analogue CCNU [1-(2-chloroethyl)-3-cyclohexyl-1-nitrosourea] to have superior activity against ic implanted tumours whilst meCCNU [1-(2-chloroethyl)-3-(4-methylcyclohexyl)-1-nitrosourea] demonstrated excellent activity against the Lewis lung (LL) tumour, a solid murine tumour believed to reflect more closely the kinetic growth characteristics of many human tumours (32, 33).

The experimental activity of these three nitrosoureas and many other analogues proved superior to that seen for any previously tested chemotherapeutic agents. This reflected both a quantitative (log kill versus sensitive tumour cells in vivo) and qualitative (a broad spectrum of activity against model systems) aspect, and included excellent activity against all six rodent tumours of the U.S. National Cancer Institute (NCI) activity screen[i.e. the P388 and L1210 leukaemias, B16 melanoma, CD8 breast, Co38 colonic and LL Lewis lung; (34)]. Despite poorer activity being seen against the 3 human xenografts used by the NCI (CX-1, colon, LX-1, lung and MX-1, breast) the 3 nitrosoureas were amongst only 6 drugs of 1635 evaluated to be positive in 6 or more screens (34). The experimental anti-tumour activity of the nitrosoureas has been reviewed in depth by Schabel (35).

Clinically the nitrosoureas have been very disappointing following the promise of their exceptional screening results. A dose-limiting myelosuppression manifested as a delayed leukopenia and thrombocytopenia [with nadir 4-6 weeks (36, 37)] has restricted their use, whilst nausea, vomiting and some hepatic and renal problems have also been evident (36).

Additionally, cumulative pulmonary toxicities have been noted in the use of BCNU (38) and, more recently there has been a suggestion that meCCNU may be leukaemiogenic (39). However, good activity was noted against brain tumours (40), although this was recognised as being only palliative since responses obtained were generally only short-lived with an MTP (mean time to progression) of only 38 weeks for malignant glioma following treatment with BCNU (41). Nitrosoureas have featured in the treatment of other cancers, notably relapsed Hodgkins lymphoma (42) and lung (38).

Despite their clinical disappointment the nitrosoureas have generated an enormous amount of research interest concerning their activity, decomposition, mode of action, metabolism, toxicology and pharmacology.

The labile nature of the drugs under physiological conditions meant that early attempts to elucidate the decomposition pathway were surrounded in controversy. The decomposition is both ionic and pH dependent and results in the formation of volatile end-products in aqueous conditions (43), including vinyl chloride, acetaldehyde and chloroethanol. Montgomery et al proposed a mechanism that proceeded via a vinyl carbonium ion (43) however Colvin, using [^{14}C]-chloroethyl-labelled BCNU (44), and Reed working with CCNU and meCCNU (45) produced evidence favouring a mechanism that proceeded via loss of the N3 proton to generate an isocyanate and a 2-chloroethyldiazohydroxide species and it was this latter mechanism, shown in figure 1.7, that appeared to be the predominant one. Further evidence from Brundrett and Colvin using deuterated BCNU confirmed this (46) whilst Chatterji showed that the generation of the chloroethyldiazonium hydroxide species was subject to base catalysis (47).

An elegant experiment by Brundrett and Colvin (48) using stereo-specifically distinct analogues of BCNU answered the question of whether the chloroethyldiazonium hydroxide species would alkylate via an SN2 mechanism or through the generation of a chloroethyl carbonium ion in favour of the former.

Figure 1.7 - Decomposition of the chloroethylnitrosoureas.

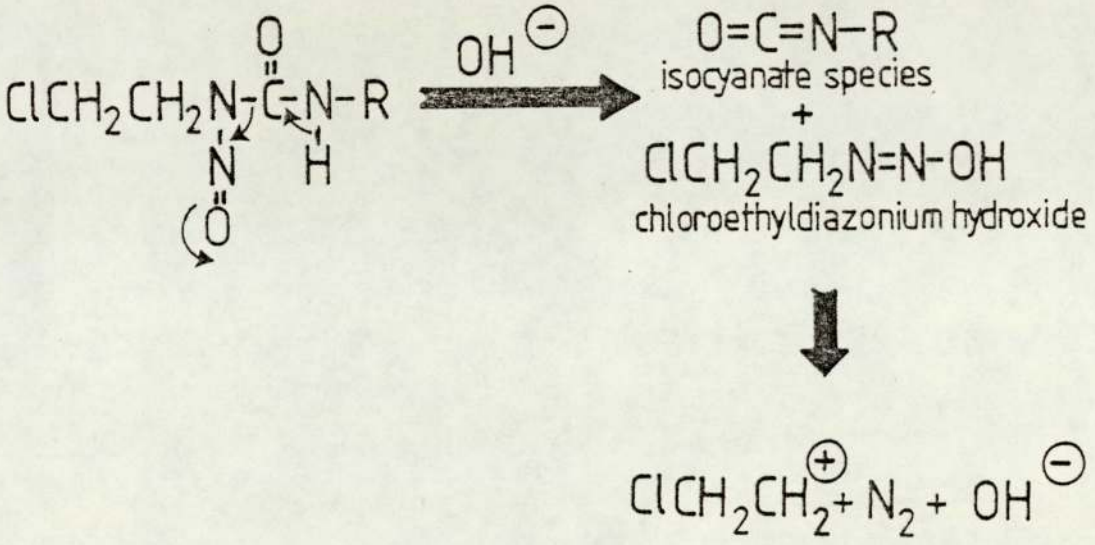

Studies on the kinetics of this process in physiological buffers revealed first order decomposition kinetics for BCNU, CCNU, and meCCNU with similar half lives in phosphate buffer at 37°C of 43-52 minutes, 48 ± 4 minutes and 70 ± 7 minutes respectively (44) and Weinkam showed an exquisite dependence upon pH in the decomposition

of BCNU (49), in phosphate buffer at pH 4-5 the half life was in excess of 500 minutes whilst at pH 8 it was only 5 minutes (50 minutes at pH 7.4). An examination of the decomposition of BCNU in human serum *in vitro* revealed a marked increase in the rate of decomposition to that seen in Ringers media at the same pH [$t_{\frac{1}{2}}$ of 11-17 minutes versus 51 minutes (50)]. Weinkam showed the same relationship with CCNU and meCCNU (51) but interestingly not for PCNU [1-(2-chloroethyl)-3-(2,6-dioxo-3-piperidyl)-1-nitrosourea]. Experiments using serum ultrafiltrates and protein solutions indicated that this increase in rate was facilitated by a non-specific protein binding to albumin which was dependent upon the lipophilicity of the drugs (BCNU, CCNU and meCCNU are considerably more lipophilic than PCNU: log P's of 1.5, 2.8, 3.3 and 0.37 respectively). The situation was further complicated by the belief that the partitioning of the very lipophilic CCNU and meCCNU into the core regions of serum lipoproteins was exerting a protective effect with respect to their decompositons (52, 53).

Studies on the mode of action of the nitrosoureas have largely been concerned with the relative importance of the two reactive species generated, with the isocyanate apparently carbamoylating the electron rich amino groups in proteins (54) and the chloroethyldiazonium hydroxide species alkylating the DNA and RNA of target cells. That the isocyanate group was probably not important with respect to reaction with DNA directly was demonstrated by Cheng *et al* (55) who showed that a [^{14}C]-ethyl label from CCNU binds to DNA, RNA and proteins but that a [^{14}C]-cyclohexyl label bound only to proteins.

The fact that CENU had excellent anti-tumour activity but cannot produce an isocyanate species suggested a minor role for the isocyanates in the anti-tumour activity of the nitrososureas (56), but Kann *et al*

showed that 2-chloroethylisocyanate inhibited the repair of DNA strand breaks in L1210 cells and so contributed to cell kill (57). It was argued by Hilton (58) that the rate of isocyanate production intracellularly and its short-lived duration (the half-life of chloroethylisocyanate under physiological conditions is approximately 17 seconds) meant that insufficient levels could be produced to inhibit repair enzymes. The popular view seemed to centre on the belief that the mode of action was via chloroethyldiazonium hydroxide-induced alkylations but that the carbamoylations of the isocyanates may contribute towards toxicity (59).

This contribution of the isocyanate group led to the development of nitrosoureas which, due to their structural properties, would self-carbamoylate upon decomposition. These include chlorozotocin, 2-[3-(2-chloroethyl)-1-3-nitrosoureido]-2-deoxy-D-glucopyranose, developed from the anti-tumour, anti-biotic streptozotocin (see figure 1.8) and HECNU [1-(2-hydroxyethyl)-3-(2-chloroethyl)-3-nitrosourea] (60, 61). The principal manifestation of nitrosourea toxicity has been myelosuppression (37) and whilst chlorozotocin has been shown in clinical trials (62, 63) to be less myelosuppressive the therapeutic results have been disappointing.

Figure 1.8 - The mechanism by which chlorozotocin self-carbamoylates upon its decomposition, thus preventing release of an isocyanate species.

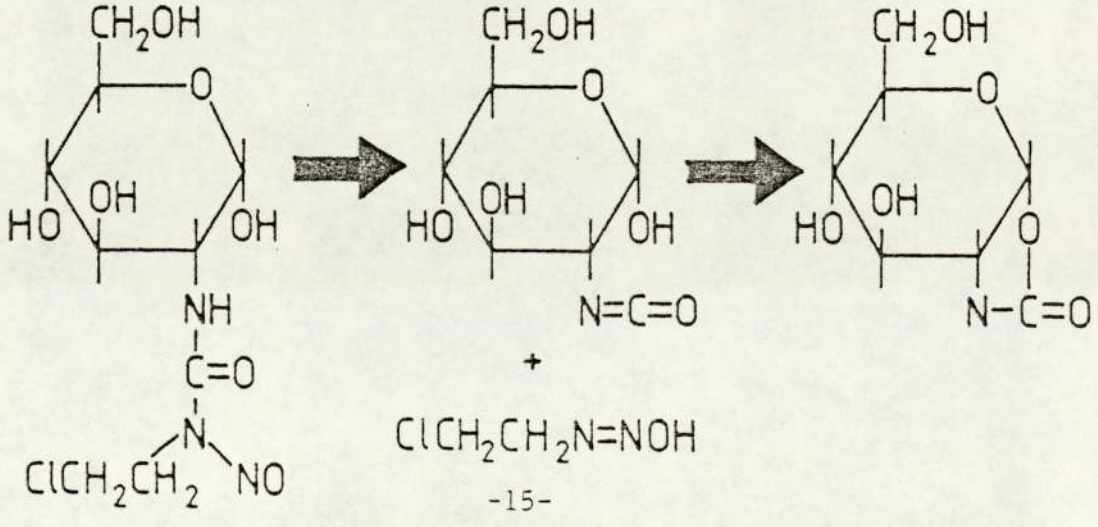

The alkylations of DNA by nitrosoureas were shown to produce single-strand breaks and cross-links (57) and studies on the nature of the cross-links showed that, unlike bifunctional alkylating agents which, it is believed, simultaneously alkylate guanine residues on opposing DNA strands, the nitrosoureas were able to cross-link via a single chloroethyl group in a two-stage alkylation process (64). An initial attachment of the chloroethyl group to one strand was followed by nucleophilic attack by a group on the opposing strand with the displacement of chloride ion and cross-link formation. This mechanism was supported by the poorer cross-linking capacity of the fluoroethylnitrosoureas. The importance of chain length to this process was demonstrated by Lown who showed the inability of chloropropyl, butyl and pentyl nitrosoureas to cross-link DNA (65).

Ewig and Kohn discovered the existence of two types of cross-link using protease-K, DNA/DNA links and DNA/protein links (66), and further showed that the nitrosourea-induced damage was not repaired within 24 hours unlike the damage induced by nitrogen mustard.

Work on isolated base adducts using ethylnitrosoureas (67) revealed the possible importance of the O6 site on guanine to cross-link formation. It was proposed that an initial alkylation here with subsequent attack from the N4 position of the paired cysteine residue would form the cross-link, a mechanism quite distinct from that proposed for bifunctional alkylators (see figure 1.9).

Erickson (68) suggested that the ability to repair cross-links may be important with respect to resistance to the nitrosoureas when he showed that a resistant human colon line, HT, was capable of cross-link repair whilst a sensitive line, BE, was not. He further showed in work with a virally transformed VA-13 line sensitive to nitrosoureas

that there was a deficiency in an ability to repair 06-methylguanine adducts (69, 70) and by extending this to 06-chloroethyl adducts postulated this as the reason for the differential susceptibility of VA-13 cells to nitrosoureas compared with normal IMR-90 cells which were capable of repair activity. Work on the precise mechanism and relative importance of the DNA interaction continues. It is recognised that this interaction is unlikely to be selective since the chloroethyldiazonium hydroxide species is believed to have a sub-second half-life in vivo such that alkylation will tend to reflect the local concentration of nucleophilic sites rather than their relative nucleophilicity (71).

Figure 1.9 - Proposed mechanism of DNA cross-link formation by chloroethylnitrosoureas.

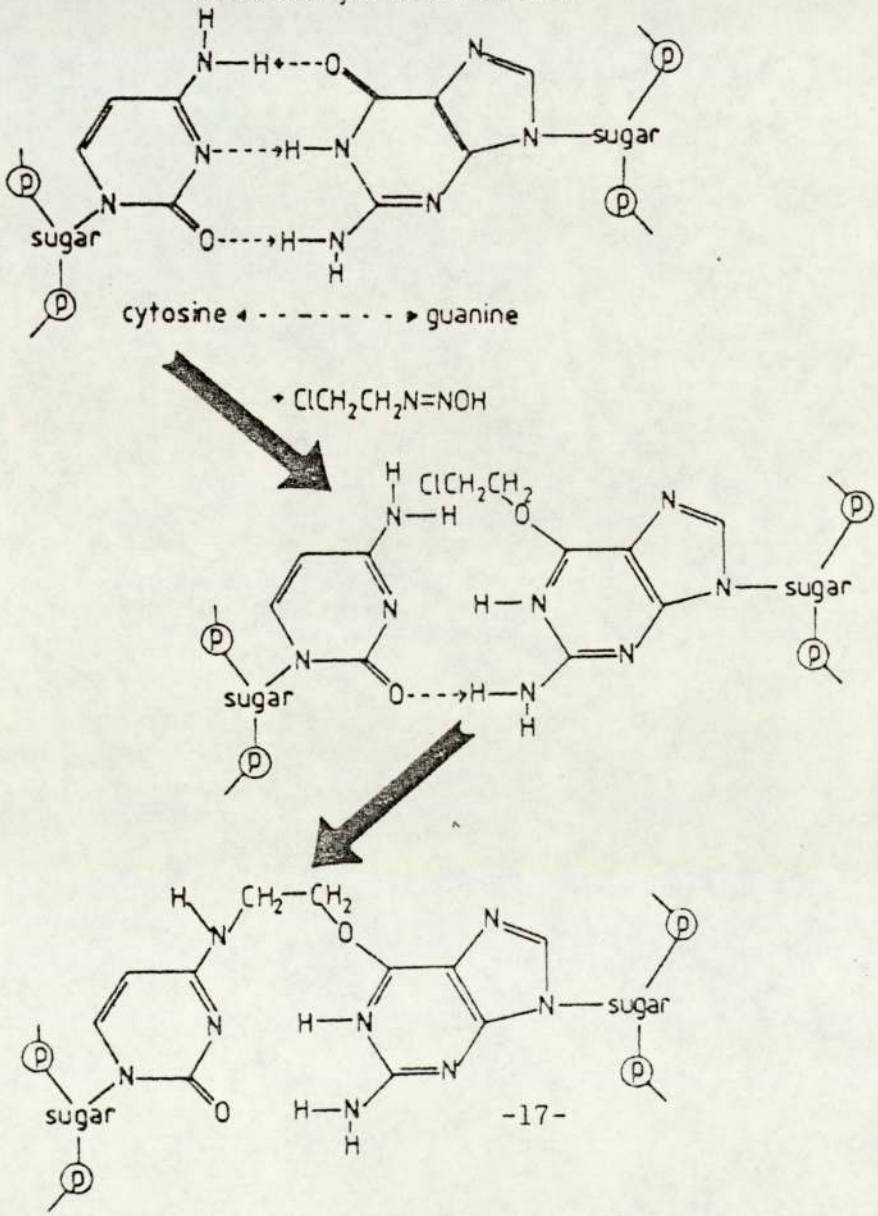

The clinical disappointment of the nitrosoureas has led to a continuing search for analogues which can carry the exceptional experimental activity through to the clinical situation.

1.4 The experimental anti-tumour activity of mitozolomide

Mitozolomide was screened for activity as an anti-tumour agent in a collaborative programme involving three screening centres, the Cancer Research Campaign experimental chemotherapy group at Aston, the Institut Jules Bordet in Brussels and Rhone-Poulenc Ltd (France) (72). This involved tests using the in vivo mouse model and various murine tumour types. These tests were carried out according to the standard protocols advocated by the NCI (73, 34). Two types of assay are employed; the survivial time assay, used in tests against systemic cancers (such as the L1210 and P388 leukaemias) where results are assessed in terms of the increased survival of the test (T) mice in comparison to the control (C) batch, and the tumour inhibition assay for solid tumours (such as the C38 adenocarcinoma) where results are assessed in terms of a measurable tumour inhibition.

Mitozolomide demonstrated a potent and broad spectrum anti-tumour activity in these tests (72, 74, 75) with a level of activity comparable to any previous drugs used against these murine models.

At doses of 20-40 $mg.kg^{-1}$ mitozolomide showed curative activity against the ip inoculated L1210 leukaemia and whilst activity was less evident against both ic and iv inoculated L1210 it was still sufficient to warrant the NCI's 'very active' categorisation (++; $T/C > 150$, see table 1.1).

Against other survival time models mitozolomide proved curative versus the P388 leukaemia, TLX5 lymphoma and colon 26 tumour in

doses ranging from 20-40 $mg.kg^{-1}$. Pronounced activity was seen against the Lewis lung, LL, model (T/C> 298 at 25 $mg.kg.^{-1}$ and 7/10 cures) whilst significant survivial time increases were seen against the B16 melanoma (T/C> 200 at 25 $mg.kg.^{-1}$) although only occasional cures were obtained.

The drug also produced excellent results in tests against the solid murine tumour models Lewis lung, LL, colon 38, M5076 reticulum cell sarcoma and ADJ/PC6A plasmacytoma although only borderline results were obtained versus the CD8F, mammary model. In addition mitozolomide was 100% effective in eliminating pulmonary metastases in the im inoculated LL model.

Table 1.1, summarises these results and compares them to those obtained for a number of clinically used anti-tumour agents using the NCI activity criteria. One immediate feature of these results is the similarity between mitozolomide and the chloroethylnitrosoureas. This aspect is accentuated by the demonstration of cross-resistance seen in tests against L1210 leukaemia lines made resistant to BCNU (72) and a KHT sarcoma made resistant to the nitrosoureas (76). Similar cross-resistance was seen in tests against an L1210 line resistant to BCTIC but L1210 and P388 lines resistant to cyclophosphamide retained their sensitivity to mitozolomide.

Whilst these results against murine tumours are very encouraging the predictive value of these screens has been questioned (35) particularly following the clinical disappointment of the chloroethylnitrosoureas.

One alternative anti-tumour screen (and one now also employed by the NCI) is the use of the xenograft model. Here, human tumour lines are grown in immunodepressed or 'nude' mice. Fødstad has recently reported results for tests against human melanomas, sarcomas

Table 1.1 - The experimental anti-tumour activity of mitozolomide compared with that of a number of clinically used agents against the NCI murine tumour panel.

		L1210	P388	B16	LL	Colon26	C38	CD8F1
T/C,NCI activity criteria	++	≥ 150	≥ 175	≥ 150	≥ 150	≥ 150	≤ 10	≤ 10
	+	≥ 125	≥ 120	≥ 125	≥ 140	≥ 130	≤ 42	≤ 42
mitozolomide		++	++	++	++	++	++	+
BCNU		++	++	++	++	++	+	++
DTIC		++	+	+	++	inactive	+	+
nitrogen mustard		++	+	++	inactive	++	+	+
cis-platinum		++	++	++	++	++	+	++
methotrexate		++	++	inactive	+	inactive	inactive	+
cyclophosphamide		++	++	++	++	++	++	++
adriamycin		++	++	++	++	++	inactive	++

and lung and colon carcinomas in xenograft systems (77). Activity was described as equal to, or better than, clinically used agents in the tumour types examined. Apparent cures were obtained against both melanoma and small cell lung carcinoma. In addition, mitozolomide completely inhibited the colony forming ability of sarcomas, melanomas, lung and colon cancers in soft agar using the clonogenic assay system (77). Workman et al showed mitozolomide to have similar activity to CCNU with both agents being ineffective against a colon and a large cell lung line but very active against a small cell lung line (76). Thus, the results obtained for mitozolomide in these alternative models also auger well for the drug.

The demonstrated activity of mitozolomide against the murine models was sufficient to initiate mode of action studies and a pre-clinical programme leading to the phase I trial of the drug.

1.5 Mode of action studies on mitozolomide

Early mode of action studies on mitozolomide focussed on the likely cellular consequences resulting from the perceived production of an alkylating chloroethyldiazonium species from the decomposition of MCTIC and a carbamoylating species (2-chloroethylisocyanate). The drug demonstrated similar in vitro cytotoxicity to that seen with both BCNU and MCTIC against TLX5 cells (with an LD_{50} of approximately 4μM) although studies on the incorporation of tritiated thymidine, uracil and adenosine following cytotoxic doses of drug (78) showed that mitozolomide and MCTIC took longer to inhibit incorporation (complete within 24 hours) than did BCNU (complete within 3 hours).

Unlike BCNU mitozolomide proved incapable of inhibiting three enzymes sensitive to carbamoylating agents, glutathione reductase,

chymotrypsin and γ-glutamyltranspeptidase (78). At doses of approximately 20μM BCNU completely inhibited glutathione reductase within 2 hours whereas no inhibition was evident in doses up to 200μM when mitozolomide was used. Similarly no effect was evident against either α-chymotrypsin or γ-glutamyltranspeptidase when mitozolomide was used in levels equivalent to a dose of BCNU which gave a 50% inhibition. These results suggest that the production of an isocyanate species from mitozolomide under these conditions is either non-existent or at such low levels as to be insignificant with respect of cytotoxicity.

Studies on the cellular uptake of mitozolomide (79) indicated that this was both rapid and linear with equilibrium levels reached within 1 minute at 37°C (10 minutes at 4°C). The uptake was demonstrated to be non-saturable over a dose-range of 0.1-20mM and unaffected by metabolic poisons indicating a passive diffusion mechanism.

Mitozolomide and MCTIC produced similar effects on the progression of 3LL cells through the cell cycle with an apparently irreversible block being induced in the late 'S' phase/G2/mitosis region of the cell cycle (80).

This further evidence for the importance of the generation of MCTIC from mitozolomide led to a series of studies concentrating on the role of interactions with biological macromolecules in the mode of action.

Gibson et al (81) used the alkaline elution method to examine the nature of any DNA damage elicited by mitozolomide and compared it to MCTIC and CENU. The three proved equitoxic to murine L1210 cells (doses of 50μM producing a >3 log cell kill) and produced quantitatively the same number of DNA cross-links, although these formed quicker with CENU (within 6 hours post-incubation) than with mitozolomide and MCTIC

(within 9 hours post-incubation). An approximately linear relationship was seen between drug concentration and cross-link formation and all 3 agents were shown to produce single strand breaks during the incubation period.

Working with normal IMR-90 and transformed VA-13 human embryo cell lines Gibson and Erickson demonstrated the same differential toxicity as had been seen with the nitrosoureas, with the 06- methylguanine repair deficient VA-13 line proving between 6 and 7 times more sensitive than the IMR-90 line to mitozolomide and MCTIC using the clonogenic assay method (82).

The experiments suggest that mitozolomide induced cross-link formation proceeds via the same 06-guanine alkylation process as previously described for the nitrosoureas (see figure 1.9) and that this lesion may be critical with respect to the cytotoxic action of the drug.

Thus, in analogy to their similar results in the murine screens mitozolomide may have the same mode of action to that implicated for the chloroethylnitrosoureas.

1.6 CCRG 81045

CCRG 81045 is the 3-methyl analogue of mitozolomide and the second of the imidazo[5,1-d]-1,2,3,5-tetrazin-4(3H)-ones to be developed for clinical evaluation. Early work on CCRG 80145 demonstrated its ability to generate the monomethyltriazene 5-(3-methyl-1-triazeno)imidazole-4-carboxamide (MTIC) in a manner analogous to the generation of MCTIC from mitozolomide [see figure 1.10 (83)].

MTIC is the proposed active metabolite arising from dacarbazine (DTIC) the clinically used triazenoimidazole first developed by Shealey et al (14, 15). Whilst DTIC is the only clinically used triazene,

compounds without the imidazole ring (such as the 1-aryl-3,3-dimethyltriazenes) have been shown to be just as active in experimental systems (84). In a series of triazenes examined using a bioassay method all dimethyl analogues demonstrated some activity and this, and other studies, identified the importance of the methyl group. The mode of action was believed to be either *via* generation of reactive diazonium compounds known to be formed in the light or acid catalysed decompositions of these agents (14, 85) or *via* metabolic activation to the monomethyltriazenes which had been shown to alkylate DNA (86). Preussman (87) showed the capability of a microsomal enzyme to dealkylate 1-aryl-3,3-dimethyltriazenes and a similar demethylation of DTIC was later demonstrated by Hill (24). This demethylation proceeds *via* the intermediate production of a hydroxymethyl species (see figure 1.9). Kolar has isolated 5-(3-hydroxymethyl-3-methyl-1-triazeno)imidazole-4-carboxamide (HMTIC) from the urine of phenobarbital pre-treated rats dosed with DTIC and speculated that this metabolite is the carrier form of the 'active' species (88).

Skibba demonstrated the N-demethylation of DTIC by rats and man (89) and the concept of metabolic activation in the mode of action of dialkyltriazenes is now generally accepted despite demonstrations of mutagenicity (90) and an apparent anti-metastatic action (91, 92) which were evident without the requirement of metabolism.

The site of the critical alkylation was believed to be the N7 position of guanine. The resultant methyl adduct was shown by Skibba (85) to be present in the urine of rats treated with DTIC. However, Ludlum showed that 7-methylguanine bases could still pair normally with cytosine bases in test systems (93) so the precise lesion and mechanism of action remains obscure.

Figure 1.10 - MTIC formation from (a) CCRG 81045 by chemical decomposition and (b) DTIC by hepatic metabolism.

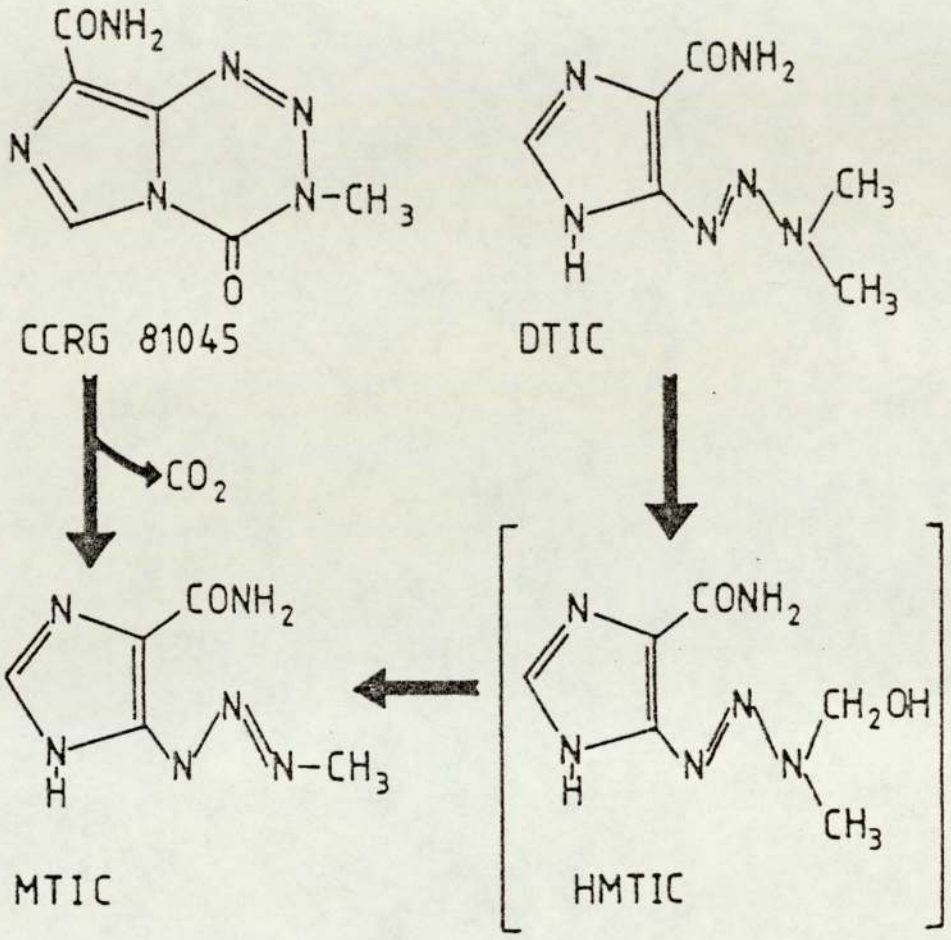

Clinically DTIC showed activity as a single agent against malignant melanoma (94, 95) but is not widely used against other malignancies. The requirement for metabolic activation may be a limiting factor in the activity of DTIC since the monomethyl intermediate has been shown to have a half-life of only 120 seconds in horse serum (96). In addition the drugs photosensitivity make it a difficult agent to use clinically and so a stable pro-drug form of the monomethyltriazene may represent a significant improvement on DTIC and the ability of CCRG 81045 to decompose chemically to MTIC has obvious possibilities in this respect.

The experimental anti-tumour activity of CCRG 81045 was shown to be superior to that of DTIC (83) with good activity against the TLX5 lymphoma and L1210 and P388 leukaemias in murine survival time assays (T/C 181-254) and excellent inhibitory action against the solid murine tumours M5076 sarcoma, PC6 plasmacytoma and B16 melanoma.

The work on CCRG 81045 presented in this thesis provides additional pharmacokinetic evidence to suggest that this agent may be a suitable clinical alternative to DTIC.

1.7 Pharmacology of the nitrosoureas and triazenoimidazoles

Early studies on pharmacological and pharmacokinetic aspects of both groups of agents were hampered by technological difficulties compounded by their instability and the problems in detecting both parent drugs and decomposition products in biological fluids.

This was particularly true for the chloroethylnitrosoureas where the use of radiolabelled drug to follow the disposition of BCNU, CCNU and meCCNU gave little information concerning the fate and kinetics of the parent compounds (97).

A variety of methods have since been employed including the use of Bratton-Marshall reagent to complex the N-nitroso group of BCNU [using this as an index of BCNU levels; (98)] and the use of pulse polarography to follow BCNU (99). However most kinetic studies have utilised direct insertion mass spectrometry and gas chromatography-mass spectrometry (GC-ms) linked methods to follow BCNU, CCNU and meCCNU pharmacokinetics (100, 101). More recently the advent of the reversed phase technique and an improvement in UV absorption detectors has resulted in HPLC (high performance liquid chromatography) methods being employed to follow CCNU (102) and BCNU (103) levels in plasma.

An additional problem in studying the pharmacokinetics and disposition of the nitrosoureas was their extensive metabolism. The belief that their short chemical half-life precluded any significant contribution from metabolic processes proved short-lived when it became apparent that rapid denitrosations and hydroxylations were occuring. Hill (104) demonstrated that an NADPH requiring enzyme present in mouse liver and lungs was capable of denitrosating BCNU to its urea [1,3-bis(2-chloroethyl)urea; BCU] at a significant rate and Huey Shin Lin and Weinkam (105) used stable isotopes to confirm that the BCU produced was being metabolically generated. Potter and Reed later showed a similar reaction for CCNU and meCCNU (106).

The cyclohexyl rings of CCNU and meCCNU were shown to be extensively hydroxylated (107-110) with hydroxylated metabolites evident in the plasma of phenobarbital induced rats 2 minutes after an iv dose of CCNU and although the rate of hydroxylation was shown to be greater in the case of CCNU than meCCNU it was evident that hydroxylation could make a significant contribution to the fate of both these agents.

Disposition and excretion balance studies on the nitrosoureas have used radiolabelled drugs. In an early study using BCNU uniformly labelled with ^{14}C in the chloroethyl carbons, De Vita et al showed that most of the activity administered to mice, dogs, monkeys and man was recovered in urine with very little or none appearing in the faeces (111). Urinary excretion in mice was rapid (62% of the dose eliminated within 4 hours) and reached a maximum within 24 hours (72% of dose). Additionally, between 7 and 10% of the dose activity was recovered as trapped $^{14}CO_2$ in the first 24 hours. Similar results were seen in the

other species examined. No differences in urinary activity were seen in man following iv and po doses (63-67% recovery at 96 hours) although slightly more activity was found in the form of $^{14}CO_2$ when dosing orally (10% vs 6%). Oliveiro showed that the disposition of label in rodents was remarkably similar following doses of BCNU, CCNU and meCCNU and that no significant tissue localization of activity was evident at 24 hours (112, 113). Comparing CCNU and BCNU Levin demonstrated that the more lipophilic CCNU attained higher levels than did BCNU in the adipose tissue of rats and suggested that higher levels of residual label following BCNU in muscle, liver, kidney and lung were indicative of its greater chemical instability (114).

Weinkam pioneered a direct insertion mass spectrometry method for the assay of BCNU and this was applied to a pharmacokinetic study in rats (115). Animals were dosed at 14 $mg.kg^{-1}$ by both iv and ip routes and the data fitted to a 2-compartment pharmacokinetic model, with peak plasma concentrations in excess of 10$\mu g.ml^{-1}$ falling rapidly in the first 30 minutes to approximately 3$\mu g.ml^{-1}$ followed by a slower elimination phase ($t_{\frac{1}{2}}$ equal to 18 minutes). Levin demonstrated a similar fit to a 2-compartment model in humans, however the distribution rate constant was greater ($t_{\frac{1}{2}}$ equal to 6 minutes versus the 12 minutes seen in the rat) as was the apparent volume of distribution at the steady state [3.25 Lkg^{-1} versus 1.9 Lkg^{-1} (115)]. In a study comparing the area under the plasma concentration/time curve (AUC) following equitoxic doses of BCNU and the hydrophilic PCNU Levin produced the interesting finding that whilst the value was higher in rats for PCNU (3.48 $mM.min^{-1}$ versus 1.76 $mM.min^{-1}$) the position was reversed in humans (0.69 $mM.min^{-1}$ versus 2.13 $mM.min^{-1}$) and by

assuming a relationship between AUC and anti-tumour efficacy presented a pharmacokinetic explanation for clinically disappointing results with PCNU (117).

Other studies have confirmed a characteristic biphasic pharmacokinetic profile for the nitrosoureas with Russo (99) reporting clinical results using a pulse polarographic determination of BCNU and Lee and Workman (102) demonstrating biphasic kinetics for CCNU using an HPLC assay. The importance of hydroxylation of the cyclohexyl ring is emphasised in this study on mice where it is argued that the α-rate constant normally associated with distribution may be influenced by metabolism and that the elimination rate may be limited by the re-distribution of parent drug from lipophilic depots. Little parent CCNU is detectable, with a maximum plasma concentration (Cp.max) of only 7.5 $ug.ml^{-1}$ and an AUC of only 43 $ug.ml.^{-1}min$, following a dose of 20 $mg.kg^{-1}$ although total nitrosourea levels are more significant (AUC approximately 473 $\mu g.ml.^{-1}min$) emphasizing the contribution of metabolism to the fate of CCNU. The situation is even more marked in humans where various studies have failed to detect any parent CCNU (111,118).

In summary, pharmacokinetic studies on the nitrosoureas indicate that the parent drug is rapidly cleared from the body ($t_{\frac{1}{2}}$ of elimination in the range of 18-53 minutes) with a biphasic plasma pharmacokinetic profile for the parent nitrosourea which may reflect the complex interactions these agents undergo with lipophilic partitioning, metabolism, and a rapid rate of hydrolysis (subject to further albumin mediated catalysis) all contributing to their fate in vivo.

In a manner analogous to the nitrosoureas, sensitive analytical methodology has limited studies on the pharmacology of the triazenoimidazoles. Early work utilised the colorimetric method

method developed by Loo and Stasswender (119). In a study on dogs Loo demonstrated a biphasic profile for DTIC with an elimination half-life of 30-45 minutes (120) and showed urinary excretion of parent drug to be complete within 6 hours, yielding 17% of dose. Administering DTIC by rapid iv injection to man resulted in a similar elimination half-life being obtained (38 minutes) but more parent drug (43%) was excreted in the urine. Householder noted an elevation in urinary levels of AIC following doses of DTIC (121) whilst a disposition study using DTIC labelled with ^{14}C in both the imidazole ring and the methyl positions showed that most label was accumulated in the liver, kidneys and small intestine 15 minutes after an iv dose. In support of the proposed metabolism of DTIC slightly higher levels of the methyl derived activity were present in the liver and 9.3% of the methyl-labelled dose was expired as $^{14}CO_2$ compared with none from the imidazole labelled dose. A 20-fold concentration of activity in bile, relative to plasma, suggested some biliary excretion whilst autoradiography identified the principal urinary components as AIC and DTIC.

Breithaupt utilised a reversed phase HPLC method in an extensive pharmacokinetic study of DTIC and AIC following the clinical administration of DTIC by various iv schedules (122). The data for a single iv dose was fitted to a two-compartment model with a $t_{\frac{1}{2}\alpha}$ of 2.4-3.6 minutes and a $t_{\frac{1}{2}\beta}$ of 30-52 minutes. Maximum plasma concentrations of 12 $\mu g.ml^{-1}$ were obtained following a dose of 500 mgs DTIC. No variation in the AUC was seen when the same total dose was given by various schedules indicating that the hepatic metabolism of the drug was not saturable at clinically tolerable doses.

A BCTIC disposition study in mice and dogs (123) indicated no

tissue localisation of radioactivity from a [^{14}C]-imidazole-label and showed that absorption from the gastro-intestinal tract was both poor and variable. The plasma half-life of total label was shown to be only 2 hours with the bulk of the activity excreted renally. More sophisticated studies on BCTIC have not been carried out, no doubt due to the extreme difficulty of working with this unstable agent.

1.8 Aims and scope of the current study

Mitozolomide is the lead compound in a novel series of imidazo[5,1-d]-1,2,3,5-tetrazin-4(3H)-ones. The screening of mitozolomide as an anti-tumour agent produced results which were comparable to those obtained by any drugs previously tested in murine tumour models. Early chemical and biochemical studies suggested that the behaviour of mitozolomide under physiological conditions bore many resemblances to that of the chloroethylnitrosoureas and the triazenoimidazoles, two groups of agents where experimental promise culminated in relatively disappointing clinical results.

For mitozolomide to succeed clinically it was evident that some aspect of its behaviour under physiological conditions would have to show a demonstrable improvement on the aforementioned agents. In order to identify such an improvement and to optimise the therapeutic potential of mitozolomide it was essential that detailed studies were carried out on its behaviour and fate under physiological conditions and in the in vivo situation.

It was the aim of the current study to attempt to identify those aspects in the metabolosm, decomposition and pharmacokinetics of the imidazo[5,1-d]-1,2,3,5-tetrazin-4(3H)-ones which would suggest clear advantages over clinically used anti-tumour agents and which would enable the maximum exploitation of their therapeutic potential.

In order to facilitate studies in these areas it was necessary to develop the required analytical methodology. An HPLC method was developed which enabled the quantification of mitozolomide and this was applied to *in vivo* and *in vitro* kinetic studies. Other HPLC methods were developed to assist in the identification and quantification of the end-products arising from mitozolomide following *in vitro* decomposition experiments and its *in vivo* administration.

Early work had suggested that the major degradative pathway was *via* the triazene MCTIC and kinetic studies and end-product assays were conducted to characterize this pathway under conditions of physiological temperature and pH and to establish a kinetic profile for the disappearance of mitozolomide under various conditions. Part of this work revealed an enhanced rate of drug breakdown in plasma (*in vitro*) when compared to degradation in physiological buffers. This effect was previously seen in studies on the decomposition of the chloroethylnitrosoureas and was investigated accordingly.

In order to enable an interpretation of the anti-tumour results in terms of plasma levels of mitozolomide pharmacokinetic studies were conducted in mice over the appropriate dose range (0.25-20 $mg.kg^{-1}$). The subsequent pharmacokinetic studies in humans carried out as part of the phase I clinical trial provided a valuable comparison of the pharmacokinetic behaviour of the drug in the two species from which predictions concerning the likely clinical efficacy of mitozolomide could be made.

The pharmacokinetics of mitozolomide were modelled using a simple one-compartment model with an apparent correlation between the *in vitro* half-life of the drug and its rate of elimination *in vivo* being evident. To examine the validity of this correlation in terms of the actual fate of the drug an excretion balance study was conducted in mice and the

resultant urines collected and assayed. The results of this and other in vitro studies were brought together and a more complicated picture of the disposition and fate of the drug presented.

Most of the current work has focussed on mitozolomide but some studies have been conducted on CCRG 81045, the second compound in the series to become a candidate for clinical evaluation. Structure-activity relationships on a series of imidazo[5,1-d]-1,2,3,5-tetrazin-4(3H)-ones had identified the apparent importance of the haloethyl group to anti-tumour activity. The activity seen in various 8-substituted imidazo[5,1-d]-1,2,3,5-tetrazin-4(3H)-ones was typically similar to that exhibited by mitozolomide with single doses at approximately 20 $mg.kg^{-1}$ proving optimally effective. CCRG 81045, the 3-methyl analogue of mitozolomide also proved to possess effective anti-tumour activity but in a schedule-dependent manner with much higher doses being required to elicit activity. This raised the possibility of an entirely different mode of action to that displayed by mitozolomide. In addition, the potential generation of MTIC in the decomposition of CCRG 81045 suggested that it may have advantages over the clinically used triazenoimidazole DTIC.

Preliminary in vitro and in vivo studies were carried out on CCRG 81045 in order to establish whether the observed differences in the anti-tumour activity compared with that of other imidazo[5,1-d]-1,2,3,5-tetrazin-4(3H)-ones had a pharmacological explanation and to investigate further the generation of MTIC under physiological conditions.

The possible implications for the future of the imidazo[5,1-d]-1,2,3,5-tetrazin-4(3H)-ones as anti-tumour agents based on the results of these studies on mitozolomide and CCRG 81045 and their potential advantages over the clinically established chloroethylnitrosoureas and triazenoimidazoles are discussed.

2 MATERIALS AND METHODS

2.1 General

2.1.1 Chemicals and solvents

Mitozolomide, CCRG 81045 and CCRG 82019 (the ethyl analogue of mitozolomide used as an internal standard in the HPLC assay of CCRG 81045) were generously supplied by Dr E Lunt of May and Baker Ltd., Dagenham, UK.

Samples of N-(2-chloroethyl)-AIC, N-(2-hydroxyethyl)-AIC and N-(2-aziridino)-AIC obtained from mitozolomide decomposition experiments in aqueous Sodium bicarbonate were kindly supplied by Dr C G Newton of May and Baker Ltd., Dagenham, UK.

3-(2-Hydroxyethyl)-1,2,3-benzotriazin-4(3H)-one, the internal standard used in the HPLC assay of mitozolomide, was synthesized by Ms G U Baig within the Department of Pharmaceutical Sciences at Aston University.

5-Aminoimidazole-4-carboxamide (AIC) was obtained as the hydrochloride salt from May and Baker Ltd., Dagenham, UK.

Heptane sulphonic acid, octane sulphonic acid and sodium dodecyl sulphate were obtained from Fisons Ltd., Loughborough, UK.

Thiofluorescein was obtained from Sigma UK Ltd.

MCTIC was synthesized as described in section 2.1.1.1.

All other chemicals used in this work were obtained commercially as ANALAR grade and used as supplied.

All solvents used in the course of this work were commercially obtained and of HPLC grade. HPLC mobile phases were degassed by vacuum filtering through a scinta glass filter prior to use. Glass distilled water was used throughout.

2.1.1.1 Synthesis of 5-[3-(2-chloroethyl)-1-triazenyl]imidazole-4-carboxamide (MCTIC)

MCTIC was synthesized by the method of Shealy (13) for use in attempted derivatisation experiments as part of the method development work described in section 3.1.4. 3.87 g of 2-chloroethylamine hydrochloride was dissolved in a minimum of water and excess sodium carbonate added. The free base was extracted into 30 mls of ethyl acetate and decanted into a foil-wrapped flask. 1.37 g of diazo-1C was added and the mix left stirring overnight, in the dark, at room temperature. The product was filtered and washed with approximately 20 mls dry ethyl acetate. The structure of the product was confirmed by comparison of its infra-red spectrum with that of an authentic sample. The product was stored at 3°C in the dark prior to use.

Yield: MCTIC - $C_6H_9ClN_6O$

product 2.035 g = 94.0%

2.1.2 Radiochemicals

Radiolabelled [^{14}C]-mitozolomide was supplied by May and Baker Ltd., Dagenham, UK. Two batches were supplied:

Batch number: DWA 3536 B

[^{14}C-chloroethyl-labelled mitozolomide; specific activity - 62.9μCi.mg^{-1}

Batch number: DWA 3409 E

[^{14}C]-imidazole-labelled mitozolomide; specific activity - 43.9 μCi.mg^{-1}

The position of the labels is shown in figure 3.24.

2.1.3 Buffer recipes

Sørensons mixed phosphates (124):

Stock solution A : 0.2 M sodium dihydrogen phosphate, 27.8 $gL.^{-1}$

Stock solution B : 0.2 M disodium hydrogenphosphate dihydrate, 55.6 $g.L.^{-1}$

For pH : 7.0 - 39 mls A + 61 mls B diluted to 200 mls with H_2O

7.2 - 28 mls A + 72 mls B " " " " " "

7.4 - 19 mls A + 81 mls B " " " " " "

7.6 - 13 mls A + 87 mls B " " " " " "

7.8 - 8.5 mls A + 91.5 mls B " " " " " "

For lower buffer concentrations samples were diluted accordingly.

Tris buffer (125) :

Stock solution A : 0.2 M tris(hydroxymethylaminomethane), 24.2 $g.L.^{-1}$

Stock solution B : 0.2 N hydrochloric acid

For pH : 9.0 - 50 mls A + 5 mls B diluted to 200 mls with H_2O

7.4 - 50 mls A + 41.4 mls B " " " " " "

Walpoles acetate buffer (126) :

Stock solution A : 0.2 M acetic acid; 11.55 $ml.L.^{-1}$

Stock solution B : 0.2 M sodium acetate, 16.4 $g.L.^{-1}$

For pH : 4.0 - 41 mls A + 9 mls B diluted to 100 mls with H_2O.

2.1.4 Animals

All animals used in the course of this work were obtained from Bamtin Kingman, Aldbrough, Horton, Yorkshire. Animals were kept in an animal house for at least a week prior to use to enable acclimatisation. Animals were maintained on Heygates modified rat and mouse breeding diet pellets throughout.

2.1.5 Weighings and measurements

All weighings below 250 mgs were performed on a Sartorius 1207 MP2 4-figure balance using pre-weighed bottles. Weighings over 250 mgs were performed on a tared Sartorius 1219 MP balance.

Unless otherwise stated all pipetted volumes were carried out using the appropriate Gilson pipetteman pipette (250µl, 1 ml or 5 ml). Volumes of 30 µl and less were pipetted using a Gilson microman positive displacement pipette. All pipettes were calibrated regularly by dispensing volumes of water at room temperature and weighing on the MP2 balance.

All pH measurements were obtained using a Beckman pH meter with standard glass electrodes.

2.2 Analytical

2.2.1 High performance liquid chromatography (HPLC)

HPLC has been the principal analytical method utilised in the course of this work. The development of the HPLC methods employed and details of the specific HPLC conditions for each analysis are detailed in section 3.1.

HPLC analysis was accomplished using a Waters Associates trimodular system comprising a M720 system controller, M710B WISP (automated injector) and M730 data module. Two model 6000A solvent delivery systems were employed and a Lamda-max 480 variable wavelength UV detector was used. Throughout these studies Waters C-18 reversed phase radial compression columns (127) have been employed with C-18 guard-pak inserts. RCM-100 radial compression modules were used for the columns.

Some method development work was performed on a composite system consisting of 2 Altex 100A pumps, an Altex system programmer

and a Rheodyne loop injector (sample loop size : 20 µl) together with a Lamda-max 480 variable wavelength detector and RCM-100 radial compression module as previously. Additionally an on-line ESI-Panax 506-C HPLC radioactivity monitor was employed for some work.

In the sample preparation procedure (see 3.1.1.1) concentration of samples was carried out using a Techne Dri-block DB-3, nitrogen flow concentrator or a Savant Speed-Vac concentrator. Centrifugation of samples was performed using a Heraeus Labofuge 2000 centrifuge.

2.2.2 Thin Layer chromatography (TLC)

Two TLC methods were found to be suitable for the analysis of mitozolomide and its breakdown and urinary end-products. These methods were originally developed for the assay of urinary imidazoles (128). 20 x 20 cm plastic backed cellulose F254 TLC plates were used (0.1 mm layer thickness; Merck Limited, UK). The samples were applied as 1 cm bands positioned 2 cm above the base of the plate and at least 2 cm in from the sides. A minimum gap of 1 cm separated adjacent bands. Samples were applied using a Hamilton microsyringe and the solvent was evaporated by applying warm air between successive applications to each band. For autoradiograms samples were applied such that the equivalent of either 10 000 dpm or 2 500 dpm of radioactivity was applied to each band. Standards of AIC and N-(2-hydroxyethyl)-AIC were prepared in water and mitozolomide standards (including a radiolabelled standard) prepared in chloroform. AIC, N-(2-hydroxyethyl)-AIC and non-radiolabelled mitozolomide were applied such that 50-100µg of standard was present in the appropriate band.

Chromatography was performed in standard TLC tanks with plates being run over a 15 cm distance. The two solvent systems used were:

(A) 7 : acetone

1 : acetic acid

2 : water

(B) 1 : water

1 : Pyridine

1 : Butan-1-ol.

Both gave suitable separations, but system A was faster and was therefore employed for general use with system B employed in a confirmatory role. Following chromatography the plates were dried and the position of the standards identified under UV light. Autoradiograms were obtained by placing the plates against X-ray film (Singul-XR-P). The films were left for 1 week where 10 000 dpm. band^{-1} had been applied and 4 weeks where 2 500 dpm. band^{-1} had been applied subsequent to developing using Kodak D76 developer and Kodafix fixer. The Rf values (distance travelled by sample/distance travelled by solvent front; measured to the centre of the band in all cases) for the standards in the two solvent systems are shown in table 2.1.

Table 2.1 - Rf values for the standards run in the two TLC systems employed.

standard	solvent system	
	A	B
mitozolomide	0.89	0.79
N-(2-hydroxyethyl)-AIC	0.63	0.69
AIC	0.55	0.59

2.2.3 - Liquid scintillation counting

Liquid scintillation counting was employed in part of the verification procedures for the quantitative HPLC analysis of mitozolomide (see section 3.1.1.3.1) and in the quantification of radioactivity levels in decomposition experiments (see section 3.3.2) and in the excretion balance study in mice (see sections 3.7 and 3.8).

In the first case samples were prepared for counting by the addition of 10 mls of Fisofluor 'mpc' multi-purpose scintillation counting fluid (Fisons, Loughborough, UK) to 1 ml of sample and counted in a Beckman LS230 liquid scintillation counter with dpm values being evaluated using an external channels ratio method (129).

All other liquid scintillation counting was performed in a Packard Tri-carb 2660 liquid scintillation counter with dpm values determined against standard quench curves (129). Fractions collected from the HPLC assay of decomposition products and mouse urine samples were counted directly following the addition of 10 mls of 'Optiphase mp' scintillation fluid (Fisons, Loughborough, UK) per ml of column eluent.

Trapped carbon dioxide and urine samples from the excretion balance study (section 3.7) were prepared for counting by diluting 50-200µl sub-samples to 1 ml with water and adding 10 mls of Optiphase mp scintillation fluid. Urine sub-samples were weighed to facilitate the accurate quantification of radioactivity levels.

A tissue solubilisation method was employed in the preparation of faeces and carcass samples from the excretion balance study for liquid scintillation counting. Each mouse carcass and faeces sample was weighed and two times the weight of water added. The diluted samples were homogenised (using a Sorval tissue homogeniser) and 50 µl sub-samples weighed into glass scintillation counting vials. 1 ml of Soluene tissue

solubiliser (Packard Ltd., Caversham, UK) was added to each sample and the vials baked in an oven at 50°C for 2 hours. 200µl of propan-2-ol and 200 µl of hydrogen peroxide were added to each vial after cooling and the vials baked for a further 2 hours at 50°C once the effervescence had subsided. The vials were cooled and 10 mls of Beckman EP Reddissolve scintillation fluid added to each. Samples were counted after a minimum 8 hours delay to allow for the subsidence of chemiluminescence.

2.3 In vitro Decomposion and protein binding experiments

2.3.1 In vitro decomposition experiments

Decomposition experiments were performed in biological buffers and media, plasma, serum, urine and a plasma ultrafiltrate for both mitozolomide and CCRG 81045, all of which employed the same basic methodology. Phosphate (pH 7.4), acetate (pH 4.0) and Tris (pH 9.0) buffers were prepared according to the recipes outlined in section 2.1.3. Samples of human plasma and serum were obtained from fresh blood samples, the serum from clotted whole blood and the plasma from heparinised blood samples after centrifugation at 2000 rpm for 10 minutes. Fresh urine samples were used in each case. RPMI/1630 tissue culture media supplemented with 10% foetal calf serum (FCS) was obtained from Gibco Ltd., Glasgow, UK. The human proteins (albumin and α-1-acid glycoprotein) were obtained from Sigma UK Ltd., as was the bovine serum albumin and reduced and oxidised forms of glutathione (GSH and GSSG).

Protein and glutathione solutions were prepared in 0.2 M Sørensons phosphate buffer for decomposition experiments investigating their effect on the breakdown kinetics of mitozolomide. Plasma ultrafiltrates were prepared by ultrafiltration using Amicon CF50A centriflow membrane cones. These exclude >97% plasma protein. 3 mls of plasma

were pipetted into each cone and the cones centrifuged at 1500 rpm (< 1000 g) in an MSE centrifuge with 35° fixed angle head for 1½ hours. The pH of the resultant ultrafiltrate was adjusted to 7.4 by the addition of dilute hydrochloric acid prior to decomposition experiments.

The general method applied for decomposition experiments in all these media was thus:

2-5 mls of the appropriate decomposition medium were pipetted into each of 3 glass tubes and the tubes equilibrated in a water bath at 37°C. The pH of the medium was measured immediately prior to the start of the experiment and at the end of it. No pH change of > 0.05 pH units was seen during the time course of any of the experiments. 20.0 mgs of mitozolomide were dissolved in 10 mls of dimethylsulphoxide (DMSO) and 10 µl of this stock solution was pipetted (using a Gilson microman pipette) into the tubes at the start of the experiment. Tubes were immediately vortexed and sampled by removing 125 µl with the 250 µl Gilson pipetteman pipette and quenching in 125 µl of 1.0N hydrochloric acid in sample collection tubes. These were vortexed and samples stored in a refrigerator prior to analysis. The tubes were further sampled at 0.25, 0.5, 0.75, 1.0, 1.5, 2.0, 3.0 and 4.0 hours in each decomposition experiment. Levels of mitozolomide in each sample were determined using the method developed in section 3.1.1 within 3 days of the experiment.

Some variations to the basic method were employed in certain experiments. In some of the phosphate buffer experiments higher starting concentrations of mitozolomide (100-250 $\mu g.ml^{-1}$) were used and the buffer concentrations varied between 0.2M and 0.07M. These manipulations had no effect upon the results (see section 3.2.1). Additional 8, 12 and 24 hour time points were taken during decompositons in RPMI/10% FCS and human urine at pH 6.0 and a further 72 hour time point taken in the

acetate buffer experiment. The rapidity of the decomposition of mitozolomide in tris buffer at pH 9.0 necessitated that this experiment was performed at room temperature (22°C).

The method employed to study the in vitro decomposition kinetics of CCRG 81045 was identical in every way to that used for mitozolomide with CCRG 81045 stock solutions prepared in DMSO and 10 µl added to the experiment tubes at T_0. Samples were analysed using the mitozolomide method modified for CCRG 81045 as described in section 3.1.1.5.

2.3.2 Protein binding of mitozolomide

The in vitro protein binding of mitozolomide to total plasma protein and to individual plasma proteins was determined using the ultrafiltration technique. This technique had been demonstrated to be a rapid and sensitive means of following the protein binding of drugs (130). Comparative studies suggested that ultrafiltration was a preferential method to equilibrium dialysis and gel filtration (131) whilst Whitlam showed that binding equilibria were unaffected by the ultrafiltration process (132).

Amicon centrifree micropartition systems (133) were used for all protein binding determinations. These contain a YMT filtration membrane which excludes >99.9% serum proteins. The binding of mitozolomide to albumin, α-1-acid glycoprotein and γ-globulins (all obtained from Sigma UK Ltd) was determined together with binding to total plasma protein. The same basic methodology was employed in all cases.

Protein solutions were prepared in 0.2M phosphate buffer and the pH adjusted to 7.4 using dilute hydrochloric acid. Blood was taken on the day of the experiment into heparinised tubes and centrifuged at 2000 rpm for 10 minutes. Supernatant plasma was removed for use in binding determinations.

A mitozolomide stock solution was prepared in DMSO and 30 µl pipetted to 6 mls of each test solution using a Gilson microman pipette giving a starting concentration of approximately 10 $\mu g.ml^{-1}$ of mitozolomide. The tubes were vortexed and allowed to stand for 30 minutes at room temperature. 3 x 750 µl of each test solution was pipetted into the sample reservoirs of centrifree systems (see figure 2.1) and 3 x 750 µl pipetted into the filtrate cups of centrifree systems to act as controls. All the centrifree systems were centrifuged at 3200 rpm (approximately 1500 g) in an MSE hi-spin 21 centrifuge with a 35° fixed angle rotor head at a temperature of 3°C for 1 hour. 125 µl was removed from each well and quenched in 125 µl 1.0N hydrochloric acid. Levels of mitozolomide in ultrafiltrate and the total plasma controls were determined by the standard HPLC assay (section 3.1.1).

Figure 2.1 - Diagram of a centrifree micropartition system.

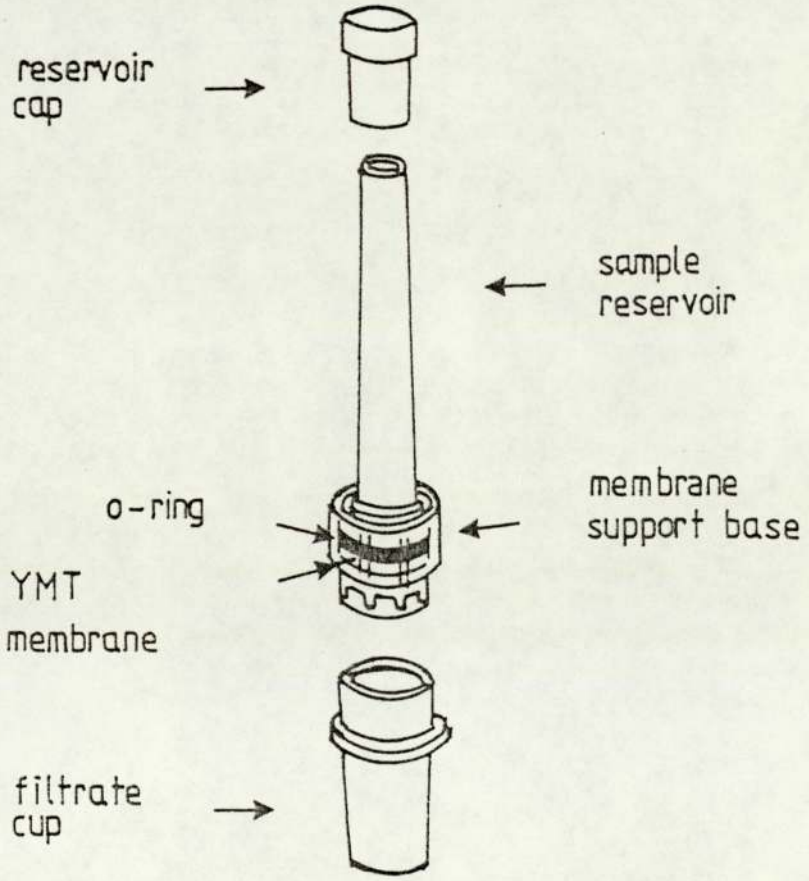

Protein binding was assessed in terms of a percentage bound figure evaluated according to the equation :

$$\% \text{ bound} = (1 - UF/T) \times 100$$

where UF = the concentration of mitozolomide in ultrafiltrate

T = the concentration of mitozolomide in total plasma.

Protein concentrations were determined by the method of Lowry (134) to enable the expression of binding in terms of the amount of protein. Plasma and protein solution samples were diluted and mixed with Lowry's alkaline copper solution (equivolumes of 1% Cu $SO_4.5H_20$ and 2% K.Na tartarate diluted to give a 2% solution in 2% Na_2C0_3 in 0.1M NaOH(aq)). 50% Folins reagent (in water) was added after 15 minutes and the samples vortexed and allowed to stand for 45 minutes at room temperature. The UV absorbance of these samples was monitored at 750 nm using a Beckman DU-7 spectrophotometer and levels of protein evaluated against a calibration curve generated using 6 human serum albumin (HSA) standards with concentrations spread evenly over the range of interest.

2.4 Murine pharmacokinetics

Murine pharmacokinetic studies were conducted using non-tumour bearing male BALB/c mice. Oral bioavailability studies were carried out for both mitozolomide and CCRG 81045 at a dose of 20 $mg.kg^{-1}$. The bioavailability of mitozolomide following topical administration was also determined at this dose. A dose escalation study using the ip route of adminstration was carried out for mitozolomide at doses of 0.25, 1.0, 5.0, 10.0, 20.0 and 40.0 $mg.kg^{-1}$.

In experiments using the ip and oral routes of administration dose volumes were based on a 200 µl dose for a 25 g mouse. Mice were weighed on the evening prior to each study and dose volumes evaluated accordingly for each mouse. Mitozolomide and CCRG 81045 were dissolved in DMSO prior to dilution in 0.9% isotonic saline to give a final formulation of drug in 1:9 DMSO/saline. Stock solutions of drug in DMSO were prepared at the start of each experimental day with volumes diluted into saline every 15-20 minutes as required. This step was taken to avoid the potential problem of drug precipitation from the saline formulation at the higher doses evaluated.

Mice were housed in standard size cages (5 mice per cage) with adequate supplies of food and water during the experiment. Blood collection tubes (microfuge tubes) containing 0.1 mls of a 3% solution of trisodium citrate (as an anti-coagulant) were cooled on ice prior to use.

The mice were dosed by ip injection using a hypodermic syringe. Oral dosing was accomplished by sliding an oral dispensing tube down into the stomach of each mouse and ejecting the dose using a syringe.

At sample times mice were anaesthetized using a Boyles apparatus with halothane and nitrous oxide as the anaesthetics (135) and 0.9 mls of blood removed by cardiac puncture from the right ventricle. The time point was recorded when the blood was in the syringe. Blood samples were transferred to the collection tubes and mixed with the anti-coagulant prior to centrifuging in a Beckman microfuge B for 2 minutes. The supernatant plasma was immediately removed to corresponding tubes and stored frozen at -20°C prior to analysis. 278 µl of the stored samples (corresponding to 250 µl plasma) were analysed by the standard HPLC method described in section 3.1.1 (mice were killed by dislocation

of the neck whilst still under anaesthesia). Mice were sampled at 0.25, 0.50, 0.75, 1.0, 1.5, 2.0, 3.0, 4.0, 6.0 and 8.0 hours following the administration of mitozolomide in the dose escalation study with additional 5 and 10 minute time points being taken following ip and oral doses of both mitozolomide and CCRG 81045 at 20 $mg.kg^{-1}$. At least 4 mice were evaluated at each time point.

For the topical administration of mitozolomide mice were anaesthetized (using a Boyles apparatus) on the day prior to the experiment and a small area ($\sim 1\ cm^2$) on the backs of the animals shaved. Mice were allowed to recover and housed in standard size cages (5 mice per cage) overnight.

Mitozolomide was formulated in DMSO such that a 10 µl volume corresponded to a dose of 20 $mg.kg^{-1}$ to a 25 g mouse. Mice were weighed on the evening prior to the study and individual dose volumes evaluated accordingly. Dosing was accomplished by anaesthetizing the mice using a Boyles apparatus and layering the appropriate dose volume onto the shaven area using a Gilson microman pipette. The mouse was transferred to a small cage and allowed to recover in isolation. Sampling was carried out as previously with mice sampled at 0.25, 0.5, 0.75, 1.0, 1.5, 2.0, 3.0, 4.0, 6.0 and 8.0 hours following administration.

2.5 Clinical Pharmacokinetics of mitozolomide

A clinical pharmacokinetic study formed part of the phase I clinical trial of mitozolomide. The phase I was a collaborative exercise conducted between two centres, one based in Birmingham under Dr G Blackledge and the other at Charing Cross Hospital in London under Dr E S Newlands. Pharmacokinetic studies on the patients treated in the Birmingham arm of the trial were conducted as part of the current

work. Results from the Charing Cross arm are included in section 3.6 to enable conclusions concerning the overall results of the clinical pharmacokinetics to be made.

The principal aim of the phase I trial was to determine the maximum tolerated dose (MTD) of mitozolomide and to establish the specific toxicities manifested in humans at toxic doses of the drug. To achieve this an iv dose escalation study was carried out. The eligibility of patients for entry into the trial was based on standard guidelines (136). All patients had microscopically confirmed, progressive cancer against which all recognised therapy had failed. Minimal haematological requirements for a white blood count (WBC) of $> 4000\ mm^{-3}$ and for a thrombocyte count of $> 100\ 000\ mm^{-3}$ were imposed together with a requirement for normal hepatic and renal function as determined by standard tests (137).

Mitozolomide was formulated for the iv dose escalation study in glass ampoules as 5 and 10% solutions in DMSO. The drug was administered as a 500 ml iv infusion in 0.9% isotonic saline. The appropriate volume of mitozolomide in DMSO was injected into a 500 ml polyfuser bag immediately prior to administration. Stability tests using HPLC analysis showed no detectable fall in mitozolomide levels in a polyfuser over a 2 hour period at room temperature. The infusion was administered over approximately 1 hour. Pharmacokinetics were monitored in all patients entered into the trial who were evaluable for response in terms of the protocol restrictions.

The recommended starting dose for a phase I trial is 1/10th of the LD_{10} in mice (135). The LD_{10} of mitozolomide was determined in CBA mice to be 40 $mg.kg^{-1}$ with the LD_{50} at 55 $mg.kg^{-1}$ (138). Because mitozolomide possessed a novel structure and studies had indicated

the cytotoxic nature of the drug the trial was started at a dose equivalent to 1/20th of the LD_{10} value. For a 70 kg man this approximates to a dose of 8.0 $mg.m^{-2}$. Doses were escalated as a modified Fibonacci search. A minimum of 3 patients and 4 courses were evaluated at non-toxic dose levels with at least 6 courses evaluated at doses where toxicity was evident. A minimum of 6 weeks was allowed between subsequent courses of treatment to individual patients at doses above 82 $mg.m^{-2}$.

Patients were infused mitozolomide over approximately 1 hour. Blood samples for the pharmacokinetic analysis were taken at the end of the infusion and at 1.5, 2.0, 2.5, 3.0, 4.0, 6.0, 8.0, 12.0 and 24.0 hours after the start of the infusion. Blood was sampled using an in-dwelling venous venflon with an attached 3-way tap. Clotting of blood in the line between sample times was prevented by the injection of 0.5 mls of 1000 $unit.ml^{-1}$ heparin after each sampling. At sample times 2 mls of blood was drawn off to waste then an approximately 10 ml sample drawn into a plastic syringe. The blood was immediately transferred to a heparinised blood sample tube (Sterilin, Ltd), mixed, and placed on ice in an enclosed ice-bucket. The sample was transferred to a nearby laboratory and 2-3 mls of whole blood separated into a 5 ml Sterilin sample tube. This was stored frozen at -20°C prior to the analysis of mitozolomide levels in whole blood. The remainder was centrifuged at 2000 rpm in an Heraeus centrifuge at a temperature of 3°C for 10 minutes. Supernatant plasma was pipetted into Sterilin sample tubes and stored frozen at -20°C prior to analysis. The analysis of patient plasma samples was accomplished using the standard method described in section 3.1.1.

The oral bioavailability of mitozolomide in man was assessed by dosing individual patients with equivalent iv and po doses. The oral dose was given as one or more 50 and 100 mg hard gelatin capsules taken in the morning on an empty stomach. An iv infusion of equivalent dose was prepared and administered as previously. The protocol was otherwise identical to that previously used in the iv study with the exception that an additional blood sample was taken 0.5 hours after the start of infusion or the administration of the gelatin capsules.

The analysis of whole blood levels of mitozolomide was accomplished by the standard method (section 3.1.1) after lysis of blood cells. Whole blood samples were defrosted and 50 µl of 1.0N HCl added per ml of blood. Cells were lysed by ultrasonication using an MSE sonic oscillator. In the assessment of the method various times and numbers of oscillatory bursts were tried and the blood subsequently centrifuged. Supernatants were assayed in a Beckman DU-7 UV spectrophotometer and lysis measured in terms of absorbance due to the colouring of the supernatant by haemaglobin released from lysed red cells. Optimal conditions were determined and the method adapted for the routine analysis of whole blood samples.

2.6 Mitozolomide excretion balance study in mice

An excretion balance study was designed to trace the fate of a [^{14}C]-radiolabel following the administration of radiolabelled mitozolomide to male BALB/c mice. Mitozolomide was available with [^{14}C]-radiolabels in two positions (see figure 3.24). 5 mice each were dosed with formulations containined [^{14}C]-chloroethyl-labelled mitozolomide and [^{14}C]-imidazole-labelled mitozolomide. The subsequent excretion of the radiolabel was monitored by collecting urine, faeces and expired carbon

dioxide over a 72 hour period. Levels of radioactivity residual in the carcass at the end of this period were also determined. Mice were dosed at 20 mg.kg $^{-1}$, administered ip , with 5-7 μCi of radioactivity in each dose.

Stock solutions of drug labelled in each position were prepared by weighing approximately 5 mgs into small sample bottles and adding 250 μl DMSO. These were stored frozen at -20°C prior to use. Sub-samples of these stock solutions (6-9 μl) were diluted with a solution of unlabelled mitozolomide in DMSO to give a final concentration of drug in DMSO of 25 mgs.ml $^{-1}$ and containing approximately 250-350 μCi.ml $^{-1}$ of radioactivity. This was diluted 1:9 in sterile isotonic saline immediately before administration to give a dose formulation such that 200 μl was equivalent to a dose of 20 mg.kg $^{-1}$ for a 25 g mouse. 20 μl of this dose formulation was removed using a Gilson microman pipette and diluted with water to 100 mls in a volumetric flask. 3 x 1 ml aliquots of this dilute solution were removed and 10 mls of 'optiphase mp' scintillant added to each prior to liquid scintillation counting in a Packard Tri-carb 2660 scintillation counter as described in section 2.2.3 for the counting of column eluent samples.

Mice were weighed on the day prior to the start of the experiment and the appropriate volume corresponding to a 20 mg.kg $^{-1}$ dose evaluated. This dose volume was taken up in a 1 ml syringe and the syringe weighed. The syringe was re-weighed after injection of the drug to enable the accurate determination of the weight of the dose administered and therefore of the starting radioactivity.

Mice were housed in glass metabolic cages during the course of the experiments and for 24 hours prior to its start. These contained a metal grid base such that urine and faeces fell through to trap vessels

attached beneath. A movable glass insert directed urine into a side-positioned trap whilst faeces fell straight through to a trap positioned directly beneath the grid. The metabolic cage was positioned over a cold bath (at a temperature of -5°C) such that the urine and faeces traps were immersed. In this way trapped samples were immediately frozen. Food and water was available to the mice *via* attached dispensers. Trap fittings and food and water dispensers were attached by ground glass connectors which were greased facilitating an air-tight seal.

Air was drawn through the cages *via* inlet and outlet lines using a small electrical pump. Calcium sulphate and soda lime traps were positioned in series at the air inlet end to remove water and carbon dioxide from input air. 2 traps each containing approximately 30 mls of a 1:4 mix of ethanolamine and ethoxyethanol were positioned in series beyond the air outlet to enable to trapping of expired carbon dioxide. A diagram of the metabolic cage set-up is shown in figure 2.2.

Mice were dosed ip and immediately placed in the metabolic cage. Samples of urine, faeces and carbon dioxide were collected at 12, 24, 48 and 72 hours after dosing. At each time point the sides of the metabolic cage were rinsed using a water wash bottle such that 2-8 mls of water were mixed into the urine in the trap. Urine, faeces and carbon dioxide traps were exchanged for clean ones ensuring that the air tight seal was broken for the minimum amount of time in the change-over.

Urine samples were thawed and washed into a pre-weighed sample bottle containing 75µl of 1.0N hydrochloric acid, re-weighed to determine the total sample weight and stored frozen at -20°C. Frozen pellets of faeces were transferred to a pre-washed sample bottle, re-weighed and then also stored frozen at -20°C. The volume of trap fluid

in each carbon dioxide trap was measured in a measuring cylinder and then a sub-sample transferred to a storage bottle prior to liquid scintillation counting. At the end of the 72 hours each mouse was killed by dislocation of the neck and the carcass stored frozen prior to analysis.

Figure 2.2 - The arrangement of equipment for the excretion balance study.

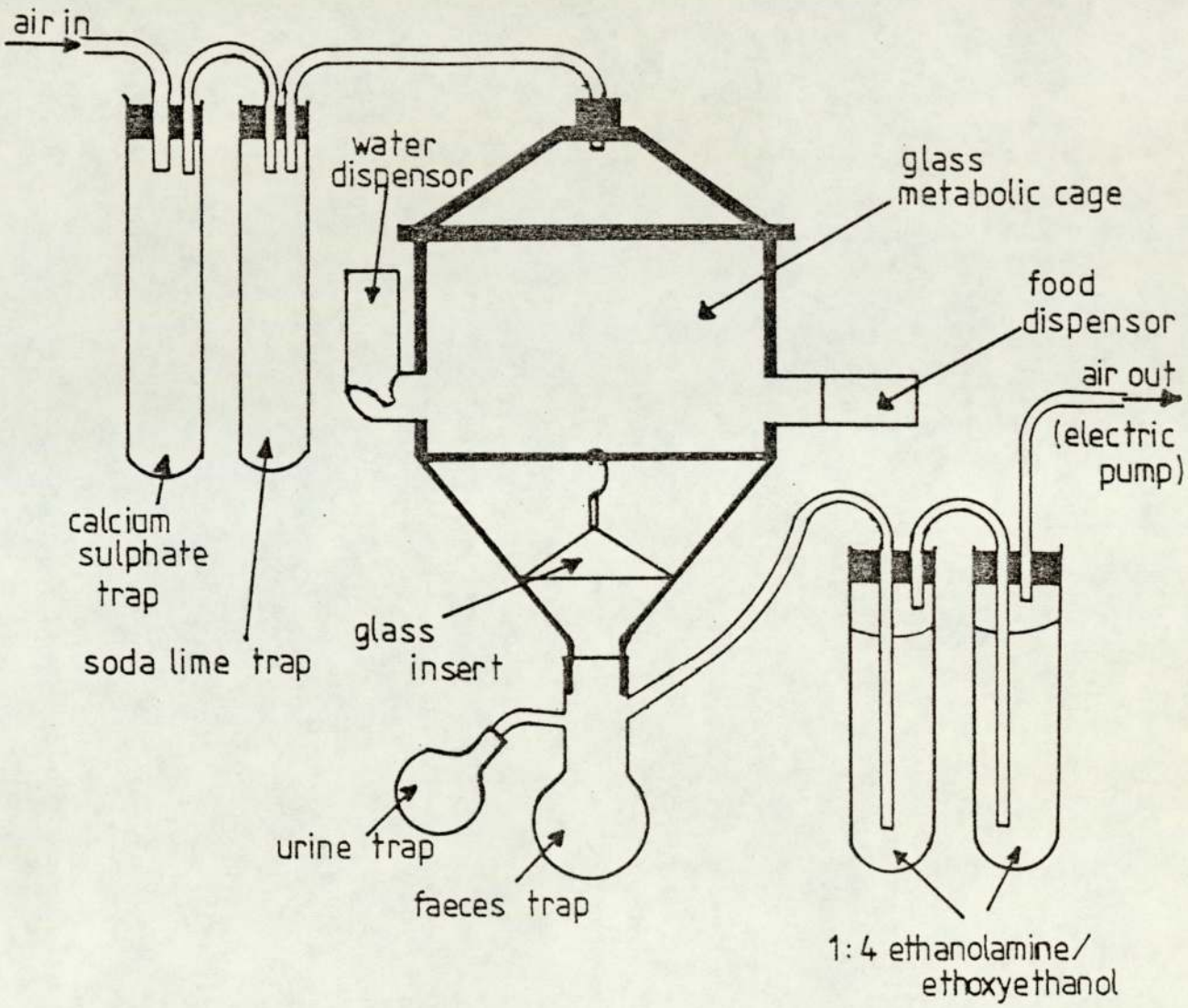

Levels of radioactivity in the urine, faeces and trapped carbon dioxide samples together with that residual in the carcass at the end of the experiment were determined by liquid scintillation counting using the methods detailed in section 2.2.3. Urine samples were also assayed by HPLC and TLC in an attempt to identify moieties containing the radioactivity (see sections 3.8.2 and 3.8.3).

3 RESULTS AND DISCUSSION

3.1 Analytical method development

3.1.1 A quantitative assay of mitozolomide and CCRG 81045

3.1.1.1 Development of the method for mitozolomide

An HPLC method was developed for the quantitative analysis of mitozolomide as a necessary pre-requisite to the various kinetic studies described in this thesis. Mitozolomide was extracted from plasma or urine subsequent to analysis by an isocratic reversed-phase HPLC method utilising UV detection. Previous studies on mitozolomide had identified a strongly absorbing chromophore at λ max.325nm (5). Quantification was determined from the peak area ratio of mitozolomide to an internal standard. Concentrations were obtained from a calibration line constructed from 6-8 evenly distributed standards over the concentration range of interest. A suitable internal standard was found to be 3-(2-hydroxyethyl)-1,2,3-benzotriazin-4(3H)-one (see figure 3.1.)

Plasma or urine samples were stored at -20°C and thawed immediately prior to use. A 20µl aliquot of the internal standard solution (in methanol) was added to a test tube followed by the addition of 50µl 1M hydrochloric acid and 0.25-1.0 mls of test plasma or urine. 2.5 mls of ethyl acetate was added and the contents vortexed. The layers were separated by centrifugation at 1500 g for 10 minutes, 2 mls of the organic layer were removed and the ethyl acetate evaporated. The residue was dissolved in 150µl of methanol followed by the immediate addition of 150µl 5% acetic acid in water. This solution was transferred to a low volume insert and stored at 4°C prior to analysis. Standard solutions were prepared over the concentration range of interest by the

addition of chloroform solutions of mitozolomide to test tubes with subsequent evaporation to dryness in a stream of nitrogen. These standards were then prepared simultaneously with the test samples using control samples of either plasma or urine.

Chromatographic conditions and examples of chromatograms obtained in the analysis of mouse plasma samples are shown in figure 3.2.

3.1.1.2 Verification of the method

Experiments were conducted to determine the efficiency of the ethyl acetate extraction and to establish the reproducibility, linearity and detection limits of the assay.

To determine the efficiency of the ethyl acetate extraction aqueous solutions of [^{14}C]-imidazole labelled mitozolomide were added to 1 ml samples of plasma to give concentrations of 1, 5, 10 and 20 mg.L^{-1}. Extraction with ethyl acetate was performed as in section 3.1.1.1 and triplicate samples of both aqueous and organic layers counted in a liquid scintillation counter. The results in table 3.1 show that extraction is constant over this concentration range at 76%. The mean total recovery of label in this experiment was in excess of 95%.

The reproducibility of the assay was assessed by preparing a plasma solution of mitozolomide (5 mg.L^{-1}) and analysing 6 x 1 ml aliquots from this solution. Using these samples it was possible to establish the coefficient of variation (n=6) for injections made from replicate samples to be 1.75% and by running multiple injections from one of these samples to establish the coefficient of variation (n=6) for replicate injections from a single sample to be 0.465%. These figures demonstrate the reproducibility of the method and are detailed in table 3.2.

Figure 3.1 - The structure of 3-(2-hydroxyethyl)-1,2,3-benzotriazin-4(3H)-one, the internal standard used in the HPLC assay of mitozolomide

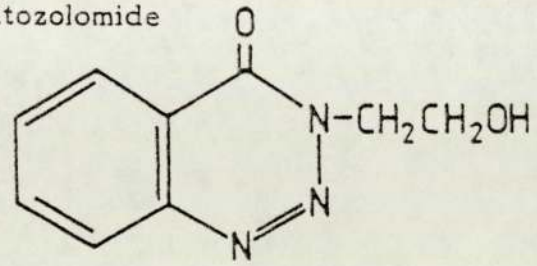

Figure 3.2 - HPLC conditions for the assay of mitozolomide and examples of the chromatograms obtained from mouse plasma.

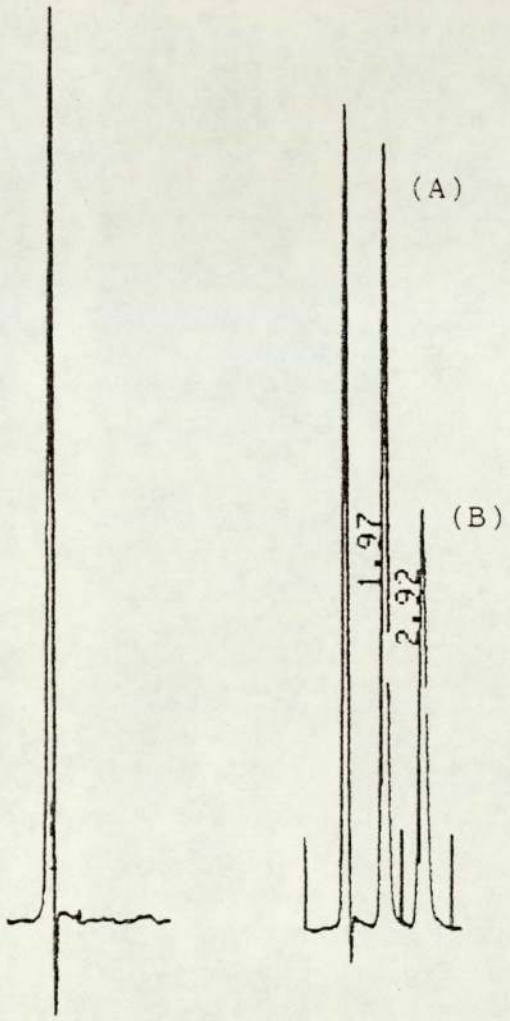

Conditions:

Column: Waters C18 RCM cartridge, 100 X 5mm, 10μ particle size + C18 guard column.

mobile phase: isocratic - 70% acetic acid (5%) 30% methanol

Flow rate: 1.5 mls.min^{-1}

detection: UV at 325nm

retention time: mitozolomide - 1.97 mins
internal standard - 2.92 mins

Chromatograms show; (i) control plasma and (ii) plasma containing 1 mg.L^{-1} mitozolomide (A) with internal standard (B). Capacity factors (k') for the assay were 1.75 for mitozolomide and 2.80 for the internal standard.

Table 3.1 - Efficiency of the ethyl acetate extraction

mitozolomide concentration (mg/L)	mean % in each fraction (n = 5)	
	ethyl acetate	plasma
20	77.56	22.44
10	76.03	23.97
5	76.53	23.47
1	75.06	24.94

Table 3.2 - Reproducibility of the assay

	mean peak area ratio mitoz/int.std (n = 6)	standard deviation (sd)	coefficient of variation sd/mean x 100%
injections from replicate samples	1.302	0.0227	1.75
multiple injections from a single sample	1.346	0.00626	0.465

Calibration curves have been constructed for each sample preparation during the course of this work which has involved concentration ranges from as low as 50-400 $ng.ml^{-1}$ to as high as 0.5-2.0 $mg.ml^{-1}$. In every case the correlation coefficient for a fit to a straight line (6-8 standards injected in duplicate) has been greater than 0.98 and in most cases in excess of 0.99. A typical calibration line derived from 8 standard solutions of mitozolomide (concentration range 50-400 $ng.ml^{-1}$, standards injected in duplicate) is shown in figure 3.3. The detection limits of the assay were obtained by preparing samples from a serially diluted plasma solution of mitozolomide and assaying these with the LM480 detector at maximum sensitivity. The maximum concentration of mitozolomide detectable with a signal to noise ratio of greater than 3 was 10 $ng.ml^{-1}$.

Figure 3.3 - A typical calibration curve generated from mitozolomide standard solutions

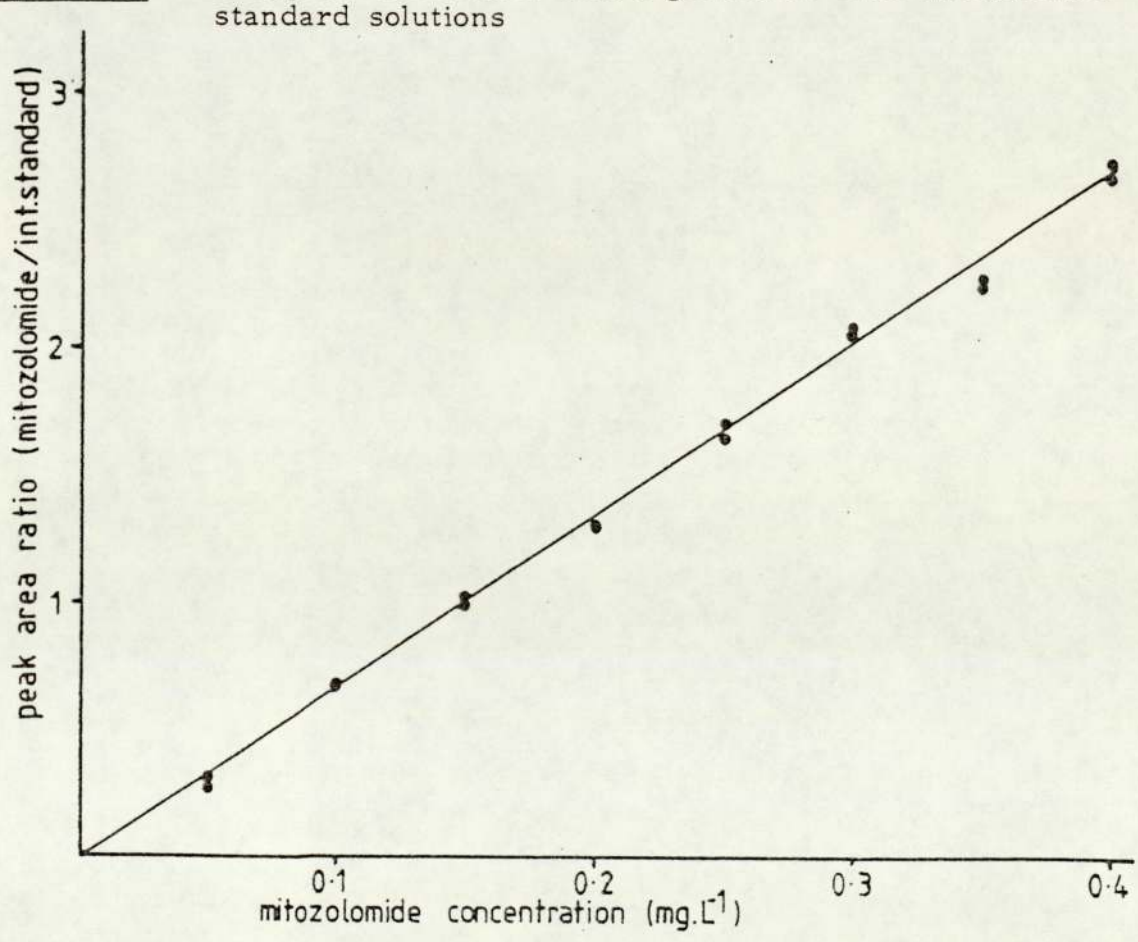

3.1.1.3 Discussion

The principal problems associated with the development of the quantitative assay are the potential interference of endogenous material or co-administered drugs (antiemetics and analgesics are commonly co-administered in cancer chemotherapy) and the inherent instability of mitozolomide. In addition, because the method was to be employed for the analysis of numerous samples from pharmacokinetic studies it was important that the chromatographic run time was kept to a minimum.

This latter point has clearly been catered for with a total run time of only 5 minutes per sample. The capacity factors obtained in this respect are a little low (1.5 for mitozolomide and 2.8 for the internal standard; it is generally recognised (139) that capacity factor values should ideally range between 2 and 7) but the strong chromophore at 325 nm has largely negated the problem of interfering polar endogenous material and baseline resolution of the 2 peaks has been obtained throughout the methods use.

The use of the method to assay blood and plasma samples from over 40 patients in the phase I clinical trial has not revealed any interfering peaks arising from either endogenous plasma moieties or co-administered drugs whilst the high stability of mitozolomide under acidic conditions means that, providing fresh samples are rapidly cooled, the anticipated problems of drug instability have also been circumvented. The verification procedures have shown that this method provides a reliable, fast and accurate means of determining mitozolomide levels in biological fluids, an essential requirement for the type of work reported herein.

3.1.1.4 Adaptation of the method for the assay of CCRG 81045

It was found that with very little modification the method developed for mitozolomide could be applied to the assay of CCRG 81045. By changing to a slightly more polar mobile phase and changing the internal standard

to the ethyl analogue of mitozolomide, 8-carbamoyl-3-ethylimidazo[5,1-d]-1,2,3,5-tetrazin-4(3H)-one (see figure 3.4) the method was found to be suitable. Figure 4 summarises the HPLC conditions employed for the assay of CCRG 81045 and shows an example of an HPLC trace for the drug in mouse plasma.

Figure 3.4 - HPLC conditions for the analysis of CCRG 81045 and examples of chromatograms obtained from mouse plasma.

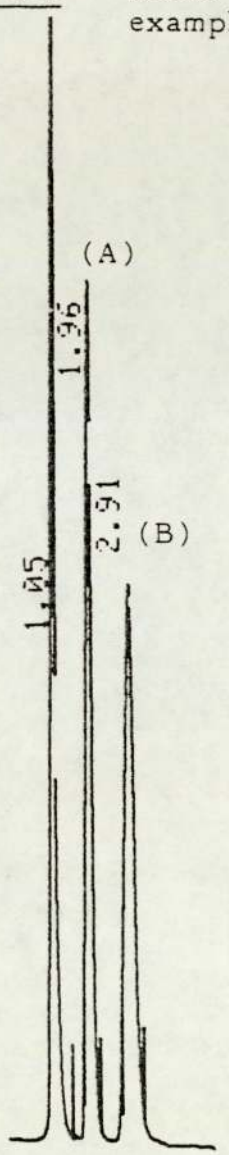

Conditions:

Column: Waters C18 RCM cartridge, 100 X 5mm 10µ particle size + C18 guard column.

mobile phase: isocratic - 90% acetic acid (5%) 10% methanol

Flow rate: 1.5 mls.min^{-1}

internal standard: CCRG 82019

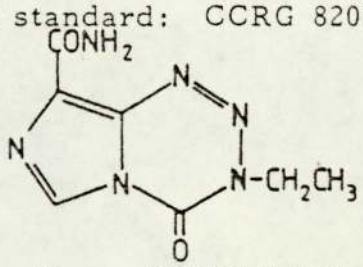

retention times: CCRG 81045 - 1.96 mins
internal standard - 2.91mins

The chromatogram shows plasma containing 10 mg.L^{-1} CCRG 81045 (A) and internal standard (B). Capacity factors (k') for the assay were 0.87 for CCRG 81045 and 1.77 for the internal standard.

3.1.2 Development of an analytical method for the assay of mitozolomide decomposition products

An analytical method was developed to elucidate the principal pathway of chemical degradation produced by mitozolomide under aqueous conditions. Scheme 1.3 shows that the likely end products arising from the two principal pathways proposed include 5-aminoimidazole-4-carboxamide (AIC) and 2-azahypoxanthine, thus a method was developed enabling the quantification of these two moieties and of any mitozolomide in the decompostion mix.

The difference in polarity of mitozolomide to both AIC and 2-azahypoxanthine proved too great to enable an isocratic method to be developed so a stepwise gradient approach was used (effectively two separate sets of isocratic conditions linked by a linear gradient). Of a variety of buffers tried in the mobile phase Walpoles acetate buffer at pH4 offered the best selectivity between AIC and 2-azahypoxanthine but the severe peak tailing obtained for AIC was unsatisfactory. Reports in the literature indicated that this is not an uncommon phenomena when assaying compounds that contain amine groups by reversed phase chromatography and is believed to arise from interactions of the basic nitrogen with unreacted silanol groups on the bonded stationary phase (140, 141). The situation can be overcome by adding 'amine modifiers' to the mobile phase and to this end diethylamine was included in the mobile phase with a resultant improvement in the peak shape of AIC. The internal standard used for the assay of mitozolomide (section 3.1.1) was found to run just behind mitozolomide in this system and was therefore used for the same purpose here. Figure 3.5 summarises the HPLC conditions for the developed method, and table 3.3 the resultant separations.

Figure 3.5 - HPLC conditions for the assay of mitozolomide, AIC and 2-azahypoxanthine arising from an aqueous decomposition study.

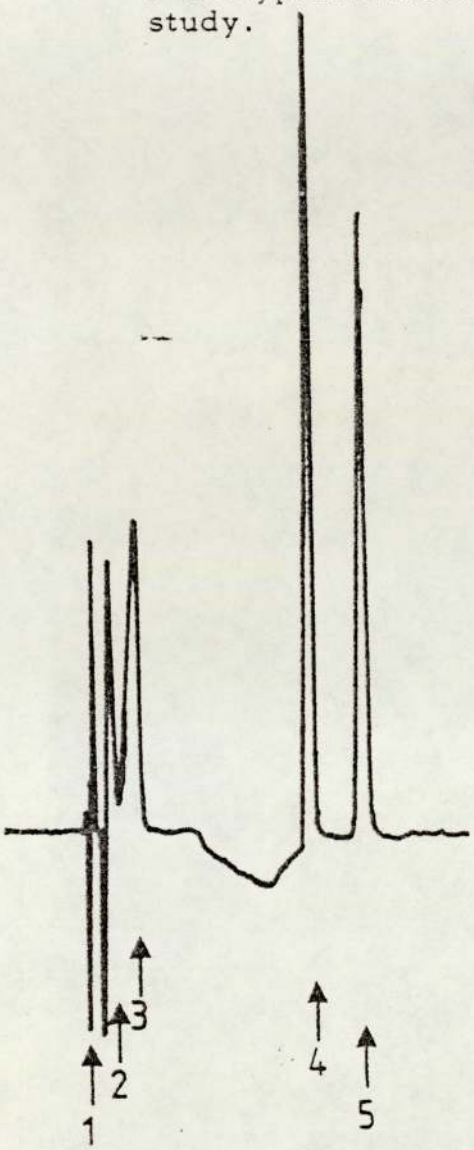

Conditions:

Column: Waters C18 RCM cartridge, 100 x 5 mm, 10μ particle size + C18 guard column.

mobile phase: gradient, flow 2.0 mls.min^{-1}

reservoir 1: Walpoles acetate buffer; pH 4 + 0.01M diethylamine.

reservoir 2: methanol

gradient table -

time	1	2
0 - 2.5 mins	95%	5%
2.5 - 4.5 mins (linear)	65%	35%
4.5 - 9.5 mins	65%	35%
9.5 - 10.5 mins (linear)	95%	5%
10.0- 15.0 mins	95%	5%

Table 3.3 - Retention times and capacity factors for the peaks 1-5.

peak No.	identity	retention time - (mins)	capacity factor (k')
1	void volume/solvent front	0.75	-
2	AIC	1.60	1.13
3	2-azahypoxanthine	2.20	1.93
4	mitozolomide	7.20	8.60
5	internal standard	8.00	9.60

3.1.2.1 Discussion

The method was developed primarily to facilitate the analysis of aqueous decomposition products and since these samples are 'clean' no sample preparative procedure was necessary. The linearity of the method was confirmed by standard curves generated using the area ratios to the internal standard method for each of the three assayed components. Correlation coefficients obtained for all three (AIC, 2-azahypoxanthine and mitozolomide) were >0.99 over a concentration range of 15-75 $\mu g ml^{-1}$ and as such the method was adequate for the decomposition experiments performed (see section 3.2).

However the method does contain a number of shortcomings which made it unsuitable for a broader range of use. UV detection was performed at 300 nm which represents a compromise between the λ max. of AIC and 2-azahypoxanthine (280-290 nm) and that of mitozolomide (325 nm) but even at this wavelength mitozolomide absorbs approximately five times as strongly as 2-azahypoxanthine and ten times as strongly as AIC which makes the detection of low levels of product difficult. Whilst the sensitivity of the assay for AIC has not been determined it is clearly not going to be much better than 0.2 $\mu g ml^{-1}$ even if absorption was monitored nearer the λ max. of 285 nm.

The major criticisms of the method are that the AIC peak is not sufficiently retained by the column ($k'=1.1$) and that although the peaks are sharp the selectivity of the separation between the AIC and the 2-azahypoxanthine peaks is insufficient with α, the selectivity coefficient between the two peaks (obtained from the ratio of the respective capacity factors) only equal to 1.7. This could mean that a low level of one component would be masked by a high level of the other and this point was accentuated by attempting to follow the decomposition of radiolabelled mitozolomide using an online L.C. radiodetector with band broadening making resolution of the two peaks impossible.

The short retention time of AIC made the method unsuitable for the assay of, for example, urine samples where polar endogenous components in the urine are shown to interfere with and mask the AIC peak. However, the method does allow the quantification of AIC and 2-azahypoxanthine arising from an aqueous or 'clean' decomposition experiment.

3.1.3 Development of an analytical method for the assay of urinary metabolites

The problems identified in the last section necessitated the development of a separate method for the assay of urinary metabolites. By this stage it was evident that the main degradative product was AIC, with N-hydroxyethyl-AIC forming the next most prevalent moiety in aqueous decompositions. A method was therefore developed which attempted to optimise the separation of these two compounds and mitozolomide. The problem of interfering endogenous material dictated that the AIC should be resolved from the solvent front as far as possible but since quantification was to be *via* fraction collection and liquid scintillation counting of radiolabelled urinary constituents the overriding requirement was one of adequate selectivity between peaks.

A feasible method for retaining AIC on the column was to use an 'ion-pairing' method (142). At low pH the protonated amine group of AIC would be attracted to a counter ion added to the mobile phase resulting in the formation of a lipophilic complex which would have greater retention. Initial results using heptane sulphonic acid as the counter ion in sodium acetate buffer were disappointing. Changing the column to one with a smaller particle size and the buffer to Sørensons mixed phosphates improved the chromatographic peak resolutions but

the ion-pair effect was still poor and could only be improved by dropping the methanol concentration to such a low value that the mitozolomide was retained for long time periods (greater than 40 minutes). Attempts to resolve the problem using gradiant elution were unsuccessful probably because of the critical importance of pH and counter-ion concentration in ion-pair chromatography and the difficulties in reproducibly controlling these factors in gradient elutions. Another approach was to use a more lipophilic counter ion. The use of SDS (sodium dodecyl sulphate) in this respect offered considerable improvement but the viscous nature of the resultant mobile phase created difficulties and this had to be abandoned. A change of counter-ion to octane-sulphonic acid improved the ion-pair effect substantially without the problems found using SDS.

A mobile phase consisting of 70% 0.002M Sørensons mixed phosphate buffer (adjusted to pH 4 using 0-phosphoric acid) mixed with 30% methanol and containing 0.005M octane-sulphonic acid gave an elution profile such that mitozolomide was eluted with a retention time of 7.8 minutes and AIC with a retention time of 12.8 minutes at a flow rate of 1 $ml.min^{-1}$. Unfortunately the N-hydroxyethyl-AIC peak, running just in front of the AIC peak, could not be resolved from AIC. Selectivity in reversed phase chromatography can sometimes be improved by changing the solvent strangth of the organic modifier added to the mobile phase (in this case methanol). In the reversed phase mode solvent strength is approximately inversely related to polarity and various polarity indices are employed to rank solvents. Krystulovich and Brown (143) employ an index of solvent strength which ranks methanol as 3.0 on a scale relative to water - 0; ethanol - 3.6; and tetrahydrofuran - 4.4.

Thus, tetrahydrofuran was substituted into the mobile phase as the organic modifer in place of methanol and the method optimized for the proportion of tetrahydrofuran giving the best selectivity. The result was a satisfactory resolution of N-(2-hydroxyethyl)-AIC from AIC and this method was used to assay urine samples from metabolism studies. The HPLC conditions and an example of a chromatogram for AIC, N-(2-hydroxyethyl)-AIC and mitozolomide in urine are summarised in figure 3.6. Whilst the broadness of the peaks and the poor UV absorption capacity of AIC limit the methods application to direct quantification on this basis the good resolution of the principal moieties and importantly the resolution of the AIC peak from interfering endogenous material facilitates the accurate quantitation of radiolabelled urinary metabolites by fraction collection and liquid scintillation counting.

3.1.4 Attempts to develop an analytical method for the assay of MCTIC

Mode of action studies (section 1.5) have already focussed on the potential importance of MCTIC in the anti-tumour activity of mitozolomide. It was apparent that the development of a method enabling the quantitative assay of MCTIC in test systems (both *in vitro* and *in vivo*) was a desirable goal.

However, the compound's inherent instability and the difficulties of extracting it unchanged from reaction mixes have complicated this task. In addition, whilst mitozolomide is stable under acidic conditions and labile in base the reverse is true for MCTIC which exhibits greater stability under basic conditions. This complicates any reaction 'quenching' approach to stabilization and isolation.

Figure 3.6 - HPLC conditions for the assay of urinary metabolites of mitozolomide and a chromatogram showing human urine 'spiked' with mitozolomide, AIC and N-(2-hydroxyethyl)-AIC.

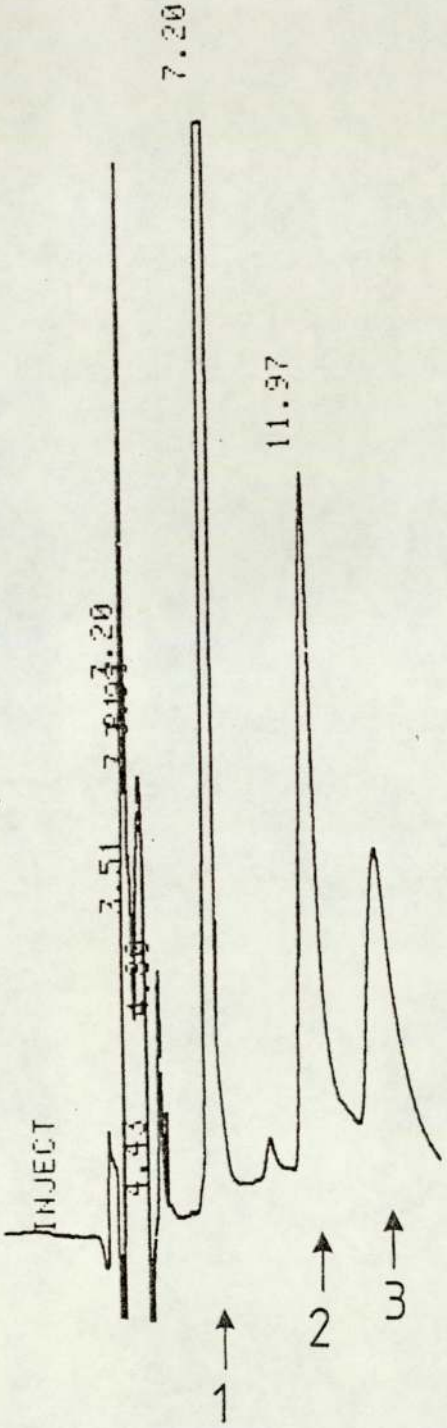

Conditions:

Column: Waters C18 RCM cartridge
100 x 8 mm, 5 μ particle size
+ C18 guard column.

mobile phase:

90 (0.002M Sørensons phosphate buffer
(+ 0.005M Octane sulphonic acid
(adjusted to pH4 with
(0-phosphoric acid

10 tetrahydrofuran

Flow rate: 1.0 mls.min^{-1}

Detection: UV at 300 nm.

Peak identifications:

1 - mitozolomide

2 - N-(2-hydroxyethyl)-AIC

3 - AIC

Two possible solutions to this problem have been pursued both based on attempts to derivatise MCTIC. Ege (144) had described a reaction for pyrazolotriazenes whereby a dehydrogenation reaction was followed by ring closure to generate the pyrazolotetrazole. Such a scheme for MCTIC is shown in figure 3.7. It was hoped that such an imidazotetrazole would be stable enough and lipophilic enough to be extracted and assayed by HPLC. The synthesis was attempted according to the method described but isolation of the tetrazole was unsuccessful. The reported method employed lead (IV) acetate as the oxidizing agent and the pyrazolotetrazole was formed in high yield. Although initial attempts to synthesize the imidazo equivalent were unsuccessful, the use of other agents in a more extensive synthetic study may prove fruitful. But, whilst this derivatisation may have offered some progress, an analytical method based on this derivative is unlikely to be sensitive enough. Since MCTIC is probably a very short-lived moiety in vivo, its formation will be dependant on a slower ring-opening of mitozolomide so it is unlikely to accumulate to significant levels. Therefore measuring the UV absorption of the tetrazole may not be a sufficiently sensitive enough method to quantify the low levels of MCTIC likely to be formed.

Figure 3.7 - The possible formation of an imidazotetrazole from MCTIC.

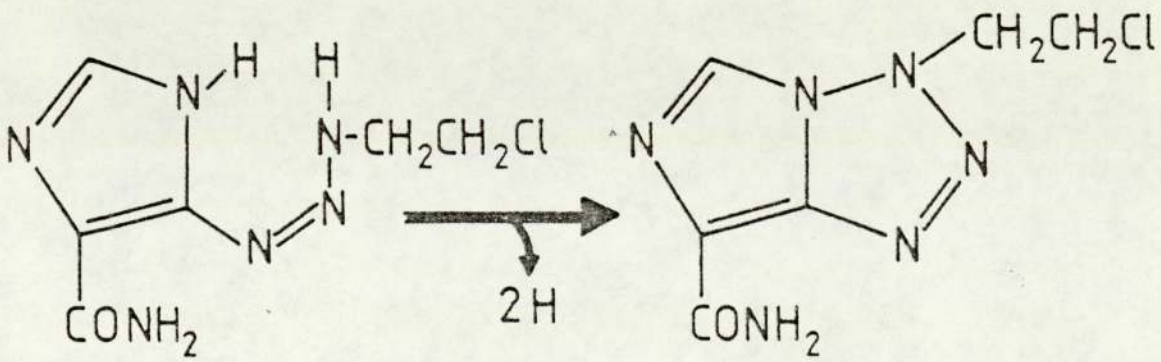

In general fluorescence spectrophotometers offer at least an order of magnitude greater sensitivity than UV absorption methods (145) and as such the derivatisation of MCTIC with a fluorescent probe is an attractive possibility. The degradation of MCTIC probably proceeds via a chloroethyldiazonium species with the possible further production of chloroethyl carbonium ions. Reaction of either of these species with a nucleophilic fluorescent probe could result in the formation of a stable adduct which could be quantified using spectrofluorimetric detection. MCTIC is labile under acidic conditions and would be expected to yield a cascade of reactive species in an acid quench of a sample (whilst stabilizing any mitozolomide present). These may react in part with a fluorescent nucleophile added simultaneously.

One possible reagent in this respect is thiofluorescein (see figure 3.8). Attempts have been made to form adducts by adding this agent in an acid quench to buffered samples of both mitozolomide and MCTIC solutions but, to date, no isolable product has been obtained. Such an approach could however produce a method sensitive enough to monitor MCTIC levels produced from mitozolomide.

Figure 3.8 - The structure of thiofluorescein a possible fluorescent probe for the derivatisation of MCTIC.

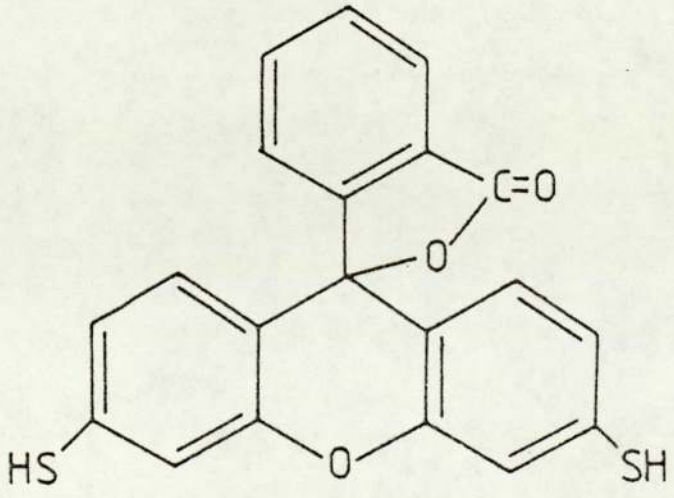

3.2 *In vitro* decomposition kinetics

3.2.1 *In vitro* kinetic studies on mitozolomide

The results for the *in vitro* decomposition experiments in various aqueous environments are summarized in table 3.4. Each experiment represents a decomposition study performed in triplicate as described in methods section 2.2.1., with analysis of mitozolomide levels by the standard HPLC method described in section 3.1.1. In all experiments plots of ln (concentration) versus time for an individual decomposition gave a correlation coefficient for a straight line of >0.98 and in most cases this was >0.99 indicating that all these *in vitro* decompositions obeyed first order kinetics. In addition variations in half-life values ($t_{\frac{1}{2}} = 0.693/k$ where k is the first order rate constant for the decomposition) within the triplicate for each experiment were within ± 3 minutes of the mean half-life value quoted in table 3.4. The exceptions to this were the more stable environments i.e. the acetate buffer, human urine (pH6) and the RPMI/10% FCS where agreement to the mean half-life value was also good. Variations in the half-life values obtained from separate experiments were however considerable and this is discussed in the next section.

Essentially the results indicate that mitozolomide is stable under acidic conditions but subject to rapid breakdown under basic conditions. Previous results (146) indicated that there was little variation in half-life values for different buffers at pH 7.4 and these results show that changing the concentration of phosphate buffer is similarly without effect. Another result of note was the finding that the rate of decomposition in plasma was consistently a factor of two times quicker than that seen in phosphate buffer at the same pH. This finding was subjected to further investigation (section 3.2.3). The half-life of 6 hours found in RPMI

tissue culture medium supplemented with 10% foetal calf serum is interesting since it infers that a stable drug pool exists in the extracellular environment during the standard dose incubation times usually employed for in vitro cellular studies. The practice of 'gassing' the cells with a CO_2/air mix lowers the media pH to the 6.5-7.0 range quoted and could make a significant difference in estimating the effective dose delivered to cells in this kind of work.

3.2.2 Decomposition kinetics of mitozolomide in phosphate buffer

Whilst variation in half-life values within the triplicates of an individual experiment was minimal the variation between experiments was relatively large with a half-life range of 0.83-1.1 hours in the seven separate experiments carried out (mean 0.92 hours; coefficient of variation 12.76%).

To attempt to explain this a closer investigation of the sensitivity of half-life to pH changes in the pH region (7-8.0) was carried out, the results of which are summarised in table 3.5. Each half-life quoted represents the mean of three decompositions at that pH and individual values were within ± 4 minutes of this mean.

The results indicate clearly that the rate of mitozolomide decomposition is exquisitely sensitive to pH in this region and it is likely that inadequate monitoring of pH was the reason for the inter-experiment variation previously noted. A similar sensitivity to pH is seen with the plasma results (table 3.4) where plasma at pH 7.66 showed a faster rate of decomposition to that at 7.4 ($t_{\frac{1}{2}}$ 0.3 versus 0.42 hours). This sensitivity to pH could have important consequences at the cellular/tissue level where local variations in pH could radically affect the amount of MCTIC being produced in a particular local environment.

Table 3.4 - Summary of the in vitro decomposition kinetics of mitozolomide in various aqueous environments.

(experiments at 37°C)	No. of expts.	pH	t 1/2 (hours)
tris buffer (0.1mM) [1]	2	9.0	0.15
acetate buffer (0.1 M)	1	4.0	240
RPMI/10% FCS	1	6.5-7.0	6
phosphate buffer (0.07 M)	2	7.4	0.97
phosphate buffer (0.2 M)	5	7.4	0.90
human plasma	3	7.4	0.42
human plasma	1	7.66	0.3
human urine	1	6.1	30.5
human urine	1	7.0	1.33

1 - experiment performed at 22°C

Table 3.5 - The sensitivity of mitozolomide breakdown kinetics to variations in pH in the range 7-8

all experiments in phosphate buffer at 37°C				
pH	7.21	7.43	7.61	7.81
t 1/2 (hours)	1.59	0.97	0.65	0.45

3.2.3 Accelerated decomposition of mitozolomide in plasma

This observed increased rate of hydrolysis of mitozolomide was also seen in decomposition studies on the chloroethylnitrosoureas. The work of Weinkam *et al* explained this finding in terms of a protein mediated non-enzymic catalysis brought about by interactions with serum albumin (51). As a first step to investigating the feasibility of such a model in the case of mitozolomide its *in vitro* plasma protein binding was investigated.

3.2.3.1 Plasma protein binding of mitozolomide

Protein binding was followed by the ultrafiltration procedure described in methods section (2.2.2). Table 3.6 summarises the results of this study and shows that the binding of mitozolomide to total plasma protein was constant over the tenfold concentration range followed. These concentrations were chosen because they reflected the range of plasma concentrations being reached in patients during the Phase I clinical trial in progress at the time. Plasma samples were acidified as part of the sample preparative procedure to ensure mitozolomide stability and the effect of this step on the protein binding is shown in table 3.6 with a drastically reduced degree of binding (17.6% versus 63.8%). Because of this the protein binding experiments were conducted at low temperature (4°C) to limit any effects of decomposition in interpretation of the results and acidification for the sample preparative procedure was only performed after ultrafiltration.

Having established that the drug underwent protein binding experiments were conducted to investigate which particular proteins were involved. Normal levels of plasma protein in humans range between 65 and 80 gL^{-1} of which the two most abundant constituents are albumin

Table 3.6 - *in vitro* plasma protein binding of mitozolomide.

approx start concentration mitozolomide (mg/L)	sample	mean concentration (mg/L, n = 3)	% bound (1-u'fil/plasma
5.0	plasma	4.341	63.78
	ultrafiltrate	1.572	
	pre-acidified ultrafiltrate	3.576	17.62
1.0	plasma	0.940	63.40
	ultrafiltrate	0.344	
0.5	plasma	0.505	62.37
	ultrafiltrate	0.190	

(50-65%) and the γ-globulins (13-22%) (147). The binding of mitozolomide to normal levels of albumin and γ-globulins was therefore investigated using solutions of the proteins in phosphate buffer (0.2M) at pH 7.4. Binding to α-1-acid glycoprotein was also studied. This plasma protein, whilst normally only present in low levels (0.5-1.5% total protein), can be elevated considerably in disease states including cancer (147) and was included for this reason. Table 3.7 summarises the results for these three proteins. The value of 60.9% bound for albumin suggests that quantitatively this is the principal site of protein binding by mitozolomide in plasma but the nature of the binding exhibited towards α-1-acid glycoprotein is approximately 4 times as specific when considered in terms of binding per gram of protein. Binding of mitozolomide to the γ-globulins is relatively poor.

3.2.3.2 Decomposition in protein solutions

To investigate whether this protein binding was a factor in the enhanced rate of breakdown in plasma decomposition experiments were performed using normal and twice normal concentrations of albumin and α-1-acid glycoprotein in 0.2M phosphate buffer at pH 7.4 with controls included of 0.2M phosphate buffer. In addition, to confirm that the phenomena was not affected by prothrombin or other elements involved in the clotting cascade a decomposition study was performed using human serum rather than plasma. The results of this study are summarised in table 3.8. Kinetics were first order in every case (correlation coefficients >0.98) with individual measurements within ± 3 minutes of the mean values quoted in the table. The fact that there is no change in the decomposition rate in albumin solutions (both human and bovine) versus phosphate buffer indicates that the catalysis must be mediated

Table 3.7 - *in vitro* protein binding of mitozolomide to individual plasma proteins.

sample	protein conc. (mg/L)	n	mean % bound	% bound/ g.protein
plasma	87.7	6	69.4	0.79
γ-globulins	20.0	3	6.4	0.32
α-1-acid glycoprotein	0.9	3	6.1	6.77
albumin	40.0	6	63.4	1.58

Table 3.8 - Decomposition of mitozolomide in protein solutions

all experiments at 37°C and pH 7.4	n	mean t 1/2 (hours)
0.2M phosphate buffer (control)	6	0.79
human serum	3	0.37
albumin at 40 g/L	3	0.81
albumin at 80 g/L	3	0.82
α-1-acid glycoprotein at 0.9 g/L	3	0.81
α-1-acid glycoprotein at 1.8 g/L	3	0.87
bovine serum albumin at 50g/L	3	0.87

via a different mechanism to that proposed for the nitrosoureas and the result with α-1-acid glycoprotein (also no change in rate) where binding is more specific suggests it may be unrelated to protein binding entirely. The serum result shows that the catalysis is unrelated to elements associated with the clotting reaction

3.2.3.3 Decomposition in ultrafiltrate

Before addressing the possibilities of an enzymic catalysis it was decided to determine whether the effect was related to high molecular weight material at all. To this end a decomposition study was conducted in plasma ultrafiltrates. Ultrafiltrates were prepared using Amicon centriflow cones which exclude 97% of plasma protein with a molecular weight cut-off of 50 000. Because removal of plasma proteins largely removes the buffering capacity of the ultrafiltrate the pH was adjusted to 7.4 by addition of dilute hydrochloric acid. The decomposition was performed by the standard method at 37°C with a simultaneous plasma control. The mean half-life seen in the ultrafiltrate was 0.41 hours (±2 mins) compared to the plasma value of 0.43 hours (±2 mins) indicating that the catalysis is being mediated by a low molecular weight component present in a plasma ultrafiltrate. The pH adjustment is critical since Weinkam had observed an intermediate decomposition rate for BCNU in serum ultrafiltrates but had not adjusted the pH (which was 7.56 compared to 7.41) and since the breakdown of BCNU is also critically dependent on pH in this region (49), the likely explanation for this is the alteration in pH. Thus, the observed maintained catalysis in ultrafiltrate at pH 7.4 is further evidence that the mechanism is one quite distinct from that suggested for the nitrosoureas. One possibility in this respect is the action of potent nucleophiles contained

in plasma to enhance the rate of ring-opening. A likely candidate would be thiol groups. The principal source of extracellular plasma thiol is the cysteine residue in glutathione with reduced glutathione (GSH) levels of between 3 and 24μM being reported (148, 149). To investigate this decomposition experiments were performed using glutathione concentrations of 10μM in the reduced form and 5μM in the oxidised (GSSG) form in 0.2M phosphate buffer (37°C). The mean half-life obtained for a 10μM GSH solution was 0.86 hours (±3 mins) and for 5μM GSSG 0.79 hours (±2 mins) compared to a phosphate buffer control of 0.80 hours (±2 mins) so it would appear that these thiols are not involved in accelerating the breakdown of the drug.

3.2.3.4 Discussion

The observed accelerated decomposition of mitozolomide in plasma is analogous to a similar effect seen with the chloroethylnitrosoureas BCNU, CCNU and meCCNU but these studies clearly demonstrate that the mechanism is not the albumin catalysed one proposed by Weinkam for the nitrosoureas. Weinkam argued that the lipophilicity of BCNU, CCNU and meCCNU (log P's of 1.5, 2.8 and 3.3 respectively) facilitated their protein binding to albumin and the resultant catalytic effect whereas the lack of effect on the decomposition of PCNU (log P of 0.37) was due to its poorer protein binding affinity consistant with its relatively hydrophilic nature (51). Interestingly the results described here show that mitozolomide, with a similar octanol:water partition coefficient to PCNU (log P of mitozolomide is 0.37) demonstrates a considerable binding affinity for albumin although in this case it appears unrelated to the accelerated decomposition observed, an explanation for which remains elusive.

The relative importance of the shorter plasma half-life *in vivo* is dependent upon pharmacokinetics and is discussed in the general discussion. However, unlike the nitrosoureas it is likely to be a consistant and predictable occurrence since mitozolomode is probably not lipophilic enough to partition into the core regions of lipoproteins which is proposed as a mechanism of stabilisation of BCNU, CCNU and meCCNU, where decomposition rates have been shown to fluctuate with changing plasma lipoprotein levels (53).

3.2.4 *In vitro* decomposition studies on CCRG 81045

Similar *in vitro* decomposition studies were conducted using CCRG 81045 to determine whether a similar accelerated decomposition was being observed as had been seen with mitozolomide. The results of these studies are summarised in table 3.9. As with mitozolomide plots of ln (concentration) versus time for an individual decompositon gave a correlation coefficient of >0.98 for a fit to a straight line indicative of first order breakdown kinetics (for disappearance of parent drug). Variations within the triplicate in each experiment were again minimal (±3 minutes in every case) but variations between the two phosphate buffer experiments were wider indicating that a similar sensitivity to pH was evident and this was supported by the faster rates of decomposition in plasma at pH 7.6 - 7.7 (0.42 hours half-life which compares to a half-life of 0.54 hours for plasma at pH 7.4) although the analagous experiment to that described in section 3.2.2 for mitozolomide has not been conducted to confirm this. The accelerated decomposition evident for mitozolomide in both plasma and a plasma ultrafiltrate was again evident in the case of CCRG 81045 suggesting that the likely mechanism of this catalysis may be universal for this group of compounds.

Comparing the rates of parent drug disappearance for CCRG 81045 and mitozolomide (tables 3.4 and 3.9) suggests that the methyl analogue is slightly the more stable of the two (phosphate buffer half-lives of mitozolomide are 0.97 hours compared to 1.24 hours for CCRG 81045).

Table 3.9 - Summary of in vitro decomposition kinetics of CCRG 81045 in various media.

all experiments at 37°C	No. of expts.	pH	t 1/2 (hours)
phosphate buffer (0.2M)	2	7.4	1.24
human plasma	1	7.4	0.54
human plasma	2	7.6-7.7	0.42
plasma ultrafiltrate	2	7.4	0.51

3.3 Assay of products arising from the decomposition of mitozolomide and MCTIC

3.3.1 Using the gradient elution method

An identification and quantification of the products arising from decompositions in phosphate buffer was attempted using the gradient method developed in Section 3.1.2. A typical chromatogram obtained from a decomposition of mitozolomide is shown compared to that obtained from MCTIC in figure 3.9. On running triplicate decompositions to completion the AIC peak was quantified as being 66.37% (± 2%) of the starting mitozolomide on a molar basis (quantitation was performed using UV peak area ratios to the internal standard versus calibration curves generated for AIC and mitozolomide). Two other principal unknowns were evident as UV peaks at 300nm, one sharp peak with a retention time (RT) of 2.47 and one less well defined with an RT of 4.67.

Previous decomposition studies had identified small amounts of the N-(2-chloroethyl)-, the N-(2-hydroxyethyl)- and the N-(2-aziridino)-AIC adducts following a decomposition in aqueous sodium bicarbonate (12) and small amounts of these standards were kindly made available by Dr C G Newton of May and Baker Limited.

Whilst none of these adducts co-chromatographed with the RT 4.67 peak the N-(2-hydroxyethyl)-AIC was found to match the earlier unknown. The sample provided was both small and known to be contaminated with AIC so accurate quantitation by a calibration curve was not possible. However, it was shown to absorb approximately 4.3 times as strongly as AIC and on this basis the amount of N-(2-hydroxyethyl)-AIC was estimated as approximately 20.5% of the starting mitozolomide on a molar basis.

Figure 3.9 - A comparison of chromatograms showing the breakdown products arising from decompositions of MCTIC and mitozolomide in phosphate buffer.

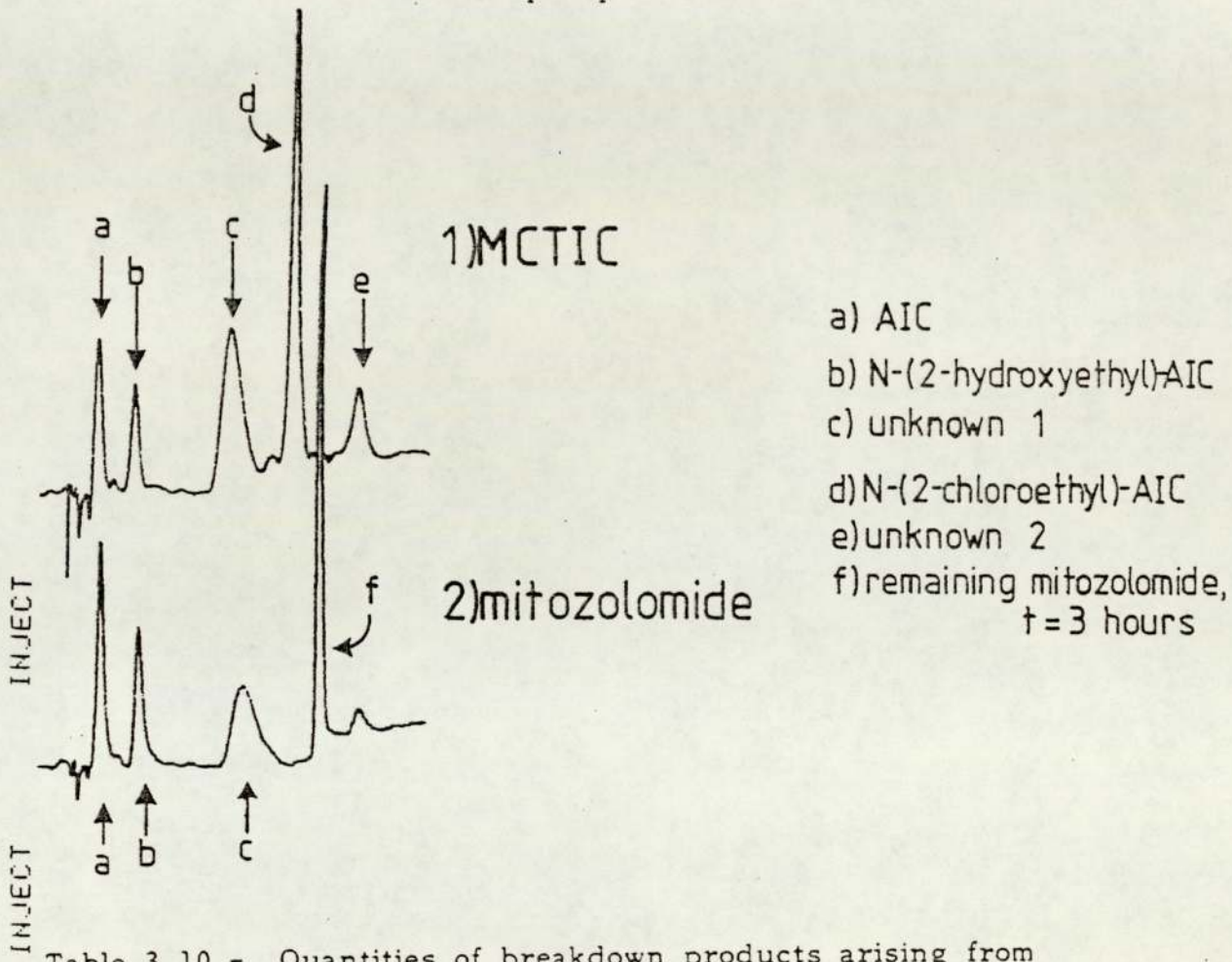

Table 3.10 - Quantities of breakdown products arising from decompositions of mitozolomide and MCTIC.

peak identification	RT (mins)	amount (mol %)	
		mitozolomide	MCTIC
AIC	1.62	66.37	44.44
N-(2-hydroxyethyl)-AIC	2.47	20.50	7.07
unknown 1	4.67	(10.50)	(17.50)
N-(2-chloroethyl)-AIC	6.45	-	20.20
unknown 2	8.10	?	unknown

The same method was used to assay the end-products from a decomposition of MCTIC. Decompositions were monitored in phosphate buffer at 22°C by adding a small volume of an MCTIC solution in DMSO (freshly dissolved) to 3.75 mls of phosphate buffer (at pH 7.46) in a WISP bottle and auto-injecting from this over a time course. Decomposition was complete within 2½ minutes since the first chromatogram obtained was identical to all later chromatograms. A typical chromatogram resulting from this decomposition is shown in figure 3.9 (compared to that obtained from an equivalent starting concentration of mitozolomide). A similar breakdown spectrum of products was seen with the addition of two new unknowns, one apparently significant (RT 6.45) and one less so (RT 8.10). The earlier of the two was identified by co-chromatography as being the N-(2-chloroethyl)- adduct of AIC. HPLC analysis suggested that the small amount of N-(2-chloroethyl)-AIC available was pure and this was used to quantify the amount of the adduct arising from the decomposition. Table 3.10 compares the relative quantities of breakdown products arising from the decomposition of mitozolomide and MCTIC.

A Problem with utilising UV quantitation is that this may not directly reflect the significance of each end-product since it relies upon them possessing a chromophore. To attempt to confirm the breakdown spectrum decompositions were performed using [^{14}C]-imidazole-labelled mitozolomide with an on-line ESI-Panax LC radiodetector. Unfortunately band broadening made the resolution of AIC and N-(2-hydroxyethyl)-AIC peaks impossible with this method. Thus the decomposition was monitored by the alternative method developed for urinary metabolites (section 3.1.3) and also by T.L.C./autoradiography.

3.3.2 Assay using the ion-pairing method

The ion pairing method developed for the urinary metabolites (section 3.1.3) was used to follow the decomposition of [^{14}C]-imidazole labelled and [^{14}C]-chloroethyl-labelled mitozolomide in phosphate buffer (ph 7.4; 37°C). Problems of reliability and band broadening led to the abandoning of attempts to utilise the on-line radiodetector and quantification was obtained by fraction collection/liquid scintillation counting .250µgml^{-1} solutions of mitozolomide containing either 42 000 dpm per 30µl of [^{14}C]-imidazole labelled or 63 000 dpm per 30µl of [^{14}C]-chloroethyl labelled mitozolomide were allowed to decompose completely in 0.2M phosphate buffer at pH 7.4 and samples were analysed by HPLC (30µl injections). Eluent fractions were collected and counted in a liquid scintillation counter. Two decompositions were performed for each label with assays of end products carried out in duplicate. Figure 3.10 shows a typical chromatogram for UV absorption at 300 nm using this method and table 3.11 summarises the results for the liquid scintillation counting.

The only problem in quantifying the imidazole labelled results was the interfering side-peak on the AIC peak. However, since this also appeared to contain the chloroethyl label its contribution could be evaluated by difference. The total AIC resulting was calculated to be 64.1%. Good agreement between the two labels was seen for the levels of N-(2-hydroxyethyl)-AIC present, with a mean level of 19.95%. The figures obtained for AIC and N-(2-hydroxyethyl)-AIC using this method (64.1% and 19.95% respectively) agree well with those obtained for the gradient elution method (66.4% and 20.5%) and confirm these as the two principal imidazole containing moieties arising from the decomposition. Further interpretation of this data was deferred until TLC autoradiograms were available.

Figure 3.10 - Chromatogram of mitozolomide decomposition products assayed by the ion-pairing method.

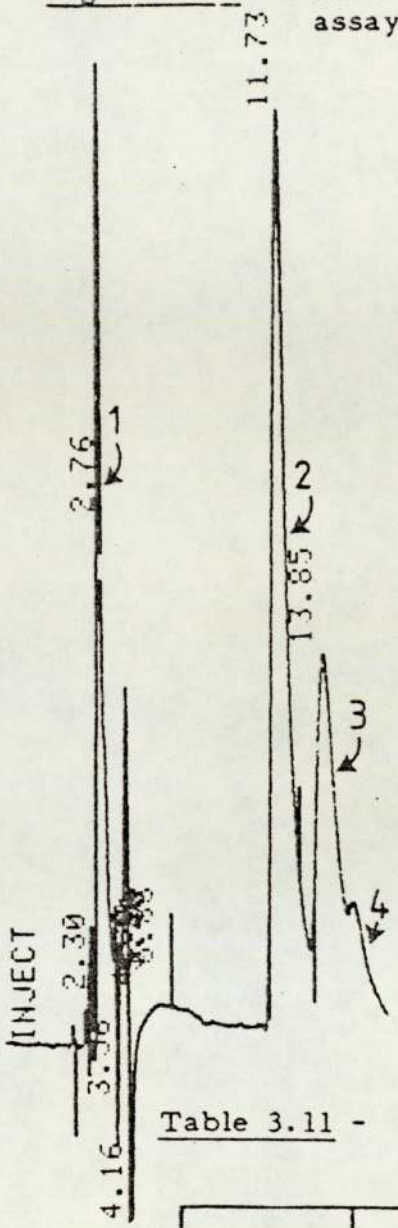

1) unknown 1

2) N-(2-hydroxyethyl)-AIC

3) AIC

4) AIC + side peak

Table 3.11 - Levels of radioactivity in eluent fractions following the HPLC of products from decompositions of radiolabelled mitozolomide.

RT (mins)	RECOVERIES			
	14C-imidazole label		14C-chloroethyl label	
	identity	mean %	identity	mean %
2.0-2.5	-	0.3	unknown A	22.2
2.5-3.5	unknown 1	8.2	unknown B	11.0
3.5-4.0	-	2.8	-	0.9
4.0-4.5	-		-	0.5
4.5-5.5	-		unknown C	37.6
5.5-6.9	-	0.3	-	0.5
6.9-8.4	(mitozolomide)	0.3	(mitozolomide)	0.4
8.4-9.6	-	0.2	-	0.3
9.6-10.7	-	0.2	-	0.3
10.7-13.2	N-(2-hyd.et)-AIC	19.3	N-(2-hyd.et)-AIC	20.6
13.2-15.0	AIC	55.0	(AIC)	2.0
15.0-16.6	AIC + side peak	11.4	side peak only	2.3
16.6-18.0	-	1.8	-	0.3

3.3.3 Assay by TLC/autoradiography

The TLC methods described in methods section 2.1 were used to assay the products from both imidazole and chloroethyl labelled mitozolomide. Autoradiograms are shown in figure 3.11 which correspond to decompositions in phosphate buffer (pH 7.4; 37°C) sampled after 2 hours. 4 bands (including mitozolomide are evident in the imidazole labelled case and at least 8 (including mitozolomide) are evident in the chloroethyl labelled case.

3.3.4 Discussion

The autoradiograms indicate that there are 3 main products containing the imidazole derived label. Two of these can be identified from co-chromatography of standards and by comparison to the HPLC data as AIC and the N-(2-hydroxyethyl)-adduct of AIC. It is likely that the third band visible by TLC with an RF of 0.08 corresponds to the unknown product 1 present in the ion-pairing separation with RT 2.5- 3.5 (see table 3.11) and the unknown 1 present in the gradient separation with RT 4.67 (see table 3.10). Quantification of the radio-label suggests this accounts for 8.2% of the starting mitozolomide on a molar basis. The identification of this unknown has not been achieved but it is not either the N-(2-chloroethyl) or the N-aziridino adducts of AIC previously isolated. The two minor components arising from the decomposition of [^{14}C]-imidazole-labelled mitozolomide (running with RT's of 3.5-4.5 and 15.0-16.6 in the ion-pairing separation (see table 3.11) were not evident in the autoradiograms and have not been identified; together they account for less than 5% of the starting mitozolomide. Identification of the array of products arising from the decomposition of [^{14}C]-chloroethyl labelled mitozolomide has not been

Figure 3.11 - Autoradiograms showing products from the decomposition of ^{14}C-chloroethyl and ^{14}C-imidazole-labelled mitozolomide.

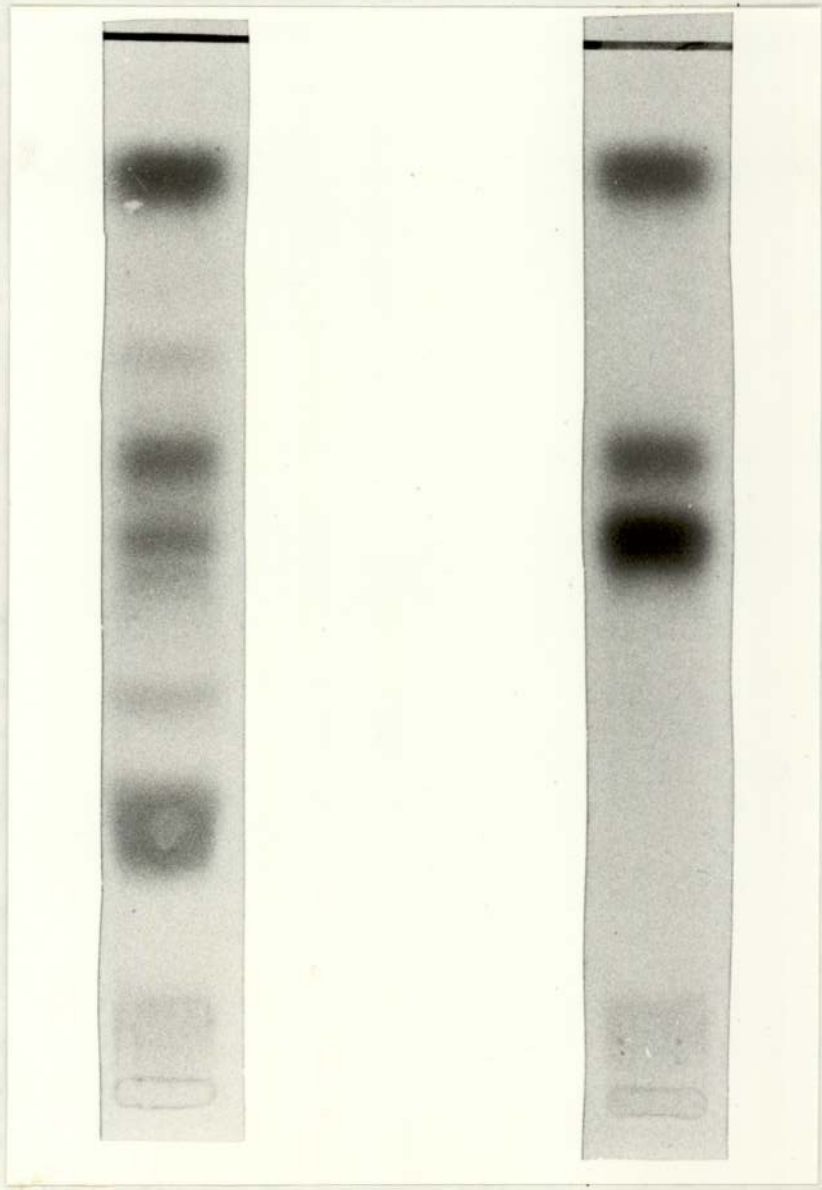

attempted, however the N-(2-hydroxyethyl)-AIC is present (20% of label) and a band is evident on TLC with an R_f of 0.08 and approximately the same intensity as the analagous band derived from the imidazole labelled decomposition suggesting it is the same component. Thus, this unknown appears to have retained both imidazole and chloroethyl parts of the parent molecule.

These decomposition studies have confirmed that under aqueous conditions and at physiological pH the principal route of degradation is *via* the triazene MCTIC and have provided the first quantification of the amount of AIC and the N-(2-hydroxyethyl)-AIC adduct produced under these circumstances.

Scaling up the decompositions and developing the assays for preparative level HPLC would facilitate the isolation of sufficient quantities of product to enable the identification of the unknowns.

It is likely that the fate of the chloroethyl fragment of mitozolomide is to 2-chloroethanol, 2-chloroacetaldehyde and 2-chloroacetic acid with other possible products including vinyl chloride and ethylene, all of which would either be predicted from decomposition *via* MCTIC or have been shown to arise in studies on the decomposition of the chloroethyldiazonium species in work on the chloroethylnitrosoureas (45).

AIC could result from nucleophilic attack on the α-CH_2 of the chloroethyl group in MCTIC (figure 3.12) and under basic conditions this may be the predominant pathway. It has been suggested that the formation of the N-(2-hydroxyethyl) adduct arises in an alternative fragmentation of the intermediate MCTIC *via* formation of an anion. However this mechanism would also predict the formation of the

N-(2-chloroethyl) adduct. This has not been seen in the studies on mitozolomide but was evident in the decomposition of MCTIC under the same conditions indicating that its formation may be dependant upon the concentration of reactive species.

The decomposition of monoalkyltriazenes is known to be proton catalysed (4) and Lown and Singh have demonstrated an increased rate of DNA alkylation with decreasing pH (150) such that the predominant pathway for the decomposition of MCTIC in vivo is likely to be the proton catalysed mechanism shown in figure 3.13. This proceeds via the generation of a chloroethyldiazonium species and reactions between this species (or subsequently formed carbonium ions) and the amine group of AIC would generate the AIC adducts seen in a manner dependent upon the concentration of the species present.

If this were the case the adducts would be less likely to be seen in vivo where competing endogenous nucleophiles would react with the generated carbonium ions whilst the earlier mechanism would predict a similar spectrum of products from decomposition in vivo.

Figure 3.12 - Formation of AIC via nucleophilic attack on the α-CH_2 group in MCTIC.

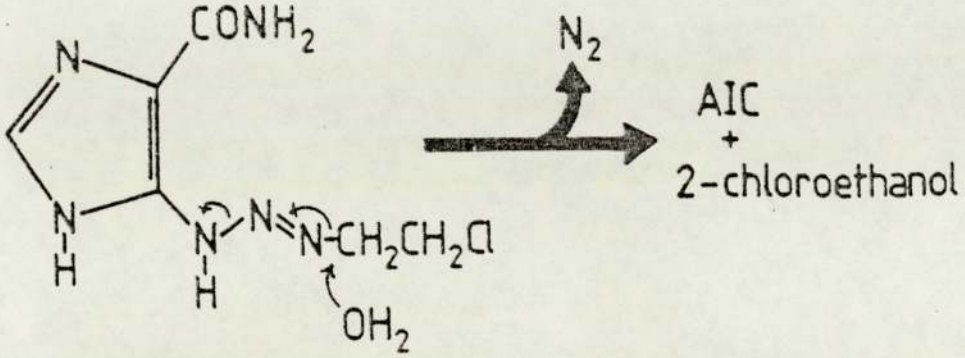

Figure 3.13 - Proton catalysed decomposion of MCTIC.

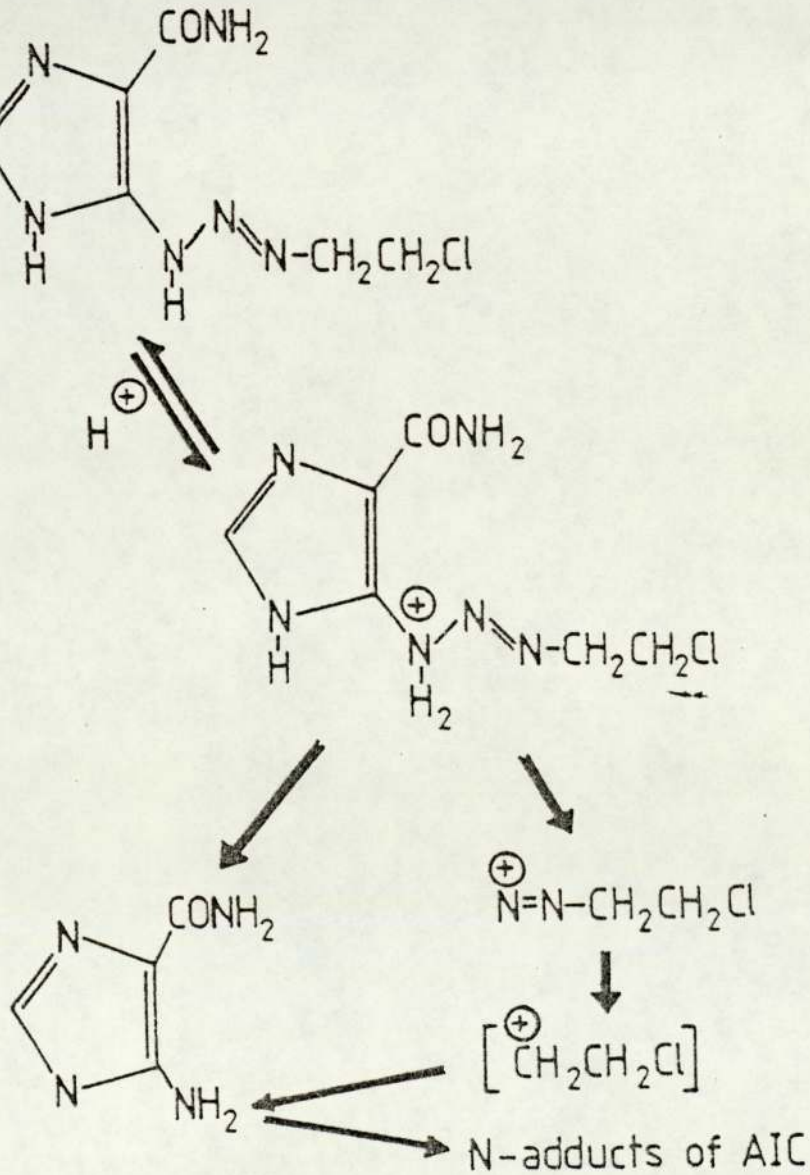

3.4 Assay of products arising from the decomposition of CCRG 81045

The assay of products arising from the decomposition of CCRG 81045 in 0.2M phosphate buffer (37°C; pH 7.4) was accomplished using the ion-pairing method (see section 3.1.3). 0.6 mgs.ml $^{-1}$ of CCRG 81045 was allowed to decompose completely and the products quantified using calibration curves generated from plots of peak area versus standard concentration. The decomposition was performed in duplicate and samples analysed in triplicate. Only 2 product peaks were evident in the resultant chromatograms and these were identified by co-chromatography with standards as being AIC and 2-azahypoxanthine. Quantification showed that virtually all the CCRG 81045 was accountable as AIC (a 97.5% yield on a molar basis) with the rest apparently being 2-azahypoxanthine. Thus, it seems that under aqueous conditions and at physiological pH CCRG 81045 degrades in a manner analogous to that of mitozolomide except that the decomposition of the intermediate triazene generates exclusively AIC.

The appearance of the azapurinone, albeit in low levels is interesting because it infers a minor contribution from the alternative decomposition pathway postulated for the imidazo[5,1-d]-1,2,3,5-tetrazin-4(3H)-ones shown in figure 1.5 (for mitozolomide) and that, as such, methyl isocyanate may also be produced from CCRG 81045. However, information from the manufacturers (May and Baker Limited) revealed a low level of methylisocyanate present in the batch of CCRG 81045 supplied (<1%). If this signified the presence of some unreacted starting materials then the 2-azahypoxanthine may be an artifact arising from the cyclisation of any unreacted diazo-IC.

3.5 Murine Pharmacokinetics

3.5.1 Dose escalation study

Screening studies had identified the optimal anti-tumour dose for therapeutic activity in mice treated with mitozolomide to be 20 $mg.kg^{-1}$ (72). Based on this information the doses selected for the ip dose escalation study were 0.25, 1.0, 5.0, 10.0, 20.0 and 40.0 $mg.kg^{-1}$. However, dosing above 20 $mg.kg^{-1}$ was complicated by formulation problems, with the mitozolomide precipitating from the formulation vehicle of 10% DMSO in saline. Initial results showed a wide variation in plasma levels indicative of this, so the study at 40.0 $mg.kg^{-1}$ was abandoned.

Plasma samples were analysed by the method described in section 3.1.1. Levels of mitozolomide were determined by fitting the peak area ratio obtained (mitozolomide peak area/internal standard peak area) to a calibration curve generated from 6-8 standards spread evenly over the concentration range of interest. The plasma from at least 4 individual mice was analysed at time points for each dose except 10 $mg.kg^{-1}$, where only 2 mice were assayed per time point.

A detailed breakdown of the plasma levels of mitozolomide found with each dose, together with values for mean and standard deviation for each time point, are tabulated in Appendix I. The data in each table is collated from at least 2 separate experiments at each dose.

At all the dose levels investigated mitozolomide was rapidly absorbed with no absorption or distribution phase evident within the first 15 minutes. The pharmacokinetic profile over this initial 15 minute period was examined only at 20 $mg.kg^{-1}$ where 5 and 10 minute time points were additionally taken. Mean plasma levels of 18.3 and 25.2 $mg.L^{-1}$ respectively indicate an absorption phase with peak plasma

levels being reached between 5 and 10 minutes after ip dosing.

Figure 3.14 summarises the results obtained for the ip dose escalation study. The data is shown as a logarithmic plot of plasma concentration versus time for 1.0 and 20.0 $mg.kg^{-1}$. The lines represent a regression of the raw data (pooled individual measurements from at least 2 separate experiments at each dose level) by the least squares method using data from 0.25 hours onward for the 1.0 $mg.kg^{-1}$ dose and 0.18 hours onward for the 20 $mg.kg^{-1}$ dose. Similar lines were obtained for the three dose levels not shown with correlation coefficients ranging from 0.9414 to 0.9820 (with the exception of the 0.25 $mg.kg^{-1}$ data which produced a lower value of 0.7755).

On the basis of these results the data was described by a simple open one-compartment pharmacokinetic model. This model assumes instantaneous distribution of the dose throughout a single compartment (in this case the whole body) followed by an exponential decline in drug levels within the compartment indicative of elimination by first order kinetics (151).

The rate constants for the elimination process (k_{el}) were estimated from the gradients generated by the linear regression of plots of ln (concentration) versus time (slope = $-k_{el}$). The AUC (area under the plasma concentration/time curve) values were estimated by the trapezoidal method from 0 to 8 hours in each case (an example of this calculation is shown in Appendix II). Other pharmcokinetic parameters for the model were determined from the following equations:

$t_{\frac{1}{2}}$ (the elimination half life) $= 0.693 / k_{el}$

Plasma clearance $= dose / AUC$

Figure 3.14 - ip route dose escalation study. The data are presented for two dose levels (20.0 and 1.0 $mg.kg^{-1}$).
The error bars indicate ± 1 standard deviation of the mean concentration at each time point.

● - 20 $mg.kg^{-1}$ ip; ■ - 1.0 $mg.kg^{-1}$ ip

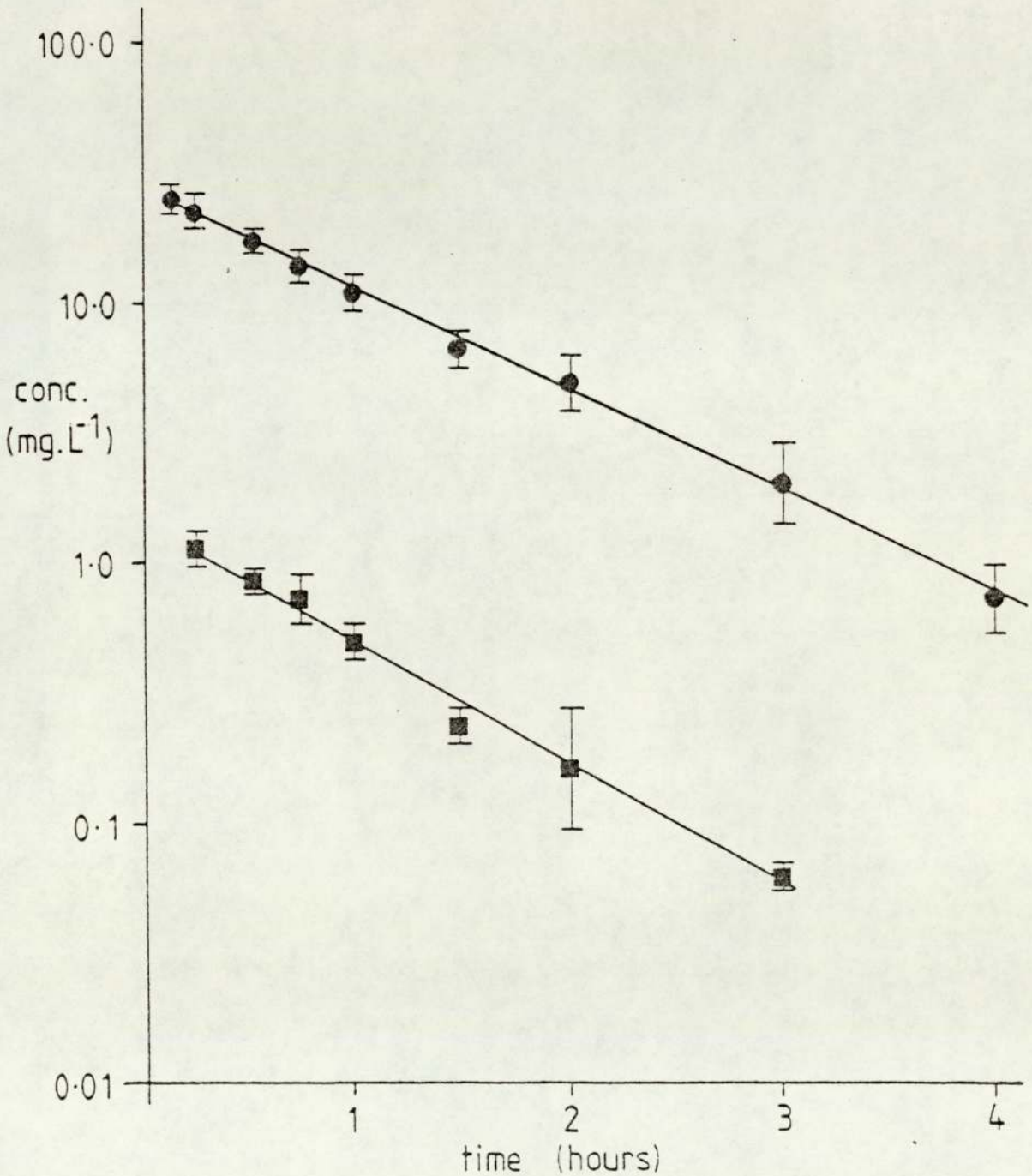

Vd, the volume of distribution (the apparent volume of fluid in which the dose would be distributed if the plasma concentration of drug reflected an even distribution throughout the body) = clearance/$k_{el.}$

Values for plasma clearance and volume of distribution were calculated on the basis of a 25g mouse weight.

The pharmacokinetic parameters evaluated from these equations are summarised in table 3.12.

Table 3.12 - Pharmacokinetic parameters for mitozolomide following ip adminstration

dose (mg/kg)	t 1/2 (hrs)	maximum plasma concentration (mg/L)	AUC (mg/hrs/L) (0-8 hrs)	Vd (L)	clearance (L/hr)
0.25	0.860	0.374	0.439	0.0176	0.0142
1.0	0.681	1.152	1.201	0.0204	0.0208
5.0	0.826	5.675	7.123	0.0209	0.0175
10.0	0.884	9.824	11.182	0.0285	0.0223
20.0	0.758	25.238	31.174	0.0173	0.0160

In addition to the linear elimination of the drug further evidence of a good fit to the one-compartment model was seen in the values obtained for the volume of distribution. These ranged from 17.5-27.4 mls (mean = 20.78) and are only slightly higher than the value for total body water which is the value predicted by this model (total body water of a mouse is 15-18 mls (151)).

The principal aim of a dose escalation study is to determine whether the pharmacokinetics of the drug are dose-dependent. Figure 3.15 shows plots of the maximum plasma concentration (Cp.max) and the AUC against ascending dose and reveals an approximately linear relationship in both cases. The values plotted for the 20 $mg.kg^{-1}$ data were evaluated omitting the 5 and 10 minute time points thereby enabling a direct comparison. These linear relationships indicate that the pharmacokinetic parameters for mitozolomide are independent of dose over the range covered.

Figure 3.15 - Plots of maximum plasma concentration (O) and AUC (●) against dose for mitozolomide over the dose range 0.25 - 20 $mg.kg^{-1}$.

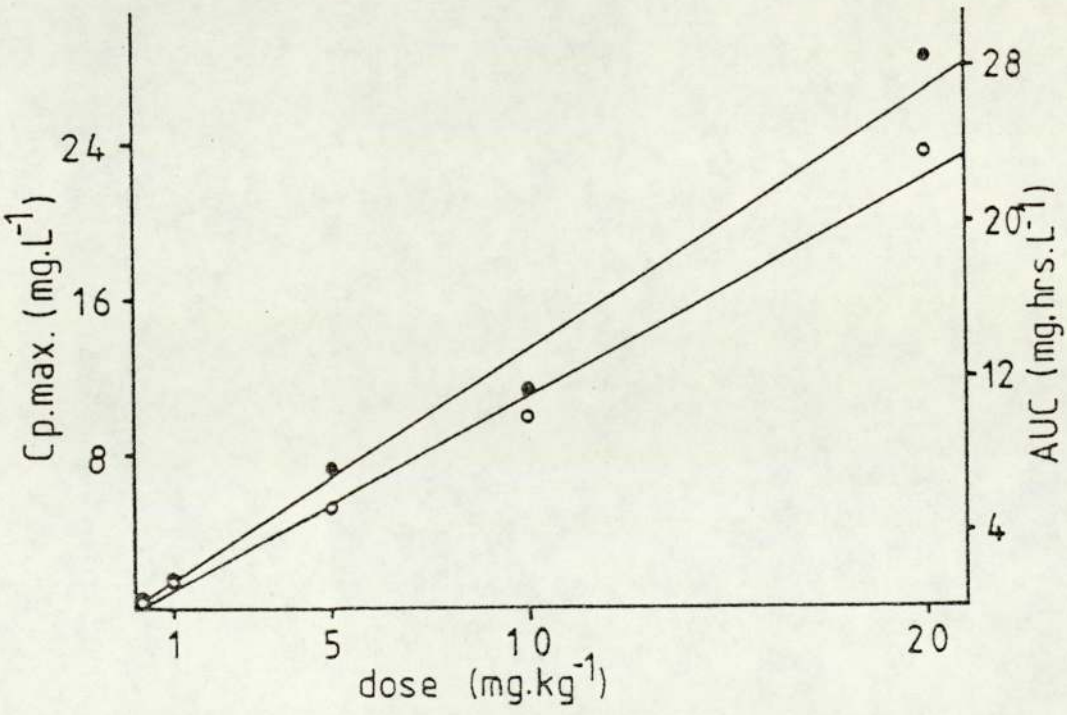

3.5.2 Oral bioavailability

The oral bioavailability of mitozolomide in mice was determined at a dose of 20 $mg.kg^{-1}$. Mice were dosed by both oral and ip routes using the same formulation vehicle (10% DMSO in saline). Plasma levels were determined as previously (section 3.5.1) with 5 mice evaluated at each time point (including 5 and 10 minute time points) for both routes of administration. The resulting pharmacokinetic profiles are shown in figure 3.16 where mean plasma concentration has been plotted against time for both sets of data. Tabulated details of the individual measurements together with the derivation of the respective AUC values by the trapezoidal method are shown in Appendix II. AUC values were estimated to be 20.346 $mg.hrs.L^{-1}$ for the oral route and 31.174 $mg.hrs.L^{-1}$ for the ip route. The oral bioavailability (or fraction of the drug absorbed, F) can be obtained from the ratio of the AUC values for the respective profiles. The calculation for mitozolomide is thus:

$$F = \frac{\text{AUC (p.o. route)}}{\text{AUC (i.p. route)}} = \frac{20.346}{31.174} = 0.653$$

By convention the denominator term should be the AUC obtained when an iv route of administration is used. In studies using mice adminstering the drug by the iv route is technically difficult, therefore the AUC value following an ip administration of mitozolomide has been substituted into the bioavailability calculation.

Figure 3.16 shows that absorption from the gastrointestinal tract was rapid with the mean peak plasma level of 13.85 $mg.L^{-1}$ being reached within 5 minutes of dosing, although the data for the 5 and 10 minute time points is variable suggesting that the absorption is probably occurring over a 5 to 15 minute time period.

Figure 3.16 - Plots of mean concentration versus time for oral and i p doses of mitozolomide. Error bars indicate ± standard deviation of the mean concentration at each time point.

○ - 20 mg.kg^{-1} i.p; ● - 20 mg.kg^{-1} p.o.

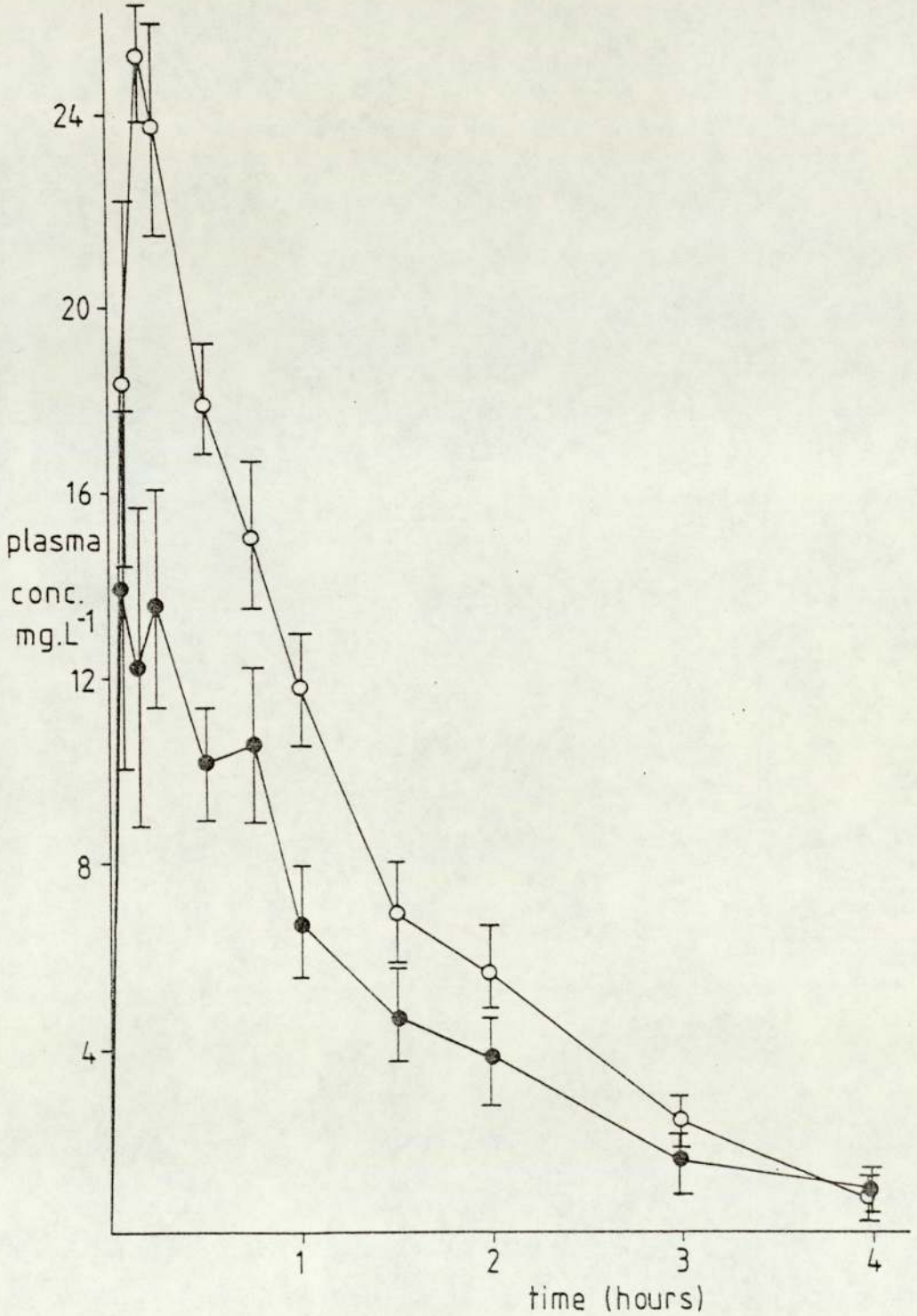

A plot of ln (concentration) versus time for the oral data produced a good fit to a straight line when the raw data was regressed using the least squares method (correlation coefficient = 0.962). This gave a value for the elimination half-life of 0.927 hours which was slightly longer than the values seen previously following ip administration.

3.5.3 Transdermal bioavailability

The bioavailability of mitozolomide adminstered topically in DMSO was investigated at a dose of 20.0 $mg.kg^{-1}$. The pharmacokinetic profile was monitored over an 8 hour period using 5 mice at each time point and determining levels of mitozolomide as previously (see section 3.5.1).

The resulting profile is shown in figure 3.17 which contrasts the plasma levels obtained with those seen following a 20 $mg.kg^{-1}$ ip dose of mitozolomide. Details of the individual measurements and the calculation of the AUC for the transdermal delivery of the drug are shown in Appendix II.

Variations in the levels seen at each time-point were greater than those seen previously, using either ip or po routes of administration but, a number of general observations could be made. The profile differs markedly from that seen for both ip and po studies in that entry of the drug into the blood stream is relatively delayed and the plasma concentrations attained relatively low (a mean Cp.max of 2.57 $mg.L^{-1}$ compared to 25.24 $mg.L^{-1}$ following the equivalent ip dose). However, these levels were sustained for most of the 8 hour period such that although maximum plasma levels were only 1/10 of those seen following an ip dose the AUC figure of 13.28 $mg.hrs.L^{-1}$ gave a bioavailable fraction, F, of 0.426 when compared to the ip figure of 31.7 $mg.hrs.L^{-1}$.

Figure 3.17 - Plot of mean concentration versus time for transdermal and ip doses of mitozolomide.
Error bars indicate ± 1 standard deviation of the mean concentration at each time point:

O - 20 $mg.kg^{-1}$ ip; ● - 20 $mg.kg^{-1}$ transdermal

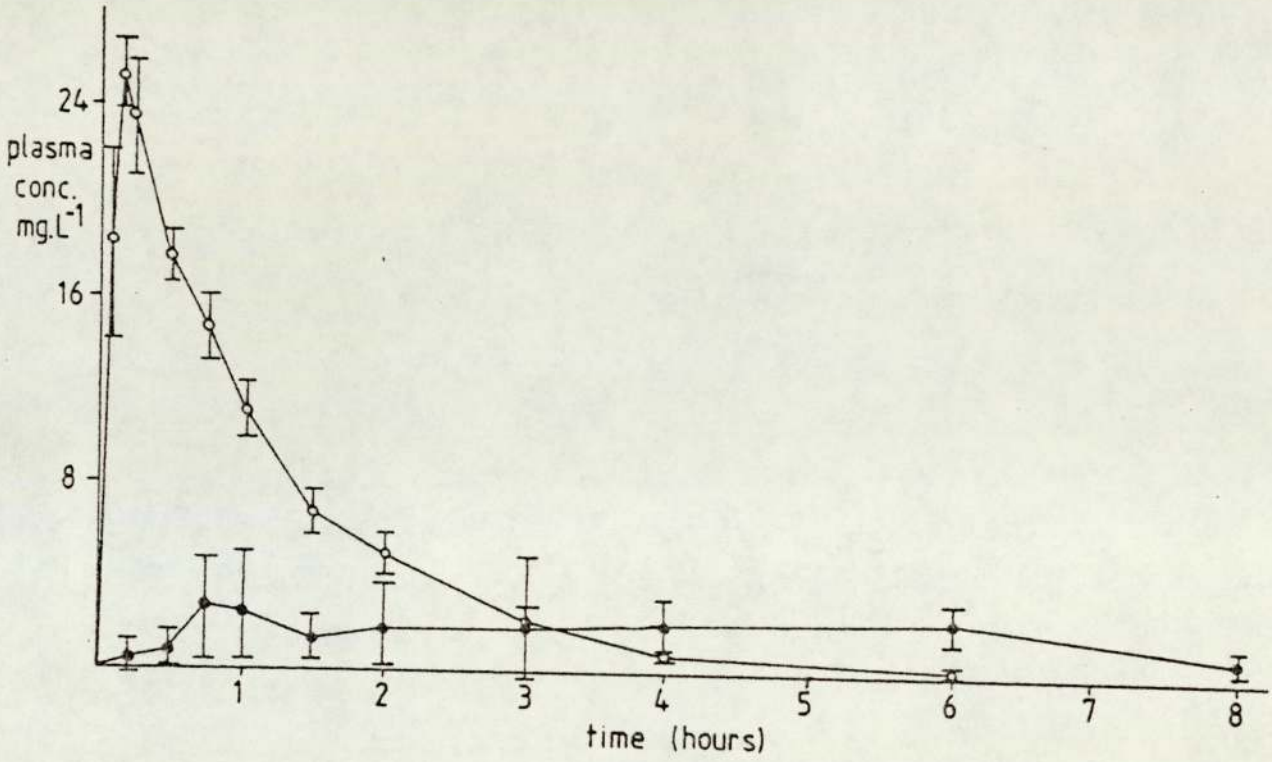

3.5.4 Discussion

The pharmacokinetics of mitozolomide in mice were fitted to a simple one-compartment model. This was supported by the lack of any apparent distribution phase following either oral or ip administration of the drug and its elimination by first order kinetics in both cases. The validity of this is further emphasized by the calculations of volume of distribution (see table 3.12) which approximate to total body water (151).

The dose escalation study was conducted using the ip route of administration. Apart from avoiding the technical problems involved in iv dosing this has facilitated a direct interpretation of the murine anti-tumour activity in terms of pharmacokinetic parameters since the majority of anti-tumour tests in mice also utilise the ip route of administration.

The dose of mitozolomide that elicited optimal activity against most of the murine tumour models was 20 $mg.kg^{-1}$. However, against some tumours, notably the P388 and L1210 leukaemias, activity was evident at single doses as low as 5 $mg.kg^{-1}$ (72).

Relating this to the pharmacokinetic parameters infers that maximum plasma concentrations of between 5 and 20 $mg.L^{-1}$ are desirable for anti-tumour activity. Also, since the results of these studies showed no dose-dependency for the pharmacokinetic parameters in the dose-range where anti-tumour activity was evident it can be argued that activity may be directly related to one of these parameters. The importance of this observation with respect to plasma concentrations and AUC values is discussed in the general discussion (section 4).

The lack of dose-dependency in the pharmacokinetics suggests that any contribution from excretion or metabolism to the fate of mitozolomide in mice is <u>via</u> mechanisms that are not saturable over the concentration range covered. The elimination of drugs is determined by contributions from metabolism, chemical degradation and excretion. Metabolism and excretion are non-reversible processes which usually follow first order kinetics and the elimination rate constant (kel) is effectively the sum of these three contributing mechanisms.

The elimination half-lives of between 0.68 hours and 0.88 hours seen in these studies agree well with the *in vitro* half-life value of 0.90 hours seen in phosphate buffer (pH 7.4; 37°C - see table 3.4) and suggest that the principal factor determining the elimination of mitozolomide *in vivo* may be chemical decomposition.

The slight decrease in the values for the $t_{\frac{1}{2}}$ over the buffer values could be due in part to the accelerated decomposition previously noted in blood plasma *in vitro* (see table 3.4). However, the contribution of this is probably limited since the volume of the plasma compartment is relatively small in comparison to that of the total body water in which the drug is distributed. Excretion and metabolism may contribute, in part, to the elimination of mitozolomide and their possible role is discussed in section 4 with reference to the results of the excretion balance and metabolism studies described in section 3.7.

The observation that mitozolomide was bioavailable following oral administration augered well for the drugs clinical development although comparison with a previous study (152) indicates that the formulation may be important with respect to the bioavailable fraction of the dose.

In this study mitozolomide was administered to mice at a dose of 20 $mg.kg^{-1}$ in a formulation of 10% DMSO in arachis oil by both ip and po routes. A higher 'F' value of 0.81 than that seen using the 10% DMSO in saline formulation was obtained but other differences in the pharmacokinetics were also seen. Absorption from both sites of administration was slower, with peak plasma levels being reached in half an hour, and the elimination half-life was longer (at 1.4 hours). In addition, the peak plasma levels attained, whilst similar by the oral route (13.16 $mg.L^{-1}$ compared to 13.85 $mg.L^{-1}$ for the DMSO/saline formulation) were much

lower following ip administration (16.31 $mg.L^{-1}$ versus 25.24 $mg.L^{-1}$). Therefore, this apparent improvement in the bioavailability using the arachis oil formulation may in fact reflect peculiarities arising from the differences in absorption characteristics when using this vehicle.

In both oral studies the drug was delivered in solution in contrast to the situation clinically where the drug would be administered using capsules containing powdered mitozolomide. As such, beyond the conclusion that the drug can be absorbed from the gastro-intestinal tract and is bioavailable in significant quantities further extrapolation of these murine results to the clinical situation is unjustified.

The use of DMSO in the formulation of mitozolomide suggested possibilites with respect to the topical administration of the drug. DMSO has been shown to be a good transdermal carrier (153) and Maddock et al previously demonstrated the successful use of transdermally applied cyclophosphamide in DMSO to treat murine tumours (154). The results described in section 3.5.3 show that significant quantities of mitozolomide are systemically available by this route although the plasma concentrations reached are only 1/10 of those seen following administration by the ip route. The use of the drug in this manner may be of value against tumours such as malignant melanoma where local application may lead to a high tumour concentration of the drug relative to host tissues.

In summary, these studies in mice show that mitozolomide fits a one-compartment pharmacokinetic model with peak plasma levels of 25.2 $mg.L^{-1}$ being reached at the optimal dose for therapeutic activity of 20 $mg.kg^{-1}$ and with a mean elimination half-life of 0.84 hours being seen over the 0.25-20 $mg.kg^{-1}$ dose range covered.

3.5.5 Pharmacokinetics of CCRG 81045

3.5.5.1 Results

The pharmacokinetics of CCRG 81045 were investigated in mice at a dose of 20 $mg.kg^{-1}$ with the principal aim of establishing the oral bioavailability of the drug. 5 mice were evaluated at each time point following administration of CCRG 81045 in 10% DMSO/saline by both oral and ip routes. Plasma samples were analysed by the method described in section 3.1.1.5 and levels of CCRG 81045 determined by reference to a calibration curve as described in section 3.5.1 for mitozolomide. The resulting pharmacokinetic profiles are shown in figure 3.18 and tabulated details of individual measurements and the AUC calculations are shown in Appendix III.

AUC values were estimated to be 37.864 $mg.hrs.L^{-1}$ for the ip route of administration and 36.914 $mg.hrs.L^{-1}$ for the oral route giving a bioavailable fraction, F, of 0.975 and indicating that CCRG 81045 is virtually completely absorbed from the gastro-intestinal tract.

Absorption of CCRG 81045 was rapid from both ip and po sites of administration with peak plasma levels being reached within 0.25 hours. Subsequent elimination was monophasic with no evident distribution phase and good agreement to a straight line was seen in both ip and po cases when plots of ln (concentration) versus time were analysed by the least squares method (correlation coefficients of 0.9625 and 0.9241 respectively). On this basis the pharmacokinetics were described by a simple one-compartment model and, because absorption from the po site was apparently complete, parameters were evaluated for both ip and po routes of administration. These parameters are shown in table 3.13. The similarities in the two sets of figures indicate

Figure 3.18 - Plots of mean concentration versus time for oral and ip doses of CCRG 81045.

● - 20 mg.kg^{-1} ip; ■ - 20 mg.kg^{-1} po.

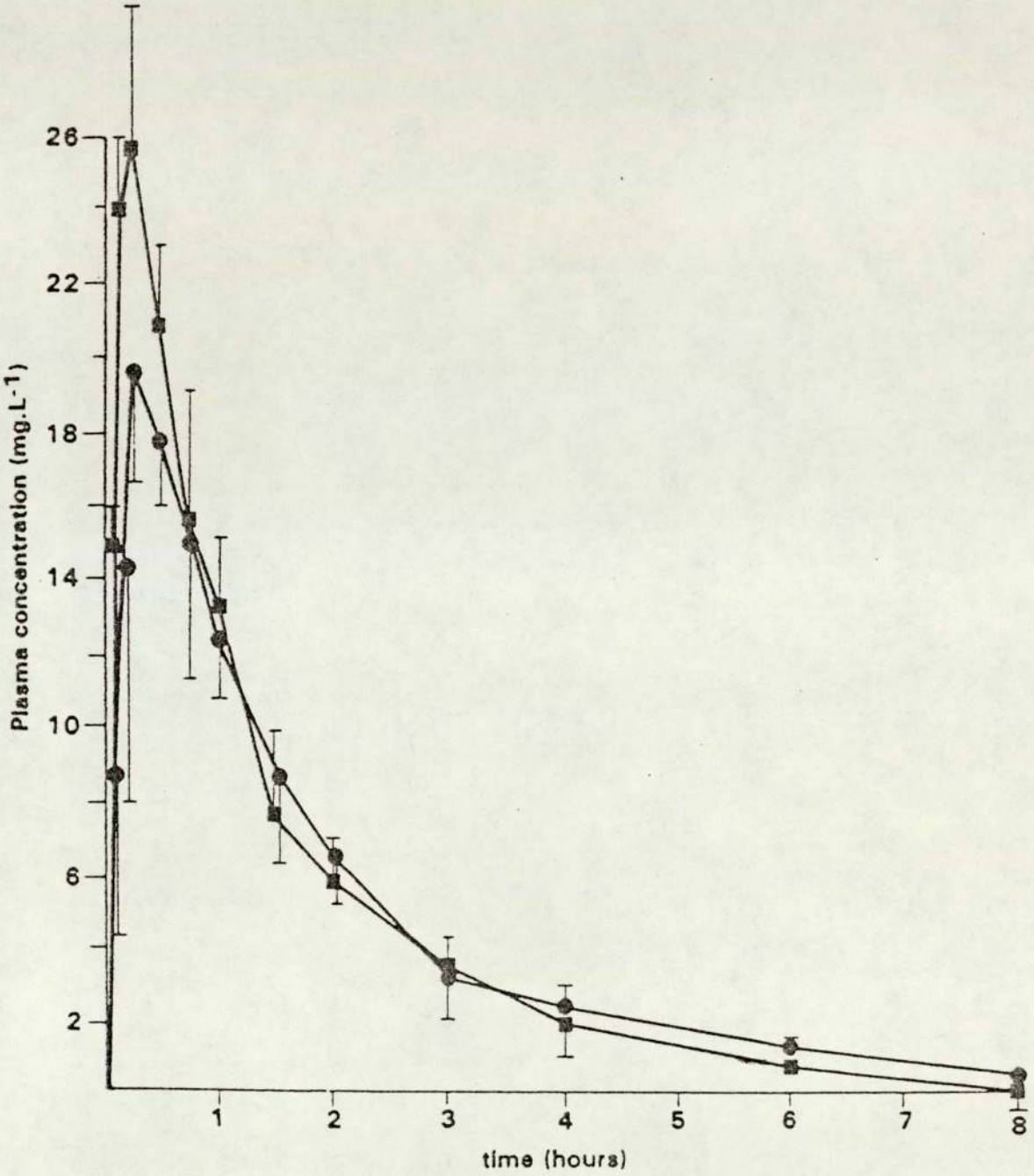

error bars indicate + (IP)/-(PO) one standard deviation of the mean value for each time point

that the pharmacokinetics are generally unaffected by oral administration although the peak plasma level following an oral dose is lower at 19.64 $mg.L^{-1}$ than the 25.84 $mg.L^{-1}$ seen following ip administration. In addition, as was found with the mitozolomide data, the elimination half-life was slightly longer (1.29 hours po compared to 1.13 hours ip). This probably reflects that the one compartment model is an over-simplification as far as detailed comparisons are concerned, with differing distribution characteristics associated with the two sites of administration accounting for the small differences observed. However, the figures for volume of distribution approximate to a compartmental volume equal to that of total body water consistent with the simple one-compartment model that has been employed.

3.5.5.2 Discussion

Although good anti-tumour activity was displayed by CCRG 81045 against murine tumours (83) it differed to that displayed by mitozolomide in that it was schedule dependent and the doses required to obtain optimal activity were much higher. Against the L1210 and P388 leukaemias doses of 100-200 $mg.kg^{-1}.day^{-1}$ over a 5 day schedule were necessary for optimal anti-tumour response compared to the single dose of 20 $mg.kg^{-1}$ used for mitozolomide.

CCRG 81045 is less soluble than mitozolomide (with a maximum solubility in saline of 4.9 $mg.ml^{-1}$) and because it was evidently less active on a molar basis than mitozolomide administering the drug iv at anything like a therapeutic dose was liable to pose severe formulation problems. Thus, if the alternative use of the oral route was to be advocated for clinical use it was essential to demonstrate a good bio-availability for CCRG 81045.

The results for this study show that in mice CCRG 81045 is essentially completely absorbed following oral administration with little change in the resulting pharmacokinetic profile. It can therefore be argued that a switch from an iv to an oral route of administration at an early stage in a clinical trial of CCRG 81045 would be justified on a pharmacokinetic basis and that this represents a valid means of by-passing the formulation problems that may be encountered in using the iv route at higher doses.

Table 3.13 - Pharmacokinetic parameters following oral and ip doses of CCRG 81045.

route	dose (mg/kg)	t 1/2 (hrs)	Cp.max. (mg/L)	AUC (mg/hrs/L)	Vd (L)
ip	20.0	1.13	25.84	37.864	0.0215
po	20.0	1.29	19.64	36.914	0.0252

3.6 Clinical Pharmacokinetics of mitozolomide

3.6.1 Dose escalation study

The pharmacokinetics of mitozolomide were monitored in all patients entered into the phase I clinical trial. The initial part of the trial involved an iv dose escalation study aimed at establishing the maximum tolerated dose (MTD) of the drug. The starting dose for the trial was set at 8.0 $mg.m^{-2}$. Doses were escalated as a "modified Fibonacci" search up to a maximum dose of 153 $mg.m^{-2}$. 30 patients received 43 doses of mitozolomide in the course of this study; 16 patients and 27 doses of which were conducted in the Birmingham half of the trial. Table 3.14 summarises the numbers of patients and courses of treatment evaluated at each dose level and shows the distribution of these between the two study centres.

Plasma samples were analysed by the method described in section 3.1.1. Levels of mitozolomide were determined from calibration curves, as previously (section 3.5.1), with 8 standards spread evenly over the concentration range of interest used to generate the calibration curve.

Table 3.14 - The number of patients and courses evaluated at each dose in the phase I trial.

	8	16.5	33	54.4	82	115	153	125
No. of patients								
Birmingham	4	4	2	3	3	4	4	2
Charing Cross	2	3	3	2	1	2	2	0
total	6	7	5	5	4	6	6	2
No. of courses								
Birmingham	4	5	2	3	3	4	4	2
Charing Cross	2	4	3	2	1	2	2	0
total	6	9	5	5	4	6	6	2

Plasma quality control samples (Q.C. samples) were routinely assayed with each sample preparation carried out. Mean Q.C. plasma concentrations of mitozolomide from each preparation were analysed for statistical variation and the results are shown in table 3.15. The mean coefficient of variation determined for the assay from the Q.C. plasma concentrations obtained from 26 separate repeats was 9.9%. It should be noted that this is an overestimate of the errors involved because:

(i) It incorporates an error margin for the dilution and preparation of the Q.C. samples themselves.

(ii) There was some evidence for a fall in the mitozolomide levels present in the Q.C. samples over their periods of use. This is emphasized by the histogram shown in figure 3.19 which plots the mean Q.C. plasma concentrations within consecutive months of use and suggests some decline in mitozolomide levels.

Table 3.15 - Statistical variation in plasma quality control samples

Q.C. batch	n	mean	standard deviation	coefficient of variation
A1	10	2.664	0.295	11.11
A2	7	3.924	0.421	11.21
A3	9	4.510	0.331	7.37
			mean	9.90

Figure 3.19 - Declining Q.C. plasma levels throughout the phase I trial of mitozolomide

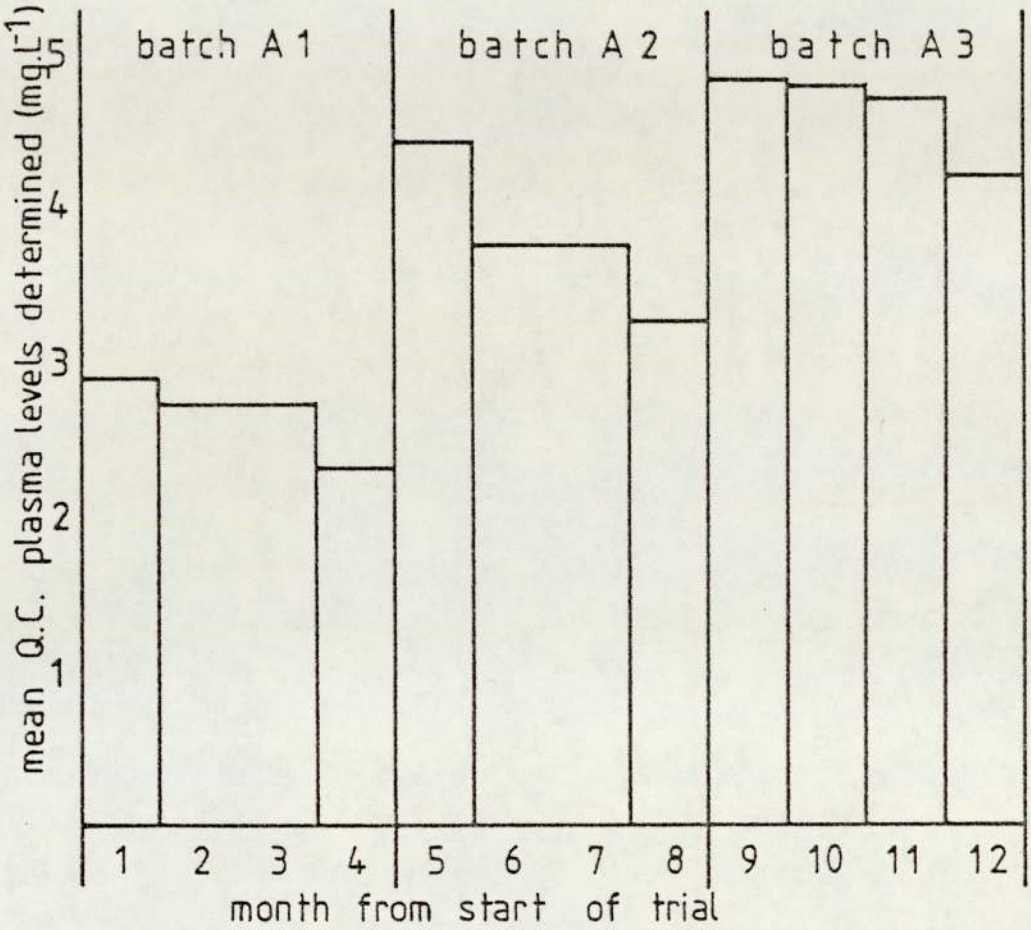

The analysis of patients' plasma samples was carried out within 20 days of treatment. The plasma levels of mitozolomide determined for the 27 courses of treatment evaluated in Birmingham are detailed in Appendix IV. Figures 3.20 and 3.21 summarise this data by showing a concentration verus time pharmacokinetic profile and a plot of ln (concentration) versus time for three courses of treatment. Plots are shown from the end of infusion (approximately 1 hour) onwards for patients 1, 13 and 21 treated at 8.0, 54.4 and 153.0 $mg.m^{-2}$ respectively, thus indicating the type of profile obtained over the range of concentrations covered. Figure 3.21 also shows that a linear regression of the ln (concentration) versus time plots by the least squares method provided a good

Figure 3.20 - Plasma concentration time profiles for three patients treated with mitozolomide

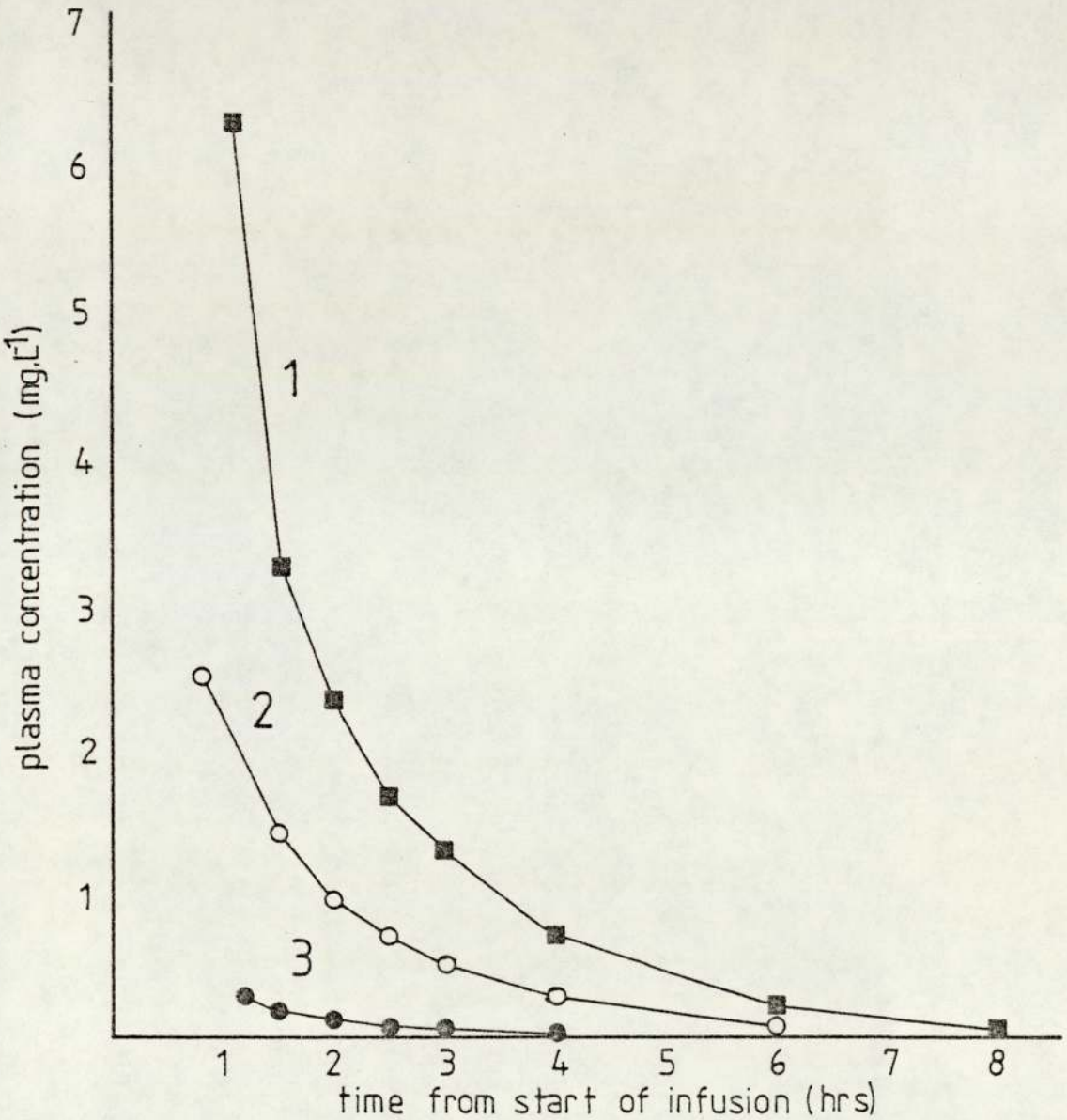

The figure shows the profiles obtained for 3 patients given iv infusions of mitozolomide during the phase I trial. Profile 1 is for patient 21 after a dose of 153 $mg.m^{-2}$ (T = 1.08 hours). Profile 2 is for patient 13 dosed at 54.4 $mg.m^{-2}$ (T = 0.8 hours) and profile 3 is for patient 1 dosed at 8.0 $mg.m^{-2}$ (T = 1.16 hours).

Figure 3.21 - Plots of ln (concentration) versus time for the three patient profiles shown in figure 3.20.

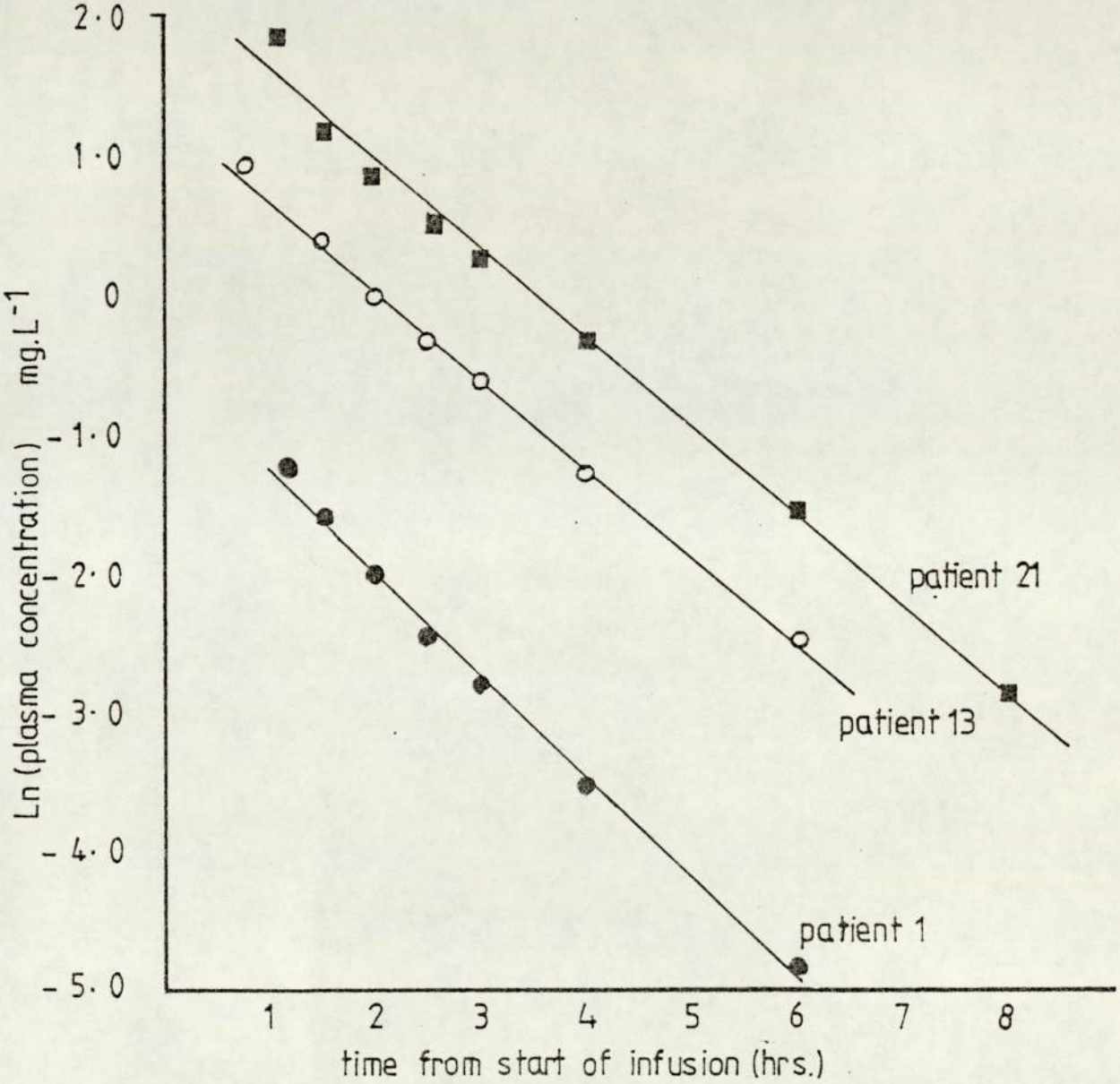

fit to a straight line. This was true throughout the study with correlation coefficients in excess of 0.97 in every case except one and >0.99 for 21 of the 27 doses; the only exception to this was patient 5 treated at 16.5 $mg.m^{-2}$ (dose 11; see Appendix IV) where a surprisingly high plasma concentration was seen at the end of the infusion. This may have been caused by the observed erratic rate of infusion of mitozolomide evident in this particular course of treatment with an accelerated infusion rate of the last 200-250 mls (giving a pseudo bolus type effect).

The results were described by a simple one compartment model and pharmacokinetic parameters evaluated accordingly. The elimination rate constant (k_{el}) was obtained from the slope of the regressed lines (slope - k_{el}) and was used to extrapolate a calculated plasma concentration at the end of infusion (Cp.ex) assuming a perfect fit to a one-compartment model. The AUC was obtained by summing the areas under the infusion and post-infusion components of the plasma concentration/time curve ($AUC_T = AUC_1 + AUC_2$). The AUC for the post-infusion phase (AUC_2) is obtained directly from the expression:

$$AUC_2 = Cp.ex./k_{el}$$

To estimate the AUC for the infusion period it is first necessary to estimate the plasma concentration at infinity (Cp.∞). Assuming a linear rate of infusion the plasma concentration at any time is given by the expression:

$$Cp.t = \frac{k_o}{Vd.k_{el}} . [1-e^{-k_{el}.t}]$$

where k_o is the first order infusion rate constant. Cp.∞ is the steady state concentration obtained when the infusion rate is balanced by the rate

of elimination and is reached only as the $e^{-k_{el.}t}$ term tends to zero - i.e. at infinity. A value for Cp.∞ can be calculated from the expression:

$$Cp.\infty = \frac{Cp.ex}{(1-e^{-k_{el.}T})}$$

This can then be substituted into an expression for the area:

$$AUC_1 = Cp. \quad [T - \frac{(1-e^{-k_{el.}T})}{k_{el}}]$$

where T is the infusion time in hours.

Calculations of plasma half-life, plasma clearance and volume of distribution were performed as previously (section 3.5.1). A detailed synopsis of the pharmacokinetic parameters evaluated for all patients in the clinical trial (both Birmingham and Charing Cross centres) together with calculations of mean and standard deviation on this data is shown in Appendix V. Table 3.16 summarises the mean pharmacokinetic parameters evaluated at each dose level.

The values for volume of distribution and clearance in this table have been normalized for variations in patient size by dividing the calculated values (tabulated in Appendix V) by the area figure for each patient (doses were determined on a $mg.m^{-2}$ basis throughout). Details of this normalization and a comparison of the variability of the data before and after normalization are shown in Appendix VI; the expected decrease in variability is seen throughout although the figures for coefficient of variation at each dose indicate considerable patient to patient variability in volume of distribution and clearance figures.

Table 3.16 - Summary of the mean pharmacokinetic parameters evaluated at each dose.

dose (mg/m2)	Cp.max. actual (mg/L)	Cp.max. calc. (mg/L)	AUC 1 (mg/hrs/L)	AUC 2 (mg/hrs/L)	AUC total (mg/hrs/L)	Vd (L/m2)	clearance (L/m2/hr)	plasma t 1/2 (hrs)
8.0	0.425	0.355	0.243	0.611	0.855	17.26	10.58	1.203
16.5	0.830	0.652	0.412	1.003	1.415	18.65	11.59	1.115
33.0	1.175	1.052	0.631	1.963	2.594	24.01	12.75	1.300
54.4	2.054	2.182	1.490	3.374	4.864	17.26	11.29	1.064
82.0	3.066	2.598	1.336	4.962	6.298	23.44	13.55	1.193
115.0	6.103	4.161	1.956	6.873	8.829	21.90	13.49	1.14
153.0	7.941	6.511	3.408	10.434	13.842	18.63	11.68	1.108
125.0	5.079	5.385	3.485	9.718	13.203	17.66	9.70	1.257

The mean value for the volume of distribution over the 43 doses covered was 19.88 Lm^{-2} (see table 3.16). An average man (weight 70 kg; height 1.65m) has an area of 1.81 m^2 and a total body water content of approximately 42 L (140). This equates to 23.2 $L.m^{-2}$ therefore the volume of distribution figure approximates to total body water and this, in combination with the good linear correlations previously described, supports the description of the pharmacokinetics in terms of a simple one-compartment model.

However, this is an oversimplification as can be seen from a comparison of the figures for Cp.max.act. and Cp.exp. (mean values are shown in table 3.16). The measured maximum plasma concentrations were consistently slightly higher than the extrapolated values with 16 of the 27 doses administered in Birmingham producing results which showed a >10% increase in Cp.max.act. values over those for Cp.exp. and only 4 doses showing no evidence of an increase. This clearly suggests a distribution phase.

The contribution of this factor to the evaluation of the pharmacokinetic parameters can be assessed by considering the data for patient 21 (profiles shown in figures 3.20 and 3.21). The measured value for the maximum plasma concentration was 6.31 $mg.L^{-1}$, approximately 35% greater than the extrapolated value of 4.65 $mg.L^{-1}$. But, a comparison of the AUC calculated assuming a one-compartment model (10.067 $mg.hrs.L^{-1}$) with that obtained from a trapezoidal estimate (10.725 $mg.hrs.L^{-1}$) shows a short fall of <10% in what was one of the more exaggerated cases of differences in calculated and measured plasma concentrations. Thus, whilst a more sophisticated modelling of the profile may have been desirable the evaluation of kinetic parameters in terms of a simple one-compartment model proved to be adequate.

Figure 3.22 shows plots of the mean values for AUC and Cp.max.act. at each dose against ascending dose and shows an approximately linear relationship in both cases with correlation coefficients for a linear regression of 0.995 and 0.989 respectively. Therefore, in agreement with the mice studies, it can be concluded that the clinical pharmacokinetics of mitozolomide exhibit no apparent dose dependency over the dose range covered.

Figure 3.22 - Plots of mean Cp.max act. and mean AUC against dose for patients entered into the iv dose escalation study.

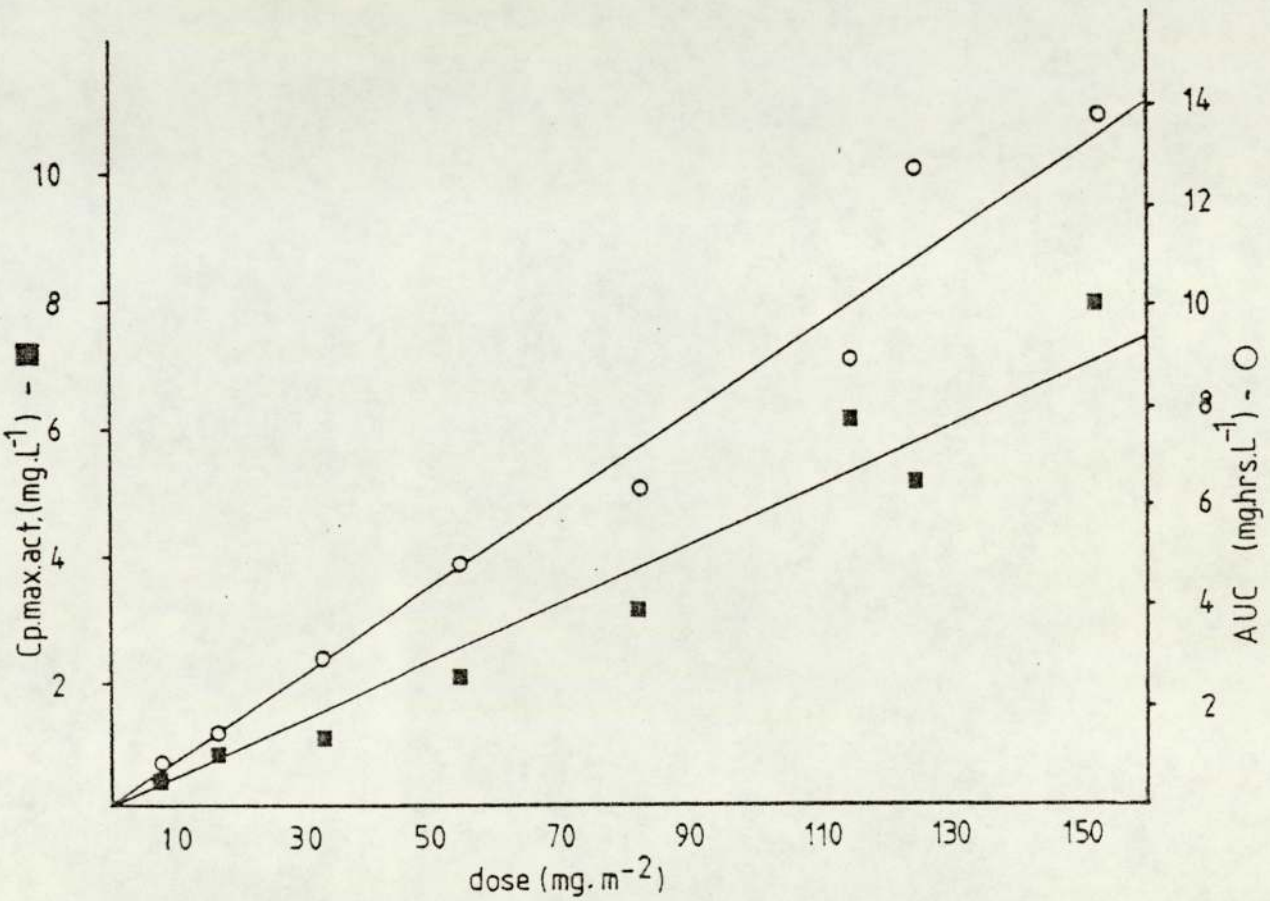

3.6.2 Oral bioavailability of mitozolomide

The oral bioavailability of mitozolomide was assessed in 7 patients as part of the phase I trial. 2 received high doses of mitozolomide (200 and 250 mgs) which necessitated a minimal 6 week gap between iv and oral doses. The other 5 patients were dosed with 50 mgs of mitozolomide on consecutive weeks. All AUC values in this part of the study were estimated by the trapezoidal method from 0 - 8 hours.

The plasma levels of mitozolomide determined for the oral and iv doses given to the 5 pateints entered into the Birmingham arm of the bioavailability study are included in Appendix IV. Figure 3.23 compares the concentration versus time profiles obtained for these 5 patients following iv and po courses of mitozolomide and table 3.17 summarises the bioavailability calculations for all 7 patients. Reference to figure 3.23 and to table 3.17 shows that mitozolomide exhibits excellent oral bioavailability with a mean F value of 0.951 (n=6). This value was obtained after omitting the results for patient 31 where an F value of 1.366 was seen. This patient was treated with 250 mgs which approximated to 140 $mg.m^{-2}$. Considerable toxicity (thrombocytopenia) was apparent such that a full 10 weeks elapsed between the oral and iv courses of treatment. Progressive disease and varying physical characteristics (e.g. weight) of the patient may have contributed to this unusual result, therefore the overall results have been considered both with and without this data (see table 3.17).

Although bioavailability of the drug in terms of total absorption (F) was high the absorption characteristics varied considerably. As figure 3.23 shows, 2 of the 5 Birmingham patients (numbers 31 and 41) exhibited rapid absorption, with the Cp.max being reached within 0.5 hours, whilst

Figure 3.23 - Plasma concentration versus time profiles for the 5 patients entered into the Birmingham part of the bio-availability study.

■ - iv dose; ● - po dose.

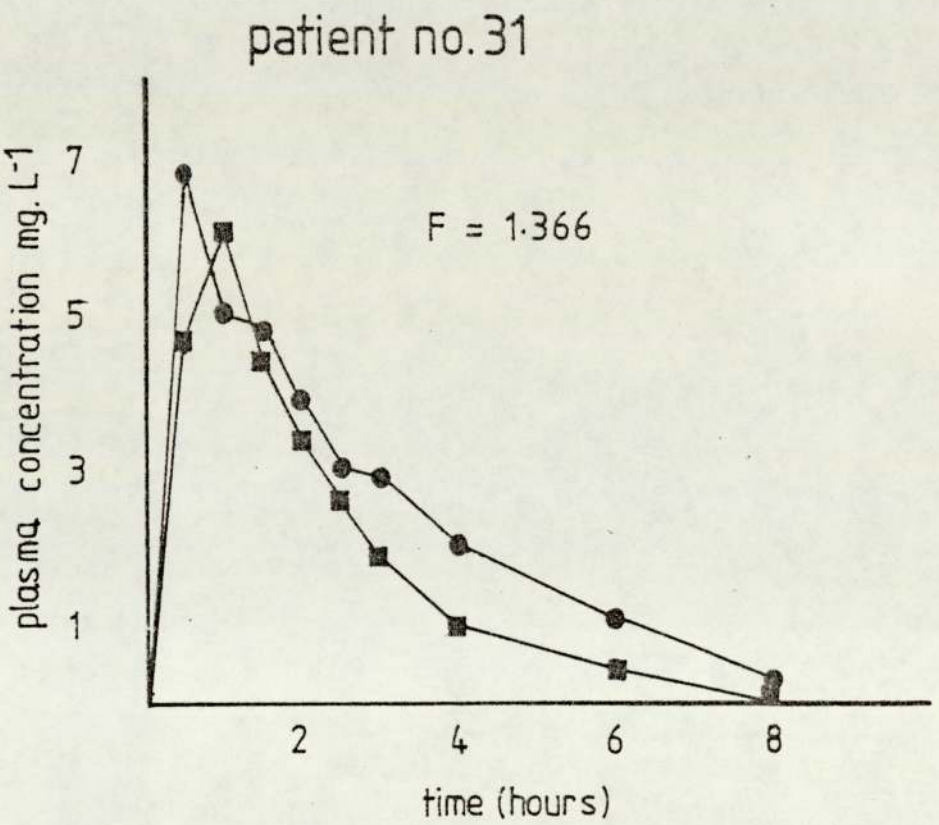

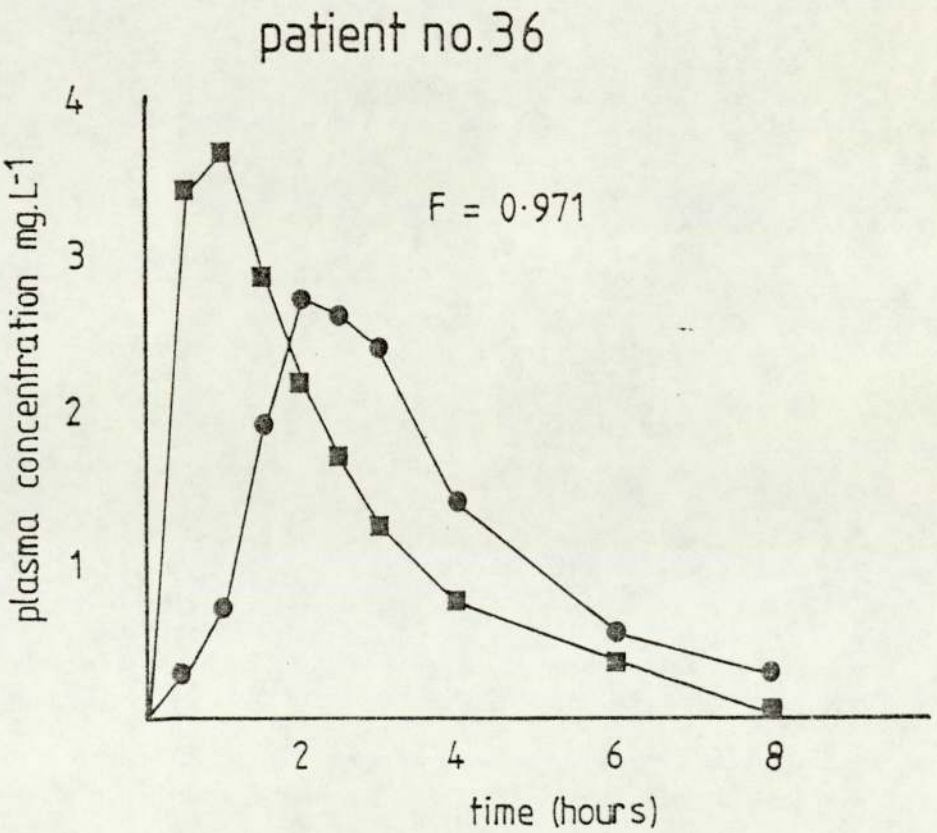

Figure 3.23 - continued

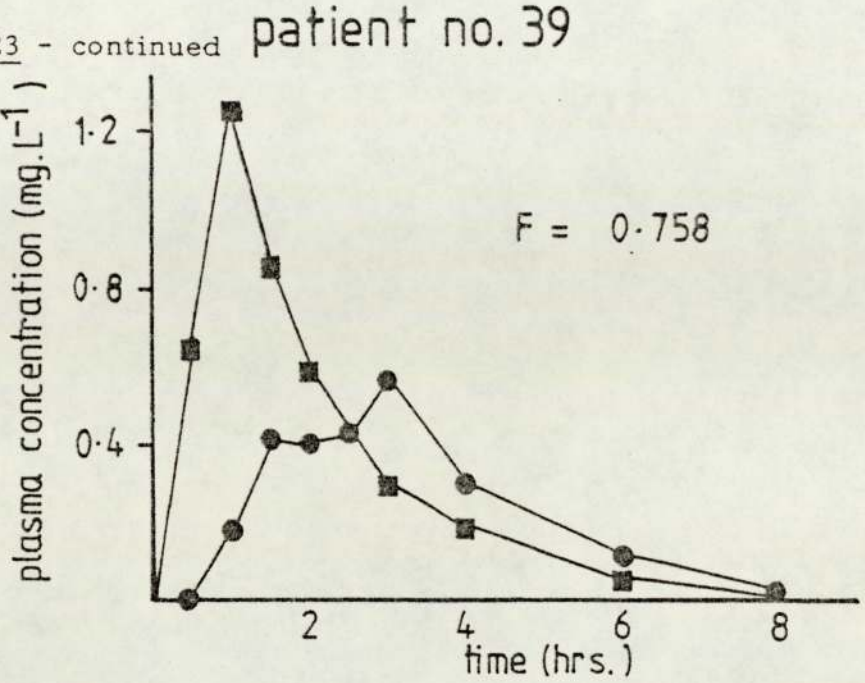

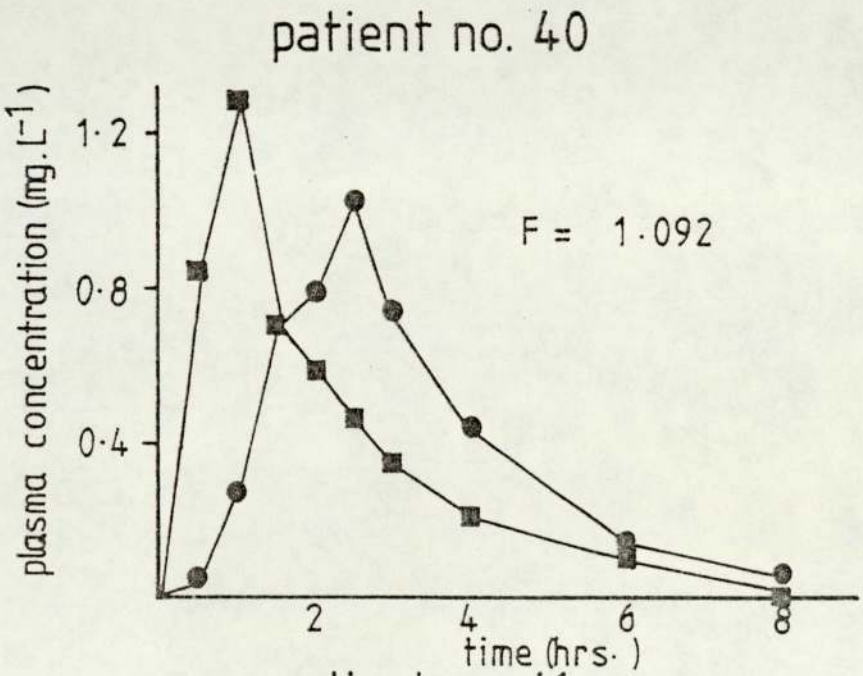

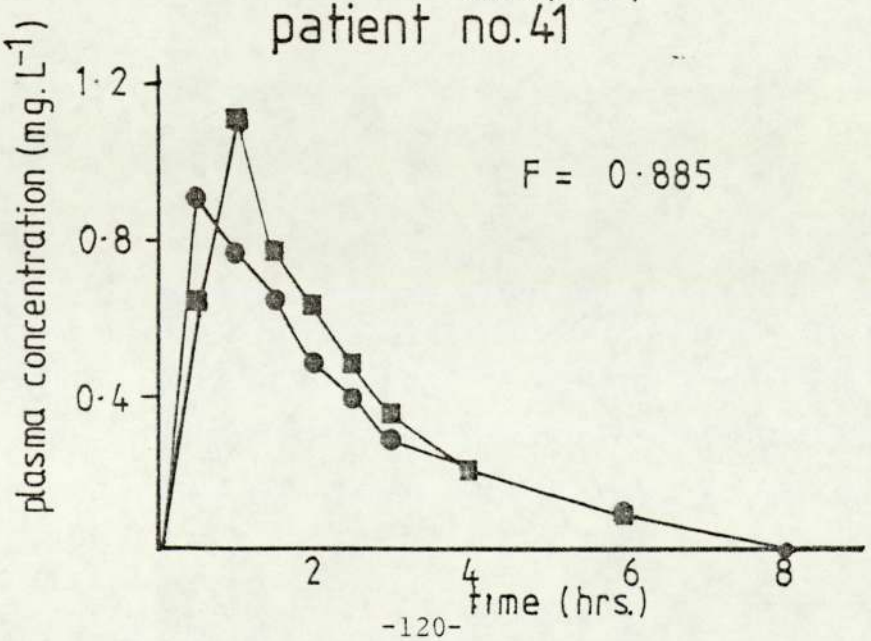

Table 3.17 - Mitozolomide oral bioavailability in the seven patients evaluated as part of the phase I trial.

pat. No.	centre	dose (mg)	AUC - iv (mg/hrs/L)	AUC - po (mg/hrs/L)	bioavailability F(AUC-iv/AUC-po)
31	B'ham	250	14.486	19.797	1.366
36	B'ham	200	9.691	9.413	0.971
38	Char.X	50	2.003	2.032	1.014
39	B'ham	50	2.491	1.889	0.758
40	B'ham	50	2.735	2.988	1.092
41	B'ham	50	2.570	2.274	0.885
42	Char.X	50	2.305	2.262	0.981
	n = 7			mean	1.010
				standard deviation	0.189
				coefficient of variation	18.754
	n = 6			mean	0.951
				standard deviation	0.115
				coefficient of variation	12.164

the other 3 (numbers 36, 39 and 40) showed a slower absorption with, in one case, no drug detectable in plasma at 0.5 hours and Cp.max values being reached between 2 and 3 hours after administration. Stomach contents often affect absorption characteristics although all these patients received oral doses in the morning having had no previous food. However, fluid intake was not monitored as stringently and this may have contributed to the variation observed if drug solubility proves to be a factor in the absorption process.

A logarithmic plot of data from the elimination phase of the plasma concentration versus time profiles following both iv and po courses was regressed to a straight line fit by the least squares method and correlation coefficients of >0.99 obtained in every case. The elimination rate constants were calculated from the slopes of these lines and the pharmacokinetic parameters evaluated assuming a fit to a one-compartment model. Table 3.18 compares the parameters evaluated for each route of administration in the 5 Birmingham patients. As the table shows values for volume of distribution and elimination half-life are not appreciably affected by oral administration and the pharmacokinetics following an oral dose of mitozolomide are therefore reasonably described by a one-compartment model.

Table 3.18 - Comparison of the pharmacokinetic parameters derived following the clinical administration of mitozolomide by both oral and iv routes.

pat. No.	route of adminstration	dose (mg)	Cp.max. (mg/L)	t 1/2 (hrs)	Vd (L)
31	iv	250	6.107	1.31	32.8
	po	250xF	6.861	1.30	32.4
36	iv	200	3.679	1.48	44.7
	po	200xF	2.671	1.80	53.6
39	iv	50	1.262	1.14	33.0
	po	50xF	0.574	1.08	31.4
40	iv	50	1.287	1.56	41.2
	po	50xF	1.033	1.33	35.2
41	iv	50	1.104	1.38	38.7
	po	50xF	0.910	1.64	46.1

3.6.3 Whole Blood Pharmacokinetics

The analysis of mitozolomide levels in samples of whole blood was performed for 10 of the doses administered in Birmingham. Samples were prepared in the same manner to that previously employed for plasma samples with the modifications described in section 2.5 incorporated. Calibration curves derived from 8 evenly spread mitozolomide concentrations in whole blood had correlation coefficients of >0.99 when regressed to a straight line fit by the least squares method. The levels of mitozolomide determined for these 10 courses of treatment are detailed in Appendix VII.

The concentration versus time profiles mirrored those previously seen in the plasma analysis except that the mitozolomide levels were lower. A regression analysis on ln (concentration) versus time plots of the data (see Appendix VII for details) produced correlation coefficients of >0.975 for the elimination phase of the drug in every case and similar values for k_{el} were determined from these plots to those previously determined for the respective plasma elimination phases. Table 3.19 compares values obtained for elimination half-life, AUC (estimated by the trapezoidal method) and 2 plasma concentrations (Cp. max and Cp.t 2 hours) from plasma and whole blood studies in all 10 patients evaluated in the whole blood study.

The slight variations in $t_{\frac{1}{2}}$ between plasma and whole blood evaluated for each patient appear to follow no particular trend as is evident from a comparison of the means in each group, with the whole blood profiles exhibiting an average $t_{\frac{1}{2}}$ of 1.390 hours and the plasma profiles an average of 1.386 hours. Thus, it would appear that the only difference between the two groups is the actual level of mitozolomide measured.

Table 3.19 - A comparison of plasma and whole blood kinetic parameters.

patient number		15	25	27	27	30	36	36	41	39	40
dose number		25	37	39	42	43	iv	po	po	iv	iv
dose,mg/m2 (T dose mgs total)		82	153	153	125	125	200T	200T	50T	50T	50T
sample age at analysis (days)	whole blood	104	55	30	13	13	12	15	11	6	6
	plasma	3	26	2	12	12	4	15	11	5	5
half-life (hours)	whole blood	1.096	1.182	1.468	1.673	1.741	1.283	1.993	1.359	0.992	1.114
	plasma	1.300	0.980	1.180	1.357	1.415	1.480	1.802	1.642	1.140	1.562
Cp.max.actual (mg/L)	whole blood	1.118	2.474	5.064	3.298	2.875	2.881	2.056	0.780	1.038	0.865
	plasma	2.976	5.827	10.218	5.761	4.397	3.679	2.671	0.910	1.262	1.287
AUC(trapezoidal) (mg/hrs/L)	whole blood	2.047	4.997	8.791	8.733	7.654	6.629	7.442	1.424	1.860	1.764
	plasma	5.568	12.279	17.554	13.248	10.306	9.691	9.412	2.274	2.491	2.735
Cp.(t = 2 hours) (mg/L)	whole blood	0.538	1.404	1.560	2.082	2.024	1.370	1.996	0.276	0.448	0.393
	plasma	1.311	3.271	3.395	3.518	2.909	2.185	2.671	0.477	0.584	0.588

3.6.4 Discussion

The clinical pharmacokinetics of mitozolomide were determined as part of the phase I trial. Plasma samples were analysed from patients who received between 8 and 153 mg.m $^{-2}$ of mitozolomide as part of the dose escalation study aimed at determining the maximum tolerated dose. Some of the patients experienced nausea and vomiting but the dose limiting toxicity was a severe thrombocytopenia with a delayed nadir at 4-6 weeks (141). The thrombocytopenia following doses of 153 mg.m $^{-2}$ of mitozolomide was at a level equivalent to WHO (World Health Organisation) grade IV and the dose was therefore reduced to 125 mg.m $^{-2}$ where 2 further patients were evaluated. The final recommended dose for the phase II studies on mitozolomide was set at 115 mg.m $^{-2}$ (141).

No dose dependency was evident in the pharmacokinetics of mitozolomide over this dose-range. It is therefore unlikely that problems associated with dose-dependent pharmacokinetics will be encountered in the clinical use of mitozolomide.

The pharmacokinetics following both oral and iv administration of mitozolomide were described in terms of a one-compartment model and it was shown that oral administration did not appreciably alter the pharmacokinetic parameters derived assuming this type of model. However, the rate of oral absorption was evidently erratic; one possible explanation for this may have been variations in fluid intake prior to dosing. This needs to be substantiated in further studies because the rate of absorption may affect the absolute concentrations of mitozolomide which can be attained and this may be important with respect to the drugs' therapeutic index. This point is discussed in section 4.

A mean elimination half-life of 1-1.4 hours agrees reasonably well with the chemical half-life at 37°C (0.97 hours in phosphate buffer pH 7.4) which, as with the mouse work, suggests that chemical degradation could

be the main mechanism for the in vivo elimination of mitozolomide. However, unlike the murine results a suggestion of a distribution phase immediately following the end of infusion suggests that a one-compartment model may be an over-simplification of the behaviour of mitozolomide in vivo.

Measured levels of mitozolomide in whole blood were consistently lower than those found in the corresponding plasma samples. Two possible explanations for this are an uneven distribution of drug between the extracellular (plasma) and intracellular (mainly red cell) blood compartments or drug instability during storage.

Table 3.19 includes data on the number of days between sample collection and analysis for both plasma and whole blood samples. Two distinct groups are immediately evident from the table, these being:

(i) patients where a long time period elapsed between the analysis of plasma and whole blood samples (i.e. data described in the first 3 columns of table 3.19 where there were gaps of 101, 29 and 28 days between analyses).

(ii) patients where there was only a short time period between plasma and whole blood analysis (i.e. data described in the remaining columns in table 3.19).

The average 70 kg man has approximately 9% of total body water present as blood (6.3L). This is distributed between the intracellular and extracellular compartments such that 4% ($\sim$ 2.8L) makes up an intracellular pool and the other 5% ($\sim$ 3.5L) is present as plasma (140). That some decomposition of mitozolomide must have occurred between the analysis of plasma and whole blood samples for the 3 patients in (i) is evident since a simple dilution of the plasma levels, assuming no drug occupied the intracellular compartment, would yield concentrations greater than those masured in whole blood.

However, unless the drug exhibits quite different stability characteristics when stored in whole blood as compared to plasma this does not explain the results seen in the other 7 patients.

An uneven distribution of the drug between the two blood compartments could result from plasma protein binding since the intracellular pool would only equilibrate with the free plasma concentration of mitozolomide. The in vitro plasma protein binding studies described in section 3.2.3.1 showed that mitozolomide was approximately 64% bound to total plasma protein. Whilst quantitiatively the importance of albumin was emphasized the binding was apparently non-specific indicating that it would vary with variations in overall plasma protein concentration. Assuming that no intracellular protein binding occurs and that transit of mitozolomide back and forth across the plasma membrane of cells is rapid (79) the nett concentration of mitozolomide in whole blood (C_{WB}) can be related to its total plasma concentration (Cp.tot) and free plasma concentration (Cp.f) by the expression:

$$C_{WB} = \frac{5.Cp.tot + 4.Cp.f}{9}$$

The free plasma concentration can be readily estimated by using the figure for in vitro plasma protein binding determined in section 2.3.2.1. Using this relationship the predicted whole blood concentrations of mitozolomide were calculated for the 10 patients assuming a range of protein binding of between 55 and 80% mitozolomide bound.

Table 3.20 compares these predicted values with the values observed in the 7 patients where plasma and whole blood samples were analysed within a short time period. 7 of the 13 values shown fall within the range with the others being very close to it. Thus, it would

Table 3.20 - A comparison of whole blood concentrations predicted assuming a 55-80% binding of mitozolomide to plasma protein to those actually measured.

patient No.	dose No.	measured whole blood conc. of mitozolomide (mg/L)		predicted range of whole blood concs. assuming binding
27	42	Cp.max.	3.298	3.71 - 4.35
		Cp.t2 hrs.	2.082	2.27 - 2.66
30	43	Cp.max.	2.875	2.83 - 3.32
		Cp.t2 hrs.	2.024	1.87 - 2.20
36	iv	Cp.max.	2.881	2.37 - 2.78
		Cp.t2 hrs.	1.370	1.40 - 1.65
36	po	Cp.max.	1.996	1.72 - 2.02
		Cp.t2 hrs.	= Cp.max.	
41	iv	Cp.max.	0.780	0.68 - 0.87
		Cp.t2 hrs.	0.276	0.28 - 0.36
39	iv	Cp.max.	1.038	0.81 - 0.95
		Cp.t2 hrs.	0.448	0.37 - 0.44
40	iv	Cp.max.	0.865	0.83 - 0.97
		Cp.t2 hrs.	0.393	0.38 - 0.44

seem that plasma protein binding offers a reasonable explanation for the observed differences in levels of mitozolomide measured in plasma and whole blood. However, the observed instability of mitozolomide during storage makes a definitive interpretation of these results difficult.

Protein binding is a dynamic situation in which the rate constants of dissociation and re-association of the drug-protein complex are unlikely to prove rate-limiting with respect to drug reactions involving the free drug pool. The binding of mitozolomide to plasma protein is therefore unlikely to affect the rate of chemical degradation of mitozolomide in vivo. Similarly, formerly held beliefs that plasma protein binding can affect the rates of metabolism and renal excretion have been largely refuted on kinetic grounds (142). Therefore, the observed protein binding is unlikely to affect the in vivo elimination of mitozolomide.

In conclusion, the clinical pharmacokinetics of mitozolomide were described by a simple one-compartment model following the analysis of patient plasma samples. An apparent volume of distribution approximating to total body water and exponential elimination of the drug supported this model. The importance of these results with respect to the therapeutic potential of mitozolomide and other anti-tumour imidazo[5,1-d]-tetrazin-4(3H)-ones are discussed in section 4.

3.7 Mitozolomide excretion balance study in mice

Excretion of a [^{14}C]-radiolabel was monitored in 2 groups of 5 mice following the administraiton of mitozolomide labelled in the chloroethyl (mice numbers 1-5) and imidazole (mice numbers 6-10) positions (see figure 3.24). Mice were dosed at 20 mg.kg $^{-1}$ (administered by the ip route) with 5-8 μCi of radioactive label in each dose.

Figure 3.24 - The structure of mitozolomide showing the positions of the two radiolabels used in the excretion balance study.

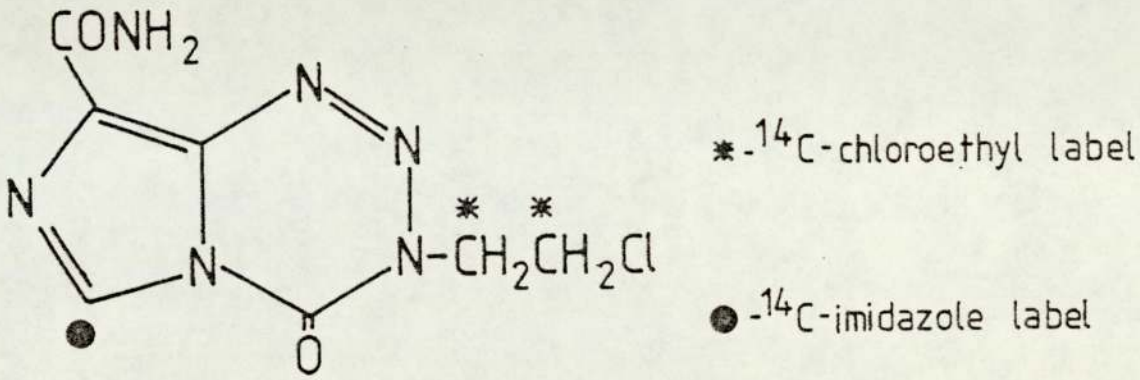

Mice were studied in pairs with urine, faeces and trapped carbon dioxide collected over a 72 hour period. Levels of radioactivity were determined by the methods described in section 2.2.3. Tabulated details of the recovery of radioactivity for each mouse during the 72 hour time course are given in Appendix VIII. Figures 3.25 and 3.26 depict the overall recoveries obtained for each mouse and show the distribution of recovered label between urine, faeces and carbon dioxide as well as the activity residual in the carcass at the end of the 72 hours. Table 3.21

Figure 3.25 - Histogram showing the recovery of label following the administration of [^{14}C]-chloroethyl-labelled mitozolomide to mice.

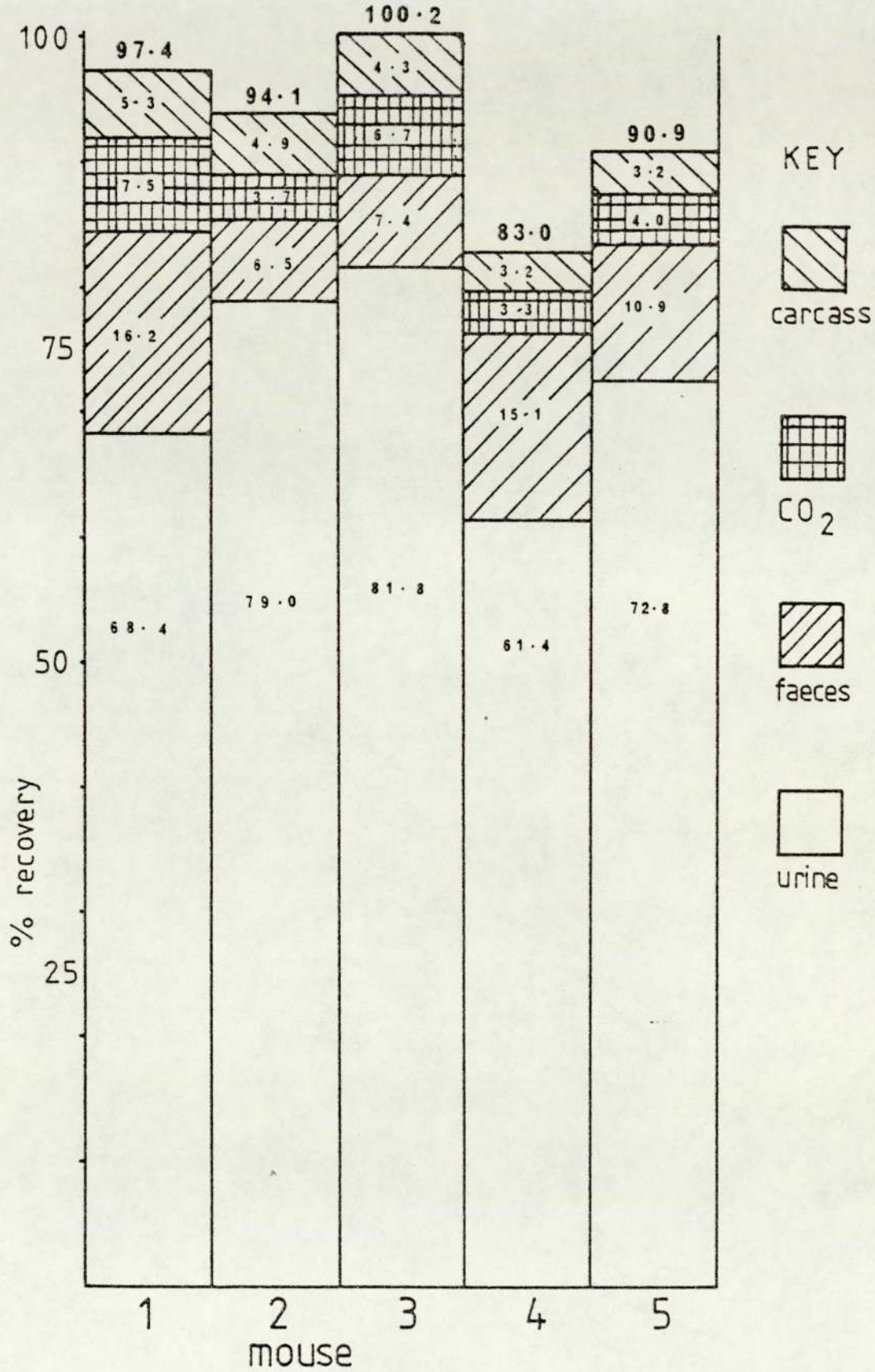

Figure 3.26 - Histogram showing the recovery of label following the administration of [^{14}C]-imidazole-labelled mitozolomide to mice.

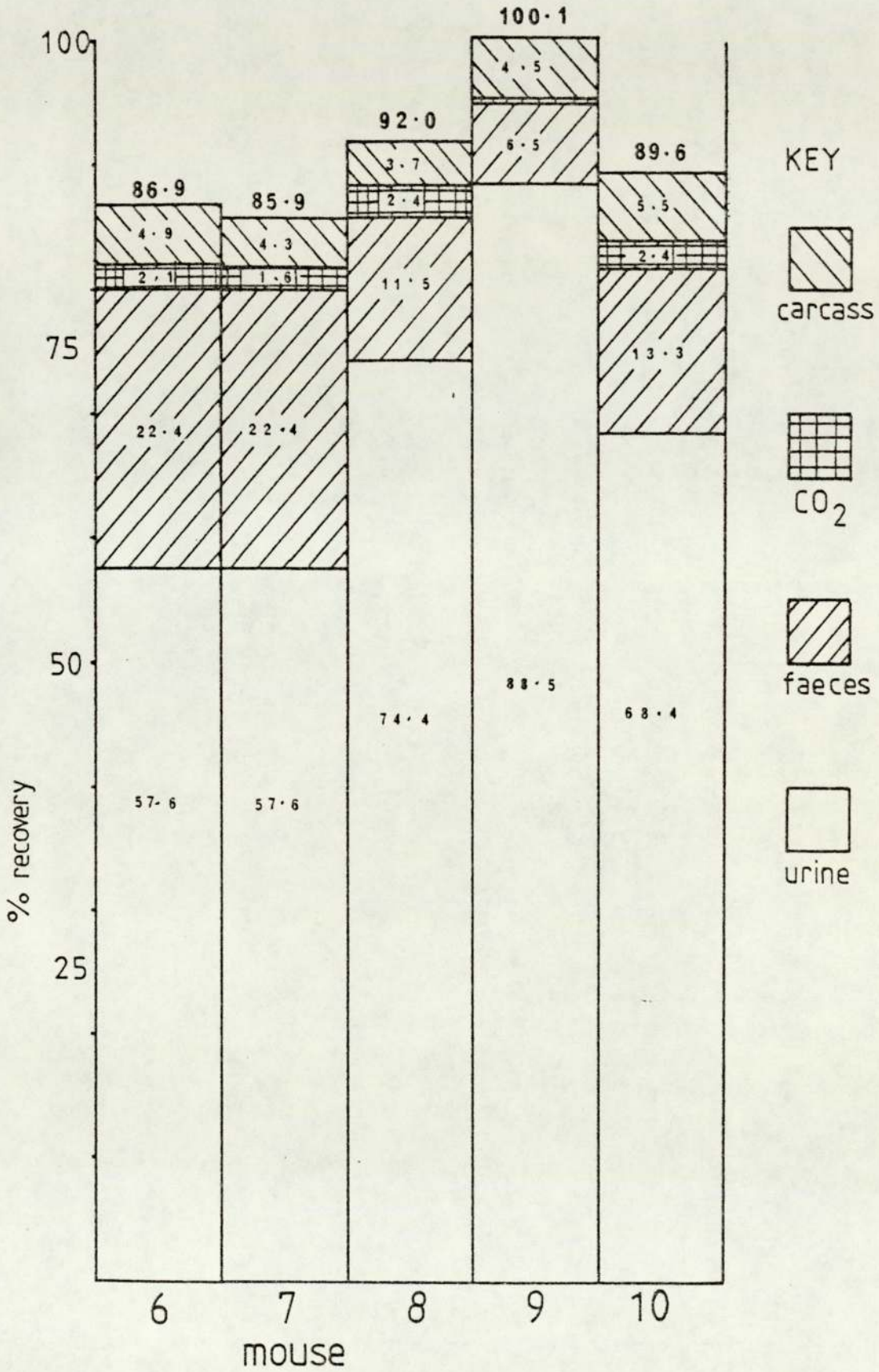

compares the mean values obtained for the 5 mice in each group.

Table 3.21 - Comparison of recoveries and distribution of radiolabel following doses of [^{14}C]-chloroethyl and [^{14}C]-imidazole labelled mitozolomide to mice.

	14C-chloroethyl label		14C-imidazole label	
	mean	coefficient of variation	mean	coefficient of variation
URINE	72.66	11.29	69.31	18.68
FAECES	11.20	39.08	15.20	46.04
CARBON DIOXIDE	5.04	38.04	1.78	46.20
CARCASS	4.20	22.91	4.60	14.63

The principal route for elimination of both labels was renal with between 57 and 88% of the dose excreted in urine. In all 10 mice the majority of this urinary excretion occurred within the first 12 hours, with only mice 1 and 9 excreting more than 10% of the dose in subsequent time periods. The next most abundant source of excreted radioactivity was the faeces where, again, the majority of this excretion occurred within the first 12 hours. Levels of between 6.5 and 22% of dose were detected in the faeces. However, problems encountered with the metabolic cages and food dispensers, whereby dislodged food altered the channelling of

urine into the appropriate trap, meant that, particularly in mice 6 and 7, the activity measured as excreted in faeces in the first 12 hour time period may have been an overestimate due to some contaminating urine derived radioactivity being included.

The amount of activity excreted as carbon dioxide was relatively insignificant being less than 8% in all cases and less than 4% in 8 out of the 10 mice (including all those treated with the imidazole labelled drug). But, there was a difference between the two labels, with a mean of 5% of the [^{14}C]-chlorethyl derived label appearing as carbon dioxide compared with only 1.8% of the [^{14}C]-imidazo derived label.

After the first 12 hour period excretion of radioactivity in both urine and faeces was at a low level and exhibited a gradual decline, whilst the radioactivity residual in the carcass at the end of the 72 hour time period was similar for both groups of mice (less than 6% of dose activity throughout). This may reflect the covalent binding of reactive intermediates to biological macromolecules or the incorporation of [^{14}C] into the metabolic pool and its subsequent excretion as a consequence of tissue metabolic turnover.

The mean overall recovery of radiolabel was in excess of 90% for both [^{14}C]-chloroethyl and [^{14}C]-imidazole labelled studies with a coefficient of variation of 7.1 and 6.25% respectively. The nature of the experiment is such that this sort of variation would be expected but the mean overall recoveries were slightly lower than anticipated. This may have been due to the loss of volatile end products particularly from the [^{14}C]-chloroethyl label since chemical decompositon is likely to yield volatile products such as 2-chloroethanol, 2-chloroacetaldehyde and 2-chloroacetic acid. However, it may also be a reflection of methodological inaccuracies. The determination of the levels of radioactivity in faeces

and carcass was *via* a homogenisation/solubilisation method which resulted in samples which are difficult to count accurately by liquid scintillation counting due to a variable sample 'quench'. Compensating quench curves partially alleviate this problem but an alternative approach using a sample oxidiser (whereby samples are combusted and $[^{14}C]$-CO_2 trapped and counted) would have been a preferable approach had this facility been available.

This excretion balance study showed that the principal route of the excretion of mitozolomide and its *in vivo* products was renal, as evidenced by the measured fate of $[^{14}C]$-radiolabels sited in the chloroethyl and imidazo positions of the molecule. However the detection of between 10 and 15% of the administered radioactivity in the faeces shows that alternative routes of excretion are also important. This may be indicative of biliary excretion but since administration of the drug was *via* the ip route concentration gradients would have been favourable for a general diffusion of drug into the gastro-intestinal tract, thus the source of this faecal radioactivity remains speculative.

In order to gain a more informed picture of the fate of mitozolomide the urine fractions were examined by HPLC and TLC.

3.8 Assay of urine samples from the excretion balance study.

3.8.1 Assay of mitozolomide levels

The 12 and 24 hour urine samples from all 10 mice used in the excretion balance study were analysed for parent drug by the standard method described in section 3.1.1. The method was adapted for this assay by using fraction collection and liquid scintillation counting as a means of quantifying the mitozolomide levels present. This was necessary because interfering endogenous material made analysis by UV peak areas impossible.

Standards were prepared consisting of known quantities of mitozolomide added to control urine. These were used to calibrate the sample preparation procedure to enable the correction of sample counts for unextracted drug and to identify the precise eluent fraction for collection. A 1 ml sub-sample of each 12 and 24 hour urine sample was assayed in duplicate. No mitozolomide was detected in any of the 24 hour urine samples. The levels determined in the 12 hour samples are summarised in table 3.22. It was evident that significant amounts of mitozolomide were being detected in the urine with a mean of 17.43% (n=10) of the dose being excreted as parent drug. However, the result obtained for mice 9 and 10 revealed a surprisingly low level of mitozolomide when compared to that seen in the other 8 mice and since the urines were also analysed by the ion-pairing HPLC method developed in section 3.13 and by TLC the detailed consideration of these results was deferred until all the analytical data was available.

Table 3.22 - Quantification of mitozolomide levels in the 12 hour urines from mice used in the excretion balance study.

mouse	mitozolomide dose		mean counts in mitozol.peak	12 hour urine mitozolomide	
	ug	dpm x 1 000 000	dpm x 1 000 000	ug	% dose
1	485.0	16.499	2.612	76.8	15.83
2	452.5	15.800	3.844	110.1	24.33
3	467.0	15.293	4.505	137.5	29.45
4	430.0	15.491	3.020	83.8	19.50
5	452.5	16.301	3.840	105.6	23.33
6	450.0	12.920	2.086	72.7	16.15
7	422.5	12.121	2.892	101.4	23.87
8	465.0	6.813	0.839	57.3	12.32
9	467.0	12.660	0.444	16.4	3.50
10	467.0	12.660	0.764	28.2	6.04
			mean, n = 10 mean, n = 8		17.43 20.60

3.8.2 Analysis of the mouse urine samples by the ion-pairing HPLC method

The 12 hour mouse urines from the excretion balance study were analysed by the HPLC method described in section 3.1.3. Samples were prepared for assay by adding 250µl of acetonitrile and 250µl of acetic acid (5%) to 500µl of urine immediately after thawing. Precipitated material

was removed by centrifugation. The analysis of each urine sample was performed in duplicate with eluent fractions collected and the levels of radioactivity determined by liquid scintillation counting. 25µl injections were made such that between 7 and 26 000 dpm were applied to the column (depending upon the urine sample).

Total recovery of radioactivity from the column was high (with a mean value of 91%) in all but two cases. Injections were performed using a WISP and variations in the metered injection volume may account for these two results. The total volume of eluent for each sample analysis was 20 mls and this dilution of the applied radioactivity imposes counting difficulties such that it would be predicted that a slightly less than 100% apparent column recovery would be obtained. Because of this all the results were normalized assuming a 100% column recovery.

The results obtained from the analysis of the 12 hour urines from the mice treated with [^{14}C]-chlorethyl-labelled mitozolomide are shown in table 3.23 and those from the mice treated with the [^{14}C]-imidazole-labelled drug in table 3.24. In both tables only distinct 'peaks' of radioactivity (>5% of that applied) have been characterized. Fractions co-eluting with mitozolomide, AIC and N-(2-hydroxyethyl)-AIC standards were characterized accordingly. This meant that one distinct fraction (RT 2.5-4 minutes) remained unidentified in the elution profiles generated by the 5 mice treated with [^{14}C]-imidazole labelled mitozolomide and 2 fractions (RT's of 1.5-4 minutes and 4-5.5 minutes) were similarly unidentified in the elution profiles generated by the mice treated with the [^{14}C]-chloroethyl-labelled drug. It was hoped that TLC analysis of the urine samples would assist in determining whether these unknown fractions consisted of one or more components.

Table 3.23 - Analysis of 12 hour urine samples from the mice treated with [^{14}C]-chloroethyl labelled mitozolomide by the 'ion-pairing' HPLC method.

FRACTION/IDENTIFICATION		1	2	3	4	5	mean	coeff. of variation
unknown, RT 1.5 - 4 mins	% urine	60.9	54.1	45.0	57.2	51.6	53.8	11.2
	% dose	34.0	37.7	32.8	27.7	32.7	33.0	10.8
unknown, RT 4 - 5.5 mins	% urine	7.4	6.7	6.3	6.6	5.3	6.5	11.8
	% dose	4.1	4.7	4.6	3.2	3.4	4.0	17.0
mitozolomide RT 7.2 - 8.95 mins	% urine	18.8	24.3	35.3	27.5	29.4	27.1	22.6
	% dose	10.5	16.9	25.7	13.3	18.7	17.0	34.1
N-(2-hydroxyethyl)-AIC RT 11.1 - 13.1 mins	% urine	3.1	7.3	5.0	4.9	5.6	5.2	29.0
	% dose	1.7	5.1	3.6	2.4	3.5	3.3	39.3

Table 3.24 - Analysis of 12 hour urine samples from the mice treated with [^{14}C]-imidazo-labelled mitozolomide by the 'ion-pairing' HPLC method.

FRACTION/IDENTIFICATION		6	7	8	9	10	mean	coeff. of variation
unknown, RT 2.5 - 4 mins	% urine	31.0	33.4	25.4	21.4	22.7	26.8	19.5
	% dose	16.9	17.1	17.2	15.3	14.0	16.1	8.7
mitozolomide RT 7.2 - 8.95 mins	% urine	18.3	16.7	17.5	27.6	27.0	21.4	25.2
	% dose	10.0	8.6	11.9	19.8	16.7	13.4	35.1
N-(2-hydroxyethyl)-AIC RT 11.1 - 13.1 mins	% urine	5.7	5.7	3.6	9.5	8.7	6.6	36.4
	% dose	3.1	2.9	4.1	6.8	5.4	4.5	36.8
AIC RT 13.9 - 17.4 mins	% urine	20.5	22.3	16.8	24.7	23.6	21.6	14.3
	% dose	11.2	11.4	11.4	17.7	14.6	13.3	21.5

3.8.3 Analysis of mouse urine samples by TLC

The 12 hour urines from all 10 mice were analysed by TLC on cellulose using the systems described in section 2.1. The urine samples from mice 6-10 (treated with the imidazole-labelled drug) were chromatographed against AIC, N-(2-hydroxyethyl)-AIC and mitozolomide standards and samples from mice 1-5 (treated with the chloroethyl-labelled drug) against N-(2-hydroxyethyl)AIC and mitozolomide. Similar autoradiograms were obtained from the 5 mice in each group with the same spectrum of bands and approximately the same relative intensity of these bands apparent in the urines from the individual mice.

Four principal bands were evident in the autoradiograms of the urines from mice numbers 6-10. These corresponded to mitozolomide (Rf 0.87), AIC (Rf 0.50), N-(2-hydroxyethyl)-AIC (Rf 0.58) and an unknown component with an Rf of 0.70. The band for the N-(2-hydroxyethyl)-AIC was diffuse indicating that more than one component was present. In addition, 4 fainter bands (visible only on autoradiograms developed over a long period) were seen with Rfs of 0.19, 0.26, 0.32 and 0.37 respectively.

Four main bands were also seen in the autoradiograms of the urines from the mice treated with [^{14}C]-chloroethyl-labelled mitozolomide (numbers 1-5). One of these corresponded to mitozolomide with the other 3 having Rf's of 0.2, 0.68 and 0.76 respectively. Interestingly a band corresponding to the Rf of N-(2-hydroxyethyl)-AIC was only very faintly visible indicating that the moiety identified as N-(2-hydroxyethyl)-AIC in the urines from mice 1-5 was wrongly assigned. 2 other bands were faintly visible, one with a similar Rf to an AIC standard (Rf 0.5) and the other with an Rf of 0.29.

Figure 3.27 - Autoradiograms showing radioactive components in 12 hour urine samples following administration of [^{14}C]-chloroethyl and [^{14}C]-imidazole labelled mitozolomide to mice with respective in vitro decomposition samples shown for comparison.

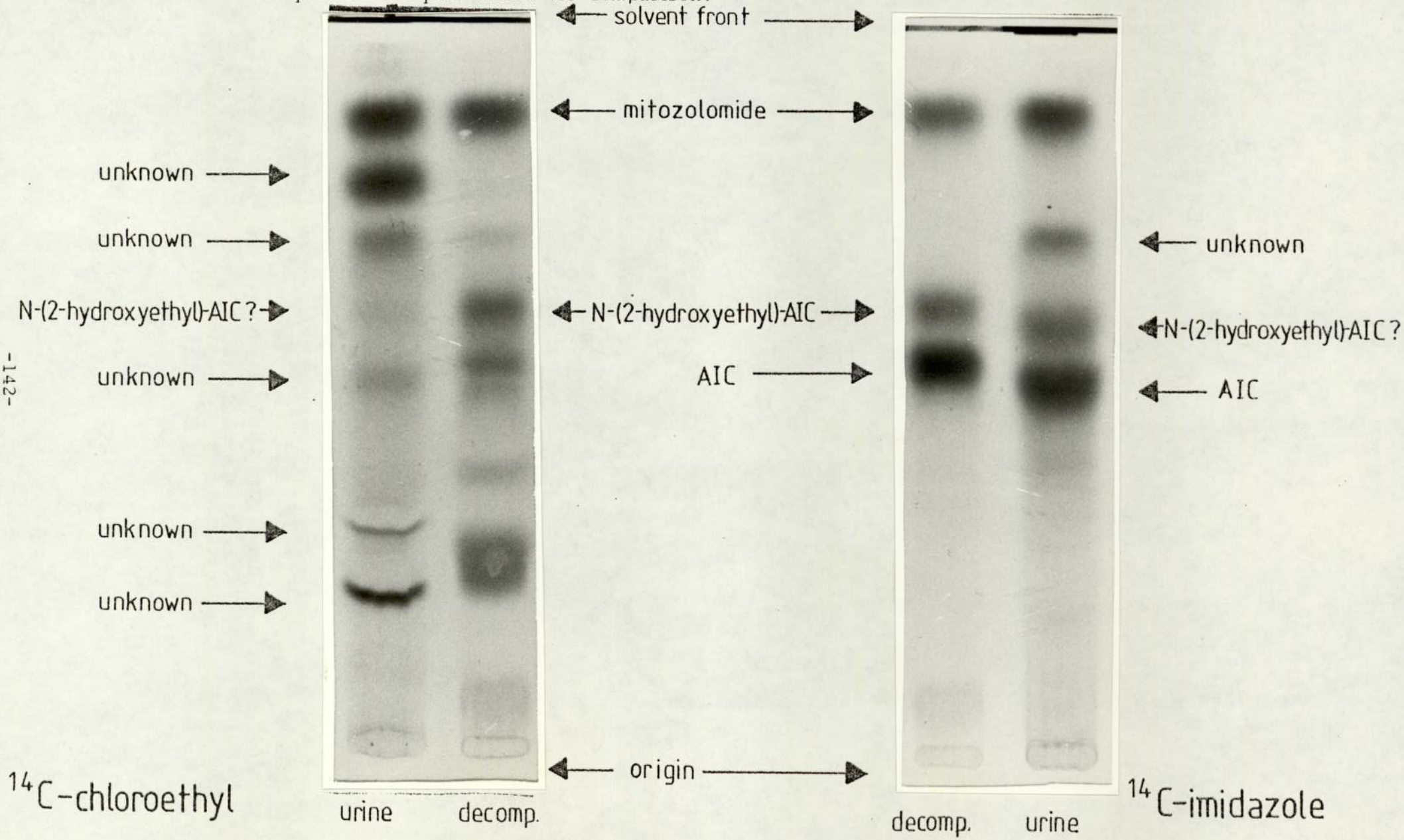

Examples of these autoradiograms are shown compared to autoradiograms derived from decompositons of mitozolomide (using both radiolabels) in figure 3.27.

3.8.4 Discussion

The excretion balance study clearly identified excretion via the renal route as being of prime importance in the elimination of [^{14}C] following the administration of [^{14}C]-labelled mitozolomide to mice. It was important to establish the levels of parent drug excreted in this manner and to attempt to identify and quantitate other products. Mitozolomide levels were determined by two methods and a comparison of the results obtained is shown in table 3.25.

The values obtained in the parent drug assay for mice 9 and 10 were surprisingly low and the results from the ion-pairing method suggest that this was a methodological error since in all the other 8 mice levels of mitozolomide determined by this latter method were lower. The reason for this is unclear but 2 possible explanations were interference, in the case of the parent drug assay, and loss of mitozolomide in the sample preparation for the ion-pairing HPLC method. Interfering endogenous material made the quantification of the mitozolomide peak by UV impossible in both assays. Despite this, the precise co-chromatography of the radiolabel peak with a mitozolomide standard made it unlikely that there was an interfering radiolabelled product in the parent drug assay whilst counting before and after the precipitation of protein showed no activity was lost in this process when using the ion-pairing method. Another explanation may be drug instability during storage. Urine samples were stored frozen but thawed and re-frozen twice in the month separating analysis by the two methods. Therefore, drug instability in storage may be the most likely explanation for the observed difference in the measured levels of mitozolomide.

Regardless of these problems it was evident that significant levels of mitozolomide were being excreted by the mice (15-20% of dose). This, and other evidence from the excretion balance study and urine assays suggests a re-assessment of the role of chemical degradation in the in vivo fate of mitozolomide may be necessary.

The in vivo studies described in section 3.3 showed AIC to be the principal imidazole containing product arising from the chemical degradation of mitozolomide in buffers at physiological pH and temperature. Quantification of AIC levels by the ion-pairing HPLC method gave a mean value of 13% of dose. It is known that AIC can be incorporated into purine biosynthesis by salvage pathways (7) but the value is still lower than might be expected if chemical degradation were the main fate of administered mitozolomide. Approximately 4% of the dose activity was quantified by the ion-pair method as being N-(2-hydroxyethyl)-AIC, the second most abundant imidazole-containing product in decomposition studies. However, TLC analysis suggested that this may have been wrongly assigned since a band with the correct Rf value was only faintly visible in the autoradiograms of the urines from the mice treated with the [^{14}C]-chloroethyl labelled mitozolomide.

TLC of the urines from the mice treated with [^{14}C]-imidazole-labelled mitozolomide showed an additional unknown moiety with an Rf of 0.7 and it is likely that the 16% of dose activity detected by the ion-pair HPLC method (in the RT range 2.5-4 minutes) in the urines from mice 6-10 consisted of this moiety and the unknown co-chromatographing with N-(2-hydroxyethyl)-AIC in the thin-layer analysis.

The excretion of 11-15% of the dose activity in the faeces (from both labels) suggested the possibility of some biliary excretion. The biliary route is usually important for the excretion of metabolites rather

than parent drug and this, in conjunction with the urine tests, implicates a contribution from metabolism to the fate of mitozolomide *in vivo*. Hepatic enzymes are known to be capable of N-dealkylation (158) and the increased excretion of $[^{14}C]$-CO_2 following administration of the chloroethyl labelled drug versus the imidazole labelled drug infers that this sort of reaction may be occurring. Other metabolic reactions (such as hydrolysis of the 8-carbamoyl group) are also possible. However, this postulated role for metabolism must remain speculative until the unknown components in the urine are identified and further metabolic studies conducted.

Table 3.25 - A comparison of the urinary levels of mitozolomide following analysis by the two methods employed.

all figures are % dose										
MITOZOLOMIDE DETERMINED BY PARENT DRUG ASSAY										
1	2	3	4	5	6	7	8	9	10	mean
15.8	24.3	29.5	19.5	23.3	16.2	23.9	12.3	3.5	6.0	20.6 n = 8
MITOZOLOMIDE DETERMINED BY ION-PAIR METHOD										
1	2	3	4	5	6	7	8	9	10	mean
10.5	16.9	25.7	13.3	18.7	10.0	8.6	11.9	19.8	16.7	15.2 n = 10

4 General discussion

It was the general aim of the work reported herein to investigate aspects of the metabolism, decomposition and pharmacokinetics of a series of compounds based on the novel imidazo[5,1-d]-1,2,3,5-tetrazin-4(3H)-one heteorcycle in the hope of identifying aspects which would lead to an improved therapeutic benefit over established anti-tumour agents. Most of the work reported concerns the lead compound in the series, mitozolomide, but some work has also been conducted on CCRG 81045 (the 3-methyl analogue).

Previous decomposition studies had identified two likely mechanistic routes for the break-down of mitozolomide (see figure 1.4), one proceeding *via* reversal of the synthetic pathway, so generating diazo-1C and 2-chloroethylisocyanate and the other by a ring-opening and decarboxylation process to generate the triazene MCTIC.

The analysis of products arising from decomposition experiments in physiological buffers confirmed the second of these pathways as the one likely to predominate *in vivo*. AIC was the principal end-product arising from this route of degradation accounting for 66% of the starting mitozolomide on a molar basis. Although the instability of MCTIC has prevented its identification in these experiments *per se* its previous isolation in chemical studies (5) and the similarity in the spectrum of products arising from MCTIC and mitozolomide decompositions reported herein is good evidence for the decomposition of mitozolomide *via* this triazene under physiological conditions.

The only apparent difference was the appearance of the N-(2-chloroethyl)- adduct of AIC in the products from the decomposition of MCTIC but not in the products from mitozolomide. The N-(2-hydroxyethyl)- adduct was identified in both cases and previous studies

had suggested a mechanism for the formation of these adducts in the decomposition of MCTIC which proceeded *via* an anion of the triazene (12). However, under physiological conditions it is likely that MCTIC degradation proceeds *via* a proton catalysed mechanism which would result in the generation of a chloroethyldiazonium species and possibly chloroethyl carbonium ions (150). Reactions between these intermediates and the amine group of AIC could also explain the formation of the adducts.

The observed appearance of the N-(2-chloroethyl)- adduct in decompositions of MCTIC but not of mitozolomide and the inconclusive appearance of the N-(2-hydroxyethyl) adduct in the mouse urines both support a situation where adduct formation is dependent upon the local concentration of reactants and the presence of competing nucleophiles. Thus, the results lend support to the latter mechanism for the observed formation of the AIC-adducts in decompositions.

The half-life for the 1st. order decomposition of mitozolomide in phosphate buffer (pH 7.4; 37°C) was shown to be 0.9 hours (see table 3.4). This ability to release MCTIC *via* chemical decomposition at an appreciable rate coupled to the relative ease of the formulation and handling of mitozolomide are immediate advantages for the drug over BCTIC. This Bis-2-chlorethyl derivative of DTIC was the most active of the triazenoimidazoles in anti-tumour screens and was postulated by Shealy to act *via* an enzymic N-dealkylation to MCTIC (13).

Mode of action studies on MCTIC and 2-chloroethylnitrosourea (see section 1.5) imply a similar cytotoxic mechanism for both these agents with the cross-linking of DNA as the putative critical lesion. Both agents are believed to decompose *via* a transient chloroethyldiazonium species which acts as the alkylating moiety.

MCTIC is a very reactive agent in its own right as evidenced by the attempts to monitor its decomposition at pH 7.4 and 22°C. Complete

decomposition was evident in the 2 - 2.5 minutes between the addition of the drug to the buffer and the first analysis. It is therefore likely that the critical factor in the action of mitozolomide is its performance as a pro-drug in generating MCTIC within the required intracellular environment. Therefore, the rate of ring-opening of the parent molecule rather than the kinetics and distribution of MCTIC itself will determine the activity of the drug. To substantiate this it is necessary to develop suitable analytical methodology for the accurate quantification of MCTIC and whilst this has been unsuccessful to date the suggested use of a fluorescent nucleophile in a derivitisation procedure may prove a fruitful approach in further investigations.

On the assumption that it is the kinetics and the locality of the generation of MCTIC which act as the determinant for cytotoxicity the observed exquisite sensitivity to pH variations in the decomposition of mitozolomide becomes a critical factor in the drugs action.

A plot of the first order rate constants for the decomposition of mitozolomide (k_{Mit}) against ascending pH over the range 7.2 - 7.8 suggested an exponential relationship between the two parameters (see table 3.5 for half-life data). This would be expected for the ring-opening of mitozolomide since this is subject to base catalysis. A linear regression of a plot of ln (k_{Mit}) versus pH produced a correlation coefficient of 0.9988 and so appeared to confirm this relationship. The regressed line was used to estimate values for k_{Mit} over the pH range of 6-9 and these estimates are shown in table 4.1.

To illustrate the potential effect of this pH sensitivity on the activity of mitozolomide a simple hypothetical model was constructed (see figure 4.1). The basis of this model was a typical tissue culture experiment with 10^6 tumour cells growing in 1 ml of medium. The total

Table 4.1 - Estimated values for the mitozolomide decomposition rate constant over the pH range 6-9 based on the measured data over the range 7.2-7.8.

pH	Kmit/hrs	ln(Kmit/hrs)	t 1/2 (hrs)
6.0	0.034	-3.381	20.36
6.4	0.079	-2.532	8.72
6.8	0.186	-1.684	3.73
7.0	0.284	-1.26	2.44
7.2	0.484	-0.836	1.59
7.4	0.663	-0.412	1.04
7.6	1.013	0.013	0.68
7.8	1.548	0.437	0.44
8.2	3.614	1.285	0.19
8.6	8.441	2.133	0.08
9.0	19.716	2.981	0.03

intracellular fluid volume can be estimated to be 4×10^{-4} ml i.e. 0.04%. If we assume that equilibration between the medium and the intracellular tumour compartment is effectively instantaneous then it can be seen that, providing the pH within the two compartments is the same (and thus

$k_{MT} = k_{MM}$), the fraction of the total active species produced within the tumour cells will be equal to a direct dilution of the total medium volume in which the drug is distributed.

Figure 4.1 - A hypothetical model to illustrate the potential effects of small pH variations on the cytotoxicity of mitozolomide.

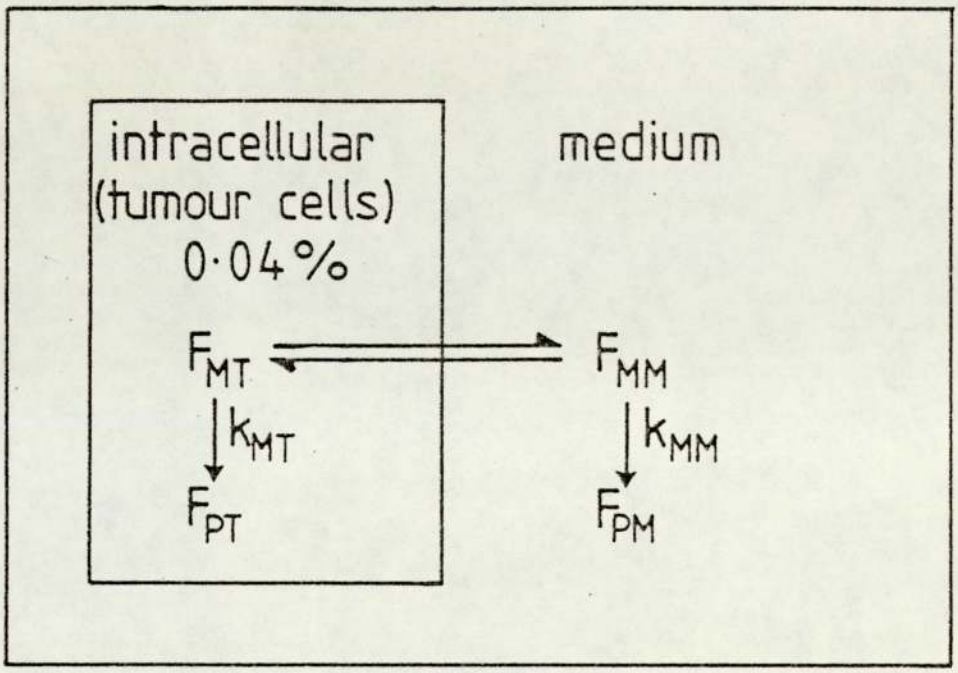

Where:

F_{MM} = Fraction of mitozolomide in the medium at any one one time (F_{PM} = fraction of products).

F_{MT} = Fraction of mitozolomide in the intracellular compartment at any one time (F_{PT} = fraction of products).

k_{MT} and k_{MM} = the rate constants for the first order decompositions intracellularly and in the medium.

If the pH of the medium is changed relative to that within the tumour cells the effect on the fractional exposure to active species can be calculated by substituting the appropriate values for k_{Mit} previously calculated. Thus, an intracellular pH of 7.4 relative to a medium pH of

6.5 would result in a fractional exposure of 26.97 x 10^{-4} i.e. 6.5 times that when the respective pH values were equal. The pH differentials are clearly very important and figure 4.2 summarises the effects of a range of pH changes on the exposure of the tumour cells to active species.

Figure 4.2 - The effect of varying intracellular and medium pH's on the fraction of total active species exposed to the tumour.

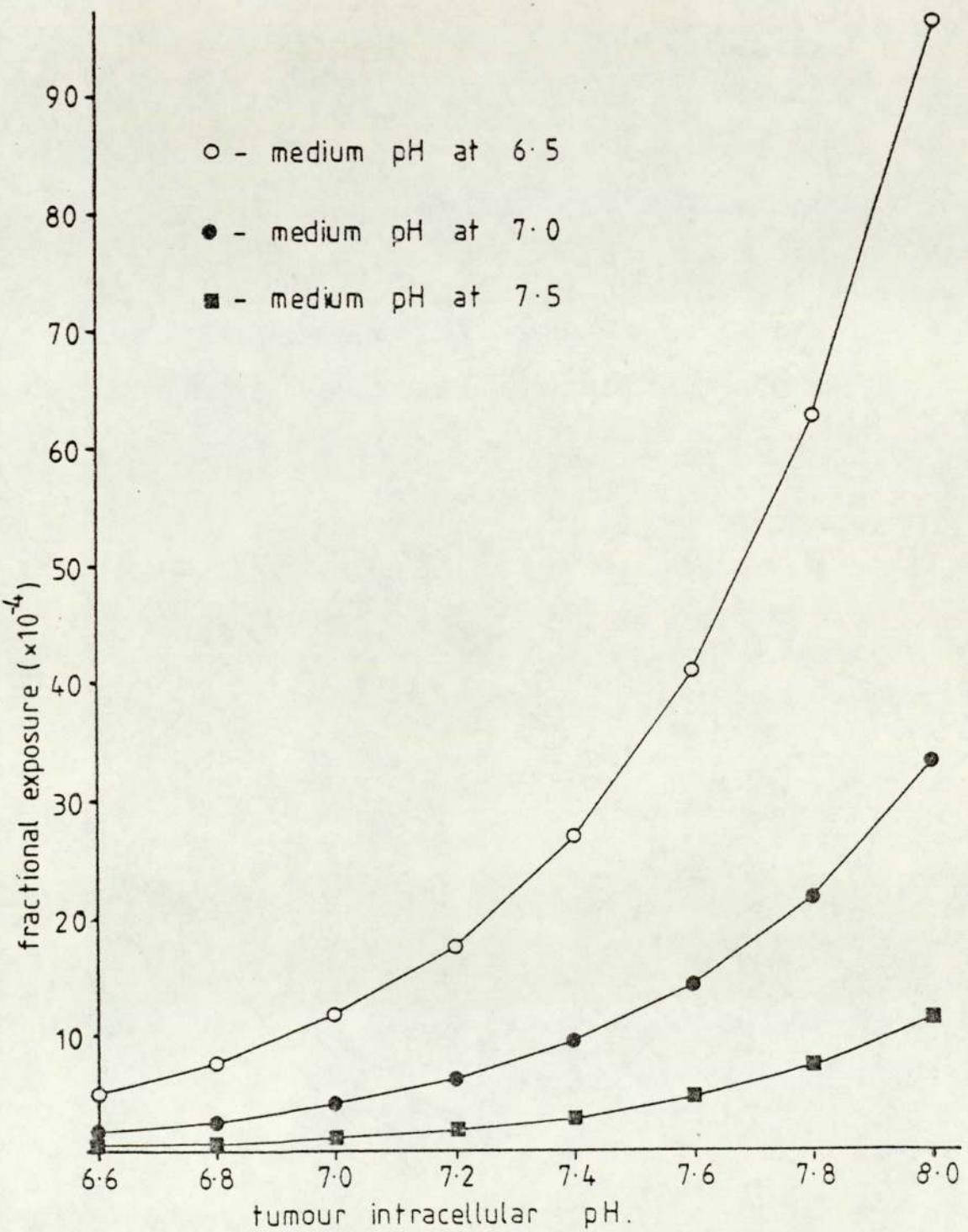

The tissue culture example is a pertinant one because such pH differences can occur due to the practice of 'gassing' cells with CO_2/O_2 mixes during incubation periods which lowers the medium pH to the 6.5 - 7.0 region. Methods for measuring intracellular pH include micro-electrodes and pH sensitive dyes (159). Waddell and Butler developed a popular method using the weak acid 5,5-dimethyl-2,4-oxazolidinedione (DMO; 160) which has only recently been superceded by the use of fluorescent dyes. These methods show that normal intracellular pH is between 7.0 and 7.4. A variety of plasma membrane transport proteins exist indicating the importance of intracellualr pH homeostasis (see reference 161 for review) and although there is evidence for a fall in intracellular pH in response to an acidic extracellular environment (162, 163) it is evident that considerable pH differentials could occur in tissue culture experiments.

The chloroethylnitrosoureas show a similar sensitivity to pH in their chemical decomposition (49) and it is possible that the variation in reported in vitro cytotoxicity parameters for these drugs (references 164 - 166 for CCNU variations) are due, in part at least, to slight variations in the pH conditions during these studies. Variations in the estimated ID_{50} figures for mitozolomide against cultured TLX-5 cells (167) could also be due to the inadequate monitoring of medium pH in these experiments because incubations were performed in RPMI/10% FCS media gassed with 10% CO_2 in air.

The potential implications of this pH sensitivity in vivo are more difficult to evaluate although it is known that increased metabolism can lead to local tissue acidosis due to the production of organic acids such as Lactate and the fact that the CO_2 produced acts as an acid via the equilibrium:

$$H_2O + CO_2 \rightleftharpoons H_2CO_3 \rightleftharpoons H^4 + HCO^2_3$$

In well perfused tissues this is normally only a transient effect (159) but where perfusion is poor, such as in the necrotic regions of many large tumours, diffusion of CO_2 and lactate becomes limiting and can lead to a permanent extracellular acidosis. Jain et al showed that the extracellular pH in an untreated Walker 256 carcinoma in a rat fell from 7.3 - 6.2 with a concomittant increase in tumour size up to 50 g (168). Interestingly these authors also showed that they could induce a tumour specific acidosis by glucose loading and this may have implications for agents like mitozolomide since it could create a marginal element of tumour directed specificity if this extracellular acidosis results in an increased intracellular exposure to active species.

The observed pH sensitivity may also be relevant to situations such as drug resistance. If a sub-population of tumour cells has reduced or altered pH homeostasis such that the intracellular pH was lowered the fractional exposure of these cells to nitrosourea or mitozolomide produced active species would also be lowered and these cells would be effectively more resistant to the drugs. Whilst this argument is somewhat speculative it presents an attractive hypothesis for further investigation and the use of the newer (non-perturbing) fluorescent indicators such as Quene I (169) to follow intracellular pH would facilitate a detailed examination of the implications and importance of this pH sensitivity in the chemistry of agents such as mitozolomide. The importance of such work to agents that are chemically labile at physiological pH is emphasized by Kennedy et al who recently demonstrated a correlation between changes in pH and DNA cross-link formation using the acid-labile anti-tumour agent mitomycin C (162). Additionally, in vitro chemosensitivity screening is, despite many shortcomings (170), becoming an increasingly important means of assessing novel anti-tumour agents with organisations such as the NCI

moving towards the adoption of tissue culture screens. This is especially true where human cell lines can be cultured(171) and it is evident that, for agents like motozolomide, the control of pH will be critical to the useful interpretation of these results.

An aspect of the chemistry of mitozolomide identified in these studies which suggested improvement over currently used drugs was the apparent non-production of an isocyanate species. The production of isocyanates in the decomposition of the chloroethylnitrosoureas was believed to contribute to their cytotoxicity without making a significant impact therapeutically (see introduction). Attempts to resolve this by developing self-carbamoylating chloroethylnitrosoureas such as chlorozotocin have been largely unsuccessful at the clinical level. Chlorozotocin is a hydrophilic agent with a log P of -1.0 (41) and it may be this aspect which, by affecting its physiological distribution, limits its therapeutic effect. Mitozolomide, with a log P of 0.35, is unlikely to be affected in this manner.

The evidence from the studies on CCRG 81045 indicate that the pH sensitivity in decomposition rates and the lack of isocyanate production are likely to be general features of the imidazo[5,1-d]-1,2,3,5-tetrazin-4(3H)-ones. Some suggestion of a limited production of methylisocyanate was inferred from the detection of 2-azahypoxanthine in decomposition studies of CCRG 80145 but this may have been due to contamination of the CCRG 81045 supplied, whilst the levels detected (<2.5%) were relatively insignificant.

Perhaps the area in which the two imidazo[5,1-d]-1,2,3,5-tetrazin-4(3H)-ones show the greatest potential improvement over the chloroethylnitrosoureas is in their pharmacokinetics. Clinical and murine results for mitozolomide and murine results for CCRG 81045 all produced

all produced reasonable fits to simple one-compartment pharmacokinetic models. Studies on the nitrosoureas (see introduction) had shown a characteristic bi-phasic pharmacokinetic profile. A comparison of pharmacokinetic parameters obtained following approximately equimolar doses of BCNU, CCNU and mitozolomide to animals is shown in table 4.2. Clearly mitozolomide exhibits higher and more sustained plasma levels (and therefore a greater AUC) than the two nitrosoureas. Results from in vitro screens indicate a similar degree of cytotoxicity for these three agents such that these sorts of pharmacokinetic differences between mitozolomide and the two chloroethylnitrosoureas would become important, especially if they are reflected in parallel differences in tumour level of drug.

Table 4.2 - A comparison of pharmacokinetic parameters derived following doses of CCNU, BCNU and mitozolomide to rodents.

drug	mol. weight	dose (mg/kg)	Cp.max. (mg/L)	AUC (mg.hrs/L)	ref
BCNU	214	14	13.0	5.988	115
CCNU	234	20	7.55	0.722 (7.883)	102
mitozolomide	242.5	20	25.84	37.864	herein

The extent of cytoxicity will be determined by the fraction of active species that can be produced within the cell over and above the capacity of the cellular repair mechanisms to cope with the resultant damage. As such, a model of a critical exposure level emerges as fundamental to cytotoxicity - that is, a model where a level of active species production beyond the threshold of the cells repair capacity is the essential parameter to the drug's effectiveness. This concept has been introduced recently by Workman (172) and the potential advantages of mitozolomide over the chloroethylnitrosoureas can be exemplified by comparing murine and clinical pharmacokinetic profiles obtained for mitozolomide and CCNU following equivalent doses of the two agents. Figures 4.3 and 4.4 show these comparisons. Both show plots for 'total nitrosourea' for the CCNU profile. This is because metabolic hydroxylation of the cyclohexyl ring is very rapid and following a clinical dose of CCNU (given orally) no parent CCNU is detectable after first pass metabolism through the liver. A hypothetical threshold level has been included at between 3 and 6 $\mu g.ml^{-1}$. This was based on the results from *in vitro* experiments (164-167) and, with respect to the previous discussion relating to the significance of such *in vitro* data, is included only as a means of emphasizing the considerable advantages in the pharmacokinetic profile of mitozolomide over the nitrosourea CCNU in this context. A similar, though less dramatic, effect is evident in comparisons with BCNU with the same basic conclusion being reached - that is, mitozolomide possesses pharmacokinetic advantages over the chloroethylnitrosoureas in its ability to deliver effectively greater amounts of drug to the cell over and above some threshold level determined by the cells ability to cope with this cytotoxic insult.

The work of Erickson *et al* (68-70) suggests that the important repair protein in the case of the chloroethylnitrosoureas and mitozolomide

Figure 4.3 - Plasma levels of mitozolomide and CCNU in mice following a dose of 20 $mg.kg^{-1}$.

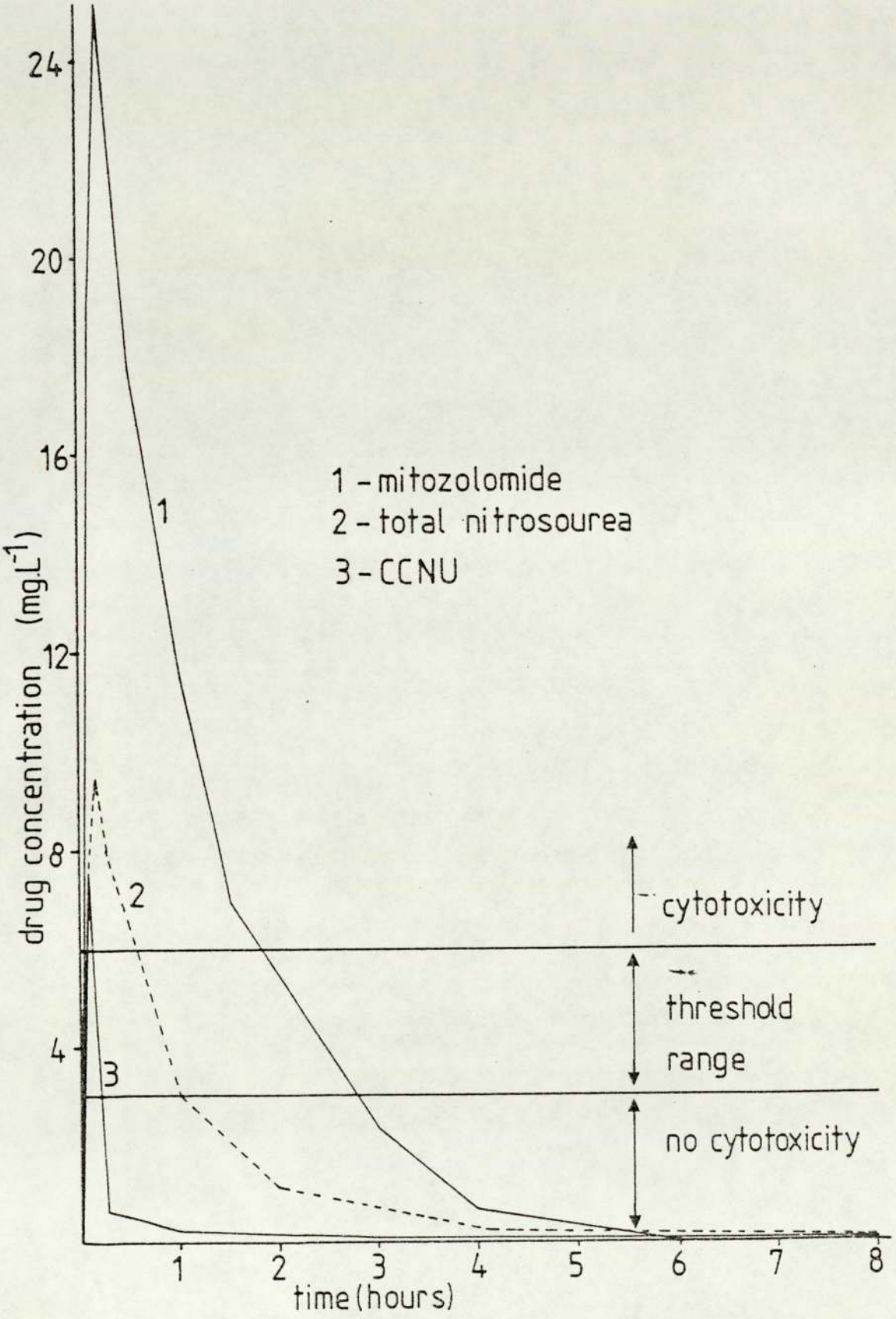

Figure 4.4 - Plasma levels of mitozolomide and CCNU obtained clinically following an oral dose of 130 $mg.m^{-2}$.

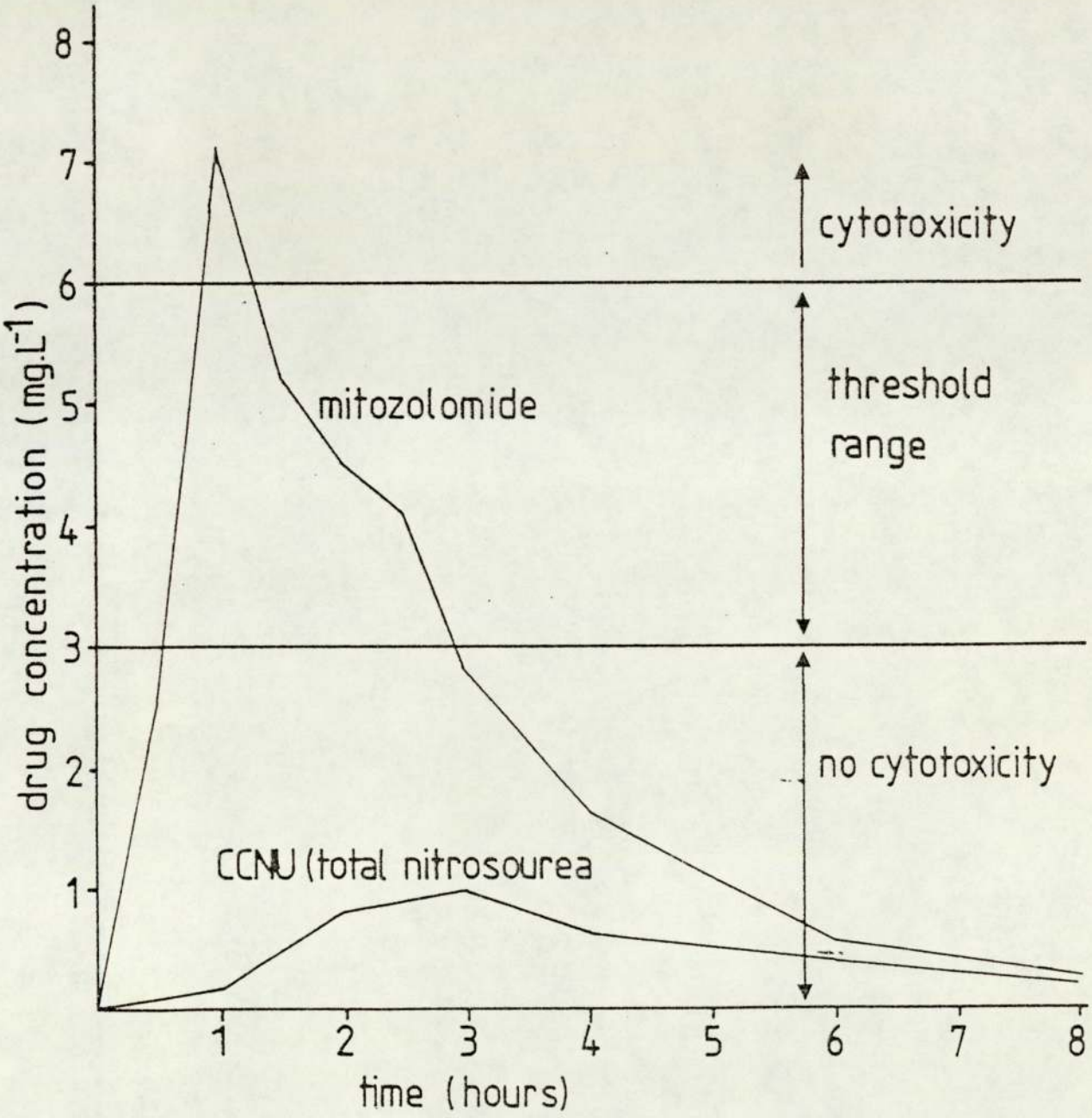

is the 'mer' protein (173, 174) and that it functions as a suicide protein which is saturable by pre-treatments with, for example, MNNG (175). In this case the threshold concept would be one where a certain saturating level of alkylations exist above which cytotoxic damage would result.

Experiments could be conducted to examine the validity of this threshold concept using an in vitro system. By 'washing out' the drug at various times following administration a variety of exposure profiles could be produced all with the same actual exposure (measured as an AUC) but with varying maximum drug concentrations enabling a detailed modelling of the necessary exposure/time profile for optimal cytotoxicity.

The pharmacokinetics of CCRG 81045 in mice suggest a similar pharmacokinetic advantage for this agent over the triazenoimidazole, DTIC. DTIC exhibited a biphasic plasma profile and an elimination half-life of 30 - 52 minutes (122).

A comparison of the pharmacokinetics of mitozolomide and CCRG 81045 shows a remarkable similarity in the behaviour of the two agents following approximately equimolar doses and this indicates that the observed differences in their anti-tumour efficacy are not related to pharmacokinetic considerations. This infers that, either the two agents are operating by a similar mode of action with one being vastly more effective than the other or, that - intriguingly - they produce their anti-tumour effects by completely different mechanisms. A second point to emerge from a comparison relates to the rates of elimination of the two agents. The in vivo elimination half-life of CCRG 81045 in the mouse was 1.13 hours (following an ip dose) which compares to the faster rate of 0.76 hours found for mitozolomide. This mirrors the in vitro situation where the decomposition half-life of CCRG 81045 in phosphate buffer

(pH 7.4; 37°C) was 1.48 hours compared to the 0.94 hours seen with mitozolomide and lends support to the supposition that chemical degradation is the principal component in the in vivo elimination process. Since it is the chemical decomposition of mitozolomide that is known to produce the putative active species this factor is important in the drug's action.

Agents such as mitozolomide, which are believed to manifest their cytotoxicity through DNA lesions, probably exhibit some selective tumour toxicity in that the DNA of tumour cells is often inherently more sensitive to chemical insult due to incumbent DNA abberations incurred during tumourogenic progression (176). In addition the implications from the pH studies previously discussed suggest another possible element of specificity in action.

The conclusions concerning the pharmacokinetic advantages of mitozolomide against the chloroethylnitrosoureas were based on plasma concentration versus time profiles and the apparent fit to a simple one-compartment pharmacokinetic model. This model implies an instant distribution of drug and the results of a concurrent tissue disposition study (177) were generally in support of this.

Tissue samples taken at 0.5 hours following the administration of mitozolomide to mice showed similar levels of drug in plasma, liver, kidney and lung (16.7, 19.8, 18.1 and 13.2 $\mu g.g^{-1}$ tissue) with slightly lower levels in muscle (10.2 $\mu g.g^{-1}$ tissue). A level of 8.2 $\mu g.g^{-1}$ tissue was measured in brain indicating the ability of the drug to cross the blood brain barrier to a significant degree. The elimination of mitozolomide from the tissues over an 8 hour time course was first order in close similarity to the plasma result with an elimination half-life of approximately 0.8 hours.

The correlation between the in vitro protein binding studies and the human whole blood kinetics suggested that protein binding may be important to the disposition of mitozolomide. However, the volume of distribution figures and the disposition study results infer that tissue binding must also occur to account for the similarity in reported levels of mitozolomide in plasma, liver, kidney and lung. The lower levels of mitozolomide in skeletal muscle and brain may be indicative of a lower capacity of these tissues to bind the drug.

The pharmacokinetic evidence suggested the principal component in the elimination of mitozolomide to be chemical decomposition. However, although the overall half-life is similar to that seen at pH 7.4 in vitro, the sensititivy of breakdown to pH changes suggests this will reflect only the composite situation.

Total body water comprises approximately 60% body weight, 40% of this being located intracellularly and 20% extracellularly. Measurements of intracellular pH range from 7.0 - 7.4 with most values suggesting a norm nearer to pH 7.0. The chemical half-life at pH 7.0 is approximately 2.4 hours compared with 1 hour at pH 7.4, thus, in 67% of the total body fluid the rate of chemical decomposition is likely to be considerably slower than the elimination half-life. Whilst plasma pH is strictly regulated that of interstitial fluid can vary, with factors such as excessive metabolic work-load producing transient tissue acidosis and therefore slower rates of degradation. Against this there is the observed two-fold enhancement of degradation rate seen in the plasma, although the plasma volume is relatively small (8% total fluid). The nett contribution of these variations in rate to the overall elimination of mitozolomide will be dependent upon the rates of re-distribution of the drug but it is conceivable from these considerations that chemical decomposition may not be the overriding factor in the elimination process.

The excretion balance study in mice showed that between 10 and 24% of administered mitozolomide was eliminated by urinary excretion and the assay of the mouse urines revealed 'unknown' products that may be indicative of a metabolic contribution.

Workman (76) has shown previously that phenobarbital pre-treatment to mice reduced the anti-tumour efficacy of mitozolomide and Brindley (178) demonstrated a concomitant increase in the rate of elimination. These results infer the existence of an inducible metabolic pathway for mitozolomide. Drug disposition studies (179) using [^{14}C]-chloroethyl- and [^{14}C]-imidazole-labelled mitozolomide showed higher levels of [^{14}C]-chloroethyl label in the liver (36 $\mu g.g^{-1}$ tissue *versus* 13 $\mu g.g^{-1}$ tissue for the imidazole label at 0.5 hours) in support of the possible N-dealkylation of mitozolomide previously postulated and suggesting that metabolism may play an important role in the fate of mitozolomide under normal circumstances.

It is essential to characterize the unidentified products detected in mouse urine and to conduct *in vitro* metabolism experiments in order to establish the nature and importance of this metabolism to the fate of mitozolomide.

Although these results suggest that a comparison of plasma concentration/time profiles obtained for mitozolomide and CCNU is an over simplification with respect to anti-tumour efficacy some solace can be obtained from the fact that the chloroethylnitrosoureas are subject to protein binding (102) and extensive metabolism such that the general conclusion that mitozolomide has pharmacokinetic advantages over these agents is sustained. A recent study by Workman *et al* showing higher tumour levels of mitozolomide following equimolar doses of mitozolomide and CCNU to mice bearing a KHT sarcoma appears to substantiate this (180).

The phase I trial of mitozolomide revealed a delayed thrombocytopenia to be the specific dose-limiting toxicity. The platelet nadir occurred some 4 - 6 weeks after dosing and may reflect some idiosyncrasies in the micro-environment of progenitor cells in the thrombopoeitic pathway. The local creation of a pH differential that may expose these cells to effectively larger doses of drug could account for the specific nature of this toxicity. An examination of this problem is hampered by the difficulties in producing a suitable model system but it is evident that an investigation into this toxicity is necessary to the future development of the drug.

Another approach to this problem would be the use of high-dose chemotherapy regimens whereby bone marrow is aspirated prior to dosing and replaced later in the hope of countering the toxicity produced by myelosuppressive agents (181). Figure 4.3 shows that mitozolomide lends itself particularly well to this sort of approach in that the effective increase in drug exposure (as measured by an increase in AUC) can be seen to be considerably larger than a similar advantage for, in this case, CCNU. Since the kinetic profile for CCNU is similar to that for BCNU an analagous advantage exists over this agent which has been used in high-dose chemotherapy regimens (182).

If the murine model is considered to be predictive of the human situation it can be seen that the plasma concentrations obtained clinically at the dose recommended for the phase II trial (approximately 6 $\mu g.ml^{-1}$) are only marginally at the level where some anti-tumour activity was evident in mice. (A Cp.max of 5.6 $\mu g.ml^{-1}$ was seen following a dose of 5 $mg.kg^{-1}$). High dose chemotherapy may enable the attainment of plasma levels of mitozolomide corresponding to those seen to produce an optimal therapeutic response in mice.

Two partial responses in patients with adenocarcinoma of the ovary (156) were obtained in the phase I trial with one non-Hodgkin's lymphoma patient showing a transient response. In addition to the dose-limiting thrombocytopenia a less severe leukopenia was evident in some patients at doses of 115 $mg.m^{-2}$ and above. The only non-myelosuppressive toxicity evident was a dose-related, but not severe, nausea and vomiting. Mitozolomide is currently undergoing a multi-centre phase II evaluation in Europe against ovarian, breast and small cell lung carcinoma and against malignant melanoma.

In conclusion, this project set out to examine the behaviour and fate of two novel imidazo[5,1-d]-1,2,3,5-tetrazin-4(3H)-ones under physiological conditions both *in vitro* and *in vivo*. The studies were designed to enable an interpretation of the anti-tumour efficacy of these drugs in terms of their chemical and biochemical behaviour *in vivo* and to establish areas in which the imidazo[5,1-d]-1,2,3,5-tetrazin-4(3H)-ones may have advantages over the chloroethylnitrosoureas and the triazenoimidazoles, two groups of agents possessing similar chemical and mode of action characteristics.

The results have enabled the construction of an *in vivo* profile for the behaviour of mitozolomide the lead compound in the series and, by analogy to CCRG 81045, to identify aspects that may be characteristic of the series. It can also be concluded that these two imidazo[5,1-d]-1,2,3,5-tetrazin-4(3H)-ones possess considerable pharmacokinetic advantages over the chloroethyl nitrosoureas and triazenoimidazoles which suggest that they will become valuable additions to the clinicians armoury of drugs for an improved treatment of cancer.

APPENDIX I

Mitozolomide pharmacokinetics in mice - Results from the ip dose escalation study.

MITOZOLOMIDE MOUSE PHARMACOKINETICS 0.25 MGS/KG

Route - ip

Time (hrs)	Plasma concentrations (mg/L) Mouse 1	2	3	4	5	Mean (1-5)	SD (1-5)	Ln (mean)
0.00	0.000	0.000	0.000	0.000	0.000	0.000	0.000	ERR
0.25	0.373	0.279	0.444	0.444	0.331	0.374	0.072	-0.983
0.50	0.278	0.153	0.343	0.296	0.296	0.273	0.071	-1.298
0.75	0.208	0.147	0.265	0.283	0.325	0.246	0.069	-1.404
1.00	0.208	0.193	0.171	0.154	0.306	0.206	0.059	-1.578
1.50	0.105	0.073	0.078	0.065	0.072	0.079	0.015	-2.543
2.00	0.086	0.065	0.065	0.299	0.143	0.132	0.099	-2.028
3.00	0.000	0.000	0.000	0.000	0.000	0.000	0.000	ERR

AUC (0-8 hrs)= 0.4386 MG.HRS/L

MITOZOLOMIDE MOUSE PHARMACOKINETICS 1.0 MGS/KG

Route - ip

Time (hrs)	Plasma concentrations (mg/L) Mouse 1	2	3	4	5	Mean (1-5)	SD (1-5)	Ln (mean)
0.00	0.000	0.000	0.000	0.000	0.000	0.000	0.000	ERR
0.25	1.059	0.971	1.200	1.367	1.162	1.152	0.150	0.141
0.50	0.792	0.862	1.304	1.027	0.923	0.982	0.200	-0.019
0.75	0.665	0.652	0.518	0.850	0.889	0.715	0.153	-0.336
1.00	0.411	0.524	0.524	0.564	0.415	0.488	0.070	-0.718
1.50	0.206	0.217	0.216	0.260	0.253	0.230	0.024	-1.468
2.00	0.076	0.129	0.284	0.186	0.201	0.175	0.078	-1.742
3.00	0.062	0.064	0.058	0.055	0.070	0.062	0.006	-2.784
4.00	0.000	0.000	0.000	0.000	0.000	0.000	0.000	ERR

AUC (0-8 hrs)= 1.2033 MG.HRS/L

MITOZOLOMIDE MOUSE PHARMACOKINETICS 5.0 MGS/KG

Route - ip

Time (hrs)	Plasma concentrations (mg/L) Mouse 1	2	3	4	5	Mean (1-5)	SD (1-5)	Ln (mean)
0.00	0.000	0.000	0.000	0.000		0.000	0.000	ERR
0.25	5.191	6.682	4.833	5.995		5.675	0.829	1.736
0.50	2.357	5.585	5.376	5.023		4.585	1.503	1.523
0.75	3.472	3.533	3.679	4.083		3.692	0.275	1.306
1.00	3.094	2.340	2.794	2.704		2.733	0.311	1.005
2.00	1.353	1.190	1.312	1.285		1.285	0.069	0.251
4.00	0.000	0.000	0.000	0.000		0.000	0.000	ERR

AUC (0-8 hrs)= 7.1236 MG.HRS/L

MITOZOLOMIDE MOUSE PHARMACOKINETICS 10.0 MGS/KG

Route - ip

Time (hrs)	Plasma concentrations (mg/L) Mouse 1	2	3	4	5	Mean (1-5)	SD (1-5)	Ln (mean)
0.00	0.000	0.000				0.000	-	ERR
0.25	6.782	12.867				9.825	-	2.285
0.50	5.030	7.720				6.375	-	1.852
0.75	4.570	7.010				5.790	-	1.756
1.00	3.980	4.500				4.240	-	1.445
1.50	1.820	2.870				2.345	-	0.852
2.00	1.560	1.960				1.760	-	0.565
3.00	0.950	0.590				0.770	-	-0.261
4.00	0.760	0.350				0.555	-	-0.589
6.00	0.000	0.000				0.000	-	ERR

AUC (0-8 hrs)= 11.182 MG.HRS/L

NB. Tabulated details of the 20.0 $mg.kg^{-1}$ ip dose are shown in Appendix II.

APPENDIX II

Mitozolomide pharmacokinetics in mice: Oral and transdermal bioavailability study - Results

MITOZOLOMIDE MOUSE BIOAVAILABILITY 20 MGS/KG

Route - ip

Time (hrs)	Plasma concentrations (mg/L) Mouse 1	2	3	4	5	Mean (1-5)	SD (1-5)	Ln (mean)
0.00	0.000	0.000	0.000	0.000	0.000	0.000	0.000	ERR
0.08	17.260	25.479	15.680	16.412	16.614	18.289	4.059	2.906
0.16	23.836	25.040	27.108	26.058	24.149	25.238	1.356	3.228
0.25	20.325	21.712	23.995	25.328	27.054	23.683	2.708	3.165
0.50	19.995	17.056	17.959	17.641	16.611	17.852	1.306	2.882
0.75	14.941	14.719	16.007	14.346		15.003	0.713	2.708
1.00	11.877	12.425	11.391	10.407	11.687	11.557	0.745	2.447
1.50	7.747	7.914	6.622	6.390	6.010	6.937	0.847	1.937
2.00	5.563	5.563	6.312	5.572	4.569	5.516	0.620	1.708
3.00	2.580	2.779	2.418	2.194	1.829	2.360	0.366	0.859
4.00	0.619	0.499	0.644	0.912	0.748	0.684	0.155	-0.379
6.00	0.000	0.000	0.000	0.000	0.000	0.000	0.000	ERR
8.00	0.000	0.000	0.000	0.000	0.000	0.000	0.000	ERR

AUC (0-8 hrs)= 31.174 MG.HRS/L

MITOZOLOMIDE MOUSE BIOAVAILABILITY 20 MGS/KG

Route - po

Time (hrs)	Plasma concentrations (mg/L) Mouse 1	2	3	4	5	Mean (1-5)	SD (1-5)	Ln (mean)
0.00	0.000	0.000	0.000	0.000	0.000	0.000	0.000	ERR
0.08	18.671	15.221	10.755	10.753		13.850	3.842	2.628
0.16	9.562	8.107	15.208	16.515	11.951	12.269	3.585	2.507
0.25	13.873	14.211	13.484	12.240		13.452	0.861	2.599
0.50	8.452	15.203	9.462	7.698	9.040	9.971	2.999	2.300
0.75	7.426	8.900	9.330	13.600	13.106	10.472	2.728	2.349
1.00	8.574	3.605	7.721	3.984	8.947	6.566	2.572	1.882
1.50	6.156	3.819	3.938	4.398		4.578	1.081	1.521
2.00	2.728	3.834	4.581			3.714	0.932	1.312
3.00	1.920	1.474	1.418	1.473	1.016	1.460	0.320	0.379
4.00	0.850	0.717	0.910	0.871		0.837	0.084	-0.178
6.00	0.438	0.925	0.000	0.000	0.000	0.273	0.411	-1.300
8.00	0.000	0.000	0.000	0.000	0.000	0.000	0.000	ERR

AUC (0-8 hrs)= 20.346 MG.HRS/L

BIOAVAILABILITY (PO/IP) = 0.653

MITOZOLOMIDE MOUSE BIOAVAILABILITY 20 MGS/KG Route - transdermal								
Time (hrs)	Plasma concentrations (mg/L) Mouse 1	2	3	4	5	Mean (1-5)	SD (1-5)	Ln (mean)
0.00	0.000	0.000	0.000	0.000	0.000	0.000	0.000	ERR
0.25	0.152	0.459	0.317	0.080	1.727	0.547	0.676	-0.603
0.50	0.237	0.195	2.071	0.389	0.967	0.772	0.789	-0.259
0.75	0.308	5.666	2.052	3.833	1.019	2.576	2.178	0.946
1.00	1.436	1.825	0.414	6.636	1.390	2.340	2.457	0.850
1.50	0.627	0.885	1.790	0.902	1.253	1.091	0.450	0.087
2.00	3.150	0.911	4.196	0.614	0.660	1.906	1.659	0.645
3.00	0.239	0.685	1.552	0.400	6.866	1.948	2.795	0.667
4.00	3.231	1.658	3.054	0.946	0.364	1.851	1.267	0.616
6.00	2.871	0.801	2.842	1.512	2.162	2.038	0.889	0.712
8.00	0.555	0.911	0.566	0.658	0.501	0.638	0.163	-0.449
					AUC (0-8 hrs)=	13.332 MG.HRS/L		

Calculation of AUC by the trapezoidal method

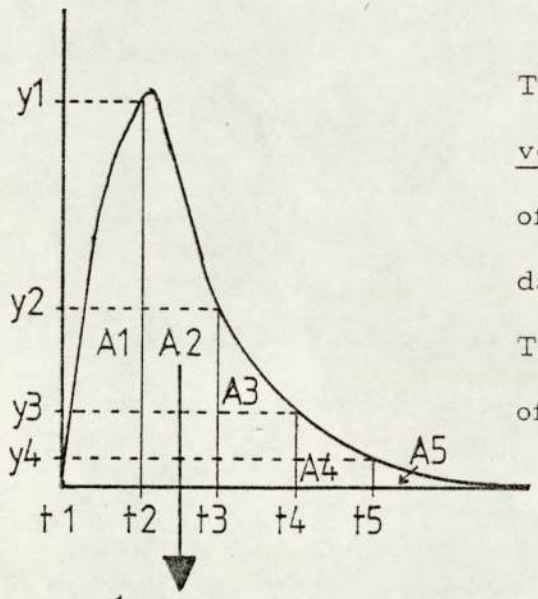

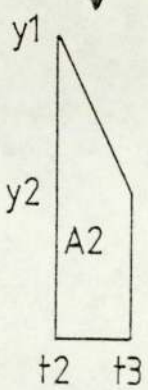

The area under the plasma concentration versus time curve is viewed as a series of trapezia with straight lines between data points approximating to the curve. The total area is the sum of the areas of the designated trapezia.

$$A2, \text{area} = 1/2(y1+y2)\times(t3-t2)$$

$$AUC = \sum (A1....A5)$$

APPENDIX III

CCRG 81045 pharmacokinetics in mice: Oral bioavailability at 20.0 $mg.kg^{-1}$

CCRG 81045 MOUSE BIOAVAILABILITY 20 MGS/KG

Route - ip

Time (hrs)	Plasma concentrations (mg/L) Mouse 1	2	3	4	5	Mean (1-5)	SD (1-5)	Ln (mean)
0.00	0.000	0.000	0.000	0.000	0.000	0.000	0.000	ERR
0.08	13.546	15.725	15.188	15.931	14.881	15.054	0.941	2.712
0.16	21.993	22.669	27.265	24.665	22.140	23.746	2.238	3.167
0.25	25.220	23.390	33.520	21.970	25.100	25.840	4.497	3.252
0.50	18.420	24.180	20.240	20.210		20.763	2.432	3.033
0.75	15.100	9.380	15.340	20.290	16.360	15.294	3.909	2.727
1.00	12.710	16.570	11.170	14.090	11.420	13.192	2.218	2.580
1.50	7.810	5.670	6.500	7.120	10.780	7.576	1.957	2.025
2.00	5.000	6.620	4.400	6.870	6.350	5.848	1.085	1.766
3.00	3.280	2.730	2.780	4.330	4.170	3.458	0.756	1.241
4.00	2.910	1.350	0.760	2.440	2.900	2.072	0.970	0.729
6.00	0.520	0.520	0.660	0.910	1.260	0.774	0.315	-0.256
8.00	0.000	0.000	0.000	0.000	0.000	0.000	0.000	ERR

AUC (0-8 hrs)= 37.864 MG.HRS/L

CCRG 81045 MOUSE BIOAVAILABILITY 20 MGS/KG

Route - po

Time (hrs)	Plasma concentrations (mg/L) Mouse 1	2	3	4	5	Mean (1-5)	SD (1-5)	Ln (mean)
0.00	0.000	0.000	0.000	0.000	0.000	0.000	0.000	ERR
0.08	5.454	10.147	3.494	18.009	6.632	8.747	5.715	2.169
0.16	23.397	18.903	10.362	6.926	12.334	14.384	6.664	2.666
0.25	19.720	19.300	18.800	15.750	24.640	19.642	3.200	2.978
0.50	15.450	17.560	18.470	18.550	18.730	17.752	1.364	2.876
0.75	13.490	16.470	17.980	18.120	9.520	15.116	3.641	2.716
1.00	9.910	12.550	12.600	14.490	12.840	12.478	1.643	2.524
1.50	10.330	5.490	8.740	10.460	7.700	8.544	2.058	2.145
2.00	7.060	7.790	4.900	8.200	4.790	6.548	1.608	1.879
3.00	2.000	1.880	6.000	3.090	3.410	3.276	1.662	1.187
4.00	1.030	0.480	3.380	3.540	3.770	2.440	1.557	0.892
6.00	1.530	0.990	1.120	1.080	1.020	1.148	0.219	0.138
8.00	0.000	0.000	0.000	1.710	0.000	0.342	0.765	-1.073

AUC (0-8 hrs)= 36.914 MG.HRS/L

BIOAVAILABILITY (PO/IP) = 0.975

APPENDIX IV

Plasma levels of mitozolomide determined for all patients in the Birmingham arm of the Phase I trial in both the dose escalation and bioavailability studies

NB - values in the 'calc ln conc' columns are derived by a regression of the ln conc values using the least squares method.

PATIENT No: 1 DOSE(mg/m2): 8.0

TIME (hr)	CONC 1 (mg/L)	LN CONC	CALC LN CONC	RESID RATIO (LN)
1.160	0.281	-1.269	-1.409	110.988
1.500	0.199	-1.614	-1.658	102.667
2.000	0.132	-2.025	-2.023	99.910
2.500	0.083	-2.489	-2.389	95.975
3.000	0.057	-2.865	-2.754	96.148
4.000	0.028	-3.576	-3.486	97.484
6.000	0.008	-4.828	-4.948	102.480

correlation coefficient: -0.9963

PATIENT No: 2 DOSE(mg/m2): 8.0

TIME (hr)	CONC 1 (mg/L)	LN CONC	CALC LN CONC	RESID RATIO (LN)
0.880	0.357	-1.030	-1.002	97.306
1.500	0.258	-1.355	-1.370	101.117
2.000	0.192	-1.650	-1.666	100.979
2.500	0.128	-2.056	-1.963	95.485
3.000	0.122	-2.104	-2.259	107.400
4.000	0.054	-2.919	-2.852	97.726

correlation coefficient: -0.9912

PATIENT No: 3 DOSE(mg/m2): 8.0

TIME (hr)	CONC 1 (mg/L)	LN CONC	CALC LN CONC	RESID RATIO (LN)
1.160	0.337	-1.088	-1.141	104.859
1.500	0.210	-1.561	-1.429	91.533
2.000	0.141	-1.959	-1.852	94.538
2.580	0.093	-2.375	-2.343	98.657
3.000	0.078	-2.551	-2.699	105.799
4.180	0.031	-3.474	-3.698	106.468
6.150	0.004	-5.521	-5.367	97.203

correlation coefficient: -0.9951

PATIENT No: 5		DOSE(mg/m2): 8.0		
TIME (hr)	CONC 1 (mg/L)	LN CONC	CALC LN CONC	RESID RATIO (LN)
1.150	0.413	-0.884	-1.149	129.986
1.660	0.231	-1.465	-1.420	96.879
2.000	0.186	-1.682	-1.600	95.106
2.500	0.143	-1.945	-1.865	95.867
3.000	0.110	-2.207	-2.129	96.470
4.000	0.062	-2.781	-2.659	95.627
6.000	0.028	-3.576	-3.718	103.994
correlation coefficient: -0.9865				

PATIENT No: 4		DOSE(mg/m2): 16.50		
TIME (hr)	CONC 1 (mg/L)	LN CONC	CALC LN CONC	RESID RATIO (LN)
1.000	0.755	-0.281	-0.379	134.905
1.500	0.538	-0.620	-0.694	111.940
2.000	0.357	-1.030	-1.009	97.930
2.500	0.248	-1.394	-1.323	94.919
3.000	0.176	-1.737	-1.638	94.301
4.000	0.094	-2.364	-2.268	95.913
6.000	0.033	-3.411	-3.527	103.392
correlation coefficient: -0.9962				

PATIENT No: 2		DOSE(mg/m2): 16.5		
TIME (hr)	CONC 1 (mg/L)	LN CONC	CALC LN CONC	RESID RATIO (LN)
1.000	0.744	-0.296	-0.380	128.645
1.500	0.565	-0.571	-0.666	116.578
2.000	0.389	-0.944	-0.951	100.695
2.500	0.258	-1.355	-1.236	91.224
3.000	0.205	-1.585	-1.521	95.981
4.000	0.108	-2.226	-2.091	93.968
6.000	0.045	-3.101	-3.232	104.222
correlation coefficient: -0.9939				

PATIENT No: 2 DOSE(mg/m2): 16.5(B)

TIME (hr)	CONC 1 (mg/L)	LN CONC	CALC LN CONC	RESID RATIO (LN)
1.000	0.655	-0.423	-0.468	110.491
1.630	0.465	-0.766	-0.836	109.141
2.150	0.311	-1.168	-1.140	97.574
2.580	0.233	-1.457	-1.391	95.485
3.120	0.166	-1.796	-1.707	95.031
4.000	0.112	-2.189	-2.221	101.444
6.000	0.035	-3.352	-3.390	101.114

correlation coefficient: -0.9981

PATIENT No: 3 DOSE(mg/m2): 16.5

TIME (hr)	CONC 1 (mg/L)	LN CONC	CALC LN CONC	RESID RATIO (LN)
1.050	0.731	-0.313	-0.502	160.138
1.500	0.343	-1.070	-0.833	77.823
1.930	0.357	-1.030	-1.149	111.547
2.620	0.186	-1.682	-1.656	98.478
3.070	0.116	-2.154	-1.987	92.256
4.150	0.070	-2.659	-2.782	104.601

correlation coefficient: -0.9791

PATIENT No: 5 DOSE(mg/m2): 16.5

TIME (hr)	CONC 1 (mg/L)	LN CONC	CALC LN CONC	RESID RATIO (LN)
0.870	2.504	0.918	0.087	9.523
1.550	0.222	-1.505	-0.694	46.138
2.070	0.182	-1.704	-1.292	75.849
2.500	0.151	-1.890	-1.787	94.509
3.000	0.132	-2.025	-2.362	116.622
4.000	0.035	-3.352	-3.511	104.739

correlation coefficient: -0.9101

PATIENT No: 4		DOSE(mg/m2): 33.0		
TIME (hr)	CONC 1 (mg/L)	LN CONC	CALC LN CONC	RESID RATIO (LN)
1.000	1.469	0.385	0.154	40.082
1.620	0.786	-0.241	-0.182	75.624
2.130	0.599	-0.512	-0.459	89.503
2.500	0.503	-0.687	-0.659	95.954
3.100	0.391	-0.939	-0.985	104.869
4.000	0.183	-1.698	-1.473	86.728
6.000	0.074	-2.604	-2.558	98.228
8.000	0.030	-3.507	-3.642	103.869
correlation coefficient: -0.9943				

PATIENT No: 12		DOSE(mg/m2): 33.0		
TIME (hr)	CONC 1 (mg/L)	LN CONC	CALC LN CONC	RESID RATIO (LN)
1.000	1.332	0.287	0.144	50.322
1.670	1.009	0.009	-0.203	*********
2.030	0.610	-0.494	-0.389	78.753
2.470	0.488	-0.717	-0.617	86.027
3.000	0.356	-1.033	-0.892	86.339
4.000	0.230	-1.470	-1.410	95.921
6.000	0.078	-2.551	-2.446	95.871
8.000	0.036	-3.324	-3.482	104.737
correlation coefficient: -0.9933				

PATIENT No: 12		DOSE(mg/m2): 54.4		
TIME (hr)	CONC 1 (mg/L)	LN CONC	CALC LN CONC	RESID RATIO (LN)
1.130	2.244	0.808	0.917	113.414
1.560	1.773	0.573	0.640	111.722
2.100	1.152	0.141	0.292	206.429
2.580	0.991	-0.009	-0.017	187.756
3.080	0.877	-0.131	-0.339	258.231
4.080	0.427	-0.851	-0.983	115.494
6.000	0.140	-1.966	-2.219	112.868
7.920	0.024	-3.730	-3.455	92.645
correlation coefficient: -0.9926				

PATIENT No: 13		DOSE(mg/m2): 54.4		
TIME (hr)	CONC 1 (mg/L)	LN CONC	CALC LN CONC	RESID RATIO (LN)
0.800	2.483	0.909	0.798	87.779
1.500	1.408	0.342	0.346	101.190
2.000	0.960	-0.041	0.023	-57.141
2.500	0.712	-0.340	-0.300	88.198
3.000	0.516	-0.662	-0.623	94.084
4.000	0.275	-1.291	-1.268	98.245
6.000	0.082	-2.501	-2.560	102.357
correlation coefficient: -0.9984				

PATIENT No: 14		DOSE(mg/m2): 54.4		
TIME (hr)	CONC 1 (mg/L)	LN CONC	CALC LN CONC	RESID RATIO (LN)
1.750	2.161	0.771	0.573	74.314
2.150	1.192	0.176	0.269	153.256
2.500	0.899	-0.106	0.004	-3.405
3.000	0.668	-0.403	-0.376	93.123
4.000	0.310	-1.171	-1.134	96.860
6.000	0.078	-2.551	-2.652	103.949
8.000	0.015	-4.200	-4.169	99.273
correlation coefficient: -0.9980				

PATIENT No: 15		DOSE(mg/m2): 82.0		
TIME (hr)	CONC 1 (mg/L)	LN CONC	CALC LN CONC	RESID RATIO (LN)
1.100	2.976	1.091	0.769	70.484
1.500	1.838	0.609	0.555	91.156
2.000	1.311	0.271	0.288	106.186
2.500	0.936	-0.066	0.020	-30.596
3.000	0.698	-0.360	-0.247	68.719
4.000	0.360	-1.022	-0.782	76.511
6.000	0.124	-2.087	-1.851	88.667
8.000	0.074	-2.604	-2.920	112.153
correlation coefficient: -0.9854				

PATIENT No: 13		DOSE(mg/m2): 82.0		
TIME (hr)	CONC 1 (mg/L)	LN CONC	CALC LN CONC	RESID RATIO (LN)
0.880	3.118	1.137	1.042	91.621
1.500	1.672	0.514	0.633	123.195
2.000	1.208	0.189	0.304	160.711
2.500	1.005	0.005	-0.026	-518.720
3.000	0.762	-0.272	-0.355	130.765
4.000	0.361	-1.019	-1.015	99.576
6.000	0.108	-2.226	-2.333	104.815
8.000	0.024	-3.730	-3.651	97.891
correlation coefficient: -0.9983				

PATIENT No: 16		DOSE(mg/m2): 82.0		
TIME (hr)	CONC 1 (mg/L)	LN CONC	CALC LN CONC	RESID RATIO (LN)
0.880	2.429	0.887	0.799	90.060
1.500	1.425	0.354	0.432	121.922
2.000	1.013	0.013	0.135	1048.909
2.500	0.889	-0.118	-0.161	136.712
3.000	0.590	-0.528	-0.457	86.648
4.000	0.375	-0.981	-1.050	107.037
6.000	0.134	-2.010	-2.235	111.208
8.000	0.028	-3.576	-3.421	95.664
correlation coefficient: -0.9960				

PATIENT No: 15		DOSE(mg/m2): 115.0		
TIME (hr)	CONC 1 (mg/L)	LN CONC	CALC LN CONC	RESID RATIO (LN)
0.750	3.690	1.306	1.164	89.178
1.500	1.944	0.665	0.693	104.307
2.000	1.481	0.393	0.379	96.611
2.500	1.016	0.016	0.065	412.282
3.000	0.714	-0.337	-0.249	73.774
4.000	0.407	-0.899	-0.876	97.499
6.000	0.112	-2.189	-2.132	97.400
8.000	0.037	-3.297	-3.388	102.771
correlation coefficient: -0.9987				

PATIENT No: 19		DOSE(mg/m2): 115.0		
TIME (hr)	CONC 1 (mg/L)	LN CONC	CALC LN CONC	RESID RATIO (LN)
0.800	3.761	1.325	1.394	105.258
1.500	2.740	1.008	0.992	98.399
2.000	2.297	0.832	0.704	84.693
2.500	1.492	0.400	0.417	104.169
3.000	1.117	0.111	0.129	116.848
4.000	0.653	-0.426	-0.446	104.589
6.000	0.178	-1.726	-1.596	92.457
8.000	0.069	-2.674	-2.746	102.700
correlation coefficient: -0.9984				

PATIENT No: 20		DOSE(mg/m2): 115.0		
TIME (hr)	CONC 1 (mg/L)	LN CONC	CALC LN CONC	RESID RATIO (LN)
0.850	9.137	2.212	1.642	74.222
1.500	3.063	1.119	1.291	115.295
2.000	2.815	1.035	1.020	98.582
2.500	1.655	0.504	0.750	148.861
3.000	1.374	0.318	0.480	150.960
4.000	0.751	-0.286	-0.061	21.304
6.000	0.321	-1.136	-1.142	100.526
8.000	0.134	-2.010	-2.224	110.631
correlation coefficient: -0.9784				

PATIENT No: 21		DOSE(mg/m2): 115		
TIME (hr)	CONC 1 (mg/L)	LN CONC	CALC LN CONC	RESID RATIO (LN)
0.850	5.317	1.671	1.384	82.827
1.500	2.635	0.969	1.024	105.732
2.000	1.948	0.667	0.748	112.154
2.500	1.456	0.376	0.471	125.442
3.000	1.143	0.134	0.195	145.679
4.000	0.648	-0.434	-0.358	82.613
6.000	0.223	-1.501	-1.465	97.609
8.000	0.086	-2.453	-2.571	104.792
correlation coefficient: -0.9951				

PATIENT No: 20		DOSE(mg/m2): 153.0		
TIME (hr)	CONC 1 (mg/L)	LN CONC	CALC LN CONC	RESID RATIO (LN)
1.070	11.271	2.422	1.910	78.837
1.500	4.710	1.550	1.627	104.998
2.000	3.301	1.194	1.299	108.747
2.500	2.259	0.815	0.970	119.057
3.000	1.446	0.369	0.642	174.013
4.000	0.896	-0.110	-0.015	13.805
6.000	0.289	-1.241	-1.329	107.063
8.000	0.079	-2.538	-2.643	104.118
correlation coefficient: -0.9885				

PATIENT No: 21		DOSE(mg/m2): 153.0		
TIME (hr)	CONC 1 (mg/L)	LN CONC	CALC LN CONC	RESID RATIO (LN)
1.080	6.310	1.842	1.538	83.478
1.500	3.230	1.172	1.269	108.217
2.000	2.338	0.849	0.949	111.696
2.500	1.660	0.507	0.628	123.998
3.000	1.287	0.252	0.308	122.169
4.000	0.712	-0.340	-0.332	97.779
6.000	0.209	-1.565	-1.613	103.033
8.000	0.057	-2.865	-2.894	101.011
correlation coefficient: -0.9960				

PATIENT No: 25		DOSE(mg/m2): 153.0		
TIME (hr)	CONC 1 (mg/L)	LN CONC	CALC LN CONC	RESID RATIO (LN)
1.120	5.827	1.763	1.821	103.340
1.500	4.780	1.564	1.554	99.328
2.000	3.271	1.185	1.202	101.429
2.500	2.361	0.859	0.850	98.957
3.000	1.600	0.470	0.498	106.004
4.000	0.840	-0.174	-0.206	117.912
6.000	0.244	-1.411	-1.613	114.363
8.000	0.042	-3.170	-3.021	95.291
correlation coefficient: -0.9983				

PATIENT No: 27		DOSE(mg/m2): 153.0		
TIME (hr)	CONC 1 (mg/L)	LN CONC	CALC LN CONC	RESID RATIO (LN)
0.470	10.218	2.324	2.142	92.171
1.500	4.355	1.471	1.537	104.462
2.000	3.395	1.222	1.243	101.708
2.500	2.531	0.929	0.949	102.236
3.000	1.855	0.618	0.656	106.100
4.000	1.001	0.001	0.068	6801.176
6.000	0.292	-1.231	-1.107	89.945
8.000	0.119	-2.129	-2.282	107.225
correlation coefficient: -0.9972				

PATIENT No: 27		DOSE(mg/m2): 125.0		
TIME (hr)	CONC 1 (mg/L)	LN CONC	CALC LN CONC	RESID RATIO (LN)
1.600	5.761	1.751	1.524	87.018
2.000	3.518	1.258	1.319	104.894
2.500	2.948	1.081	1.064	98.421
3.000	1.957	0.671	0.809	120.442
4.000	1.281	0.248	0.298	120.280
6.000	0.419	-0.870	-0.724	83.199
8.000	0.203	-1.595	-1.745	109.456
correlation coefficient: -0.9930				

PATIENT No: 30		DOSE(mg/m2): 125.0		
TIME (hr)	CONC 1 (mg/L)	LN CONC	CALC LN CONC	RESID RATIO (LN)
1.400	4.397	1.481	1.289	87.060
2.000	2.909	1.068	0.996	93.230
2.500	2.064	0.725	0.751	103.597
3.000	1.342	0.294	0.506	171.980
4.000	0.931	-0.071	0.016	-22.765
6.000	0.355	-1.036	-0.963	92.983
8.000	0.164	-1.808	-1.942	107.430
correlation coefficient: -0.9928				

APPENDIX IV - continued

PATIENT No: 31		DOSE(mgs):		250 iv
TIME (hr)	CONC 1 (mg/L)	LN CONC	CALC LN CONC	RESID RATIO (LN)
1.000	6.107	1.809	1.743	96.302
1.500	4.435	1.490	1.479	99.297
2.000	3.365	1.213	1.216	100.177
2.500	2.643	0.972	0.952	97.961
3.000	1.916	0.650	0.689	105.902
4.000	0.998	-0.002	0.162	*********
6.000	0.456	-0.785	-0.892	113.624
correlation coefficient: -0.9954				
0.500	4.679			

PATIENT No: 31		DOSE(mgs):		250 po
TIME (hr)	CONC 1 (mg/L)	LN CONC	CALC LN CONC	RESID RATIO (LN)
0.500	6.861	1.926	1.984	103.023
1.000	5.060	1.621	1.783	109.939
1.500	4.840	1.577	1.581	100.256
2.000	3.936	1.370	1.379	100.674
2.500	3.066	1.120	1.178	105.129
3.000	2.995	1.097	0.976	89.000
4.000	2.038	0.712	0.573	80.505
6.000	1.184	0.169	-0.233	-137.985
8.000	0.244	-1.411	-1.039	73.677
correlation coefficient: -0.9776				

PATIENT No: 36		DOSE(mgs):		200.0 iv
TIME (hr)	CONC 1 (mg/L)	LN CONC	CALC LN CONC	RESID RATIO (LN)
1.000	3.679	1.303	1.236	94.885
1.500	2.845	1.046	1.002	95.825
2.000	2.185	0.782	0.768	98.234
2.500	1.666	0.510	0.534	104.564
3.000	1.252	0.225	0.300	133.318
4.000	0.735	-0.308	-0.169	54.751
6.000	0.371	-0.992	-1.105	111.437
correlation coefficient: -0.9941				
0.500	3.440			

PATIENT No: 36 DOSE(mgs): 200.0 po

TIME (hr)	CONC 1 (mg/L)	LN CONC	CALC LN CONC	RESID RATIO (LN)
2.000	2.671	0.982	1.102	112.177
2.500	2.574	0.945	0.910	96.225
3.000	2.431	0.888	0.717	80.767
4.000	1.368	0.313	0.333	106.214
6.000	0.569	-0.564	-0.436	77.400
8.000	0.318	-1.146	-1.206	105.237

correlation coefficient: -0.9919

0.500	0.278
1.000	0.718
1.500	1.922

PATIENT No: 41 DOSE(mgs): 50 iv

TIME (hr)	CONC 1 (mg/L)	LN CONC	CALC LN CONC	RESID RATIO (LN)
1.500	0.773	-0.257	-0.262	101.788
2.000	0.635	-0.454	-0.507	111.722
2.500	0.485	-0.724	-0.753	104.014
3.000	0.347	-1.058	-0.998	94.284
4.000	0.209	-1.565	-1.489	95.087
6.000	0.089	-2.419	-2.470	102.089

correlation coefficient: -0.9975

0.500	0.639
1.000	1.104

PATIENT No: 41 DOSE(mgs): 50 po

TIME (hr)	CONC 1 (mg/L)	LN CONC	CALC LN CONC	RESID RATIO (LN)
0.500	0.910	-0.094	0.228	-242.273
1.000	0.758	-0.277	-0.017	6.062
1.500	0.643	-0.442	-0.262	59.347
2.000	0.477	-0.740	-0.507	68.541
2.500	0.384	-0.957	-0.753	78.638
3.000	0.282	-1.266	-0.998	78.835
4.000	0.187	-1.677	-1.489	88.779
6.000	0.098	-2.323	-2.470	106.322

correlation coefficient: -0.9950

PATIENT No: 39		DOSE(mgs):		50 iv
TIME (hr)	CONC 1 (mg/L)	LN CONC	CALC LN CONC	RESID RATIO (LN)
1.500	0.856	-0.155	-0.221	142.190
2.000	0.584	-0.538	-0.525	97.620
2.500	0.440	-0.821	-0.829	100.979
3.000	0.288	-1.245	-1.133	91.018
4.000	0.181	-1.709	-1.741	101.852
6.000	0.053	-2.937	-2.957	100.658
correlation coefficient: -0.9981				
0.500	0.652			
1.000	1.262			

PATIENT No: 39		DOSE(mgs):		50 po
TIME (hr)	CONC 1 (mg/L)	LN CONC	CALC LN CONC	RESID RATIO (LN)
3.000	0.574	-0.555	-0.481	86.607
4.000	0.317	-1.149	-1.120	97.476
6.000	0.116	-2.154	-2.398	111.320
8.000	0.022	-3.817	-3.676	96.318
correlation coefficient: -0.9930				
0.500	0.000			
1.000	0.190			
1.500	0.422			
2.000	0.418			
2.500	0.428			

PATIENT No: 40		DOSE(mgs):		50.0 iv
TIME (hr)	CONC 1 (mg/L)	LN CONC	CALC LN CONC	RESID RATIO (LN)
1.500	0.712	-0.340	-0.345	101.688
2.000	0.588	-0.531	-0.567	106.815
2.500	0.468	-0.759	-0.789	103.916
3.000	0.352	-1.044	-1.011	96.810
4.000	0.214	-1.542	-1.454	94.334
6.000	0.101	-2.293	-2.342	102.137
correlation coefficient: -0.9975				
0.500	0.841			
1.000	1.287			

PATIENT No: 40		DOSE(mgs):		50.0 po
TIME (hr)	CONC 1 (mg/L)	LN CONC	CALC LN CONC	RESID RATIO (LN)
2.500	1.033	0.032	-0.021	-64.825
3.000	0.744	-0.296	-0.281	94.968
4.000	0.439	-0.823	-0.800	97.224
6.000	0.149	-1.904	-1.840	96.625
8.000	0.059	-2.830	-2.879	101.713
correlation coefficient: -0.9991				
0.500	0.042			
1.000	0.268			
1.500	0.699			
2.000	0.787			

APPENDIX V - Pharmacokinetic parameters calculated for all patients in the phase I trial

Patient. No.	Dose No.	Dose (mg/M2)	Dose (mg)	Infusion Time (hours)	Cmax actual (mg/L)	Cmax extrap. (mg/L)	AUC1 (mg.hr/L)	AUC2 (mg.hr/L)	AUC Total (mg.hr/L)	Volume Distribution (L)	Clearance (L/hr)	Plasma Half life (hr)
1	1	8.0	13.000	1.160	0.281	0.244	0.161	0.334	0.495	35.900	26.300	0.950
2	2	8.0	13.400	0.880	0.357	0.367	0.176	0.619	0.795	28.500	16.900	1.170
3	3	8.0	16.200	1.160	0.337	0.320	0.215	0.377	0.592	32.200	27.300	0.820
5	6	8.0	12.500	1.150	0.413	0.317	0.201	0.599	0.800	29.500	15.600	1.310
6	7	8.0	15.500	1.220	0.835	0.585	0.401	0.954	1.355	18.700	11.400	1.130
7	8	8.0	12.000	1.850	0.329	0.297	0.306	0.784	1.090	29.100	11.100	1.840
Average		8.0	13.767	1.237	0.425	0.355	0.243	0.611	0.855	28.983	18.100	1.203
Standard Deviation		---	1.695	0.323	0.205	0.119	0.092	0.236	0.320	5.735	7.120	0.356
Coefficient of Variation		---	12.316	26.151	48.248	33.661	37.975	38.669	37.398	19.787	39.336	29.600
2	4	16.5	27.400	1.000	0.744	0.684	0.373	1.199	1.572	30.600	17.400	1.220
4	5	16.5	32.200	1.000	0.755	0.684	0.378	1.086	1.464	34.900	22.000	1.100
2	9	16.5	27.400	1.000	0.655	0.627	0.344	1.072	1.416	33.100	19.355	1.186
3	10	16.5	34.500	1.050	0.731	0.606	0.359	0.823	1.182	39.900	29.200	0.940
5	11	16.5	24.800	0.870	2.504	1.091	0.552	0.950	1.502	14.400	16.500	0.600
6	12	16.5	32.000	1.270	0.633	0.579	0.585	0.932	1.517	34.000	21.100	1.120
6	13	16.5	32.000	1.330	0.530	0.587	0.437	1.083	1.520	38.900	21.100	1.280
8	14	16.5	22.500	1.130	0.567	0.524	0.390	0.975	1.365	30.700	16.500	1.290
9	15	16.5	29.500	1.080	0.349	0.486	0.287	0.911	1.198	46.200	24.600	1.300
Average		16.5	29.144	1.081	0.830	0.652	0.412	1.003	1.415	33.634	20.862	1.119
Standard Deviation		---	3.930	0.144	0.641	0.177	0.098	0.113	0.142	8.766	4.144	0.225
Coefficient of Variation		---	13.485	13.296	77.226	27.167	23.734	11.311	10.051	26.062	19.870	20.165
4	16	33.0	64.400	1.000	1.469	1.166	0.636	2.151	2.787	42.600	23.100	1.280
10	17	33.0	56.000	1.330	1.146	0.912	0.682	1.608	2.290	43.100	24.400	1.220
9	18	33.0	55.900	1.000	1.047	1.219	0.667	2.130	2.797	34.900	20.000	1.210
11	19	33.0	70.000	1.230	0.879	0.810	0.545	1.694	2.239	65.500	31.300	1.450
12	20	33.0	63.400	1.000	1.332	1.155	0.627	2.230	2.857	42.800	22.200	1.340
Average		33.0	61.940	1.112	1.175	1.052	0.631	1.963	2.594	45.780	24.200	1.300
Standard Deviation		---	6.019	0.157	0.232	0.180	0.053	0.288	0.303	11.548	4.281	0.099
Coefficient of Variation		---	9.717	14.153	19.780	17.108	8.430	14.699	11.662	25.225	17.689	7.596
11	21	54.4	114.000	1.100	1.865	2.190	1.343	3.479	4.822	37.600	23.600	1.100
12	22	54.4	104.400	1.130	2.244	2.501	1.583	3.884	5.467	29.700	19.100	1.080
13	23	54.4	77.200	0.800	2.483	2.222	0.966	3.441	4.407	27.100	17.500	1.070
14	24	54.4	98.500	1.750	2.161	1.773	1.885	2.337	4.222	30.800	23.300	0.910
18	28	54.4	76.200	1.330	1.516	2.226	1.674	3.728	5.402	23.600	14.100	1.160
Average		54.4	94.060	1.222	2.054	2.182	1.490	3.374	4.864	29.760	19.520	1.064
Standard Deviation		---	16.789	0.351	0.373	0.261	0.352	0.608	0.565	5.186	4.018	0.093
Coefficient of Variation		---	17.849	28.696	18.165	11.963	23.600	18.007	11.611	17.426	20.583	8.731

APPENDIX V - continued

Patient. No.	Dose No.	Dose (mg/M2)	Dose (mg)	Infusion Time (hours)	Cmax actual (mg/L)	Cmax extrap. (mg/L)	AUC1 (mg.hr/L)	AUC2 (mg.hr/L)	AUC Total (mg.hr/L)	Volume Distribution (L)	Clearance (L/hr)	Plasma Half life (hr)
15	25	82.0	149.200	1.100	2.976	2.157	1.297	4.036	5.333	52.300	27.980	1.300
13	26	82.0	116.000	0.880	3.118	2.834	1.368	6.441	7.809	22.500	14.850	1.050
16	27	82.0	143.500	0.880	2.429	2.224	1.067	3.753	4.820	50.200	29.770	1.170
24	36	82.0	147.000	0.950	3.740	3.177	1.610	5.618	7.228	36.700	20.370	1.250
Average		82.0	138.925	0.953	3.066	2.598	1.336	4.962	6.298	40.425	23.243	1.193
Standard Deviation		---	15.463	0.104	0.539	0.492	0.224	1.283	1.445	13.805	6.922	0.109
Coefficient of Variation		---	11.130	10.889	17.574	18.926	16.742	25.853	22.945	34.150	29.781	9.145
15	29	115.0	201.300	0.750	3.690	3.204	1.298	5.102	6.397	30.094	31.457	1.100
19	30	115.0	189.800	0.800	3.761	4.033	1.736	7.013	8.749	37.710	21.690	1.210
20	31	115.0	200.100	0.850	9.137	5.165	2.363	9.554	11.917	31.050	16.790	1.280
21	32	115.0	300.100	0.850	5.317	3.990	1.830	7.214	9.044	59.990	33.180	1.250
22	33	115.0	213.000	0.830	4.400	4.221	1.893	7.193	9.086	39.950	23.440	1.180
26	38	115.0	230.000	1.050	10.315	4.354	2.619	5.159	7.778	35.040	29.570	0.820
Average		115.0	222.383	0.855	6.103	4.162	1.956	6.877	8.834	42.260	26.022	1.140
Standard Deviation		-----	40.469	0.103	2.890	0.629	0.469	1.638	1.817	10.727	6.361	0.169
Coefficient of Variation		-----	18.198	12.013	47.357	15.097	23.978	23.910	20.684	25.448	24.472	14.793
20	34	153.0	266.000	1.070	11.271	6.749	4.032	10.274	14.305	28.163	18.501	1.060
21	35	153.0	370.000	1.080	6.310	4.653	2.800	7.267	10.067	57.390	36.750	1.080
25	37	153.0	266.000	0.980	5.827	6.863	3.746	9.751	13.497	28.020	19.720	0.980
27	39	153.0	225.000	0.470	10.218	8.518	2.115	14.496	16.611	23.050	13.550	1.180
28	40	153.0	260.000	1.170	4.580	4.166	2.711	7.171	9.882	45.290	26.310	1.190
29	41	153.0	230.000	1.120	9.440	8.117	5.047	13.643	18.690	20.680	12.310	1.160
Average		153.0	269.500	0.982	7.941	6.511	3.408	10.434	13.842	39.766	21.190	1.108
Standard Deviation		-----	52.451	0.258	2.718	1.774	1.028	3.097	3.501	14.300	9.048	0.083
Coefficient of Variation		-----	19.462	26.324	34.231	27.249	31.598	29.686	25.584	41.942	42.269	7.449
27	42	125.0	185.000	1.600	5.761	6.330	4.110	11.170	15.280	14.429	8.171	1.223
30	43	125.0	227.500	1.170	4.397	4.440	2.860	8.265	11.125	20.917	11.237	1.290
Average		125.0	206.250	1.385	5.079	5.385	3.485	9.718	13.203	17.668	9.703	1.257

APPENDIX VI

Normalization of volume of distribution (Vd) and clearance figures for variation in patient size and a comparison of the variability of the data before and after normalization.

DOSE MG/M2	DOSE No.	PATIENT AREA(M2)	Vd(L)	Vd(L/M2)	CLEARANCE (L/hr)	CLEARANCE (L/hr/M2)
8.0	1	1.59	35.90	22.58	26.30	16.54
8.0	2	1.66	28.50	17.17	16.90	10.18
8.0	3	2.02	32.20	15.94	27.30	13.51
8.0	6	1.56	29.50	18.91	15.60	10.00
8.0	7	1.95	18.70	9.59	11.40	5.85
8.0	8	1.50	29.10	19.40	11.10	7.40
MEAN			28.98	17.26	18.10	10.58
STANDARD DEVIATION			5.24	4.00	6.50	3.59
COEFFICIENT OF VARIATION			18.06	23.19	35.91	33.89
DOSE MG/M2	DOSE No.	PATIENT AREA(M2)	Vd(L)	Vd(L/M2)	CLEARANCE (L/hr)	CLEARANCE (L/hr/M2)
16.5	4	1.66	30.60	18.43	17.40	10.48
16.5	5	1.95	34.90	17.90	22.00	11.28
16.5	9	1.66	33.11	19.95	19.36	11.66
16.5	10	2.09	39.90	19.09	29.20	13.97
16.5	11	1.50	14.40	9.60	16.50	11.00
16.5	12	1.95	34.00	17.44	21.10	10.82
16.5	13	1.95	38.90	19.95	21.10	10.82
16.5	14	1.55	30.70	19.81	16.50	10.65
16.5	15	1.80	46.20	25.67	24.60	13.67
MEAN			33.63	18.65	20.86	11.59
STANDARD DEVIATION			8.26	3.92	3.90	1.24
COEFFICIENT OF VARIATION			24.57	21.01	18.72	10.66
DOSE MG/M2	DOSE No.	PATIENT AREA(M2)	Vd(L)	Vd(L/M2)	CLEARANCE (L/hr)	CLEARANCE (L/hr/M2)
33.0	16	1.95	42.60	21.85	23.10	11.85
33.0	17	1.70	43.10	25.35	24.40	14.35
33.0	18	1.80	34.90	19.39	20.00	11.11
33.0	19	2.10	65.50	31.19	31.30	14.90
33.0	20	1.92	42.80	22.29	22.20	11.56
MEAN			45.78	24.01	24.20	12.76
STANDARD DEVIATION			10.33	4.06	3.83	1.56
COEFFICIENT OF VARIATION			22.56	16.90	15.82	12.21

APPENDIX VI - continued

DOSE MG/M2	DOSE No.	PATIENT AREA(M2)	Vd(L)	Vd(L/M2)	CLEARANCE (L/hr)	CLEARANCE (L/hr/M2)
54.4	21	2.10	37.60	17.90	23.60	11.24
54.4	22	1.92	29.70	15.47	19.10	9.95
54.4	23	1.42	27.10	19.08	17.50	12.32
54.4	24	1.81	30.80	17.02	23.30	12.87
54.4	28	1.40	23.60	16.86	14.10	10.07
MEAN			29.76	17.27	19.52	11.29
STANDARD DEVIATION			4.64	1.20	3.59	1.17
COEFFICIENT OF VARIATION			15.59	6.94	18.41	10.38
DOSE MG/M2	DOSE No.	PATIENT AREA(M2)	Vd(L)	Vd(L/M2)	CLEARANCE (L/hr)	CLEARANCE (L/hr/M2)
82.0	25	1.82	52.30	28.74	27.98	15.37
82.0	26	1.42	22.50	15.85	14.85	10.46
82.0	27	1.75	50.20	28.69	29.77	17.01
82.0	36	1.79	36.70	20.50	20.37	11.38
MEAN			40.43	23.44	23.24	13.56
STANDARD DEVIATION			11.96	5.52	5.99	2.72
COEFFICIENT OF VARIATION			29.57	23.55	25.79	20.06
DOSE MG/M2	DOSE No.	PATIENT AREA(M2)	Vd(L)	Vd(L/M2)	CLEARANCE (L/hr)	CLEARANCE (L/hr/M2)
115.0	29	1.75	50.09	28.63	31.46	17.98
115.0	30	1.65	37.71	22.85	21.69	13.15
115.0	31	1.74	31.05	17.84	16.79	9.65
115.0	32	2.61	59.99	22.98	33.18	12.71
115.0	33	1.85	39.95	21.59	23.44	12.67
115.0	38	2.00	35.04	17.52	29.57	14.79
MEAN			42.31	21.90	26.02	13.49
STANDARD DEVIATION			9.83	3.72	5.83	2.51
COEFFICIENT OF VARIATION			23.23	16.98	22.41	18.64
DOSE MG/M2	DOSE No.	PATIENT AREA(M2)	Vd(L)	Vd(L/M2)	CLEARANCE (L/hr)	CLEARANCE (L/hr/M2)
153.0	34	1.73	28.16	16.28	18.50	10.69
153.0	35	2.42	57.39	23.71	36.75	15.19
153.0	37	1.74	28.02	16.10	19.72	11.33
153.0	39	1.47	23.05	15.68	13.55	9.22
153.0	40	1.70	45.29	26.64	26.31	15.48
153.0	41	1.50	20.68	13.79	12.31	8.21
MEAN			33.77	18.70	21.19	11.69
STANDARD DEVIATION			13.17	4.73	8.32	2.77
COEFFICIENT OF VARIATION			39.02	25.28	39.25	23.67
DOSE MG/M2	DOSE No.	PATIENT AREA(M2)	Vd(L)	Vd(L/M2)	CLEARANCE (L/hr)	CLEARANCE (L/hr/M2)
125.0	42	1.47	24.36	16.57	12.44	8.46
125.0	43	1.82	42.62	23.42	20.87	11.47
MEAN			33.49	19.99	16.66	9.96
STANDARD DEVIATION			-	-	-	-

APPENDIX VII

Whole blood levels of mitozolomide

PATIENT No: 15		DOSE(mg/m2): 82.0 WB		
TIME (hr)	CONC 1 (mg/L)	LN CONC	CALC LN CONC	RESID RATIO (LN)
1.100	1.118	0.112	-0.124	-111.190
2.000	0.538	-0.620	-0.693	111.776
2.500	0.315	-1.155	-1.009	87.340
3.000	0.209	-1.565	-1.325	84.640
4.000	0.127	-2.064	-1.957	94.838
6.000	0.048	-3.037	-3.221	106.081
correlation coefficient: -0.9818				

PATIENT No: 27		DOSE(mg/m2): 125.0 WB		
TIME (hr)	CONC 1 (mg/L)	LN CONC	CALC LN CONC	RESID RATIO (LN)
1.600	3.298	1.193	1.002	83.969
2.000	2.082	0.733	0.836	114.047
2.500	2.042	0.714	0.629	88.138
3.000	1.375	0.318	0.422	132.560
4.000	1.065	0.063	0.008	12.617
6.000	0.299	-1.207	-0.820	67.956
8.000	0.250	-1.386	-1.649	118.939
correlation coefficient: -0.9755				

PATIENT No: 30		DOSE(mg/m2): 125.0 WB		
TIME (hr)	CONC 1 (mg/L)	LN CONC	CALC LN CONC	RESID RATIO (LN)
1.400	2.875	1.056	0.895	84.747
2.000	2.024	0.705	0.656	93.054
2.500	1.523	0.421	0.457	108.641
3.000	1.334	0.288	0.258	89.515
4.000	0.677	-0.390	-0.140	35.932
6.000	0.336	-1.091	-0.936	85.860
8.000	0.216	-1.532	-1.733	113.065
correlation coefficient: -0.9857				

PATIENT No: 25		DOSE(mg/m2):	153.0 WB	
TIME (hr)	CONC 1 (mg/L)	LN CONC	CALC LN CONC	RESID RATIO (LN)
1.120	2.474	0.906	0.689	76.012
1.500	1.689	0.524	0.471	89.816
2.000	1.404	0.339	0.184	54.284
2.500	0.548	-0.601	-0.102	17.018
3.000	0.701	-0.355	-0.389	109.477
4.000	0.333	-1.100	-0.962	87.488
6.000	0.145	-1.931	-2.108	109.179
correlation coefficient: -0.9679				

PATIENT No: 27		DOSE(mg/m2):	153.0 WB	
TIME (hr)	CONC 1 (mg/L)	LN CONC	CALC LN CONC	RESID RATIO (LN)
0.470	5.064	1.622	1.244	76.691
1.500	2.122	0.752	0.758	100.744
2.000	1.560	0.445	0.522	117.383
3.000	0.872	-0.137	0.050	-36.546
4.000	0.534	-0.627	-0.422	67.246
6.000	0.190	-1.661	-1.366	82.237
8.000	0.147	-1.917	-2.310	120.460
correlation coefficient: -0.9761				

PATIENT No: 36		DOSE(mgs):	200poWB	
TIME (hr)	CONC 1 (mg/L)	LN CONC	CALC LN CONC	RESID RATIO (LN)
2.500	2.056	0.721	0.644	89.306
3.000	1.589	0.463	0.470	101.455
4.000	1.032	0.031	0.122	387.840
6.000	0.556	-0.587	-0.573	97.650
8.000	0.291	-1.234	-1.269	102.764
correlation coefficient:-0.8892				
0.500	0.263			
1.000	0.656			
1.500	1.628			
2.000	1.996			

PATIENT No: 36		DOSE(mgs):		200 WB
TIME (hr)	CONC 1 (mg/L)	LN CONC	CALC LN CONC	RESID RATIO (LN)
1.000	2.881	1.058	0.940	88.790
1.500	2.053	0.719	0.670	93.085
2.000	1.370	0.315	0.400	126.934
2.500	1.141	0.132	0.130	98.281
3.000	0.873	-0.136	-0.140	103.317
4.000	0.439	-0.823	-0.680	82.629
6.000	0.163	-1.814	-1.760	97.028
8.000	0.065	-2.733	-2.840	103.899
correlation coefficient: -0.9975				
0.500	2.405			

PATIENT No: 39		DOSE(mgs):		50ivWB
TIME (hr)	CONC 1 (mg/L)	LN CONC	CALC LN CONC	RESID RATIO (LN)
1.000	1.038	0.037	-0.027	-73.149
1.500	0.741	-0.300	-0.382	127.417
2.000	0.448	-0.803	-0.737	91.734
2.500	0.318	-1.146	-1.091	95.247
3.000	0.224	-1.496	-1.446	96.644
4.000	0.111	-2.198	-2.155	98.043
6.000	0.030	-3.507	-3.574	101.919
correlation coefficient: -0.9984				
0.500	0.447			

PATIENT No: 40		DOSE(mgs):		501vWB
TIME (hr)	CONC 1 (mg/L)	LN CONC	CALC LN CONC	RESID RATIO (LN)
1.000	0.865	-0.145	-0.222	153.007
1.500	0.582	-0.541	-0.539	99.598
2.000	0.393	-0.934	-0.856	91.688
2.500	0.296	-1.217	-1.174	96.396
3.000	0.230	-1.470	-1.491	101.432
4.000	0.121	-2.112	-2.125	100.624
6.000	0.034	-3.381	-3.394	100.372
correlation coefficient: -0.9990				
0.500	0.615			

PATIENT No: 41		DOSE(mgs):		50poWB
TIME (hr)	CONC 1 (mg/L)	LN CONC	CALC LN CONC	RESID RATIO (LN)
0.500	0.779	-0.250	-0.426	170.444
1.000	0.522	-0.650	-0.681	104.701
1.500	0.407	-0.899	-0.936	104.081
2.000	0.276	-1.287	-1.191	92.484
2.500	0.217	-1.528	-1.446	94.615
3.000	0.146	-1.924	-1.701	88.380
4.000	0.113	-2.180	-2.211	101.382
6.000	0.045	-3.101	-3.230	104.170
correlation coefficient: -0.9900				

APPENDIX VIII

Mitozolomide excretion balance in mice:
Details of radioactivity recoveries

MITOZOLOMIDE EXCRETION BALANCE IN MICE (C1ET)

MOUSE No: 1 DOSE ACTIVITY: 7.432 uCi (16 499 000 dpm)

URINE

sample time (h)	mean dpm	mean wgt sub-samp (g)	sample weight (g)	total dpm (x10exp6)	% dose
12	39440	0.050	11.683	9.216	55.855
24	8610	0.050	5.590	0.963	5.834
48	14700	0.101	4.404	0.641	3.885
72	2250	0.095	19.333	0.458	2.775
			TOTAL	11.277	68.350

FAECES

sample time (h)	mean dpm	mean wgt sub-samp (g)	sample weight (g)	total dpm (x10exp6)	% dose
12	8620	0.050	7.552	1.302	7.891
24	4590	0.060	3.171	0.243	1.470
48	1540	0.037	15.554	0.647	3.924
72	3880	0.095	11.594	0.474	2.870
			TOTAL	2.665	16.155

CARCASS

sample time (h)	mean dpm	mean wgt sub-samp (g)	sample weight (g)	total dpm (x10exp6)	% dose
72	1040	0.086	72.950	0.882	5.347

CARBON DIOXIDE

sample time (h)	mean dpm	mean vol sub-samp (mls)	sample volume (mls)	total dpm (x10exp6)	% dose
12-1	2880	0.100	34.000	0.979	5.935
12-2	550	0.200	36.000	0.099	0.600
24-1	290	0.100	36.000	0.104	0.633
24-2	$\leq$ 100	0.200	43.000	-	-
48-1	240	0.200	26.000	0.031	0.189
48-2	170	0.200	31.000	0.026	0.160
72-1	$\leq$ 100	0.200	28.000	-	-
72-2	$\leq$ 100	0.200	33.000	-	-
			TOTAL	1.240	7.516
			TOTAL RECOVERY	16.065	97.368

MITOZOLOMIDE EXCRETION BALANCE IN MICE (CiET)

MOUSE No: 2 DOSE ACTIVITY: 7.117 uCi (15 800 000 dpm)

URINE

sample time (h)	mean dpm	mean wgt sub-samp (g)	sample weight (g)	total dpm (x10exp6)	% dose
12	90114	0.052	6.357	11.016	69.725
24	7000	0.051	5.563	0.764	4.833
48	5640	0.097	8.198	0.477	3.017
72	4502	0.097	4.830	0.224	1.419
			TOTAL	12.481	78.994

FAECES

sample time (h)	mean dpm	mean wgt sub-samp (g)	sample weight (g)	total dpm (x10exp6)	% dose
12	7450	0.051	2.834	0.414	2.620
24	6358	0.058	3.190	0.350	2.213
48	4223	0.047	1.932	0.174	1.099
72	864	0.053	5.645	0.092	0.582
			TOTAL	1.029	6.515

CARCASS

sample time (h)	mean dpm	mean wgt sub-samp (g)	sample weight (g)	total dpm (x10exp6)	% dose
72	1552	0.107	52.960	0.768	4.862

CARBON DIOXIDE

sample time (h)	mean dpm	mean vol sub-samp (mls)	sample volume (mls)	total dpm (x10exp6)	% dose
12-1	2255	0.100	25.000	0.564	3.568
12-2	132	0.200	29.000	0.019	0.121
24-1	$\leq$ 100	0.100	28.000	-	-
24-2	$\leq$ 100	0.200	32.000	-	-
48-1	$\leq$ 100	0.200	20.000	-	-
48-2	$\leq$ 100	0.200	31.000	-	-
72-1	$\leq$ 100	0.200	11.000	-	-
72-2	$\leq$ 100	0.200	19.000	-	-
			TOTAL	0.583	3.689
			TOTAL RECOVERY	14.861	94.060

MITOZOLOMIDE EXCRETION BALANCE IN MICE (C1ET)

MOUSE No: 3 DOSE ACTIVITY: 6.889 uCi (15 293 580

URINE

sample time (h)	mean dpm	mean wgt sub-samp (g)	sample weight (g)	total dpm (x10exp6)	% dose
12	105316	0.050	5.296	11.155	72.940
24	8185	0.048	5.410	0.923	6.032
48	2895	0.104	8.299	0.231	1.511
72	2440	0.095	7.826	0.201	1.314
			TOTAL	12.510	81.796

FAECES

sample time (h)	mean dpm	mean wgt sub-samp (g)	sample weight (g)	total dpm (x10exp6)	% dose
12	6653	0.053	3.114	0.391	2.556
24	6009	0.073	4.816	0.396	2.592
48	1902	0.051	4.001	0.149	0.976
72	1377	0.063	8.579	0.188	1.226
			TOTAL	1.124	7.350

CARCASS

sample time (h)	mean dpm	mean wgt sub-samp (g)	sample weight (g)	total dpm (x10exp6)	% dose
72	1065	0.089	55.650	0.666	4.354

CARBON DIOXIDE

sample time (h)	mean dpm	mean vol sub-samp (mls)	sample volume (mls)	total dpm (x10exp6)	% dose
12-1	4036	0.100	19.000	0.767	5.014
12-2	1481	0.200	30.000	0.222	1.453
24-1	150	0.100	22.000	0.033	0.216
24-2	$\leq$100	0.200	30.000	-	-
48-1	$\leq$100	0.200	18.000	-	-
48-2	$\leq$100	0.200	31.000	-	-
72-1	$\leq$100	0.200	20.000	-	-
72-2	$\leq$100	0.200	31.000	-	-
			TOTAL	1.022	6.682
			TOTAL RECOVERY	15.322	100.183

MITOZOLOMIDE EXCRETION BALANCE IN MICE (C1ET)

MOUSE No: 4 DOSE ACTIVITY: 6.978 (15 491 000 dpm

URINE

sample time (h)	mean dpm	mean wgt sub-samp (g)	sample weight (g)	total dpm (x10exp6)	% dose
12	27912	0.052	13.976	7.502	48.427
24	2430	0.052	9.079	0.424	2.739
48	1044	0.109	15.711	0.150	0.971
72	688	0.975	8.332	0.006	0.038
washings				1.427	9.209
			TOTAL	9.509	61.384

FAECES

sample time (h)	mean dpm	mean wgt sub-samp (g)	sample weight (g)	total dpm (x10exp6)	% dose
12	14190	0.054	7.385	1.941	12.527
24	1372	0.058	8.694	0.206	1.328
48	1206	0.115	9.120	0.096	0.617
72	999	0.121	11.746	0.097	0.626
			TOTAL	2.339	15.098

CARCASS

sample time (h)	mean dpm	mean wgt sub-samp (g)	sample weight (g)	total dpm (x10exp6)	% dose
72	820	0.078	47.840	0.503	3.247

CARBON DIOXIDE

sample time (h)	mean dpm	mean vol sub-samp (mls)	sample volume (mls)	total dpm (x10exp6)	% dose
12-1	1865	0.100	24.000	0.448	2.889
12-2	< 100	0.200	31.000	-	-
24-1	172.5	0.200	24.000	0.021	0.134
24-2	179	0.200	30.000	0.027	0.173
48-1	192	0.200	18.000	0.017	0.112
48-2	< 100	0.200	30.000	-	-
72-1	< 100	0.200	18.000	-	-
72-2	< 100	0.200	30.000	-	-
			TOTAL	0.512	3.308
			TOTAL RECOVERY	12.863	83.037

MITOZOLOMIDE EXCRETION BALANCE IN MICE (C1ET)

MOUSE No: 5 DOSE ACTIVITY: 7.343 (16 301 000 dpm

URINE

sample time (h)	mean dpm	mean wgt sub-samp (g)	sample weight (g)	total dpm (x10exp6)	% dose
12	46088	0.055	12.349	10.348	63.479
24	2975	0.053	11.670	0.655	4.018
48	1765	0.103	13.018	0.223	1.368
72	4015	0.107	12.228	0.459	2.815
washings				0.181	1.112
			TOTAL	11.866	72.792

FAECES

sample time (h)	mean dpm	mean wgt sub-samp (g)	sample weight (g)	total dpm (x10exp6)	% dose
12	13938	0.068	6.724	1.378	8.455
24	1595	0.059	7.604	0.206	1.261
48	1519	0.125	7.294	0.089	0.544
72	1445	0.108	7.451	0.100	0.612
			TOTAL	1.772	10.871

CARCASS

sample time (h)	mean dpm	mean wgt sub-samp (g)	sample weight (g)	total dpm (x10exp6)	% dose
72	1025	0.091	46.180	0.520	3.191

CARBON DIOXIDE

sample time (h)	mean dpm	mean vol sub-samp (mls)	sample volume (mls)	total dpm (x10exp6)	% dose
12-1	2449	0.100	18.000	0.441	2.704
12-2	1034	0.200	30.000	0.155	0.951
24-1	227	0.200	20.000	0.023	0.139
24-2	$\leq$ 100	0.200	26.000	-	-
48-1	264	0.200	13.000	0.017	0.105
48-2	$\leq$ 100	0.200	30.000	-	-
72-1	169	0.200	10.000	0.008	0.052
72-2	142	0.200	14.000	0.010	0.061
			TOTAL	0.654	4.013
			TOTAL RECOVERY	14.813	90.867

MITOZOLOMIDE EXCRETION BALANCE IN MICE (IMID)

MOUSE No: 6 DOSE ACTIVITY: 5.82 (12 920 000 dpm)

URINE

sample time (h)	mean dpm	mean wgt sub-samp (g)	sample weight (g)	total dpm (x10exp6)	% dose
12	37526	0.051	9.564	7.037	54.466
24	1401	0.056	6.030	0.151	1.168
48	2001	0.105	9.168	0.175	1.352
72	747	0.106	11.451	0.081	0.625
			TOTAL	7.443	57.610

FAECES

sample time (h)	mean dpm	mean wgt sub-samp (g)	sample weight (g)	total dpm (x10exp6)	% dose
12	45427	0.063	3.415	2.462	19.058
24	1718	0.055	8.412	0.263	2.034
48	471	0.051	8.892	0.082	0.636
72	512	0.061	9.887	0.083	0.642
			TOTAL	2.890	22.370

CARCASS

sample time (h)	mean dpm	mean wgt sub-samp (g)	sample weight (g)	total dpm (x10exp6)	% dose
72	638	0.050	49.130	0.627	4.852

CARBON DIOXIDE

sample time (h)	mean dpm	mean vol sub-samp (mls)	sample volume (mls)	total dpm (x10exp6)	% dose
12-1	594	0.100	22.000	0.131	1.011
12-2	532	0.200	27.000	0.072	0.556
24-1	215	0.200	21.000	0.023	0.175
24-2	100	0.200	28.000	0.014	0.108
48-1	146	0.200	29.000	0.021	0.164
48-2	< 100	0.200	25.000	-	-
72-1	100	0.200	20.000	0.010	0.077
72-2	< 100	0.200	27.000	-	-
			TOTAL	0.270	2.092
			TOTAL RECOVERY	11.231	86.924

MITOZOLOMIDE EXCRETION BALANCE IN MICE (IMID)

MOUSE No: 7 DOSE ACTIVITY: 5.46 (12 121 000 dpm)

URINE

sample time (h)	mean dpm	mean wgt sub-samp (g)	sample weight (g)	total dpm (x10exp6)	% dose
12	32439	0.053	10.160	6.218	51.303
24	2413	0.048	8.539	0.429	3.541
48	2090	0.103	11.165	0.227	1.869
72	935	0.102	11.657	0.107	0.882
			TOTAL	6.981	57.595

FAECES

sample time (h)	mean dpm	mean wgt sub-samp (g)	sample weight (g)	total dpm (x10exp6)	% dose
12	23259	0.046	2.850	1.441	11.889
24	10124	0.056	6.008	1.086	8.961
48	869	0.067	8.324	0.108	0.891
72	818	0.038	3.543	0.076	0.629
			TOTAL	2.711	22.369

CARCASS

sample time (h)	mean dpm	mean wgt sub-samp (g)	sample weight (g)	total dpm (x10exp6)	% dose
72	618	0.055	46.560	0.523	4.316

CARBON DIOXIDE

sample time (h)	mean dpm	mean vol sub-samp (mls)	sample volume (mls)	total dpm (x10exp6)	% dose
12-1	201	0.100	27.000	0.054	0.448
12-2	< 100	0.200	30.000	-	-
24-1	593	0.200	23.000	0.068	0.563
24-2	< 100	0.200	29.000	-	-
48-1	150	0.200	19.000	0.014	0.118
48-2	330	0.200	29.000	0.048	0.395
72-1	240	0.200	10.000	0.012	0.099
72-2	< 100	0.200	25.000	-	-
			TOTAL	0.197	1.622
			TOTAL RECOVERY	10.412	85.902

MITOZOLOMIDE EXCRETION BALANCE IN MICE (IMID)

MOUSE No: 8 DOSE ACTIVITY: 3.069 (6 813 0000 dpm)

URINE

sample time (h)	mean dpm	mean wgt sub-samp (g)	sample weight (g)	total dpm (x10exp6)	% dose
12	43696	0.052	5.493	4.616	67.748
24	1999	0.053	7.915	0.299	4.382
48	1454	0.105	7.896	0.109	1.605
72	687	0.106	6.831	0.044	0.650
			TOTAL	5.068	74.385

FAECES

sample time (h)	mean dpm	mean wgt sub-samp (g)	sample weight (g)	total dpm (x10exp6)	% dose
12	7758	0.060	4.679	0.605	8.880
24	6020	0.050	0.361	0.043	0.638
48	1078	0.065	6.608	0.110	1.609
72	147	0.059	9.002	0.022	0.329
			TOTAL	0.780	11.455

CARCASS

sample time (h)	mean dpm	mean wgt sub-samp (g)	sample weight (g)	total dpm (x10exp6)	% dose
72	391	0.079	51.330	0.254	3.729

CARBON DIOXIDE

sample time (h)	mean dpm	mean vol sub-samp (mls)	sample volume (mls)	total dpm (x10exp6)	% dose
12-1	258	0.100	22.000	0.057	0.833
12-2	118	0.200	28.000	0.017	0.242
24-1	464	0.200	22.000	0.051	0.749
24-2	<100	0.200	29.000	-	-
48-1	128	0.200	20.000	0.013	0.188
48-2	100	0.200	31.000	0.016	0.228
72-1	110	0.200	21.000	0.012	0.170
72-2	<100	0.200	25.000	-	-
			TOTAL	0.164	2.410
			TOTAL RECOVERY	6.267	91.978

MITOZOLOMIDE EXCRETION BALANCE IN MICE (IMID)

MOUSE No: 9 DOSE ACTIVITY: 5.703 (12 660 000 dpm

URINE

sample time (h)	mean dpm	mean wgt sub-samp (g)	sample weight (g)	total dpm (x10exp6)	% dose
12	75202	0.052	6.273	9.072	71.655
24	4782	0.050	13.394	1.281	10.118
48	1937	0.101	14.565	0.279	2.206
72	1266	0.101	11.632	0.146	1.152
washings				0.431	3.406
			TOTAL	11.209	88.536

FAECES

sample time (h)	mean dpm	mean wgt sub-samp (g)	sample weight (g)	total dpm (x10exp6)	% dose
12	15937	0.058	1.680	0.462	3.646
24	3565	0.054	0.654	0.043	0.341
48	2889	0.115	6.895	0.173	1.368
72	1268	0.110	12.771	0.147	1.163
			TOTAL	0.825	6.518

CARCASS

sample time (h)	mean dpm	mean wgt sub-samp (g)	sample weight (g)	total dpm (x10exp6)	% dose
72	961	0.087	52.040	0.575	4.540

CARBON DIOXIDE

sample time (h)	mean dpm	mean vol sub-samp (mls)	sample volume (mls)	total dpm (x10exp6)	% dose
12-1	160	0.100	29.000	0.046	0.366
12-2	$\leq$ 100	0.200	27.000	-	-
24-1	$\leq$ 100	0.200	19.000	-	-
24-2	$\leq$ 100	0.200	32.000	-	-
48-1	140	0.200	10.000	0.007	0.055
48-2	$\leq$ 100	0.200	27.000	-	-
72-1	$\leq$ 100	0.200	21.000	-	-
72-2	$\leq$ 100	0.200	27.000	-	-
			TOTAL	0.053	0.422
			TOTAL RECOVERY	12.663	100.017

MITOZOLOMIDE EXCRETION BALANCE IN MICE (IMID)

MOUSE No: 10 DOSE ACTIVITY: 5.703 (12 660 000 dpm

URINE

sample time (h)	mean dpm	mean wgt sub-samp (g)	sample weight (g)	total dpm (x10exp6)	% dose
12	57343	0.054	7.366	7.822	61.782
24	1424	0.054	6.806	0.179	1.418
48	4525	0.103	7.786	0.342	2.702
72	1543	0.102	8.999	0.136	1.075
washings				0.183	1.444
			TOTAL	8.663	68.421

FAECES

sample time (h)	mean dpm	mean wgt sub-samp (g)	sample weight (g)	total dpm (x10exp6)	% dose
12	27540	0.066	2.268	0.946	7.475
24	13436	0.062	1.712	0.371	2.930
48	3331	0.120	6.470	0.180	1.419
72	1894	0.114	11.072	0.184	1.453
			TOTAL	1.681	13.277

CARCASS

sample time (h)	mean dpm	mean wgt sub-samp (g)	sample weight (g)	total dpm (x10exp6)	% dose
72	1256	0.085	47.560	0.703	5.551

CARBON DIOXIDE

sample time (h)	mean dpm	mean vol sub-samp (mls)	sample volume (mls)	total dpm (x10exp6)	% dose
12-1	1845	0.200	15.000	0.138	1.093
12-2	806	0.200	28.000	0.113	0.891
24-1	278	0.200	25.000	0.035	0.274
24-2	$\leq$ 100	0.200	19.000	-	-
48-1	104	0.200	26.000	0.014	0.107
48-2	$\leq$ 100	0.200	30.000	-	-
72-1	$\leq$ 100	0.200	10.000	-	-
72-2	$\leq$ 100	0.200	29.000	-	-
			TOTAL	0.299	2.365
			TOTAL RECOVERY	11.346	89.614

REFERENCES

REFERENCES

1. PRATT, W.B. and RUDDON, R.W. (1979)
Combination chemotherapy. In: The Anti-cancer drugs. pp. 52-57. Oxford University Press. UK.

2. CARTER, S.K., BAKOWSKI, M.T.and HELLMAN, K. (1981).
Chemotherapy of advanced adult solid tumours. In: Chemotherapy of Cancer. pp. 130-243. John Wiley & Sons Ltd., New York, USA.

3. STEVENS, M.F.G. (1976)
The medicinal chemistry of 1,2,3-triazines.
Prog.Med.Chem. 13, 205-269.

4. VAUGHAN, K. and STEVENS, M.F.G. (1978)
Monoalkyltriazenes
Chem.Soc.Rev. 7, 377-397.

5. STEVENS, M.F.G., HICKMAN, J.A., STONE, R., GIBSON, N.W., BAIG, G.U., LUNT, E. and NEWTON, C.S. (1984)
Anti-tumour imidazotetrazines. Part I. Synthesis and chemistry of mitozolomide; a novel, broad spectrum anti-tumour agent.
J. Med. Chem. 27, 196-204.

6. STONE, R. (1981)
Cyclic and acyclic modifications of 5-aminoimidazole-4-carboxamide.
PhD thesis. Aston University, UK.

7. METZLER, D.E. (1977)
The metabolism of pyrimidines and purines. In: Biochemistry. The chemical reactions of living cells. pp. 873-882. Academic Press, London, UK.

8. CARTER, S.K. and FRIEDMAN, M.A. (1972)
5-(3,3-Dimethyl-1-triazeno)-imidazole-4-carboxamide. A new anti-tumour agent with activity against malignant melanoma.
Eur. J. Cancer. 8, 85-92.

9. SHEALY, Y.F. (1970)
Syntheses and biological activity of 5-aminoimidazoles and 5-triazenoimidazoles.
J. Pharm. Sci. 59, 1533-1557.

10. EGE, G and GILBERT, K. (1979)
[7+2] and [11+2] cycloaddition reactions of diazo-azoles with isocyanates to azolo[5,1-d]-1,2,3,5-tetrazine-4(3H)-ones.
Tet. Letters. 44, 4253-4257.

11. BAIG, G.U., STEVENS, M.F.G., STONE, R. and LUNT, E. (1982).
Triazines and related products. Part 24. Synthesis of pyrazol-4-ylidenehydrazinoimidazoles by hydrazinolysis of imidazo[5,1-c]-1,2,4-triazines and 2-arylazoimidazoles by diazonium coupling reactions.
J. Chem. Soc. Perkin Trans. 1811-19.

12. NEWTON, C.G. (1984).
May and Baker Ltd., Dagenham, UK.
Personal communication.

13. SHEALY, Y.F. (1975)
5-[3-(2-Chloroethyl)-1-triazenyl]imidazole-4-carboxamide and a possible mechanism of action of 5-[3,3-bis(2-chloroethyl)-1-triazenyl]imidazole-4-carboxamide.
J. Pharm. Sci.64 , 177-180.

14. SHEALY, Y.F., MONTGOMERY, J.A. and LASTER, W.R. (1962).
Anti-tumour activity of triazenoimidazoles.
Biochem. Pharmacol. 11, 674-676.

15. SHEALY, Y.F., STRUCK, R.F., LEE, B.H. and MONTGOMERY, J.A. (1961).
Synthesis of potential anti-cancer agents XXIX. 5-Diazoimidazole-4-carboxamide and 5-diazo-v-triazole-4-carboxamide.
J. Org. Chem. 26, 2396-2401.

16. SHEALY, Y.F. and KRAUTH, C.A. (1966).
Complete inhibition of mouse leukaemia L1210 by 5(or4)-[3,3-bis(2-Chloroethyl)-1-triazeno]imidazole-4(or 5)-carboxamide (NSC 82196).
Nature 210, 208-209.

17. SHEALY, Y.F., KRAUTH, C.A., HOLUM, L.B. and FITZGIBBON, W.E. (1968).
Synthesis and properties of the anti-leukaemic agent 5(or 4)-[3,3-bis(2-Chloroethyl)-1-triazeno]imidazole-4(or 5)-carboxamide.
J. Pharm. Sci. 57, 83-86.

18. FALKSON, G., VAN DER MERWE, A.M. and FALKSON, H.C. (1972).
Clinical experience with 5-[3,3-bis(2-chloroethyl)-1-triazeno]imidazole-4-carboxamide in the treatment of metastatic malignant melanoma.
Canc. Chem. Reps. I. 56, 671-677.

19. KOMP, D.M., LAND, V.J. and NITSCHKE, R. (1975)
5[3,3-bis(2-Chloroethyl)-1-triazeno]imidazole-4-carboxamide in the treatment of childhood malignancy.
Canc. Chem. Rep. I. 59, 371-376.

20. LEVIN, V.A., CRAFTS, D., WILSON, C.B., KABRA, P., HANSCH, C., BOLDREY, E., ENOT, J. and NEELY, M. (1975).
Imidazole carboxamides. Relationship of lipophilicity to activity against intracerebral murine glioma 26 and pre-liminary phase II clinical trial of 5-[3,3-bis(2-chloroethyl)-1-triazeno]imidazole-4-carboxamide in primary and secondary brain tumours.
Canc. Chem. Reps. I. 59, 327-331.

21. AHMANN, D.L., BISEL, H.F. and HAHN, R.G. (1973).
Difficulties in designing clinical trials as exemplified by a phase II drug evaluation of 5[3,3-bis(2-chloroethyl)-1-triazenyl]imidazole-4-carboxamide and 1-(2-chloroethyl)-3-cyclohexyl-1-nitrosourea in patients with disseminated breast cancer.
Canc. Res. 33. 1707-1710.

22. MOERTEL, C.G., SHUTT, A.J. REITEMEIER, R.J. and HAHN, R.G.(1972).
A phase II study of 5[3,3-bis(2-chloroethyl)-1-triazenyl]imidazoale-4-carboxamide in advanced gastro-intestinal cancer.
Canc. Chem. Reps. I. 56, 267-269.

23. VOGEL, C.L., DENHAM, C., WAALKES, T.P. and DEVITA, V.T. (1970).
The physiological disposition of the carcinostatic imidazole-4(or 5)-carboxamide, 5(or4)-[3,3,-bis(2-chloroethyl)-1-triazeno] (NSC 82196) (imidazole mustard) in mice and dogs.
Canc. Res. 30, 1651-1657.

24. HILL, D.L. (1975).
Microsomal metabolism of triazenylimidazoles.
Canc.Res. 35, 3106-3110.

25. GIBSON, N.W. (1982).
Mechanism of action of antineoplastic nitrosoureas.
PhD thesis, Aston University, UK.

26. COLVIN, M. and BRUNDRETT, R.A. (1981).
Chemical decomposition of chloroethylnitrosoureas.
In: Nitrosoureas, current status and new developments.
ed. Prestayko, A.W., Crooke, S.T., Baker, L.H., Carter, S.K. and Schein, P.S. pp. 43-50.
Academic Press, London.

27. GREENE, M.O. and GREENBERG, J. (1960).
The activity of nitrosoguanidine against ascites tumours in mice.
Canc. Res. 20, 1166-1173.

28. HYDE, K.A., ACTON, E., SKINNER, W.A., GOODMAN, L., GREENBERG, J. and BAKER, B.R. (1962).
Potential anti-cancer agents LXII. The relationship of chemical structure to anti-leukaemic activity with analogs of 1-methyl-3-nitro-1-nitrosoguanidine.
J. Med. Pharm. Chem. 5, 1-14,

29. SKIPPER, H.E., SCHABEL, F.M., TRADER, M.W. and THOMSON, R.J. (1961).
Experimental evaluation of potential anti-cancer drugs. VI. Anatomical distribution of leukaemic cells and failure of chemotherapy.
Canc. Res. 21, 1154-1164.

30. JOHNSTON, T.P., McCALEB, G.S. and MONTGOMERY, J.A. (1963).
The synthesis of anti-neoplastic agents. XXXII. N-Nitrosoureas.
J. Med. Chem. 6, 669-681.

31. SCHABEL, F.M. JOHNSTON, T.P. McCALEB, G.S., MONTGOMERY, J.A., LASTER, W.R. and SKIPPER, H.E. (1963).
Experimental evaluation of potential anti-cancer agents VIII. Effects of certain nitrosoureas on intracerebral L1210 leukaemia.
Canc. Res. 23, 725-733.

32. MONTGOMERY, J.A. (1976).
Chemistry and structure-activity studies of the nitrosoureas.
Canc. T. Reps. 60, 651-664.

33. MONTGOMERY, J.A., McCALEB, G.S., JOHNSON, T.P., MAYO, J.P. and LASTER, W.R. (1977).
Inhibition of solid tumours by nitrosoureas. I. Lewis Lung carcinoma.
J. Med. Chem. 20, 291-295.

34. STAQUET, M.J., BYAR, D.P., GREEN, S.B. and ROZENCWEIG, M. (1983).
Clinical predictivity of transplantable tumour systems in the selection of new drugs for solid tumours. Rationale for a three-stage strategy.
Canc. T. Reps. 67, 753-765.

35. SCHABEL, F.M. (1976).
Nitrosoureas: A review of experimental anti-tumour activity.
Canc. T. Reps. 60, 665-698.

36. MACDONALD, J.S., WEISS, R.B., FOSTER, D. and DUQUE-HAMMERSHAIMB, L. (1981).
Sub-acute and chronic toxicities associated with nitrosourea therapy. In: Nitrosoureas, current status and new developments. ed. Prestakyo, A.W., Crooke, S.T., Baker, L.H., Carter, S.K. and Schein, P.S. pp. 145-155.
Academic Press. London.

37. WASSERMAN T.H., SLAVIK, M. and CARTER, S.K. (1973)
Clinical comparison of the nitrosoureas.
Cancer. 36, 1258-1268.

38. WEISS, R.B. (1981).
The nitrosoureas and pulmonary toxicity.
Canc. Treat. Rev. 8, 111-125.

39. AMES, M.M. and POWIS, G. (1983).
Pharmacokinetics of nitrosoureas.
In: Pharmacokinetics of anti-cancer agents in humans. ed. Ames, M.M., Powis, G. and Kovach, J.S. pp. 113-134.
Elsevier, The Netherlands.

40. HANSEN, H.H. (1971)
Treatment of malignant brain tumours with nitrosoureas
Canc. Chem. Rep. 1. 55, 99-100.

41. LEVIN, V.A. (1981).
Chemotherapy of re-current brain tumours.
In: Nitrosoureas, current status and new developments.
ed. Prestakyo, A.W., Crooke, S.T., Baker, L.H., Carter, S.K. and Schein, P.S. pp. 259-268.
Academic Press. London.

42. MAURICE, P., GLIDEWELL, O., JACQUILLET, C., SILVER, R.T., CAREY, R., TENPAS, A., CORNELL, C.J., BURNINGHAM, R.A., NISSEN, N.I. and HOLLAND, J.F. (1978).
Comparison of methyl-CCNU and CCNU in patients with advanced forms of Hodgkins disease, lymphosarcoma and reticulum cell carcinoma.
Cancer, 41, 1658-1663.

43. MONTGOMERY, J.A., JAMES, R., McCALEB, G.S. and JOHNSTON, T.P. (1967).
The modes of decomposition of 1,3-bis(2-chloroethyl)-1-nitrosourea and related compounds.
J. Med. Chem. 10, 668-674.

44. COLVIN, M., COWENS, J.W., BRUNDRETT, R.B., KRAMER, B.S. and LUDLAM, D.B. (1974).
Decomposition of BCNU (1,3-bis(2-chloroethyl)-1-nitrosourea) in aqueous solution.
Biochem. Biophys. Res. Comm. 60, 515-521.

45. REED, D.J., MAY, H.E., BOOSE, R.B., GREGORY, K.M. and BEILSTEIN, M.A. (1975).
2-Chloroethanol formation as evidence for a 2-chloroethyl alkylating intermediate during chemical degradation of 1-(2-chloroethyl)-3-cyclohexyl-1-nitrosourea and 1-(2-chloroethyl)-3-(trans-4-methylcyclohexyl)-1-nitrosourea.
Canc. Res. 35, 568-576.

46. BRUNDRETT, R.B., COLVIN, M. and COWENS, J.W. (1976).
Chemistry of Nitrosoureas. Decomposition of deuterated 1,3-bis(2-chloroethyl)-1-nitrosourea.
J. Med. Chem. 19, 958-962.

47. CHATTERJI, D.C., GREENE, R.F. and GALLELLI, J.F. (1978).
Mechanism of hydrolysis of halogenated nitrosoureas.
J. Pharm. Sci. 67, 1527-1533.

48. BRUNDRETT, R.B. and COLVIN, M. (1977).
Chemistry of nitrosoureas. Decomposition of 1,3-bis(threo-3-chloro-2-butyl)-1-nitrosurea and 1,3-bis(erythro-3-chloro-2-butyl)-1-nitrosourea.
J. Org. Chem. 42, 3538-3541.

49. WEINKAM, R.J. and LIN, H.S. (1979).
Reactions of 1,3,-bis(2-chloroethyl)-1-nitrosourea and 1-(2-chloroethyl)-3-cyclohexyl-1-nitrosourea in aqueous solution.
J. Med. Chem. 22, 1193-1199.

50. LEVIN, V.A., HOFFMAN, W. and WEINKAM, R.J. (1978).
Pharmacokinetics of BCNU in humans. A preliminary study of 20 patients.
Canc. T. Reps. 62, 1305-1312.

51. WEINKAM, R.J., TSUI-YUN, J.L. and LIN, H.S. (1980).
Protein mediated chemical reactions of chloroethylnitrosoureas.
Chem - Biol. Interact. 31, 167-177.

52. MAKER, H.S., SYED, H.H. and LEHRER, G.M. (1978).
Cyclohexyl-1-nitrosourea in aqueous suspension.
J. Nat. Canc. Inst. 60, 1055-1057.

53. WEINKAM, R.J., FINN, A., LEVIN, V.A. and KANE, J.P. (1980).
Lipophilic drugs and Lipoproteins. Partitioning effects on chloroethylnitrosourea reaction rates in serum.
J. Pharmacol. Exp. Ther. 214, 318-323.

54. WHEELER, G.P., BOWDON, B.J. and STRUCK, R.F. (1975).
Carbamoylation of amino acids, peptides and proteins by nitrosoureas.
Canc. Res. 35, 2974-2985.

55. CHENG, C.J., FUJIMURA, S., GRUNBERGER, D. and WEINSTEIN, B. (1972).
Interaction of 1-(2-chloroethyl)-3-cyclohexyl-1-nitrosourea with nucleic acids and proteins in vivo and in vitro.
Canc. Res. 32, 22-27.

56. COLVIN, M., BRUNDRETT, R.B., COWENS, W., JARDINE, I. and LUDLUM, D.B. (1976).
A chemical basis for the anti-tumour activity of chloroethylnitrosoureas
Biochem. Pharmacol. 25, 695-699.

57. KANN, H.E., KOHN, K.W. and LYLES, J.M. (1974).
Inhibition of DNA repair by the 1,3-bis(2-chloroethyl)-1-nitrosourea breakdown product, 2-chloroethyl isocyanate.
Canc. Res. 34, 398-402.

58. HILTON, J., MALDARELLI, F. and SARGENT, S. (1978).
Evaluation of the role of isocyanates in the action of therapeutic nitrosoureas.
Biochem. Pharmacol. 27, 1359-1363.

59. BONO, V.H. (1976).
Review of mechanism of action studies of the nitrosoureas.
Canc. T. Reps. 60, 699-702.

60. SPREAFICO, F., FILIPPESCHI, S., FALAUTANO, P. and EISENBRAND, G.(1981),
EORTC studies with novel nitrosoureas.
In: Nitrosoureas, current status and new developments. ed. Prestakyo, A.W., Crooke, S.T., Baker, L.H., Carter, S.K. and Schein, P.S. pp. 27-42.
Academic press, London.

61. ANDERSON, T., McMANAMIN, M.G. and SCHEIN, P. (1975).
Chlorozotocin, 2-[3-(2-chloroethyl)-3-nitrosoureido]-D-glucopyranose, an anti-tumour agent with modified bone marrow toxicity.
Canc. Res. 35, 761-765.

62. KOVACH, J.S., MOERTEL, C.G., SCHUTT, A.J., FRYTAK, S., O'CONNELL, M.J., RUBIN, J. and INGLE, J.N. (1979).
A phase I study of chlorozotocin.
Cancer 43, 2189-2196.

63. TALLEY, R.W., SAMSON, M.K., BROWNLEEE, R.W., SAMHOURI, A.M., FRAILES, R.J. and BAKER, L.H. (1981).
Phase II evaluation of chlorozotocin in advanced human cancer.
Eur. J. Cancer. 17, 337-343.

64. KOHN, K.W. (1977).
Interstrand cross-linking of DNA by 1,3-bis(2-chloroethyl)-1-nitrosourea and other 1-(2-haloethyl)-1-nitrosoureas.
Canc. Res. 37, 1450-1454.

65. LOWN, J.W. and McLAUGHLIN, L.W. (1979).
Mechanism of action of 2-haloethylnitrosoureas on deoxyribonucleic acid.
Biochem. Pharmacol. 28, 2123-2128.

66. EWIG, R.A. and KOHN, K.W. (1978).
DNA-protein cross-linking and DNA interstrand cross-linking by haloethylnitrosoureas in L1210 cells.
Canc. Res. 38, 3197-3203.

67. SUN, L. and SINGER, B. (1975).
The specificity of different classes of ethylating agents towards various sites of HeLa cell DNA in vitro and in vivo.
Biochemistry. 14, 1795-1802.

68. ERICKSON, L.C., OSIEKA, R. and KOHN, K.W. (1978).
Differential repair of 1-(2-chloroethyl)-3-(4-methylcyclohexyl)-1-nitrosourea-induced DNA damage in 2 human colon tumour cell lines.
Canc. Res. 38, 802-807.

69. ERICKSON, L.C., BRADLEY, M.O., DUCORE, J.M., EWIG, R.A. and KOHN, K.W. (1980).
DNA cross-linking and cytotoxicity in normal and transformed human cells treated with anti-tumour nitrosoureas.
Proc. Nat. Acad. Sci. 77, 467-471.

70. ERICKSON, L.C., LAURENT, G., SHARKEY, N.A. and KOHN, K.W. (1980).
DNA cross-linking and monoadduct repair in nitrosourea treated human tumour cells.
Nature. 288, 727-729.

71. WEINKAM, R.J. and DEEN, D.F. (1982).
Quantitative dose response relations for the cytotoxic activity of chloroethylnitrosoureas in cell culture.
Canc. Res. 42, 1008-1014.

72. HICKMAN, J.A., STEVENS, M.F.G., GIBSON, N.W., LANGDON, S.P., FIZAMES, C., LAVELLE, F., ATASSI, G. and LUNT,E. (1985).
The experimental anti-tumour activity of 8-carbamoyl-3-(2-chloroethyl)imidazo[5,1-d]-1,2,3,5-tetrazin-4(3H)-one, a broad spectrum agent.
Canc. Res. 45, 3008-3019.

73. GERAN, R.I., GREENBERG, N.H., MACDONALD, M.M. SCHUMACHER, A.M. and ABBOT, B.J. (1972).
Protocols for screening chemical agents and natural products against animal tumours and other biological systems.
Canc. Chem. Rep. III, 3, 1-103.

74. HICKMAN, J.A., STEVENS, M.F.G., GIBSON, N.W. STONE, R., LAVELLE, F. and FIZAMES, C. (1982).
M&B 39565, a novel heteorocycle with potent anti-tumour activity in mice.
In: Proceedings of 13th International cancer conference. p. 551. UICC. Geneva.

75. STEVENS, M.F.G., HICKMAN, J.A. STONE, R., GIBSON, N.W. and LUNT, E. (1983).
Synthesis and properties of a new bicyclic anti-tumour agent CCRG 81010.
Br. J. Cancer. 48, 120.

76. WORKMAN, P. and LEE, F.Y.F. (1984).
Experimental anti-tumour activity and mechanism of action of the novel anti-cancer agent CCRG 81010.
Br. J. Cancer. 50, 251-252.

77. FØDSTAD, O., AAMDAL, S., PIHL, A. and BOYD, M.R. (1985).
Activity of mitozolomide (NSC 353451), a new imidazotetrazine, against xenografts from human melanomas, sarcomas and lung and colon carcinomas.
Canc. Res. 45, 1778-1786.

78. HORGAN, C.M.T. and TISDALE, M.J. (1984).
Anti-tumour imidazotetrazines - IV. An investigation into the mechanism of anti-tumour activity of a novel and potent anti-tumour agent, mitozolomide.
Biochem. Pharmacol. 33, 2185-2192.

79. HORGAN, C.M.T. and TISDALE, M.J. (1985).
Anti-tumour imidazotetrazines - VIII - Uptake and decomposition of a novel anti-tumour agent, mitozolomide, in TLX5 lymphoma cells in vitro.
Biochem. Pharmacol. 34, 217-221.

80. HORGAN, C.M.T. and TISDALE, M.J. (1983).
An investigation into the mechanism of action of a novel and potent anti-tumour agent, mitozolomide.
Br. J. Cancer. 48, 132-138.

81. GIBSON, N.W., ERICKSON, L.C. and HICKMAN, J.A. (1984).
Effects of the anti-tumour agent 8-carbamoyl-3-(2-chloroethyl) imidazo[5,1-d]-1,2,3,5-tetrazin-4(3H)-one on the DNA of mouse L1210 cells.
Canc. Res. 44, 1767-1771.

82. GIBSON, N.W., HICKMAN, J.A. and ERICKSON, L.C. (1984).
DNA cross-linking and cytotoxicity in normal and transformed human cells treated in vitro with 8-carbamoyl-3-(2-chloroethyl)imidazo[5,1-d]-1,2,3,5-tetrazin-4(3H)-one.
Canc. Res. 44, 1772-1775.

83. LANGDON, S.P., STONE, R., STEVENS, M.F.G., GIBSON, N.W., CHUBB, D., HICKMAN, J.A. and LAVELLE, F. (1985).
CCRG 81045 - A novel imidazotetrazinone with broad spectrum activity against murine tumours.
Proc. Amer. Assoc. Canc. Res. 26, 255.

84. STANLEY-AUDETTE, R.C., CONNORS, T.A., MANDEL, H.G., MERAI, K. and ROSS, W.C.J. (1973).
Studies on the mechanism of action of the tumour inhibitory triazenes.
Biochem. Pharmacol. 22, 1855-1864.

85. STEVENS, M.F.G. and PEATEY, L. (1978).
Photodegradation of solutions of the anti-tumour drug DTIC.
J. Pharm. Pharmacol. 30, 47P.

86. SKIBBA, J.L. and BRYAN, G.T. (1971).
Methylation of nucleic acids and urinary excretion of ^{14}C-labelled 7-methylguanine by rats and man after administration of 4(5)-(3,3-dimethyl-1-triazeno)-imidazole-5(4)-carboxamide.
Toxicol. App. Pharmacol. 18, 707-719.

87. PREUSSMAN, R., von HODENBERG, A. and HENGY, H. (1969).
Mechanism of carcinogenesis with 1-aryl-3,3-dialkyltriazenes. Enzymatic dealkylation by rat liver microsomal fraction in vitro.
Biochem. Pharmacol. 18, 1-13.

88. KOLAR, G.F., MAURER, M. and WILDSCHÜTTE, M. (1980).
5-(3-hydroxymethyl-3-methyl-1-triazeno)imidazole-4-carboxamide is a metabolite of 5-(3,3-dimethyl-1-triazeno)imidazole-4-carboxamide.
Canc. Lett. 10, 235-241.

89. SKIBBA, J.L., BEAL, D.D., RAMIREZ, G. and BRYAN, G.T. (1970).
N-demethylation of the anti-neoplastic agent 4(5)-(3,3-dimethyl-1-triazeno)imidazole-5(4)-carboxamide by rats and man.
Canc. Res. 30, 147-150.

90. BARTOLI-KLUGMAN, F., PANI, B., BABUDRI, N., MONTIGRADIN, C., TAMARO, M. and VENTURINI, S. (1982).
In vitro mutagenic activity of 5-(3,3-dimethyl-1-triazeno)imidazole-4-carboxamide (DTIC) in eukaryotic and prokaryotic cells.
Carcinogenesis 3, 467-471.

91. GIRALDI, T., GUARINO, A.M., NISI, C., TAYLOR, D.M. and SAVA, G. (1978).
Anti-metastatic action of some triazene derivatives against the Lewis Lung carcinoma in mice.
Canc. T. Reps. 62, 721-725.

92. SAVA, G., GIRALDI, T., LASSIANI, L. and NISI, C. (1982).
Metabolism and mechanism of the anti-leukaemic action of isomeric aryldimethyltriazenes.
Canc. T. Reps. 66, 1751-1755.

93. LUDLUM, D. (1979).
The properties of 7-methylguanine-containing templates for ribonucleic acid polymerase.
J. Biol. Chem. 245, 477-482.

94. LUCE, J.K., THURMAN, W.G. and ISAACS, B.L. (1970).
Clinical trials with the anti-tumour agent 5-(3,3-dimethyl-1-triazeno)imidazole-4-carboxamide.
Canc. Chem. Rep. I. 54, 119-124.

95. BURKE, P.J., McCARTHY, W. and MILTON, G.W. (1971).
Imidazole carboxamide therapy in advanced malignant melanoma.
Cancer. 27, 744-750.

96. DELBEN, F., PAOLETTI, S., MANZINI, G. and NISI, C. (1981).
Influence of serum albumins on decomposition rates of para-substituted 1 phenyl-3-methyltriazenes and 5-(3-methyl-1-triazeno)imidazole-4-carboxamide in near physiological conditions.
J. Pharm. Sci. 70, 892-897.

97. WALKER, M.D. and HILTON, J. (1976).
Nitrosourea pharmacodynamics in relation to the central nervous system.
Canc. T. Reps. 60, 725-728.

98. ENSMINGER, W.D., THOMPSON, M., COME, S. and EGAN, E.M. (1978).
Hepatic arterial BCNU; A pilot clinical-pharmacologic study in patients with liver tumours.
Canc. T. Reps. 62, 1509-1512.

99. RUSSO, R., BARTOSEK, I., PIAZZA, E., SANTI, A-M., LIBRETTI, A. and GARATTINI, S. (1981).
Differential pulse polarographic determination of BCNU pharmacokinetics in patients with lung cancer.
Canc. T. Reps. 65, 555-562.

100. WEINKAM, R.J., WEN, J.H.C., FURST, D.E. and LEVIN, V.A. (1978).
Analysis for 1,3-bis(2-chloroethyl)-1-nitrosourea by chemical ionization mass spectrometry.
Clin. Chem. 24, 45-49.

101. SMITH, R.G. and CHEUNG, L.K. (1982).
Determination of two nitrosourea anti-tumour agents by chemical ionization gas chromatography mass spectrometry.
J. Chromatog. 229, 464-469.

102. LEE, F.Y.F. and WORKMAN, P. (1983).
Modification of CCNU pharmacokinetics by misonidazole - a major mechanism for chemosensitization in mice.
Br. J. Cancer. 47, 659-669.

103. YEAGER, R.L., OLDFIELD, E.H. and CHATTERJI, D.C. (1984).
Quantitation of 1,3-bis(2-chloroethyl)-1-nitrosourea in plasma using high performance liquid chromatography.
J. Chromatog. 305 (1984) 496-501.

104. HILL, D.L., KIRK, M.C. and STRUCK, R.F. (1975).
Microsomal metabolism of nitrosoureas.
Canc. Res. 35, 296-301.

105. LIN, H-S. and WEINKAM, R.J. (1981).
Metabolism of 1,3-bis(2-chloroethyl)-1-nitrosourea by rat hepatic microsomes.
J. Med. Chem. 24, 761-763.

106. POTTER, D.W. and REED, D.J. (1982).
Denitrosation of carcinostatic nitrosoureas by purified NADPH cytochrome P.450 reductase and rat liver microsomes to yield nitric oxide under anaerobic conditions.
Arch. Biochem. Biophys. 216, 158-169.

107. HILTON, J. and WALKER, M.D. (1975).
Hydroxylation of 1-(2-chloroethyl)-3-cyclohexyl-1-nitrosourea.
Biochem. Pharmacol. 24, 2153-2158.

108. MAY, H.E., BOOSE, R. and REED, D.J. (1974).
Hydroxylation of the carcinostatic 1-(2-chloroethyl)-3-cyclohexyl-1-nitrosourea by rat liver microsomes.
Biochem. Biophys. Res. Comm. 57, 426-453.

109. MAY, H.E., BOOSE, R. and REED, D.J. (1975).
Microsomal monooxygenation of the carcinostatic 1-(2-chloroethyl)-3-cyclohexyl-1-nitrosourea. Synthesis and identification of cis and trans mono-hydroxylated products.
Biochemistry. 14, 4723-4730.

110. MAY, H.E., KOHLHEPP, S.J., BOOSE, R.B. and REED, D.J. (1979).
Synthesis and identification of products derived from the metabolism of the carcinostatic 1-(2-chloroethyl)-3-(trans-4-methylcyclohexyl)-1-nitrosourea by rat liver microsomes.
Canc. Res. 39, 762-772.

111. DE VITA, V.T., DENHAM, C., DAVIDSON, J.D. and OLIVERIO, V.T. (1967).
The physiological disposition of the carcinostatic 1,3-bis(2-chloroethyl)-1-nitrosourea (BCNU) in man and animals.
Clin. Pharmacol. Ther. 8, 566-577.

112. OLIVERIO, V.T. (1973).
Toxicology and pharmacology of the nitrosoureas.
Canc. Chem. Reps. pt 3. 4, 13-20.

113. OLIVERIO, V.T. (1976).
Pharmacology of the nitrosoureas: an overview.
Canc. T. Reps. 60, 703-707.

114. LEVIN, V.A., KABRA, P.A. and FREEMAN-DOVE, M.A. (1978).
Relationship of 1,3-bis(2-chloroethyl)-1-nitrosourea (BCNU) and 1-(2-chloroethyl)-3-cyclohexyl-1-nitrosourea (CCNU). Pharmacokinetics of uptake, distribution and tissue/plasma partitioning in rat organs and intracerebral tumours.
Canc. Chem. Pharmacol. 1, 233-242.

115. LEVIN, V.A., STEARNS, J., BYRD, A., FINN, A. and WEINKAM, R.J. (1979).
The effect of phenobarbital pretreatment on the anti-tumour activity of 1,3-bis(2-chloroethyl)-1-nitrosourea (BCNU), 1-(2-chloroethyl)-3-cyclohexyl-1-nitrosourea (CCNU) and 1-(2-chloroethyl)-3-(2,6-dioxo-3-piperidyl)-1-nitrosourea (PCNU) and on the plasma pharmacokinetics and biotransformation of BCNU.
J. Pharmacol. Exp. Ther. 208, 1-6.

116. LEVIN, V.A. (1981).
Clinical pharmacology of the nitrosoureas.
In: Nitrosoureas, current status and new developments. ed. Prestakyo, A.W., Crooke, S.T., Baker, L.H., Carter, S.K. and Schein, P.S.
pp. 171-181, Academic Press, London.

117. LEVIN, V.A., LIU, J. and WEINKAM, R.J. (1981).
Comparative pharmacokinetics of 1-(2-chloroethyl)-3-(2,6-dioxo-1-piperidyl)-1-nitrosourea in rats and patients and extrapolation to clinical trials.
Canc. Res. 41, 3475-3477.

118. LEE, F.Y., WORKMAN, P., ROBERTS, J.T., BLEEHEN, N.M. (1985).
Clinical pharmacokinetics of oral CCNU (lomustine).
Canc. Chem. Pharmacol. 14, 125-131.

119. LOO, T.L. and STASSWENDER, E.A. (1967).
Colorimetric determination of dialkyltriazenoimidazoles.
J. Pharm. Sci. 56, 1016-1018.

120. LOO, T.L., LUCE, J.K., JARDINE, J.H. and FREI, E. (1968).
Pharmacologic studies of the anti-tumour agent 5-(dimethyl-triazeno)imidazole-4-carboxamide.
Canc. Res. 28, 2448-2453.

121. HOUSEHOLDER, G.E. and LOO, T.L. (1971)
Disposition of 5-(3,3-dimethyl-1-triazeno)imidazole-4-carboxamide, a new anti-tumour agent.
J. Pharmacol. Exp. Ther. 179, 386-395.

122. BREITHAUPT, H., DAMMANN, A. and AIGNER, K. (1982).
Pharmacokinetics of dacarbazine (DTIC) and its metabolite 5-aminoimidazole-4-carboxamide (AIC) following different dose schedules.
Canc. Chem. Pharmacol. 9, 103-109.

123. VOGEL, C.L., DENHAM, C., WALLKES, T.P. and DEVITA, V.T. (1970).
The physiological disposition of the carcinostatic imidazole-4-(or 5)-carboxamide, 5(or 4)-[3,3-bis(2-chloroethyl)-1-triazeno] (NSC 82196) (imidazole mustard) in mice and dogs.
Canc. Res. 30, 1651-1657.

124. SØRENSON, S.P.L. (1909).
Supplement to the paper, Ensyme studies II. Concerning the measurement and significance of hydrogen ion concentrations in ensymmatic processes.
Biochem. Zeitschrift. 22, 352-356.

125. GOMORI, G. (1948).
Histochemical demonstration of sites of choline esterase activity.
Proc. Soc. Exp. Biol. Med. 68, 354-358.

126 WALPOLE, G.S. (1914).
Hydrogen potentials of mixtures of acetic acid and sodium acetate.
J. Chem. Soc. 105, 2501-2530.

127. FALLICK, G.J. and RAUSCH, C.W. (1979).
Radial compression separation system: an advance in analytical LC column technology.
Am. Lab. 11, 87-97.

128. DHONDT, J.L., CARTIGNY, B. and FARRIAUX, J.P. (1974).
Etude des derives imidazoles urinaires pour chromatographie sur conche-mince.
Clin. Chim. Acta. 50, 297-300.

129. TURNER, J.C. (1971)
In: Sample preparation for liquid scintillation counting.
Radiochemical centre, Amersham, UK.

130. PAULUS, H. (1969).
A rapid and sensitive method for measuring the binding of radioactive ligands to proteins.
Anal. Biochem. 32, 91-100.

131. KURZ, H., TRUNK, H. and WEITZ, B. (1977).
Evaluation of methods to determine the protein binding of drugs. Equilibrium dialysis, ultrafiltration, ultracentrifugation, gel-filtration.
Arzneim-Forsch. 27, 1373-1380.

132. WHITLAM, J.B. and BROWN, K.F. (1981).
Ultrafiltration in serum protein binding determinations.
J. Pharm. Sci. 70, 146-150.

133. SHAH, V.P., WALLACE, S.M. and RIEGELMAN, S. (1974).
Microultrafiltration technique for drug protein-binding determination in plasma.
J. Pharm. Sci. 63, 1364-1367.

134. LOWRY, O.H., ROSEBROUGH, N.J. and FARR, A.L. (1951).
Protein measurement with the Folin phenol reagent.
J. Biol. Chem. 193, 265-275.

135. CROSSLAND, J. (1980).
Gaseous and volatile anaesthetics. In: Lewis's Pharmacology.
pp. 498-503.
Churchill Livingstone, Edinburgh, UK.

136. CALVERT, A.H. (1985).
clinical aspects of phase I trials.
Br. J. Cancer. In press.

137. NEWLANDS, E.S., BLACKLEDGE, G., SLACK, J.A., GODDARD, C., BRINDLEY, C.J., HOLDEN, L. and STEVENS, M.F.G. (1985).
Phase I trial of mitozolomide (CCRG 81010; M & B 39565; NSC 353451).
Canc. T. Reps. In press.

138. TILSON, R. (1984).
May and Baker Ltd., Dagenham, UK.
Personal communciation.

139. LKB Ltd. (1982)
In: High performance liquid chromatography for the Biochemist.
LKB Ltd., Bromma, Sweden.

140. ENGELHARDT, H., DREYER, B. and SCHMIDT, H. (1982).
Properties and diversity of C18 bonded phases.
Chromatographia. 16, 11-18.

141. GILL, R., ALEXANDER, S.P. and MOFFAT, A.C. (1982).
Comparison of amine modifiers used to reduce peak tailing of 2-phenylethylamine drugs in reversed-phase high performance liquid chromatography.
J. Chrom. 247, 39-45.

142. KRUSTULOVIC, A. and BROWN, p. (1983).
Ion-pair cromatography. In: Reversed phase high performance liquid chromatography. pp. 170-191.

143. KRUSTULOVIC, A. and BROWN, P. (1983).
Basic principles. In: Reversed phase high performance liquid chromatography. pp. 17-32
Academic Press, UK.

144. EGE, G., HECK, R. and GILBERT, K-H. (1983).
Reactions with diazo-azoles. Part VI. Unequivocal synthesis of 3-methyl-3H-azolotetrazoles. Correction of the formerly described 3-methylazolotetrazoles in favour of mesoionic 2-methylazolotetrazoles.
J. Het. Chem. 20, 1629-1639.

145. RHYS-WILLIAMS, A.T. (1980).
In: Fluorescence detection in liquid chromatography.
Perkin-Elmer, Beaconsfield, UK.

146. HORGAN, C.M.T. (1985).
Studies on mitozolomide (CCRG 81010) a new anti-neoplastic agent.
PhD Thesis, Aston University, UK.

147. DIEM, K. and LENTNER, C. (1975).
In: Documenta Geigy. Scientific Tables. pp.579-583
Geigy Pharmaceuticals, Macclesfield, UK.

148. ANDERSON, M.E. and MEISTER, A. (1980).
Dynamic state of glutathione in blood plasma.
J. Biol. Chem. 255, 9530-9533.

149. WENDEL, A. and CIKRYT, P. (1980).
The level and half-life of glutathione in human plasma.
FEBS Lett. 120, 209-211.

150. LOWN, J.W. and SINGH, R. (1982).
Mechanism of action of anti-tumour 3-(2-haloethyl)aryltriazenes on deoxyribonucleic acid.
Biochem. Pharmacol. 31, 1257-1266.

151. CURRY, S.H. (1980).
Elementary pharmacokinetics.
In: Drug disposition and pharmacokinetics. pp. 177-210.
Blackwell Scientific, Oxford, UK.

152. SLACK, J.A., STEVENS, M.F.G., GOODARD, C. and KAHN, A. (1983).
The analysis and pharmacokinetics of CCRG 81010 in mice.
Proc. Amer. Assoc. Canc. Res. 24, 291.

153. WOOD, D.C. and WOOD, J. (1975).
Pharmacologic and biol considerations of dimethyl-sulphoxide.
N.Y. Acad. Sci. 243, 7-35.

154. MADDOCK, G.L., GREEN, M.N. and BROWN, B.L. (1966).
Topical administration of anti-tumour agents to locally implanted neoplasms.
Proc. Amer. Assoc. Canc. Res. 7, 46.

155. CURRY, S.H. (1980).
Disposition and fate.
In: Drug disposition and pharmacokinetics. pp. 22-87.
Blackwell Scientific, Oxford, UK.

156. NEWLANDS, E.S., BLACKLEDGE, G., SLACK, J.A., GODDARD, C., BRINDLEY, C.J., HOLDEN, L. and STEVENS, M.F.G. (1985).
Phase I trial of mitozolomide (CCRG 81010; M & B 39565; NSC 353451).
Canc. T. Reps. In press.

157. CURRY, S.H. (1980).
Binding to plasma proteins.
In: Drug distribution and pharmacokinetics. pp 88-101.
Blackwell Scientific, Oxford, UK.

158. MANDEL, H.G. (1972).
Pathways of drug biotransformation: Biochemical conjugations.
In: Fundamentals of drug metabolism and drug disposition. ed. La Du, B.N., Mandel, H.G. and Ways, E.L. pp. 34-363.
Williams and Wilkins, Baltimore, USA.

159. WOODBURY, J.W. (1974).
Body acid-base state and its regulation.
In: Physiology and Biophysics II. ed. Ruch, T.C. and Patton, H.D. pp. 48-521. W.B. Saudners, London, UK.

160. WADDELL, W.J. and BUTLER, T.C. (1959)
Calculation of intracellular pH from the distribution of 5,5-dimethyl-2,4-oxazolidinedione (DMO). Application to skeletal muscle of the dog.
J. Clin. Invest. 38, 720-729.

161. FORTE, J.G. and REENSTRA, W.W. (1985).
Plasma membrane proton pumps in animal cells.
Bioscience 35, 38-42.

162. KENNEDY, K.A. McGURL, J.D., LEONDARIDIS, L. and ALABASTER, O. (1985).
pH dependant interstrand cross-linking by mitomycin C in aerobic EMT 6 tumour cells.
Proc. Amer. Assoc. Canc. Res. 26, 211.

163. BROPHY, G.T. and SLADEK, N.E. (1983).
Influence of pH on the cytotoxic activity of chlorambucil.
Biochem. Pharmacol. 32, 79-84.

164. WHEELER, K.T., LEVIN, V.A. and DEEN, D.F. (1978).
The concept of drug dose for in vitro studies with chemotherapeutic agents.
Radiation Res. 76, 441-446.

165. MULCAHY, R.T., DEMBS, N.L. and UBLACKER, G.A. (1984).
Enhancement of nitrosourea cytotoxicity by misonidazole in vitro : correlation with carbamoylating potential.
Br. J. Cancer. 49, 307-310.

166. TWENTYMAN, P.R. and BLEEHAN, N.M. (1975).
Changes in sensitivity to cytoxic agents occuring during the life history of monolayer cultures of a mouse tumour cell line.
Br. J. Cancer. 48, 17-25.

167. SKIPPER, H.E., SCHABEL, F.M. MELLETT, L.B., MONTGOMERY, J.A., WILKOFF, L.J., LLOYD, H.H. and BROCKMAN, R.W. (1970).
Implications of biochemical, cytokinetic, pharmacologic and toxicologic relationships in the design of optimal therapeutic schedules.
Canc. Chem. Reps. I. 54, 431-440.

168. JAIN, R.K., SHAH, S.A. and FINNEY, P.L. (1984).
Continuous non-invasive monitoring of pH and temperature in rat Walker 256 carcinoma during normoglycemia and hyperglycemia.
J. Nat. Canc. Inst. 73, 429-436.

169. ROGERS, J., HESKETH, R., SMITH, G.A. and METCALFE, J.C. (1983).
Intracellular pH of stimulated thymocytes measured with a new fluorescent indicator.
J. Biol. Chem. 258, 5994-5997.

170. TWENTYMAN, P.R. (1985).
Predictive chemosensitivity testing.
Br. J. Cancer. 51, 295-299.

171. SHOEMAKER, R., WOLPERT-De FILIPPES, R.S and VENDITTI, J. (1985).
Anti-tumour drug screening using fresh human lung tumour specimens in an in vitro colony forming assay.
Proc. Amer. Assoc. Canc. Res. 26, 369.

172. WORKMAN, P. (1985).
The role of pre-clinical and clinical pharmacokinetics in phase I trials.
Br. J. Cancer. In press.

173. YAROSH, D.B., (1985).
The role of 06-methylguanine-DNA methyltransferase in cell survival, mutagenesis and carcinogenesis.
Mut. Res. 145, 1-16.

174. GIBSON, N.W., ZLOTOGORSKI, C. and ERICKSON, L.C. (1985).
Specific DNA repair mechanisms may protect some human tumour cells from DNA interstrand cross-linking by chloroethylnitrosoureas but not from cross-linking by other anti-tumour alkylating agents.
Carcinogen. 6, 445-450.

175. ZLOTOGORSKI, C., and ERICKSON, L.C. (1984).
Pre-treatment of human colon tumour cells with DNA methylating agents inhibits their ability to repair chloroethyl monoadducts.
Carcinogen. 5, 83-87.

176. NOWELL, P.C. (1982).
Cytogenetics In: Cancer - a comprehensive treatise. Vol 1. Etiology: Chemical and physical carcinogenesis. pp. 3-46.
Plenum Press, New York, USA.

177. BRINDLEY, C.J., ANTONIW, P., NEWLANDS, E.S. and BAGSHAWE, K.D. (1984).
Plasma and tissue disposition of CCRG 81010 in mice.
Proc. Amer. Assoc. Canc. Res. 25, 355.

178. BRINDLEY, C.J., ANTONIW, P. and NEWLANDS, E.S. (1985).
Plasma and tissue disposition of mitozolomide in mice.
Br. J. Cancer. In press.

179. KESTELL, P., BRINDLEY, C.J., ANTONIW, P., SLACK, J.A. and NEWLANDS, E.S. (1985).
Tissue disposition of radiolabelled mitozolomide in mice.
Br. J. Cancer. In press.

180. WORKMAN, P., LEE, F.V.F. and DONALDSON, J. (1985).
Pharmacokinetic factors affecting comparative tumour response to CCNU and mitozolomide.
Br. J. Cancer. In press.

181. VOGLER, W.R. (1982).
Autologous bone marrow transplantation: Current studies and future directions.
Prog. Clin. Canc. 8, 45-56.

182. PHILLIPS, G.L., FAY, J.W., HERZIG, G.P., HERZIG, R.H., WEINER, R.S., WOLFF, S.N., LAZARUS, H.M., KARANES, C. and ROSS, W.E. (1983).
Intensive 1,3-bis(2-chloroethyl)-1-nitrososurea (BCNU) and cryopreserved autologous bone marrow transplantation for refactory cancer. A phase I-II study.
Cancer. 52. 1792-1802.